Final Report

Synthesis and biological evaluation of novel indole-triazole hybrids

By Assoc.Prof. Ratchanok Pingaew

May 2015

Contract No. MRG5680001

Final Report

Synthesis and biological evaluation of novel indole-triazole hybrids

Assoc.Prof. Ratchanok Pingaew Srinakharinwirot University

This project granted by the Thailand Research Fund, the office of the Higher Education Commission, and Srinakharinwirot University

Abstract

Project Code : MRG5680001

Project Title : Synthesis and biological evaluation of novel indole-triazole hybrids

Investigator : Assoc.Prof. Ratchanok Pingaew

E-mail Address : ratchanok@swu.ac.th

Project Period : 2 Years

A series of arylsulfonyl mono-indoles, bis-indoles and tris-indoles have been synthesized and evaluated for their cytotoxicity toward four human cancer cell lines including HuCCA-1 (cholangiocarcinoma), HepG2 (hepatocellular carcinoma), A-549 (lung carcinoma) and MOLT-3 (lymphoblastic leukemia). The results disclosed that *N*-arylsulfonyl bis-indoles bearing phenolic groups are potentially interesting lead pharmacophores of anticancer agents that should be further investigated in more detail. In addition, a series of 1,4-disubstituted-1,2,3-triazoles containing sulfonamide moiety were synthesized and evaluated for their aromatase inhibitory effects. Most triazoles with open-chain sulfonamide showed significant aromatase inhibitory activity (IC_{50} = 1.3-9.4 μM). Interestingly, the *meta* analog of triazole-benzene-sulfonamide bearing 6,7-dimethoxy substituents on the isoquinoline ring displayed the most potent aromatase inhibitory activity (IC_{50} = 0.2 μM) without affecting normal cell. Furthermore, a new series of chalcone-coumarin derivatives linked by the 1,2,3-triazole ring were synthesized through the azide/alkyne dipolar cycloaddition. Hybrid molecules were evaluated for their cytotoxic activity against four cancer cell lines (e.g., HuCCA-1, HepG2, A549 and MOLT-3) and antimalarial activity toward *Plasmodium falciparum*. Most of the synthesized hybrids displayed cytotoxicity against MOLT-3 cell line without affecting normal cells. These works provide the novel lead molecules for further development.

Keywords : indole; triazole; tetrahydroisoquinoline; cytotoxicity; anti-aromatase; antimalarial activity

1. Objective

1.1 To study the dipolar cycloaddition for the synthesis of triazole scaffold

1.2 To study the Friedel Crafts reaction for the synthesis of bis-indole and tris-indole

1.3 To evaluate the biological activity of indole and triazole derivatives

1.4 To study the structure-activity relationships

2. Research methodology

2.1 Synthesis of mono-indoles (type I), bis-indoles (type II-IV) and tris-indoles (type V) **10-32** was outlined in Scheme 1 and 2.

Various mono-indoles **10-15** were readily prepared by the condensation of tryptamine with corresponding arylsulfonyl chlorides in the presence of sodium carbonate in good yields (85-95%).

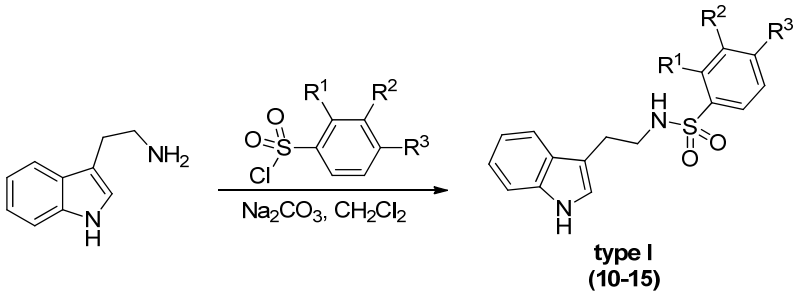

Scheme 1

Subsequently, alkylations of *N*-sulfonyltryptamines **11-15** with benzaldehyde (**a**), *o*-hydroxybenzaldehyde (**b**), *p*-hydroxybenzaldehyde (**c**) or isatin (**d**) catalyzed by 20 mol% $H_4O_{40}SiW_{12}$·aq in acetonitrile were investigated. The reactions readily furnished BIMs (type II-IV) and TIMs (type V) in moderate to good yields (34-75%) (Scheme 2).

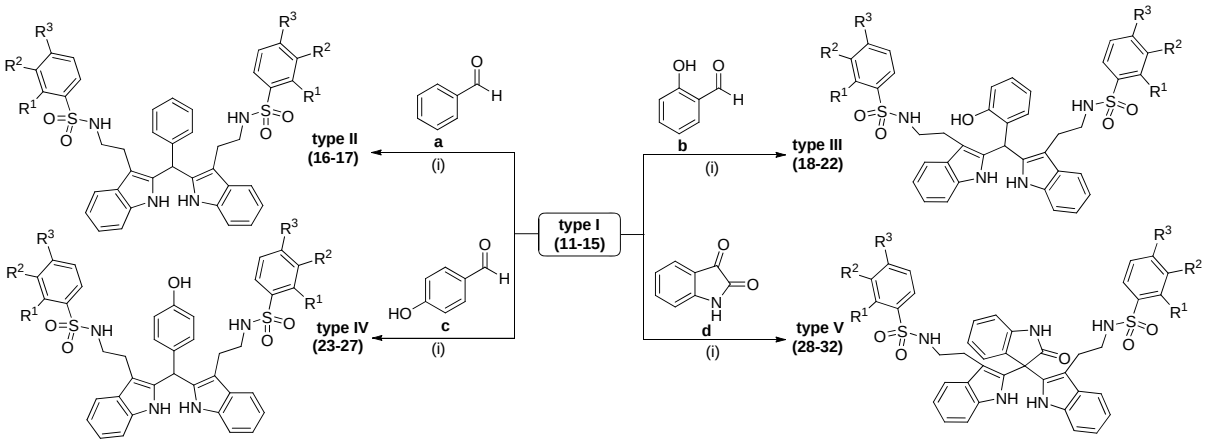

Reagents and conditions: (i) $H_4O_{40}SiW_{12}$·aq (20 mol%), CH_3CN, rt

Scheme 2

2.2 Synthesis of triazole derivatives **1-39** was outlined in Scheme 3.

The open chain THIQ analogs of triazoles **1-16** (type I) were prepared through a sequential sulfonation/reduction/diazotization/cycloaddition reactions (route a; steps i-iv). In the same manner, the synthesis of triazoles type II **17-35** and type III **36-39** was carried out via route b (steps i-v), in which an additional step (i.e., step v) was performed using the Pictet-Spengler reaction to form isoquinoline ring prior to steps ii-iv.

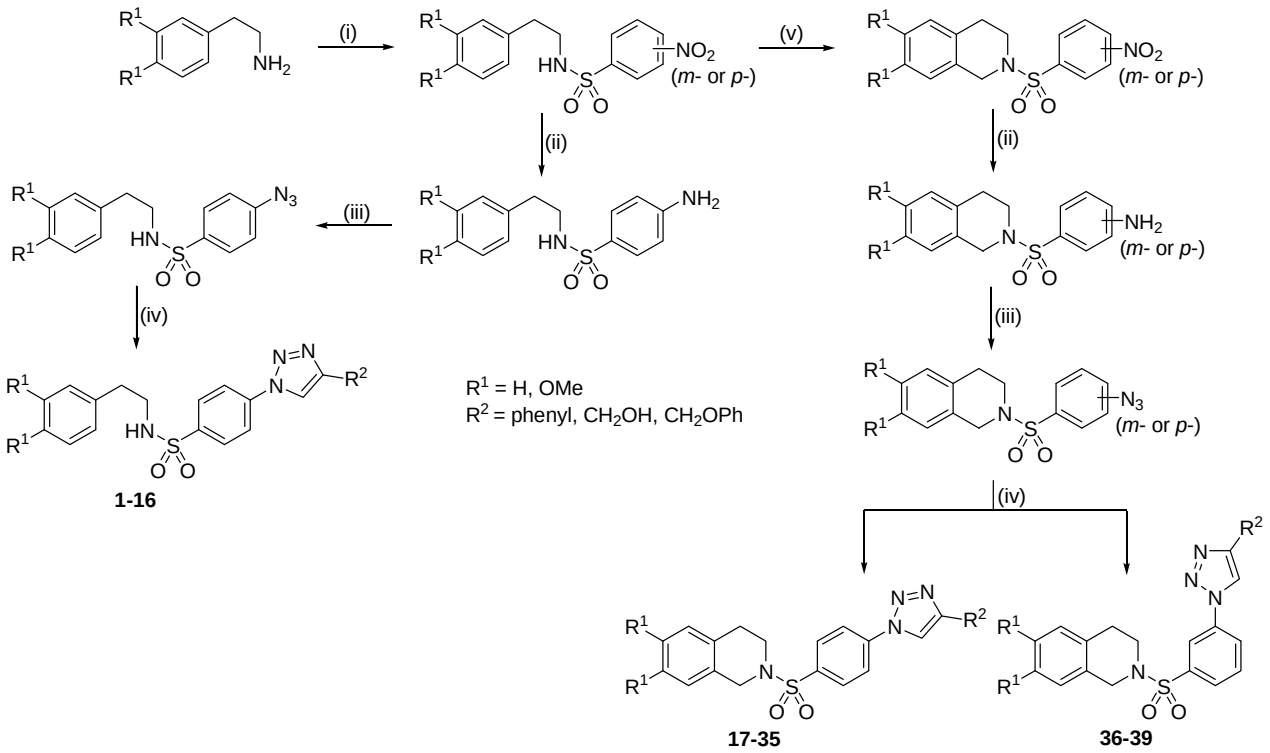

(i) 3- or 4-benzenesulfonyl chloride, Na_2CO_3, CH_2Cl_2, rt; (ii) $SnCl_2 \cdot 2H_2O$, EtOH, reflux ;(iii) $NaNO_2$, HCl/CH_3COOH, 0 ^oC, NaN_3, rt; (iv) ≡—R^2, $CuSO_4 \cdot 5H_2O$, sodium ascorbate, *t*-BuOH/H_2O, rt; (v) $(CH_2O)_n$, HCOOH, reflux

Scheme 3

2.3 Synthesis of chalcone-coumarin hybrids **1-11** was outlined in Scheme 4.

Chalcones were synthesized using the base-catalyzed Claisen-Schmidt condensation of various aromatic aldehydes with two aminoacetophenones (3- or 4-NH_2). Subsequently, azotization reaction of the aminochalcones using sodium nitrite and sodium azide in a mixture of glacial acetic acid and concentrated hydrochloric acid afforded the corresponding azidochalcones. The azide/alkyne dipolar cycloaddition, represented as the Click-type reaction, is the key route to the synthesis of 1,2,3-triazole linkage. Finally, the azides readily underwent cycloaddition with alkynes to afford the novel desired hybrid molecules (**1-11**) in moderate to good yields (50-88%).

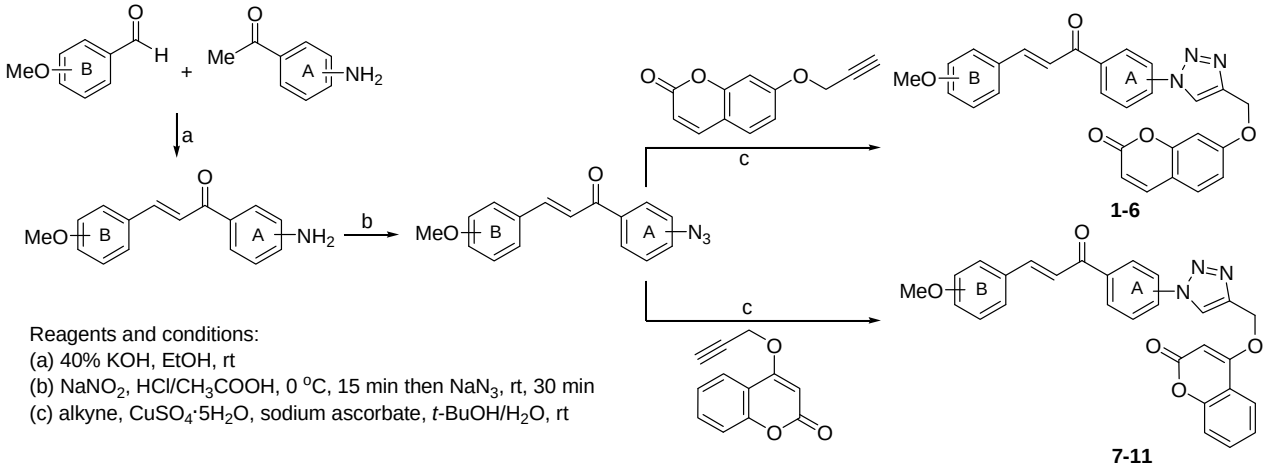

Scheme 4

3. Results

3.1 Cytotoxic activity of mono-indoles (type I), bis-indoles (type II-IV) and tris-indoles (type V)

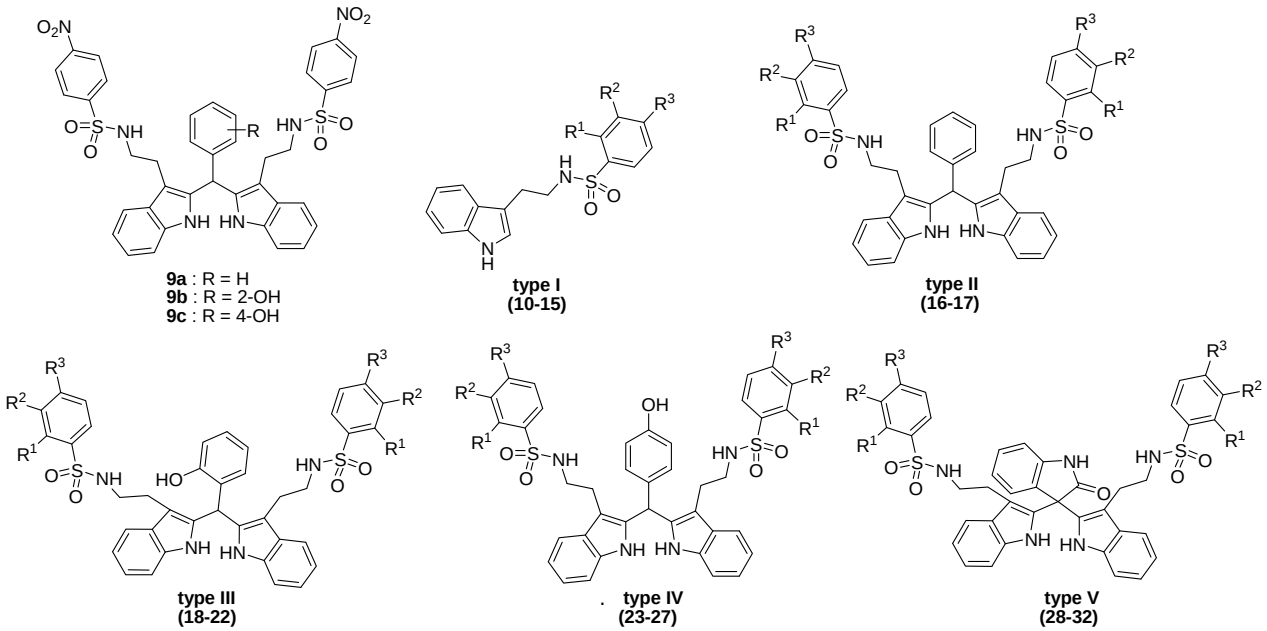

Table 1 Cytotoxic activity of compounds (**10-32**) against four cancer cell lines[a].

Compound	R^1	R^2	R^3	Cytotoxic activity (IC_{50}, μM)[b]			
				HuCCA-1	HepG2	A549	MOLT-3
10	H	H	NO_2	136.09±1.14	95.55±2.82	124.50±1.41	68.91±2.63
11	H	H	Me	128.18±1.53	83.75±4.73	132.00±2.12	50.41±1.69
12	H	H	OMe	134.69±6.36	86.77±2.08	119.55±0.71	50.15±1.41
13	H	H	Cl	Inactive	69.68±2.89	71.68±0.64	46.23±1.65
14	H	NO_2	H	Inactive	99.40±4.04	128.85±4.95	54.38±2.34
15	NO_2	H	H	Inactive	Inactive	Inactive	59.21±3.13
9a[c]	H	H	NO_2	Inactive	Inactive	Inactive	Inactive
16	H	H	Me	Inactive	Inactive	Inactive	Inactive
17	H	H	OMe	Inactive	Inactive	Inactive	Inactive
9b[c]	H	H	NO_2	Inactive	22.23±2.08	Inactive	4.97±0.13
18	H	H	Me	15.69±0.71	11.15±1.44	64.13±1.41	6.94±0.90
19	H	H	OMe	30.72±0.71	18.73±2.08	47.06±2.83	7.35±0.54
20	H	H	Cl	7.75±0.37	8.62±1.04	8.74±0.79	6.06±0.81
21	H	NO_2	H	Inactive	26.00±4.04	Inactive	5.47±0.68
22	NO_2	H	H	61.65±1.41	22.02±3.79	Inactive	9.95±0.82
9c[c]	H	H	NO_2	Inactive	22.02±2.08	Inactive	2.04±0.10
23	H	H	Me	14.33±2.12	9.55±1.73	15.69±0.71	6.30±0.91
24	H	H	OMe	33.99±1.41	13.30±1.44	Inactive	7.22±1.21
25	H	H	Cl	9.69±0.16	9.91±1.04	12.39±0.58	7.13±0.34
26	H	NO_2	H	Inactive	26.00±1.15	Inactive	8.49±1.19
27	NO_2	H	H	20.93±3.76	9.94±1.93	Inactive	5.06±0.56
28	H	H	Me	Inactive	Inactive	Inactive	5.49±0.58
29	H	H	OMe	Inactive	Inactive	Inactive	53.84±8.25
30	H	H	Cl	15.95±0.37	12.52±0.58	Inactive	6.25±0.35
31	H	NO_2	H	Inactive	Inactive	Inactive	31.57±4.71
32	NO_2	H	H	Inactive	Inactive	Inactive	Inactive

Inactive = IC_{50} > 50 μg/mL

[a] Cancer cell lines are comprised of the following: HuCCA-1 Human cholangiocarcinoma cancer cell; HepG2 Human hepatocellular carcinoma cell line; A549 Human lung carcinoma cell line; and MOLT-3 Human lymphoblastic leukemia cell line; [b] The assays were performed in triplicate.; [c] Data from reference (Pingaew R, Prachayasittikul S, Ruchirawat S, Prachayasittikul V. Archives Pharmacal Research 2012; 35: 949-954); [d,e] Etoposide and doxorubicin were used as reference drugs.

3.2 Biological activity of triazole derivatives **1-39**

Table 2 Cytotoxic activity and aromatase inhibitory activity (IC_{50}, μM) of triazoles (**1-39**).

	compound	Cytotoxic activity (IC_{50}, μM)[a]				Aromatase[b]
		HuCCA-1	HepG2	A549	MOLT-3	
1	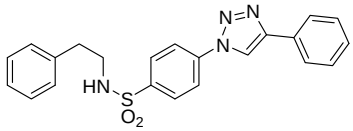	8.65±1.70	9.07±1.15	34.54±0.89	Inactive	Inactive
2	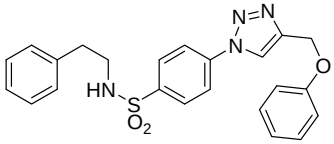	Inactive	57.54±8.66	Inactive	Inactive	9.4±1.6
3	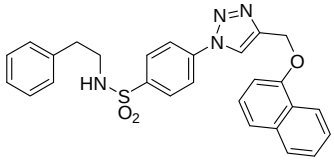	Inactive	Inactive	Inactive	Inactive	3.4±1.5
4	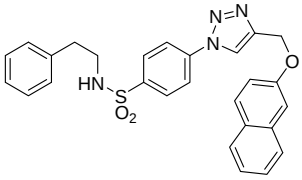	Inactive	28.21±2.89	Inactive	74.23±5.08	1.3±0.4
5	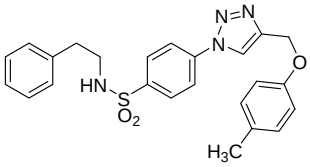	Inactive	81.75±2.89	Inactive	Inactive	8.0±0.2
6	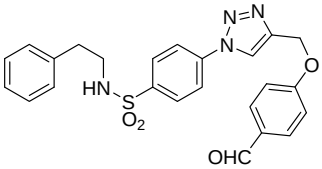	87.89±0.92	100.54±2.12	Inactive	32.02±0.76	7.9±0.7
7	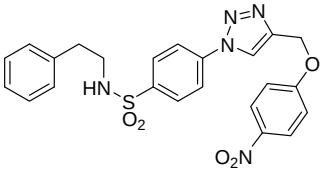	Inactive	Inactive	Inactive	61.42±1.01	2.9±0.1
8	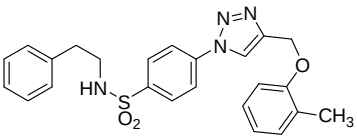	Inactive	41.62±1.15	Inactive	34.24±3.11	3.4±0.1
9	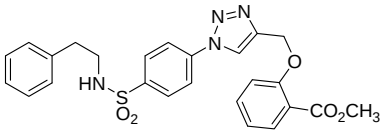	Inactive	49.40±4.04	Inactive	8.81±0.42	-
10	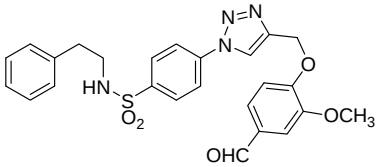	Inactive	57.52±6.51	79.18±14.15	9.22±0.48	-

11	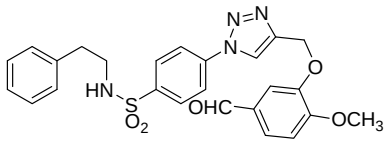	Inactive	34.51±4.36	39.04±0.37	10.33±0.08	-
12	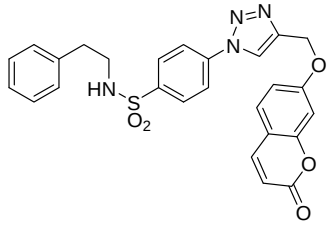	16.12±0.71	12.44±1.71	19.60±2.33	88.97±3.42	Inactive
13	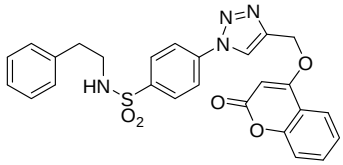	Inactive	Inactive	Inactive	10.65±0.48	1.8±0.5
14	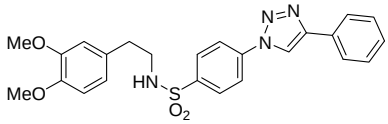	Inactive	23.89±3.00	18.19±0.35	60.99±6.66	4.6±2.0
15	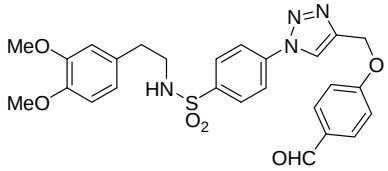	Inactive	Inactive	28.03±1.63	17.43±0.41	-
16	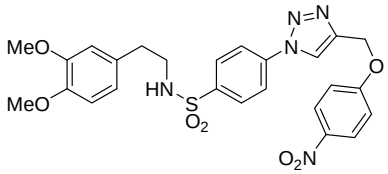	Inactive	Inactive	Inactive	10.10±0.27	2.7±0.1
17	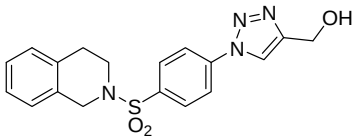	51.35±5.66	Inactive	Inactive	Inactive	-
18	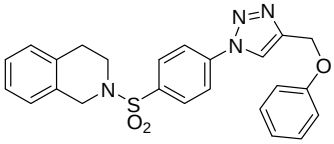	Inactive	6.50±0.14	Inactive	Inactive	-
19	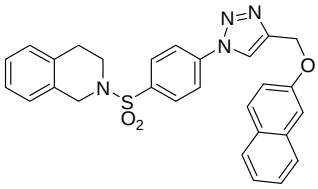	Inactive	60.48±14.14	Inactive	Inactive	-
20	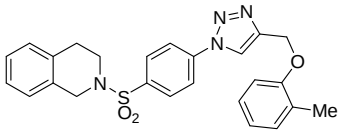	Inactive	Inactive	66.30±0.70	Inactive	-
21	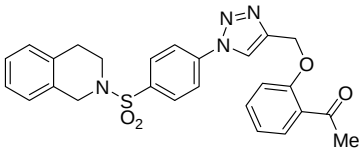	30.16±4.07	19.12±3.06	14.90±1.02	21.86±3.67	Inactive

22	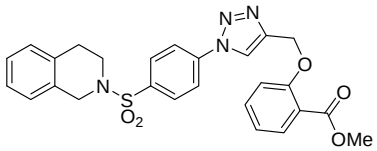	0.63±0.04	12.36±1.97	0.57±0.02	18.63±1.62	-
23	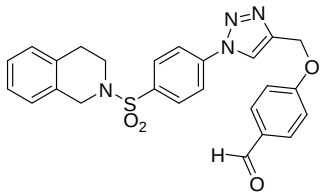	Inactive	5.27±0.71	59.07±11.31	Inactive	-
24	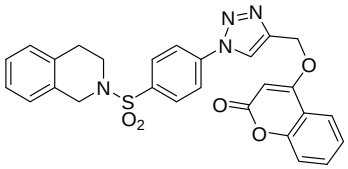	24.80±2.19	Inactive	25.29±10.78	80.78±10.23	Inactive
25	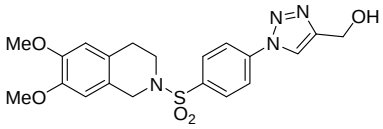	72.0±10.54	31.79±2.89	41.04±9.40	Inactive	-
26	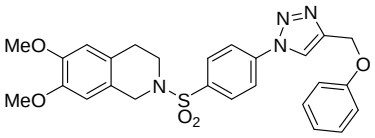	Inactive	2.57±0.99	Inactive	Inactive	-
27	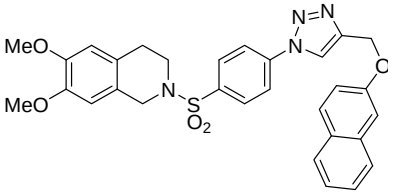	Inactive	1.26±0.42	Inactive	36.35±1.36	-
28	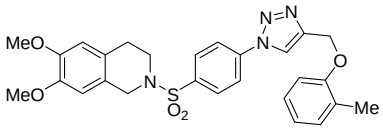	39.71±1.48	1.48±0.61	27.21±1.77	Inactive	Inactive
29	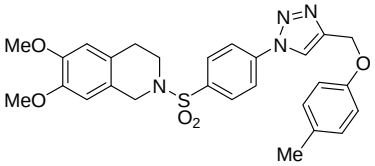	Inactive	0.56±0.01	Inactive	Inactive	-
30	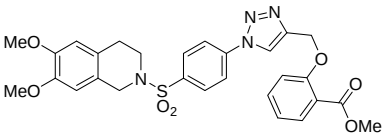	4.79±0.28	3.37±0.96	8.43±2.79	11.74±4.97	-
31	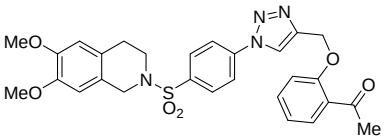	Inactive	Inactive	Inactive	Inactive	Inactive
32	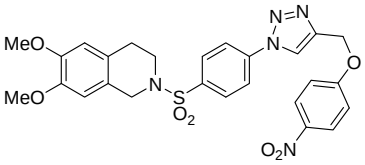	Inactive	Inactive	Inactive	Inactive	Inactive

33	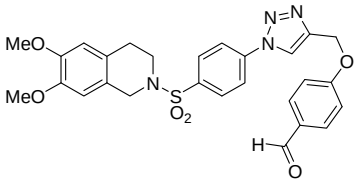	31.09±8.91	12.49±2.47	31.84±8.13	34.12±0.97	-
34	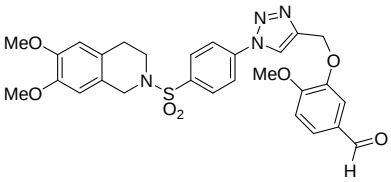	76.15±1.77	41.36±2.89	31.91±9.76	5.82±0.85	Inactive
35	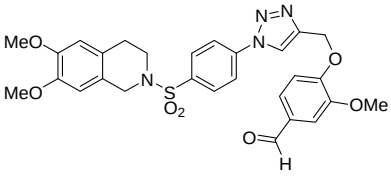	39.98±4.03	Inactive	Inactive	5.50±0.61	-
36	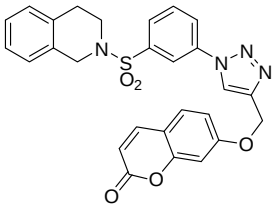	46.88±0.1	22.04±3.21	21.59±5.94	Inactive	-
37	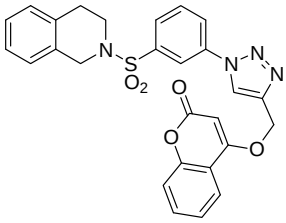	Inactive	Inactive	Inactive	Inactive	Inactive
38	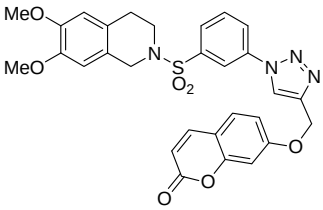	Inactive	36.58±6.56	37.33±0.66	Inactive	0.2±0.1
39	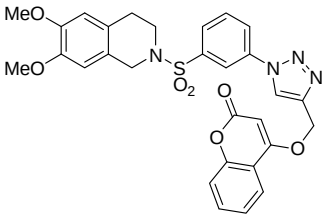	Inactive	7.40±0.35	Inactive	Inactive	1.8±0.2

[a] Inactive = IC_{50} > 50 μg/mL

[b] Inactive = IC_{50} > 12.5 μM

3.3 Biologucal activity of chalcone-coumarin hybrids **1-11**

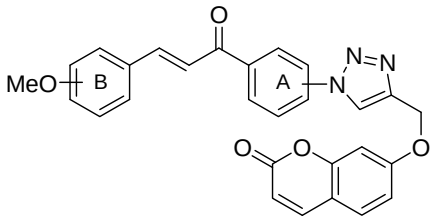

1-6

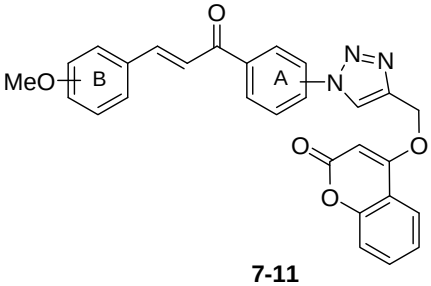

7-11

Table 3 Cytotoxic and antimalarial activities (IC_{50}, μM) of hybrid compounds (**1-11**).

cpd	A-ring	B-ring	Cancer cell lines[a]				Antimalarial[b]	Vero cell line
			HuCCA-1	HepG2	A549	MOLT-3		
1	3-triazole	3,4-diOMe	33.37±0.84	Non-cytotoxic	Non-cytotoxic	3.12±0.11	Inactive	Non-cytotoxic
2	3-triazole	2,3-diOMe	11.13±0.40	15.70±2.00	31.40±1.00	5.16±0.69	6.63	35.03
3	4-triazole	2,3-diOMe	4.81±0.92	8.18±0.76	7.95±3.04	Non-cytotoxic	Inactive	Non-cytotoxic
4	3-triazole	2,3,4-triOMe	Non-cytotoxic	Non-cytotoxic	Non-cytotoxic	3.89±0.28	13.03	Non-cytotoxic
5	4-triazole	2,3,4-triOMe	Non-cytotoxic	Non-cytotoxic	Non-cytotoxic	22.50±3.63	Inactive	Non-cytotoxic
6	4-triazole	3,4,5-triOMe	Non-cytotoxic	Non-cytotoxic	Non-cytotoxic	79.49±1.44	Inactive	Non-cytotoxic
7	3-triazole	3,4-diOMe	38.57±1.48	Non-cytotoxic	Non-cytotoxic	3.91±0.34	Inactive	Non-cytotoxic
8	3-triazole	2,3-diOMe	2.36±0.14	4.26±0.29	18.06±1.07	0.53±0.08	4.73	3.91
9	3-triazole	2,3,4-triOMe	6.13±0.06	Non-cytotoxic	Non-cytotoxic	1.13±0.18	7.47	Non-cytotoxic
10	4-triazole	2,3,4-triOMe	Non-cytotoxic	22.85±0.51	Non-cytotoxic	12.33±1.78	1.60	Non-cytotoxic
11	4-triazole	3,4,5-triOMe	Non-cytotoxic	Non-cytotoxic	Non-cytotoxic	6.58±1.78	Inactive	Non-cytotoxic

Non-cytotoxic = IC_{50} > 50 μg/mL.

Inactive = IC_{50} > 10 μg/mL.

Vero cell line = African green monkey kidney cell line.

[a] Cancer cell lines comprise the following: HuCCA-1 human cholangiocarcinoma cell line, HepG2 human hepatocellular carcinoma cell line, A549 human lung carcinoma cell line, MOLT-3 human lymphoblastic leukemia cell line.

[b] Antimalarial against *Plasmodium falciparum*.

4. Conclusion and Discussion

A variety of mono-, bis- and tris-indole sulfonamide derivatives have been synthesized and evaluated for their cytotoxic activity. Most of the indole analogs with various substituents (R^1-R^3) on the benzene ring of the sulfonamide moiety displayed cytotoxicity against MOLT-3 cell lines. Significantly, bis-indoles containing phenolic groups and chloro tris-indole showed higher anticancer activity against HepG2 cell than the control drug, etoposide. The phenolic bis-indoles seem to be the most important core structures responsible for strong antiproliferative activity observed in all of the tested cancer cell lines. In addition, a series of 1,2,3-triazole-based sulfonamides have been synthesized using the Click reaction as a key step. Their aromatase inhibitory activities were explored. It was observed that most open-chain sulfonamide triazoles exerted aromatase inhibitory activity (IC_{50} = 1.3-9.4 μM). The triazoles containing 6,7-dimethoxy substituents (R^1) on the THIQ core, and coumarinyloxymethyl (R^2) on the triazole ring; and *m*-substitution of sulfonyl group and triazole ring on the phenyl moiety of sulfonamide displayed potent activity. Furthermore, eleven conjugated molecules derived from chalcones and coumarins linked by 1,2,3-triazole ring have been successfully synthesized *via* the Click reaction. Cytotoxic activity testing revealed that most of the hybrids displayed cytotoxicity against MOLT-3 cell line.

5. Output (Acknowledge the Thailand Research Fund)

5.1 International Journal Publication (* corresponding author)

1. **Pingaew R**,* Prachayasittikul V, Mandi P, Nantasenamat C, Prachayasittikul S, Ruchirawat S, Prachayasittikul V.* Synthesis and molecular docking of 1,2,3-triazole-based sulfonamides as aromatase inhibitors. *Bioorganic & Medicinal Chemistry* 2015; In Press. (Impact factor = 2.951)

2. **Pingaew R**,* Saekee A, Mandi P, Nantasenamat C, Prachayasittikul S, Ruchirawat S, Prachayasittikul V. Synthesis, biological evaluation and molecular docking of novel chalcone-coumarin hybrids as anticancer and antimalarial agents. *European Journal of Medicinal Chemistry* 2014; 85: 65-76. (Impact factor = 3.432) *Featured in ScienceDirect, Ranked 3rd and Ranked 6th in Top 25 Hottest Articles in European Journal of Medicinal Chemistry (3rd quarter of 2014 and 4th quarter of 2014)*

3. **Pingaew R**,* Mandi P, Nantasenamat C, Prachayasittikul S, Ruchirawat S, Prachayasittikul V. Design, synthesis and molecular docking studies of novel *N*-benzenesulfonyl-1,2,3,4-tetrahydroisoquinoline-based triazoles with potential anticancer activity. *European Journal of Medicinal Chemistry* 2014; 81: 192-203. (Impact factor = 3.432)

4. **Pingaew R**,* Prachayasittikul S, Ruchirawat S, Prachayasittikul V. Synthesis and cytotoxicity of novel 4-(4-(substituted)-1*H*-1,2,3-triazol-1-yl)-*N*-phenethylbenzenesulfonamides. *Medicinal Chemistry Research* 2014; 23: 1768-1780. (Impact factor = 1.612)

5. **Pingaew R**,* Prachayasittikul S, Ruchirawat S, Prachayasittikul V. Synthesis and structure–activity relationship of mono-indole-, bis-indole-, and tris-indole-based sulfonamides as potential anticancer agents. *Molecular Diversity* 2013; 17: 595-604. (Impact factor = 2.544)

5.2 Application (Award)

1. Asian CORE Program (ACP) Lectureship Award to China, presented at the 9th International Conference on Cutting-Edge Organic Chemistry in Asia (ICCEOCA-9), Malaysia (1-4 December 2014)

5.3 Others e.g. national journal publication, proceeding, international conference, book chapter, patent

1. **Pingaew R**, Mandi P, Nantasenamat C, Prachayasittikul S, Ruchirawat S, Prachayasittikul V. “Design, synthesis and molecular docking of novel tetrahydroisoquinoline-triazole hybrids as potential anticancer agents” The 9th International Conference on Cutting-Edge Organic Chemistry in Asia (ICCEOCA-9)/5th New phase International Conference on Cutting-Edge Organic Chemistry in Asia (NICCEOCA-5), 1-4 December 2014, Malaysia.

Bioorganic & Medicinal Chemistry xxx (2015) xxx–xxx

Contents lists available at ScienceDirect

Bioorganic & Medicinal Chemistry

journal homepage: www.elsevier.com/locate/bmc

Synthesis and molecular docking of 1,2,3-triazole-based sulfonamides as aromatase inhibitors

Ratchanok Pingaew [a,*], Veda Prachayasittikul [b], Prasit Mandi [b,c], Chanin Nantasenamat [b,c], Supaluk Prachayasittikul [c], Somsak Ruchirawat [d,e], Virapong Prachayasittikul [b,*]

[a] Department of Chemistry, Faculty of Science, Srinakharinwirot University, Bangkok 10110, Thailand
[b] Department of Clinical Microbiology and Applied Technology, Faculty of Medical Technology, Mahidol University, Bangkok 10700, Thailand
[c] Center of Data Mining and Biomedical Informatics, Faculty of Medical Technology, Mahidol University, Bangkok 10700, Thailand
[d] Laboratory of Medicinal Chemistry, Chulabhorn Research Institute, and Program in Chemical Biology, Chulabhorn Graduate Institute, Bangkok 10210, Thailand
[e] Center of Excellence on Environmental Health and Toxicology, Commission on Higher Education (CHE), Ministry of Education, Thailand

ARTICLE INFO

Article history:
Received 12 February 2015
Revised 9 April 2015
Accepted 10 April 2015
Available online xxxx

Keywords:
Triazole
Sulfonamide
Tetrahydroisoquinoline
Anti-aromatase activity
Structure–activity relationships
Molecular docking

ABSTRACT

A series of 1,4-disubstituted-1,2,3-triazoles (**13**–**35**) containing sulfonamide moiety were synthesized and evaluated for their aromatase inhibitory effects. Most triazoles with open-chain sulfonamide showed significant aromatase inhibitory activity (IC_{50} = 1.3–9.4 μM). Interestingly, the *meta* analog of triazole-benzene-sulfonamide (**34**) bearing 6,7-dimethoxy substituents on the isoquinoline ring displayed the most potent aromatase inhibitory activity (IC_{50} = 0.2 μM) without affecting normal cell. Molecular docking of these triazoles against aromatase revealed that the compounds could snugly occupy the active site of the enzyme through hydrophobic, π–π stacking, and hydrogen bonding interactions. The potent compound **34** was able to form hydrogen bonds with Met374 and Ser478 which were suggested to be the essential residues for the promising inhibition. The study provides compound **34** as a potential lead molecule of anti-aromatase agent for further development.

© 2015 Elsevier Ltd. All rights reserved.

1. Introduction

Breast cancer is one of the leading causes of cancer-related mortality among women worldwide from different age groups. The vast majority of breast cancers in postmenopausal women are deriving from estrogens production.[1–3] Estrogens are biosynthesized from androgens catalyzed by aromatase (CYP19), an enzyme belonging to the P450 family of monooxygenase heme proteins. Two main strategies to control or block breast cancer progression include binding of the estrogen receptors (ERs) with receptor antagonists (ERAs such as tamoxifen), and inhibiting the production of estrogen with aromatase inhibitors (AIs).[3] AIs were found to have less side effects than ERAs owing to the the lack of estrogenic activity on uterus and vasculature.[3]

Triazoles are common pharmacophore found in a diverse range of biologically active molecules due to their potential structural features (i.e., capability of hydrogen bonding, stable to metabolic degradation and less undesired effects).[4] Among the AIs, letrozole (**1**) and anastrozole (**2**), both containing 1,2,4-triazole ring, were approved by the Food and Drug Administration (FDA) and using as the first-line therapy in the treatment of breast cancer in postmenopausal women since they have been shown to be superior to tamoxifen.[3] Based on the AIs, the triazole ring plays a pivotal role in chelation with heme iron.[5] Along the line, Touaibia group has studied on an aromatase inhibitory activity of various substituted-1,2,3-triazole letrozole-based analogs.[6] The results revealed that 1,2,3-trizole (**3**) analog of letrozole showed equipotent activity to the parent compound. In addition, the 1,4-disubstituted-1,2,3-triazole (**4**) was shown to be the most potent compound (IC_{50} = 1.36 μM) among the tested 1,4-disubstituted-1,2,3-triazole series. Aromatase inhibitors **1**–**4** are shown in Figure 1. However, the interaction mode of the 1,4-disubstituted-1,2,3-triazole series with the target enzyme remains to be explored.

Recently, 1,4-disubstituted-1,2,3-triazoles bearing 1,2,3,4-tetrahydroisoquinoline (THIQ) and its open-chain derivatives **5** (Fig. 2) with cytotoxic activity against four cancer cell lines (e.g., HuCCA-1, HepG2, A549 and MOLT-3) have been reported by our group.[7,8] Based on the molecular docking study, an aldoketo reductase 1C3 (AKR1C3) has been identified to be a plausible target responsible for anticancer activity of the THIQ analogs.[8]

* Corresponding authors. Tel.: +66 2 649 5000x18253; fax: +66 2 260 0128 (R.P.); tel.: +66 2 441 4376; fax: +66 2 441 4380 (V.P.).
E-mail addresses: ratchanok@swu.ac.th (R. Pingaew), virapong.pra@mahidol.ac.th (V. Prachayasittikul).

http://dx.doi.org/10.1016/j.bmc.2015.04.036
0968-0896/© 2015 Elsevier Ltd. All rights reserved.

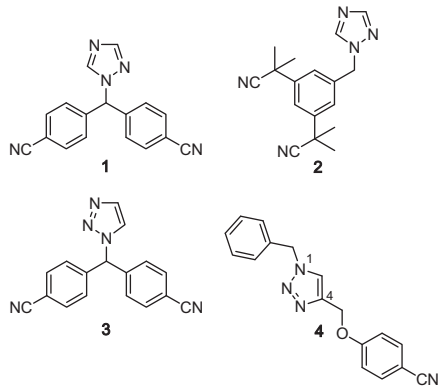

Figure 1. Aromatase inhibitors containing triazole **1**–**4**.

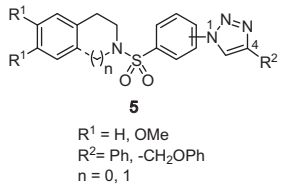

Figure 2. Cytotoxic agents containing triazole **5**.

In general, two structural features of the aromatase active site associate with highly hydrophobic and H-bonding interactions.[9] Therefore, to design and seek for a novel class of aromatase inhibitor, many in-house 1,2,3-triazoles (series I and II) and four novel 1,2,3-triazoles of THIQ (series III) were synthesized through the Click reaction, and evaluated for their aromatase inhibitory effects. Herein, the molecules of rational designed inhibitors (Fig. 2) bearing THIQ, benzene, naphthalene and coumarin rings might be anticipated in forming hydrophobic interaction. In addition, various functional groups of the designed compounds such as sulfonamide, triazole, ether and carbonyl moieties would participate in hydrogen bonding formation. Moreover, molecular docking of the synthesized compounds against the aromatase was also performed to give insights into their binding modes governing the investigated aromatase inhibitory activities.

2. Results and discussion

2.1. Chemistry

The synthesis of triazoles (e.g., types I and II) has been previously reported by our group.[7,8] The open chain THIQ analogs of triazoles **13**–**24** (type I) were prepared through a sequential sulfonation/reduction/diazotization/cycloaddition reactions (route a; steps i–iv) as outlined in Scheme 1. In the same manner, the synthesis of triazoles type II **25**–**31** and type III **32**–**35** was carried out via route b (steps i–v) in which an additional step (i.e., step v) was performed using the Pictet–Spengler reaction to form isoquinoline ring (**10**) prior to steps ii–iv.

Structures of the novel 1,2,3-triazoles **32**–**35** were confirmed based on their ^{1}H NMR, ^{13}C NMR, HRMS and IR spectra. For instance the triazole **34**, its ^{1}H NMR spectra revealed two triplets at δ 2.86 and 3.47 ppm which were assigned to the methylene protons of C4- and C3-THIQ, respectively. The methylene protons at C1-THIQ ring appeared as a singlet at δ 4.31 ppm whereas two methoxy protons at C6- and C7-positions of the THIQ part were noted as a singlet at δ 3.83 ppm. In addition, the methylene protons of –CH_2O– group were found to be displayed as a singlet at δ 5.39 ppm. Aromatic protons of THIQ ring (H-5 and H-8) displayed as two singlets at δ 6.54 ppm and 6.56 ppm. Two methine protons of coumarin ring appeared as a multiplet at δ 6.92–6.98 (H-6 and H-8). The rest of three methine protons of coumarin moiety were observed as three doublets at δ 6.30 (J = 9.5 Hz), δ 7.39 (J = 9.2 Hz) and δ 7.63 (J = 9.5 Hz) ppm, which were assigned to methine protons of C3, C5 and C4, respectively. A triplet at δ 7.70 ppm (J = 8.0 Hz), two doublets at δ 7.87 (J = 7.8 Hz) and 7.99 ppm (J = 7.6 Hz) and a singlet at δ 8.17 ppm were attributed

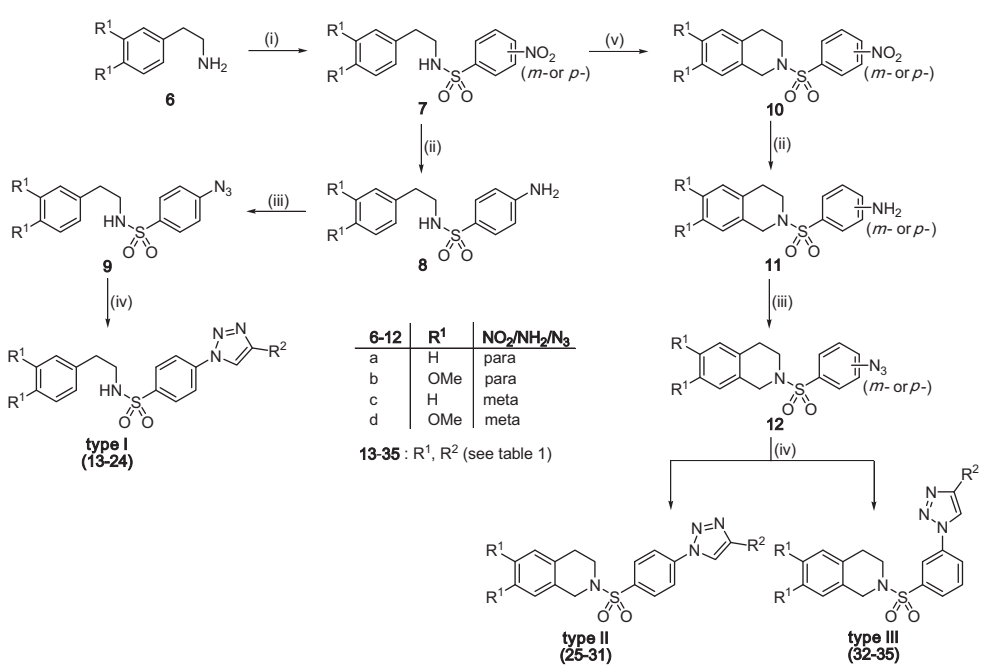

6-12	R^1	$NO_2/NH_2/N_3$
a	H	para
b	OMe	para
c	H	meta
d	OMe	meta

Scheme 1. Synthesis of 1,2,3-triazole-based sulfonamides **13**–**35** through the Click reaction. Reagents and conditions: (i) 3- or 4-benzenesulfonyl chloride, Na_2CO_3, CH_2Cl_2, rt; (ii) $SnCl_2{\cdot}2H_2O$, EtOH, reflux; (iii) $NaNO_2$, HCl/CH_3COOH, 0 °C, NaN_3, rt; (iv) ≡–R^2, $CuSO_4{\cdot}5H_2O$, sodium ascorbate, t-BuOH/H_2O, rt; (v) $(CH_2O)_n$, HCOOH, reflux; route a = steps i–iv; route b = steps i–v.

to four aromatic protons of benzenesulfonyl moiety. A singlet of a methine proton of the triazole ring appeared down field chemical shift at δ 8.13 ppm.

In the ^{13}C NMR spectra, three methylene carbons (C1, C3 and C4) of THIQ ring were visible at δ 28.2, 43.8 and 47.2 ppm whereas a methylene carbon of $-CH_2O-$ group was observed at δ 62.2 ppm. Two methoxy carbons (at C6 and C7) of THIQ ring were noted at 55.9 and 56.0 ppm. Two tertiary aromatic carbons of THIQ ring appeared at chemical shift 109.0 (C8) and 111.5 ppm (C5), and C5 of triazole ring was observed at δ 121.2 ppm. Five tertiary carbons (C3, C4, C5, C6 and C8) of coumarin ring were seen at chemical shift 102.2, 112.7, 113.7, 129.0 and 143.2 ppm. The rest of tertiary aromatic carbons of phenyl ring were noted at chemical shift 119.4, 124.4, 127.6 and 130.8 ppm. Four quaternary aromatic carbons (C4a, C8a, C6 and C7) of THIQ ring resonated at corresponding chemical shift 122.9, 124.8, 147.9 and 148.1 ppm, and C4 of triazole ring was observed at δ 144.5 ppm. Two quaternary aromatic carbons (C1 and C7) of phenyl ring were appeared at chemical shift 137.3 and 139.4 ppm whereas three quaternary aromatic carbons (C4a, C8a, C7) and one carbonyl carbon (C2) were observed at chemical shift 113.2, 155.8, 160.9 and 161.1 ppm.

The HRMS-TOF experiment showed molecular ion $[M+H]^+$ peak at 575.1589 corresponding to the molecular formula of $C_{29}H_{27}N_4O_7S$. The IR spectra exhibited the vibration absorption bands of C=O group at 1723 cm^{-1} and S=O moiety at 1347 and 1163 cm^{-1}.

2.2. Biological activity

A series of 1,2,3-triazole-based sulfonamides types I–III (**13**–**35**), bearing disubstituents at position 1 (phenyl sulfonamide) and position 4 (R^2), were evaluated for their aromatase inhibitory activities. All tested triazoles had inhibition effect at 12.5 μM in the range of 14–97% (data not shown), except for compound **32** (could not be evaluated due to its insolubility in the assay). The triazoles type I (**14**–**20**, **22**–**24**) and type III (**34** and **35**) with inhibition >50% were further explored to determine their IC_{50} values as summarized in Table 1. The derivatives with the inhibition ⩽50% were identified as inactive compound (IC_{50} >12.5 μM). Ketoconazole (IC_{50} = 2.6 μM) and letrozole (IC_{50} = 3.3 nM) were used as the reference drugs.

Results showed that sulfonamide substituents as open-chain (type I) and restricted-THIQ analogs on the phenyl ring (types II and III); and R^2 substituents as phenyl, phenoxymethyl, naphthalene oxymethyl and coumarin oxymethyl on the triazole core play crucial roles in governing their anti-aromatase activities. Obviously, most of the triazoles in types I and III displayed aromatase inhibition activity (IC_{50} = 0.2–9.4 μM) whereas the triazoles in type II were shown to be inactive (IC_{50} >12.5 μM). Structure–activity relationship (SAR) studies of the tested compounds are discussed hereafter.

No significant inhibition effect was observed for triazole **13** (R^2 = phenyl substituent); however, triazoles bearing R^2 as phenoxymethyls (**14**–**18**) displayed the inhibition effect with IC_{50} values in the range of 2.9–9.4 μM. Among these compounds, 4-nitrophenoxymethyl (R^2) analog **17** (IC_{50} = 2.9 μM) exerted the highest activity having comparable IC_{50} value with that of the ketoconazole (IC_{50} = 2.6 μM). When the phenyl group of compound **14** was replaced with naphthalenyl rings as found in compounds **19** and **20**, and with a 4-coumarinyl ring as found in compound **22**, the enhanced inhibitory potency was observed. In comparison between 4-coumarinyl of open-chain (**22**) and restricted THIQ (**26**) analogs (R^1 = H), the activity was noted for compound **22** (IC_{50} = 1.8 μM) but not for compound **26** (IC_{50} >12.5 μM). Apparently, the triazoles **20** and **22** exerted inhibition activity higher than that of the ketoconazole. On the other hand, the triazole was substituted with 7-coumarinoxymethyl substituent (R^2) led to the compound **21** with loss of the activity as compared to the 4-coumarinyl group of compound **22** (IC_{50} = 1.8 μM). Inhibition potency was distinctively appeared as noted in compound **23** (IC_{50} = 4.6 μM) when dimethoxy groups (R^1) were introduced to 3,4-positions on phenethyl moiety of analog **13** (R^1 = H, IC_{50} >12.5 μM). However, no aromatase inhibition was observed for triazole type II (**25**–**31**) containing R^1 = H and OMe on the THIQ. Both triazole types I and II constituting sulfonyl group at *para* position on phenyl ring, anti-aromatase activity was observed for type I compounds, except for compounds **13** and **21** (IC_{50} >12.5 μM). Surprisingly, when the sulfonyl group on the phenyl ring was moved to *meta* position, the activity of compounds was remarkably manifested. Promisingly, 7-coumarinyl analog **34** (R^1 = OMe) was shown to be the most potent compound with IC_{50} value of 0.2 μM. Potent activity was also found in dimethoxy THIQ of 4-coumarinyl analog **35** (R^1 = OMe, IC_{50} 1.8 μM). However, without 6,7-dimethoxy groups on the THIQ ring, 4-coumarinyl analog **33** (R^1 = H) was shown to be an inactive aromatase inhibitor.

The SAR results imply that lipophilic effect of dimethoxy groups (R^1) enhances the activity of triazoles type I and type III. Our results are in-line with earlier studies, in which the lipophilicity is responsible for high aromatase inhibition of xanthone[10] and coumarin[11] derivatives. Even with or without dimethoxy groups, the triazoles type II with restricted THIQ were shown to be inactive compounds. This could be possibly due to their structural features, that is, flexible or rigid conformation, isomeric effect and binding interaction with the target site of action. Therefore, the aid of molecular docking may provide insight into their mechanism of action.

To determine the safety index, these compounds were also tested against the noncancerous (Vero) cell line derived from African green monkey kidney (Table 1). It was found that the potent analogs (**14**–**20**, **22**–**24**, **34** and **35**) were non-cytotoxic toward normal cell, except for compound **35**. However, the triazole **35** had high safety index with a selective index value of 48.

2.3. Molecular docking

Molecular docking of triazoles **13**–**35** to the aromatase enzyme was performed to investigate their binding modes. The most potent compound **34** (Fig. 3) was able to form hydrogen bonds with Met374 and Ser478 using the sulfonyl oxygen (bond distance = 2.3 Å) and the oxycoumarinyl group (bond distance = 2.0 Å), respectively. The 2D ligand–protein interaction map of the co-crystallized ligand ASD (Fig. S1) displayed hydrophobic interaction involving steroidal backbone with amino acids residues (i.e., Ile133, Phe134, Trp224 and Leu477), and hydrogen bonding of the CO group at position 17 with the amino group of Met374.

Interestingly, isomeric coumarinyl and naphthalenyl triazoles play crucial roles in exerting more potent aromatase inhibitory activity than other tested compounds. This could be attributed to their binding interactions with the aromatase enzyme. Docking results (Figs. S2 and S3) of 4-coumarinyl triazoles (**22** and **35**) with the same potency (IC_{50} = 1.8 μM) showed that compound **22** occupied the binding cavity in a more straight extended form when compared with that of compound **35**. The binding of compound **22** (Fig. S2) facilitated hydrophobic interaction of phenethyl phenylsulfonamide moiety with Ile133, Val370, Ser478, Thr310 and Trp224 along with the interaction of 4-coumarinyl ring with Phe221; π–π stacking interaction of triazole and 4-coumarinyl rings with Phe221; and hydrogen bonding of coumarin-2-one with the amino group of Arg192. Docking of triazole **35** (Fig. S3) involves hydrophobic interactions of dimethoxy THIQ with Ile133, of sulfonyl phenyl with Asp309 and Thr310 as well as of the

Table 1
Aromatase inhibitory activity and cytotoxic activity (IC_{50}, μM) of triazoles (**13**–**35**)

Series	Compound	R^1	R^2	Inhibitory activity (aromatase)	Cytotoxic activity (Vero cell line)	Selective index[a]
I	**13**	H		>12.5	Non-cytotoxic	–
	14	H	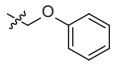	9.4 ± 1.6	Non-cytotoxic	>12.24
	15	H	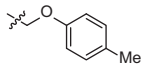	8.0 ± 0.2	Non-cytotoxic	>13.93
	16	H	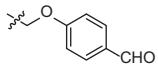	7.9 ± 0.7	Non-cytotoxic	>13.68
	17	H	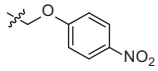	2.9 ± 0.1	Non-cytotoxic	>35.96
	18	H	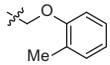	3.4 ± 0.1	Non-cytotoxic	>32.79
	19	H	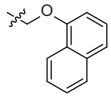	3.4 ± 1.5	Non-cytotoxic	>30.35
	20	H	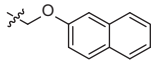	1.3 ± 0.4	Non-cytotoxic	>79.37
	21	H	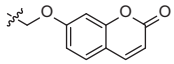	>12.5	Non-cytotoxic	–
	22	H	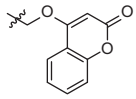	1.8 ± 0.5	Non-cytotoxic	>55.27
	23	OMe		4.6 ± 2.0	Non-cytotoxic	>23.40
	24	OMe	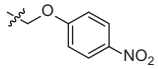	2.7 ± 0.1	Non-cytotoxic	>34.32
II	**25**	H	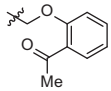	>12.5	Non-cytotoxic[b]	–
	26	H	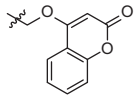	>12.5	28.58[b]	–
	27	OMe	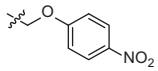	>12.5	Non-cytotoxic[b]	–
	28	OMe	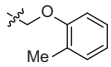	>12.5	Non-cytotoxic[b]	–
	29	OMe	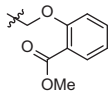	>12.5	2.82[b]	–
	30	OMe	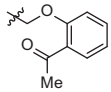	>12.5	37.23[b]	–
	31	OMe	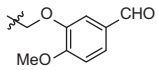	>12.5	Non-cytotoxic[b]	–
III	**32**	H	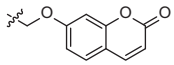	–[c]	91.54	–
	33	H	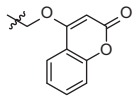	>12.5	Non-cytotoxic	–
	34	OMe	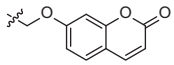	0.2 ± 0.1	Non-cytotoxic	>435.09

Table 1 (*continued*)

Series	Compound	R^1	R^2	Inhibitory activity (aromatase)	Cytotoxic activity (Vero cell line)	Selective index[a]
	35	OMe	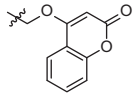	1.8 ± 0.2	86.32	47.96
Ketoconazole[d]				2.6 ± 0.7	–	–
Letrozole[d]				0.0033 ± 0.0004	–	–
Ellipticine[d]				–	1.94	–

Vero cell line = African green monkey kidney cell line.
Non-cytotoxic = IC_{50} >50 μg/mL.
[a] Selective index = IC_{50} for Vero cells/IC_{50} for aromatase.
[b] Data from reference number 8.
[c] Insoluble in testing medium
[d] Ketoconazole, letrozole and ellipticine were used as reference drugs.

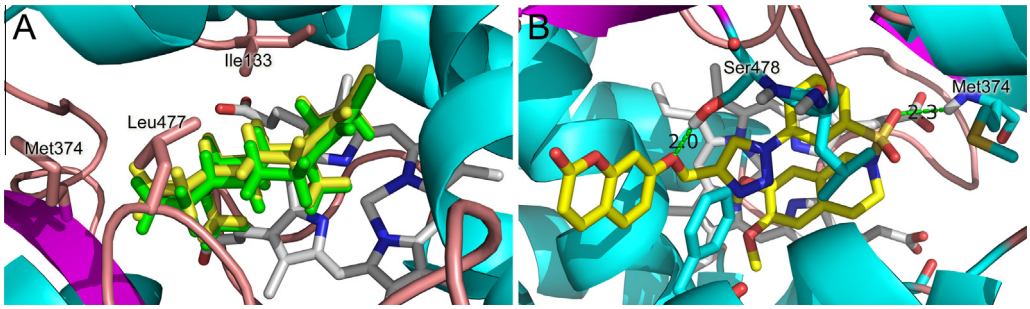

Figure 3. Molecular docking of 1,2,3-triazole sulfonamides to aromatase enzyme. Redocking of co-crystallized androstenedione (ASD) yielded RMSD of 0.711 Å (A). Docking pose of the most potent compound **34** (B) is shown where green dashed lines indicate distances of hydrogen bonds.

4-coumarinyl ring with Phe221 and His480. This molecular arrangement induced π–π stacking of phenylsulfonyl, triazole and 4-coumarinyl rings with Phe221; and hydrogen bonding of triazole (N3 position) with Ser478, and oxycoumarinyl moiety with Arg192. Such interactions involve molecules in the bent form (**35**), which arises from *m*-substitution of the sulfonyl group and triazole ring on the phenyl ring of sulfonamide. The results suggested that the Ser478 and Arg192 residues were essential for the inhibition of aromatase. It should be noted that both Ser478 and Arg192 played crucial roles in anti-aromatase activity of the natural substrate ASD.[9] Accordingly, such amino acids participated in a water-mediated network of hydrogen bonding, thereby allowing the interaction between the aromatase and the C3-keto oxygen of androstenedione to undergo enolization.[9] Furthermore, Ser478 was capable of promoting the aromatase inhibition confirmed by the mutagenesis study.[12] In addition, such amino acid was the residue responsible for the inhibition and selectivity.[13,14]

The triazole **26** (Fig. S4), a restricted THIQ analog of **22**, similarly showed hydrophobic and π–π stacking interactions with the aromatase. The triazole **21** (Fig. S5), an isomeric analog of **22**, showed that both terminal ends (phenethyl and 7-coumarinyl) could interact with the hydrophobic pockets. However, no hydrogen bonding with Arg192 was noted for compounds **26** and **21**. This could likely result in the absence of inhibitory activity for the compounds **26** and **21** (IC_{50} >12.5 μM) as compared to that of compound **22** (IC_{50} 1.8 μM).

Comparison of THIQs with 4-coumarinyl moiety **33** (R^1 = H, Fig. S6) and **35** (R^1 = OMe, Fig. S3) revealed that both compounds displayed similar hydrophobic and hydrogen bonding interactions with the binding pockets of the aromatase. It was observed that lipophilic dimethoxy groups were essential for the interaction of compound **35** with Ile133 in exerting its activity (IC_{50} = 1.8 μM) while compound **33** without dimethoxy groups was shown to be an inactive compound (IC_{50} >12.5 μM).

Considering the most potent dimethoxy THIQ bearing 7-coumarinyl analog **34** (Fig. 4), additional hydrophobic interactions with Val370, Ser478, Leu477 and Trp224 were observed as compared to compound **35** (Fig. S3). Furthermore, the compound **34** was arranged in such a way to appropriately form hydrogen bonding of the sulfonyl group with the amino group of Met374 as well as hydrogen bonding of oxycoumarinyl moiety with Ser478. These hydrophobic and hydrogen bonding interactions were suggested to play pertinent roles contributing to the most potent activity of

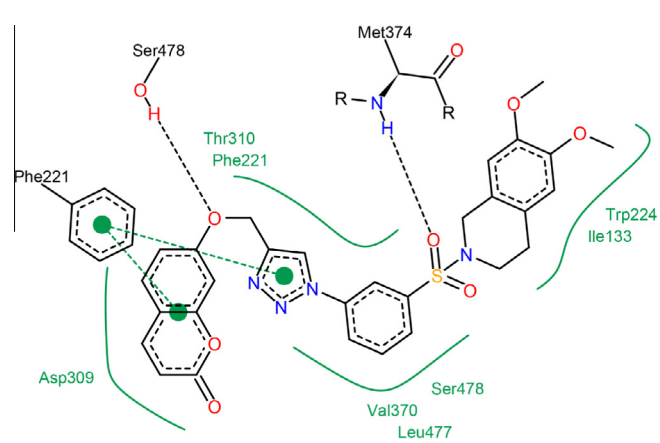

Figure 4. 2D-ligand–protein interaction scheme of compound **34**.

compound **34** (IC_{50} = 0.2 μM). Importantly, Leu477 and Trp224 were the same hydrophobic residues interacting with steroidal skeleton of ASD (Fig. S1). The H-bonding formations with Ser478 and Met374 (bond distance = 3.11 and 2.31 Å) were also noted in the antiestrogenic letrozole in which it used two benzonitrile groups to form such interactions.[15] However, the compound **34** showed lower potency than letrozole. This may be due to the lack of chelation with heme iron. Notably, the Met374 played a crucial role in anti-aromatase activity of the natural substrate ASD through H-bonding interaction with the C17-keto oxygen.[9] In addition, Met374 and/or Ser478 were suggested to be the crucial residues found in many classes of aromatase inhibitors such as coumarin,[11] acridone,[13] xanthone[14] and flavonoids.[16,17]

Unfortunately, 7-coumarinyl analog **32** (R^1 = H) was not tested for the activity due to its insolubility in the testing system. Therefore, the activity of 7-coumarinyl **32** cannot be compared with 7-coumarinyl **34** (R^1 = OMe, Fig. 4). However, the 2D ligand–protein interaction of **32** (Fig. S7) showed hydrophobic and π–π stacking interactions but without hydrogen bond forming.

In addition, the analysis of triazole type I analog of naphthalenyl (R^2), particularly the highly potent 2-naphthalenyl compound **20** (Fig. S8), was found to be in the extended form when occupying the binding site via hydrophobic interaction of phenethyl with Ile133, Val370 and Thr310, phenyl sulfonyl with Leu477 and Ser478 as well as 2-naphthalenyl with Phe221, Asp309 and His480; through π–π stacking of triazole and naphthalenyl rings with Phe221; and hydrogen bonding of oxy-naphthalenyl moiety with Ser478. On the other hand, the less extended form of 1-naphthalenyl compound **19** (Fig. S9) showed hydrophobic interaction of phenethyl phenyltriazole with Ile133, Thr310, Phe221, Ser478 and Asp309 as well as 1-naphthalenyl ring with Gln218; π–π stacking of triazole and 1-naphthalenyl rings with Phe221; but no hydrogen bonding was observed. The results implied that the presence of H-bonding interaction with Ser478 contributed to the better activity of compound **20** (IC_{50} = 1.3 μM) over compound **19** (IC_{50} = 3.4 μM).

Taken together, the molecular requirements for the most potent triazole inhibitor (**34**) included the restricted THIQ with 6,7-dimethoxy groups (R^1), 7-coumaryloxymethyl (R^2) at position 4 of the triazole ring, and *m*-substitution of triazole and sulfonyl moieties on the phenyl ring. Such structural features were essential for engaging in hydrophobic, π–π stacking and H-bonding interactions with the aromatase enzyme, particularly, hydrogen bond forming with Met374 and Ser478. Obviously, triazole **34** was the only compound that engaged in the hydrogen bonding interactions. In comparison with letrozole and ASD, the sulfoyl and coumarinyl ether moieties of compound **34** could act as hydrogen bond acceptors to mimic the benzonitrile groups of the letrozole whereas mimicking the steroidal backbone and the C17-keto oxygen of ASD was responsible by the hydrophobic moieties (6,7-dimethoxy THIQ and phenyl rings) and the sulfonyl oxygen of compound **34**, respectively.

3. Conclusions

A series of 1,2,3-triazole-based sulfonamides (**13**–**35**) have been synthesized using the Click reaction as a key step. Their aromatase inhibitory activities and molecular docking were explored. It was observed that most open-chain sulfonamide triazoles (Type I) exerted aromatase inhibitory activity (IC_{50} = 1.3–9.4 μM). All triazoles (Type II) with restricted THIQ analogs were shown to be inactive compounds. The triazoles **34** and **35** displayed potent activity where they contained 6,7-dimethoxy substituents (R^1) on the THIQ core, and coumarinyloxymethyl (R^2) on the triazole ring; and *m*-substitution of sulfonyl group and triazole ring on the phenyl moiety of sulfonamide. Particularly, the triazole **34** was shown to be the most potent inhibitor (IC_{50} = 0.2 μM) without affecting the normal cell line. Moreover, the molecular docking study revealed that the investigated triazoles could snugly occupy the active site of aromatase through the interactions of hydrophobic, π–π stacking and H-bonding. The most potent compound (**34**) was the only one that displayed H-bonding interactions with both Met374 and Ser478 which were suggested to be the essential amino acid residues for the inhibitory activity.

4. Experimental

4.1. Chemistry

Column chromatography was carried out using silica gel 60 (70–230 mesh ASTM). Analytical thin-layer chromatography (TLC) was performed with silica gel 60 F_{254} aluminum sheets. ^1H and ^{13}C NMR spectra were recorded on a Bruker AVANCE 300 NMR spectrometer (operating at 300 MHz for ^1H and 75 MHz for ^{13}C). The following standard abbreviations were used for signal multiplicities: singlet (s), doublet (d), triplet (t), quartet (q) and multiplet (m). FTIR spectra were obtained using a universal attenuated total reflectance attached on a Perkin–Elmer Spectrum One spectrometer. Mass spectra were recorded on a Bruker Daltonics (microTOF). Melting points were determined using a Griffin melting point apparatus and were uncorrected.

Data associated with the compounds **13**–**31** were reported in our previous work.[7,8]

4.2. General procedure for the synthesis of nitrobenzenesulfonamides (7c–d)

A solution of phenylethylamine **6** (10 mmol) in dichloromethane (50 mL) was added dropwise to a stirred mixture of 3-nitrobenzenesulfonyl chloride (10 mmol) and sodium carbonate (14 mmol) in dichloromethane (20 mL). The reaction mixture was stirred at room temperature overnight, and added distilled water (20 mL). The organic phase was separated and the aqueous phase was extracted with dichloromethane (2 × 30 mL). The organic extracts were combined and washed with water (30 mL). The organic layer was dried over anhydrous sodium sulfate (anhyd Na_2SO_4), filtered and evaporated to dryness under reduced pressure. The crude product was further purified by recrystallization.

^1H NMR of 3-nitro-*N*-phenethylbenzenesulfonamide (**7c**) was consistent with that reported in the literature.[18]

4.2.1. *N*-(3,4-Dimethoxyphenethyl)-3-nitrobenzenesulfonamide (7d)

Pale yellow solid. 87%. Mp 103–104 °C. IR (UATR) cm^{-1}: 3233, 1607, 1592, 1534, 1332, 1162 cm^{-1}. ^1H NMR (300 MHz, $CDCl_3$) δ 2.77 (t, *J* = 6.6 Hz, 2H, ArCH_2), 3.31 (q, *J* = 6.6 Hz, 2H, CH_2NH), 3.82, 3.86 (s, 6H, 2× OCH_3), 4.65 (br t, 1H, N*H*), 6.58 (s, 1H, Ar*H*), 6.64 (d, *J* = 8.1 Hz, 1H, Ar*H*), 6.76 (d, *J* = 8.1 Hz, 1H, Ar*H*), 7.70 (t, *J* = 8.0 Hz, 1H, Ar*H*), 8.10 (d, *J* = 8.0 Hz, 1H, Ar*H*), 8.43 (d, *J* = 8.1 Hz, 1H, Ar*H*), 8.62 (s, 1H, Ar*H*). ^{13}C NMR (75 MHz, $CDCl_3$): δ 35.5, 44.5, 55.8, 55.9, 111.4, 111.7, 120.8, 122.2, 127.0, 130.0, 130.3, 132.4, 142.3, 148.1, 148.3, 149.2. HRMS-TOF: *m*/*z* $[M+H]^+$ 367.0957 (Calcd for $C_{16}H_{19}N_2O_6S$: 367.0958).

4.3. General procedure for the synthesis of 1,2,3,4-tetrahydroisoquinolines (10c–d)

A mixture of sulfonamide **7** (6.7 mmol) and paraformaldehyde (7.2 mmol) in formic acid (30 mL) was refluxed for 2 h, and then allowed to cool to room temperature. The reaction mixture was added to 30 mL of water, and the product was extracted with

CH_2Cl_2 (2 × 30 mL). Combined extracts were washed with saturated aqueous $NaHCO_3$, dried (anhyd Na_2SO_4) and evaporated to dryness under reduced pressure. The crude product was recrystallized from methanol.

^{1}H NMR of 2-((3-nitrophenyl)sulfonyl)-1,2,3,4-tetrahydroisoquinoline (**10c**) was consistent with that reported in the literature.[19]

4.3.1. 6,7-Dimethoxy-2-((3-nitrophenyl)sulfonyl)-1,2,3,4-tetrahydroisoquinoline (10d)

Pale yellow solid. 80%. Mp 133–134 °C. IR (UATR) cm^{-1}: 1611, 1532, 1519, 1351, 1175, 1117. ^{1}H NMR (300 MHz, $CDCl_3$) δ 2.86 (t, *J* = 5.8 Hz, 2H, C4-*H*), 3.47 (t, *J* = 5.8 Hz, 2H, C3-*H*), 3.84 (s, 6H, 2× OC*H*$_3$), 4.30 (s, 2H, C1-*H*), 6.54, 6.55 (2s, 2H, C-5, C-8), 7.76 (t, *J* = 8.1 Hz, 1H, Ar*H*), 8.16 (d, *J* = 7.7 Hz, 1H, Ar*H*), 8.44 (d, *J* = 8.0 Hz, 1H, Ar*H*), 8.68 (s, 1H, Ar*H*). ^{13}C NMR (75 MHz, $CDCl_3$) δ 28.1, 43.8, 47.2, 55.9, 56.0, 108.9, 111.4, 122.7, 124.6, 127.2, 130.5, 132.9, 139.4, 147.9, 148.1, 148.3. HRMS-TOF: *m*/*z* [M+Na]$^+$ 401.0768 (Calcd for $C_{17}H_{18}N_2NaO_6S$: 401.0778).

4.4. General procedure for the synthesis of 1,2,3,4-tetrahydroisoquinolines (11c–d)

A mixture of nitroisoquinoline **10** (4 mmol) and $SnCl_2{\cdot}2H_2O$ (20 mmol) in absolute ethanol (20 mL) was stirred under reflux for 4 h then concentrated under reduced pressure. Water (20 mL) was added and extracted with EtOAc (3 × 20 mL). The organic extracts were combined and washed with water (20 mL) and brine (20 mL). The organic layer was dried over anhyd Na_2SO_4, filtered and concentrated. The crude product was recrystallized from methanol.

^{1}H NMR of 2-((3-aminophenyl)sulfonyl)-1,2,3,4-tetrahydroisoquinoline (**11c**) was consistent with that reported in the literature.[19]

4.4.1. 2-((3-Aminophenyl)sulfonyl)-6,7-dimethoxy-1,2,3,4-tetrahydroisoquinoline (11d)

Pale yellow solid. 80%. Mp 170–171 °C. IR (UATR) cm^{-1}: 3468, 3374, 1626, 1599, 1519, 1317, 1158, 1117. ^{1}H NMR (300 MHz, DMSO-d_6) δ 2.76 (t, *J* = 5.8 Hz, 2H, C4-*H*), 3.18 (t, *J* = 5.8 Hz, 2H, C3-*H*), 3.64 (s, 6H, 2× OC*H*$_3$), 4.00 (s, 2H, C1-*H*), 5.62 (s, 2H, N*H*$_2$), 6.67, 6.72 (2s, 2H, C-5, C-8), 6.80 (dd, *J* = 8.0, 1.3 Hz, 2H, Ar*H*), 6.85 (d, *J* = 8.0 Hz, 1H, Ar*H*), 6.97 (s, 1H, Ar*H*), 7.22 (t, *J* = 7.8 Hz, 1H, Ar*H*). ^{13}C NMR (75 MHz, DMSO-d_6) δ 28.2, 44.2, 47.4, 56.0, 110.0, 110.3, 112.1, 112.3, 114.5, 118.4, 123.7, 125.3, 130.2, 147.8, 148.0, 150.0. HRMS-TOF: *m*/*z* [M+Na]$^+$ 371.1039 (Calcd for $C_{17}H_{20}N_2NaO_4S$: 371.1036).

4.5. General procedure for the synthesis of 2-((3-azidophenyl)sulfonyl)-1,2,3,4-tetrahydroisoquinolines (12c–d)

To a cold solution of amine **11** (3 mmol) in HCl/CH_3COOH (3:3 mL) at 0 °C, a solution of sodium nitrite (9 mmol) in water (5 mL) was added. The stirred reaction mixture was maintained for 15 min and then added dropwise a solution of sodium azide (9 mmol) in water (5 mL). The reaction mixture was allowed to stir at room temperature for 0.5 h, then the precipitate was filtered and washed with cold water. The crude product was recrystallized from methanol.

4.5.1. 2-((3-Azidophenyl)sulfonyl)-1,2,3,4-tetrahydroisoquinoline (12c)

Pale yellow solid. 94%. Mp 120–121 °C. IR (UATR) cm^{-1}: 2154, 2109, 1595, 1337, 1169. ^{1}H NMR (300 MHz, $CDCl_3$) δ 2.93 (t, *J* = 6.0 Hz, 2H, C4-*H*), 3.42 (t, *J* = 6.0 Hz, 2H, C3-*H*), 4.31 (s, 2H, C1-*H*), 7.02-7.18 (m, 4H, Ar*H*), 7.22 (d, *J* = 7.9 Hz, 1H, Ar*H*), 7.47 (s, 1H, Ar*H*), 7.51 (t, *J* = 7.9 Hz, 1H, Ar*H*), 7.60 (d, *J* = 7.8 Hz, 1H, Ar*H*). ^{13}C NMR (75 MHz, $CDCl_3$) δ 28.7, 43.7, 47.5, 118.0, 123.1, 123.7, 126.3, 126.5, 126.9, 128.8, 130.5, 131.4, 133.0, 138.8, 141.6. HRMS-TOF: *m*/*z* [M+Na]$^+$ 337.0737 (Calcd for $C_{15}H_{14}N_4NaO_2S$: 337.0730).

4.5.2. 2-((3-Azidophenyl)sulfonyl)-6,7-dimethoxy-1,2,3,4-tetrahydroisoquinoline (12d)

Pale yellow solid. 85%. Mp 86–87 °C. IR (UATR) cm^{-1}: 2155, 2106, 1592, 1518, 1465, 1346, 1167, 1116. ^{1}H NMR (300 MHz, $CDCl_3$) δ 2.81 (t, *J* = 5.8 Hz, 2H, C4-*H*), 3.37 (t, *J* = 5.8 Hz, 2H, C3-*H*), 3.80 (s, 6H, 2× OC*H*$_3$), 4.20 (s, 2H, C1-*H*), 6.50, 6.53 (s, 2H, Ar*H*), 7.21 (d, *J* = 7.7 Hz, 1H, Ar*H*), 7.44 (s, 1H, Ar*H*), 7.48 (t, *J* = 7.9 Hz, 1H, Ar*H*), 7.56 (d, *J* = 7.7 Hz, 1H, Ar*H*). ^{13}C NMR (75 MHz, $CDCl_3$) δ 28.3, 43.8, 47.2, 55.9, 56.0, 109.0, 111.5, 118.0, 123.1, 123.7, 124.9, 130.5, 141.5, 147.9, 148.1. HRMS-TOF: *m*/*z* [M+Na]$^+$ 397.0925 (Calcd for $C_{17}H_{18}N_4NaO_4S$: 397.0941).

4.6. General procedure for the synthesis of triazoles (32–35)

To a stirred solution of azido **12** (0.2 mmol) and the corresponding alkyne (0.2 mmol) in *t*-BuOH/H_2O (3:3 mL), $CuSO_4{\cdot}5H_2O$ (0.2 mmol) and ascorbic acid (0.5 mmol) were added. The reaction mixture was stirred at room temperature for 2–12 h (monitored by TLC), then concentrated under reduced pressure. The residue was added water (10 mL) and extracted with dichloromethane (3 × 20 mL). The combined organic phases were washed with water (20 mL), dried over anhyd Na_2SO_4 and evaporated to dryness. The crude product was purified using silica gel column chromatography and eluted with methanol/dichloromethane (1:50).

4.6.1. 7-((1-(3-((3,4-Dihydroisoquinolin-2(1*H*)-yl)sulfonyl)phenyl)-1*H*-1,2,3-triazol-4-yl)methoxy)-2*H*-chromen-2-one (32)

White solid. 88%. Mp 180–181 °C. IR (UATR) cm^{-1}: 1725, 1616, 1486, 1342, 1229, 1163, 1127. ^{1}H NMR (300 MHz, $CDCl_3$) δ 2.95 (t, *J* = 5.9 Hz, 2H, C4-THIQ*H*), 3.50 (t, *J* = 5.9 Hz, 2H, C3-THIQ*H*), 4.38 (s, 2H, C1-THIQ*H*), 5.39 (s, 2H, C*H*$_2$O), 6.30 (d, *J* = 9.5 Hz, 1H, Ar*H*), 6.96–7.02 (m, 2H, Ar*H*), 7.03–7.18 (m, 4H, Ar*H*), 7.44 (d, *J* = 9.3 Hz, 1H, Ar*H*), 7.68 (d, *J* = 9.5 Hz, 1H, Ar*H*), 7.74 (t, *J* = 8.0 Hz, 1H, Ar*H*), 7.93 (d, *J* = 8.0 Hz, 1H, Ar*H*), 8.06 (d, *J* = 8.0 Hz, 1H, Ar*H*), 8.17 (s, 1H, C*H*N), 8.20 (s, 1H, Ar*H*). ^{13}C NMR (75 MHz, $CDCl_3$) δ 28.6, 43.8, 47.5, 62.2, 102.2, 112.7, 113.2, 113.7, 119.3, 121.2, 124.5, 126.3, 126.5, 127.0, 127.6, 128.9, 129.0, 130.9, 131.1, 132.8, 137.4, 139.3, 143.2, 144.4, 155.8, 161.0, 161.1. HRMS-TOF: *m*/*z* [M+H]$^+$ 515.1390 (Calcd for $C_{27}H_{23}N_4O_5S$: 515.1384).

4.6.2. 4-((1-(3-((3,4-Dihydroisoquinolin-2(1*H*)-yl)sulfonyl)phenyl)-1*H*-1,2,3-triazol-4-yl)methoxy)-2*H*-chromen-2-one (33)

White solid. 91%. Mp 168–170 °C. IR (UATR) cm^{-1}: 1712, 1623, 1566, 1494, 1455, 1372, 1336, 1248, 1191, 1153. ^{1}H NMR (300 MHz, $CDCl_3$) δ 2.95 (t, *J* = 5.9 Hz, 2H, C4-THIQ*H*), 3.51 (t, *J* = 5.9 Hz, 2H, C3-THIQ*H*), 4.40 (s, 2H, C1-THIQ*H*), 5.47 (s, 2H, C*H*$_2$O), 5.93 (s, 1H, C*H*CO), 7.04–7.20 (m, 4H, Ar*H*), 7.30 (t, *J* = 7.6 Hz, 1H, Ar*H*), 7.35 (d, *J* = 7.6 Hz, 1H, Ar*H*), 7.59 (dt, *J* = 7.8, 1.6 Hz, 1H, Ar*H*), 7.76 (t, *J* = 8.0 Hz, 1H, Ar*H*), 7.85 (dd, *J* = 7.9, 1.5 Hz, 1H, Ar*H*), 7.95 (d, *J* = 8.1 Hz, 2H, Ar*H*), 8.08 (d, *J* = 8.1 Hz, 2H, Ar*H*), 8.22, 8.23 (2s, 2H, Ar*H*, C*H*N). ^{13}C NMR (75 MHz, $CDCl_3$) δ 28.6, 43.8, 47.5, 62.5, 91.4, 115.4, 116.9, 119.4, 121.6, 123.1,

124.0, 124.6, 126.3, 126.6, 127.0, 127.8, 128.9, 131.0, 131.1, 132.7, 132.8, 137.3, 153.4, 162.5, 164.9. HRMS-TOF: m/z $[M+H]^+$ 515.1385 (Calcd for $C_{27}H_{23}N_4O_5S$: 515.1384).

4.6.3. 7-((1-(3-((6,7-Dimethoxy-3,4-dihydroisoquinolin-2(1*H*)-yl)sulfonyl)phenyl)-1*H*-1,2,3-triazol-4-yl)methoxy)-2*H*-chromen-2-one (34)

White solid. 92%. Mp 180–181 °C. IR (UATR) cm^{-1}: 1723, 1613, 1522, 1466, 1347, 1226, 1163, 1120. ^1H NMR (300 MHz, $CDCl_3$) δ 2.86 (t, J = 5.8 Hz, 2H, C4-THIQ*H*), 3.47 (t, J = 5.9 Hz, 2H, C3-THIQ*H*), 3.83 (s, 6H, 2× OCH_3), 4.31 (s, 2H, C1-THIQ*H*), 5.39 (s, 2H, CH_2O), 6.30 (d, J = 9.5 Hz, 1H, Ar*H*), 6.54, 6.56 (2s, 2H, Ar*H*), 6.92–6.98 (m, 2H, Ar*H*), 7.39 (d, J = 9.2 Hz, 1H, Ar*H*), 7.63 (d, J = 9.5 Hz, 1H, Ar*H*), 7.70 (t, J = 8.0 Hz, 1H, Ar*H*), 7.87 (d, J = 7.8 Hz, 1H, Ar*H*), 7.99 (d, J = 7.6 Hz, 1H, Ar*H*), 8.13 (s, 1H, C*H*N), 8.17 (s, 1H, Ar*H*). ^{13}C NMR (75 MHz, $CDCl_3$) δ 28.2, 43.8, 47.2, 55.9, 56.0, 62.2, 102.2, 109.0, 111.5, 112.7, 113.2, 113.7, 119.4, 121.2, 122.9, 124.4, 124.8, 127.6, 129.0, 130.8, 137.3, 139.4, 143.2, 144.5, 147.9, 148.1, 155.8, 160.9, 161.1. HRMS-TOF: m/z $[M+H]^+$ 575.1589 (Calcd for $C_{29}H_{27}N_4O_7S$: 575.1595).

4.6.4. 4-((1-(3-((6,7-Dimethoxy-3,4-dihydroisoquinolin-2(1*H*)-yl)sulfonyl)phenyl)-1*H*-1,2,3-triazol-4-yl)methoxy)-2*H*-chromen-2-one (35)

White solid. 90%. Mp 211–213 °C. IR (UATR) cm^{-1}: 1717, 1622, 1518, 1457, 1384, 1343, 1238, 1156, 1114. ^1H NMR (300 MHz, $CDCl_3$) δ 2.86 (t, J = 5.7 Hz, 2H, C4-THIQ*H*), 3.48 (t, J = 5.7 Hz, 2H, C3-THIQ*H*), 3.83 (s, 6H, 2× OCH_3), 4.35 (s, 2H, C1-THIQ*H*), 5.48 (s, 2H, CH_2O), 5.94 (s, 1H, C*H*CO), 6.54, 6.56 (2s, 2H, Ar*H*), 7.29 (t, J = 7.7 Hz, 1H, Ar*H*), 7.35 (d, J = 8.3 Hz, 1H, Ar*H*), 7.59 (t, J = 7.6 Hz, 1H, Ar*H*), 7.76 (t, J = 7.8 Hz, 1H, Ar*H*), 7.85 (d, J = 7.9 Hz, 1H, Ar*H*), 7.94 (d, J = 7.7 Hz, 1H, Ar*H*), 8.07 (d, J = 7.6 Hz, 2H, Ar*H*), 8.24 (s, 2H, Ar*H*, C*H*N). ^{13}C NMR (75 MHz, $CDCl_3$) δ 28.2, 43.9, 47.3, 55.9, 56.0, 62.5, 91.4, 108.9, 111.4, 115.4, 116.9, 119.5, 121.6, 122.9, 123.1, 124.0, 124.5, 124.8, 127.8, 130.9, 132.7, 137.2, 139.5, 142.9, 147.9, 148.1, 153.4, 162.5, 164.9. HRMS-TOF: m/z $[M+H]^+$ 575.1597 (Calcd for $C_{29}H_{27}N_4O_7S$: 575.1595).

4.7. Aromatase inhibition assay

Aromatase inhibitory effect was performed using the modified method reported by Stressor et al.[20] This method was carried out according to the Gentest kit using CYP19 enzyme and *O*-benzyl fluorescein benzyl ester (DBF) as a fluorometric substrate. DBF was dealkylated by aromatase and then hydrolyzed to give the fluorescein product.

Briefly, 100 μL of cofactor, containing 78.4 μL of 50 mM phosphate buffer (pH 7.4); 20 μL of 20× NADPH-generating system (26 mM $NADP^+$, 66 mM glucose-6-phosphate, and 66 mM $MgCl_2$); and 1.6 μL of 100 U/mL glucose-6-phosphate dehydrogenase, were pipetted into a 96-well black plate and preincubated in 37 °C (water bath) for 10 min. The reaction was initiated by addition of 100 μL of enzyme/substrate (E/S) mixture containing 77.3 μL of 50 mM phosphate buffer (pH 7.4); 12.5 μL of 16 pmol/mL CYP19; 0.2 μL of 0.2 mM DBF, and 10 μL of tested sample or 10% DMSO as a negative control or ketoconazole/letrozole as a positive control. Fluorescence signal was recorded using an excitation wavelength of 490 nm and emission wavelength of 530 nm with cutoff 515 nm. Percentage of inhibition (% inhibition) was calculated as shown in Eq. 1. Samples with % inhibition greater than 50 were further calculated according to Eq. 1 to obtain their IC_{50} values.

$$\%\,\text{inhibition} = 100 - [(\text{sample} - \text{blank})/(\text{DMSO} - \text{blank}) \times 100] \quad (1)$$

4.8. Cytotoxicity assay: primate cell line (Vero)

The cytotoxicity was carried out by using the Green Fluorescent Protein (GFP) detection method.[21] The GFP-expressing Vero cell line was generated in-house by stably transfecting the African green monkey kidney cell line (Vero, ATCC CCL-81), with pEGFP-N1 plasmid (Clontech). The assay was performed by adding 45 μL of cell suspension at 3.3×10^4 cells/mL to each well of 384-well plates containing 5 μL of test compounds diluted in 0.5% DMSO. After incubation for 4 days in 37 °C incubator with 5% CO_2. Fluorescence signals were measured using SpectraMax M5 microplate reader (Molecular Devices, USA) with excitation and emission wavelengths of 485 and 535 nm, respectively. IC_{50} values were deduced from dose-response curves, using 6 concentrations of 3-fold serially diluted samples, by the SOFTMax Pro software (Molecular device). Ellipticine and 0.5% DMSO were used as a positive and a negative control, respectively.

4.9. Molecular docking

Molecular docking was performed to elucidate interactions of investigated compounds toward its target protein namely the aromatase enzyme. Initially, the crystal structure of the human placental aromatase (cytochrome P450, member 19A1) co-crystallized with the androstenedione (ASD) substrate was retrieved from the Protein Data Bank (PDB ID: 3EQM). Investigated compounds (**13**–**35**) were constructed using Marvin Sketch version 6.0 and were geometrically optimized by Gaussian 09[22] using Becke's three-parameter hybrid method with the Lee–Yang–Parr correlation functional (B3LYP) together with the 6-31 g(d) basis set. Prior to docking, the protein structure was prepared by addition of H atoms and side chain repair using the WHAT IF software.[23] Subsequently, the Gasteiger and Kollman charges were added to the ligands (the co-crystallized ligand ASD and optimized compounds **13**–**35**) and protein structures, respectively, using the PyRx 0.6 software.[24] A grid box with a size of 62.06 × 71.95 × 51.46 Å was created by the AutoGrid software to cover all area of aromatase. The center of the grid box was allocated using x, y, z coordinates of 83.4375, 50.1006 and 46.3803, respectively. Molecular docking was performed using AutoDock Vina, which is a part of the PyRx 0.6 software.[24] The co-crystallized ligand ASD was re-docked to aromatase as to validate the docking protocol. The re-docking was evaluated by the calculation of root mean standard deviation (RMSD) between the original and re-docked position of the co-crystallized ligand using the Chimera software.[25] Docking poses of investigated compounds (**13**–**35**) were visualized using the PyMoL software[26] and the ligand–protein interactions were generated using online available tool, PoseViewWeb version 1.97.0.[27]

Acknowledgments

This project is financially supported from Srinakharinwirot University and the Higher Education Research Promotion (HERP). R.P. is grateful for the Thailand Research Fund (MRG5680001). Great supports from the Office of Higher Education Commission and Mahidol University under the National Research Universities Initiative are appreciated. We are also indebted to Chulabhorn Research Institute for recording mass spectra and bioactivity testing.

Supplementary data

Supplementary data associated with this article can be found, in the online version, at http://dx.doi.org/10.1016/j.bmc.2015.04.036.

References and notes

1. Palmieri, C.; Patten, D. K.; Januszewski, A.; Zucchini, G.; Howell, S. J. *Mol. Cell. Endocrinol.* **2014**, *382*, 695.
2. Gobbi, S.; Rampa, A.; Belluti, F.; Bisi, A. *Anticancer Agents Med. Chem.* **2014**, *14*, 54.
3. Favia, A. D.; Nicolotti, O.; Stefanachi, A.; Leonetti, F.; Carotti, A. *Expert Opin. Drug Discov.* **2013**, *8*, 395.
4. Agalave, S. G.; Maujan, S. R.; Pore, V. S. *Chem. Asian J.* **2011**, *6*, 2696.
5. Neves, M. A. C.; Dinis, T. C. P.; Colombo, G. *J. Med. Chem.* **2009**, *52*, 143.
6. Doiron, J.; Soultan, A. H.; Richard, R.; Touré, M. M.; Picot, N.; Richard, R.; Čuperlović-Culf, M.; Robichaud, G. A.; Touaibia, M. *Eur. J. Med. Chem.* **2011**, *46*, 4010.
7. Pingaew, R.; Prachayasittikul, S.; Ruchirawat, S.; Prachayasittikul, V. *Med. Chem. Res.* **2014**, *23*, 1768.
8. Pingaew, R.; Mandi, P.; Nantasenamat, C.; Prachayasittikul, S.; Ruchirawat, S.; Prachayasittikul, V. *Eur. J. Med. Chem.* **2014**, *81*, 192.
9. Ghosh, D.; Griswold, J.; Erman, M.; Pangborn, W. *Nature* **2009**, *457*, 219.
10. Recanatini, M.; Bisi, A.; Cavalli, A.; Belluti, F.; Gobbi, S.; Rampa, A.; Valenti, P.; Palzer, M.; Palusczak, A.; Hartmann, R. W. *J. Med. Chem.* **2001**, *44*, 672.
11. Stefanachi, A.; Favia, A. D.; Nicolotti, O.; Leonetti, F.; Pisani, L.; Catto, M.; Zimmer, C.; Hartmann, R. W.; Carotti, A. *J. Med. Chem.* **2011**, *54*, 1613.
12. Kao, Y.-C.; Korzekwa, K. R.; Laughton, C. A.; Chen, S. *Eur. J. Biochem.* **2001**, *268*, 243.
13. Abadi, A. H.; Abou-Seri, S. M.; Hu, Q.; Negri, M.; Hartmann, R. W. *MedChemComm* **2012**, *3*, 663.
14. Cavalli, A.; Recanatini, M. *J. Med. Chem.* **2002**, *45*, 251.
15. Wood, P. M.; Woo, L. W. L.; Thomas, M. P.; Mahon, M. F.; Purohit, A.; Potter, B. V. L. *ChemMedChem* **2011**, *6*, 1423.
16. Narayana, B. L.; Kishore, D. P.; Balakumar, C.; Rao, K. V.; Kaur, R.; Rao, A. R.; Murthy, J. N.; Ravikumar, M. *Chem. Biol. Drug Des.* **2012**, *79*, 674.
17. Bonfield, K.; Amato, E.; Bankemper, Y.; Agard, H.; Steller, J.; Keeler, J. M.; Roy, D.; McCallum, A.; Paula, S.; Ma, L. *Bioorg. Med. Chem.* **2012**, *20*, 2603.
18. Pingaew, R.; Prachayasittikul, S.; Ruchirawat, S.; Prachayasittikul, V. *Med. Chem. Res.* **2013**, *22*, 267.
19. Jamieson, S. M. F.; Brooke, D. G.; Heinrich, D.; Atwell, G. J.; Silva, S.; Hamilton, E. J.; Turnbull, A. P.; Rigoreau, L. J. M.; Trivier, E.; Soudy, C.; Samlal, S. S.; Owen, P. J.; Schroeder, E.; Raynham, T.; Flanagan, J. U.; Denny, W. A. *J. Med. Chem.* **2012**, *55*, 7746.
20. Stresser, D. M.; Turner, S. D.; McNamara, J.; Stocker, P.; Miller, V. P.; Crespi, C. L.; Patten, C. J. *Anal. Biochem.* **2000**, *284*, 427.
21. Hunt, L.; Jordan, M.; De Jesus, M.; Wurm, F. M. *Biotechnol. Bioeng.* **1999**, *65*, 201.
22. Frisch, M. J.; Trucks, G. W.; Schlegel, H. B.; Scuseria, G. E.; Robb, M. A.; Cheeseman, J. R.; Scalmani, G.; Barone, V.; Mennucci, B.; Petersson, G. A.; Nakatsuji, H.; Caricato, M.; Li, X.; Hratchian, H. P.; Izmaylov, A. F.; Bloino, J.; Zheng, G.; Sonnenberg, J. L.; Hada, M.; Ehara, M.; Toyota, K.; Fukuda, R.; Hasegawa, J.; Ishida, M.; Nakajima, T.; Honda, Y.; Kitao, O.; Nakai, H.; Vreven, T.; Peralta, J. A. M. Jr., J. E.; Ogliaro, F.; Bearpark, M.; Heyd, J. J.; Brothers, E.; Kudin, K. N.; Staroverov, V. N.; Kobayashi, R.; Normand, J.; Raghavachari, K.; Rendell, A.; Burant, J.C.; Iyengar, S.S.; Tomasi, J.; Cossi, M.; Rega, N.; Millam, J. M.; Klene, M.; Knox, J. E.; Cross, J. B.; Bakken, V.; Adamo, C.; Jaramillo, J.; Gomperts, R.; Stratmann, R. E.; Yazyev, O.; Austin, A. J.; Cammi, R.; Pomelli, C.; Ochterski, J. W.; Martin, R. L.; Morokuma, K.; Zakrzewski, V. G.; Voth, G. A.; Salvador, P.; Dannenberg, J. J.; Dapprich, S.; Daniels, A. D.; Farkas, Ö.; Foresman, J. B.; Ortiz, J. V.; Cioslowski, J.; Fox, D. J. Gaussian, Inc., Wallingford CT, 2009.
23. Vriend, G. *J. Mol. Graphics* **1990**, *8*, 52.
24. Dallakyan, S. PyRx Version 0.6., 2013. http://pyrx.scripps.edu.
25. Pettersen, E. F.; Goddard, T. D.; Huang, C. C.; Couch, G. S.; Greenblatt, D. M.; Meng, E. C.; Ferrin, T. E. *J. Comput. Chem.* **2004**, *25*, 1605.
26. Delano, W. *PyMOL Release 0.99*; DeLano Scientific LLC: Pala Alto, CA, 2002.
27. Stierand, K.; Rarey, M. *ACS Med. Chem. Lett.* **2010**, *1*, 540.

Please cite this article in press as: Pingaew, R.; et al. *Bioorg. Med. Chem.* (2015), http://dx.doi.org/10.1016/j.bmc.2015.04.036

European Journal of Medicinal Chemistry 85 (2014) 65–76

Contents lists available at ScienceDirect

European Journal of Medicinal Chemistry

journal homepage: http://www.elsevier.com/locate/ejmech

Original article

Synthesis, biological evaluation and molecular docking of novel chalcone–coumarin hybrids as anticancer and antimalarial agents

Ratchanok Pingaew [a,*], Amporn Saekee [a], Prasit Mandi [b,c], Chanin Nantasenamat [b,c], Supaluk Prachayasittikul [b], Somsak Ruchirawat [d,e,f], Virapong Prachayasittikul [c]

[a] Department of Chemistry, Faculty of Science, Srinakharinwirot University, Bangkok 10110, Thailand
[b] Center of Data Mining and Biomedical Informatics, Faculty of Medical Technology, Mahidol University, Bangkok 10700, Thailand
[c] Department of Clinical Microbiology and Applied Technology, Faculty of Medical Technology, Mahidol University, Bangkok 10700, Thailand
[d] Chulabhorn Research Institute, Bangkok 10210, Thailand
[e] Program in Chemical Biology, Chulabhorn Graduate Institute, Bangkok 10210, Thailand
[f] Center of Excellence on Environmental Health and Toxicology (EHT), CHE, Ministry of Education, Thailand

ARTICLE INFO

Article history:
Received 13 March 2014
Received in revised form
19 July 2014
Accepted 24 July 2014
Available online 24 July 2014

Keywords:
Chalcone
Coumarin
Triazole
Molecular docking
Cytotoxicity
Antimalarial activity

ABSTRACT

A new series of chalcone–coumarin derivatives (**9**–**19**) linked by the 1,2,3-triazole ring were synthesized through the azide/alkyne dipolar cycloaddition. Hybrid molecules were evaluated for their cytotoxic activity against four cancer cell lines (e.g., HuCCA-1, HepG2, A549 and MOLT-3) and antimalarial activity toward *Plasmodium falciparum*. Most of the synthesized hybrids, except for analogs **10** and **16**, displayed cytotoxicity against MOLT-3 cell line without affecting normal cells. Analogs (**10**, **11**, **16** and **18**) exhibited higher inhibitory efficacy than the control drug, etoposide, in HepG2 cells. Significantly, the high cytotoxic potency of the hybrid **11** was shown to be non-toxic to normal cells. Interestingly, the chalcone–coumarin **18** was the most potent antimalarial compound affording IC_{50} value of 1.60 μM. Molecular docking suggested that the cytotoxicity of reported hybrids could be possibly due to their dual inhibition of α- and β-tubulins at GTP and colchicine binding sites, respectively. Furthermore, falcipain-2 was identified to be a plausible target site of the hybrids given their antimalarial potency.

© 2014 Elsevier Masson SAS. All rights reserved.

1. Introduction

Chalcones (1,3-diaryl-2-propen-1-ones) belonging to the flavonoid class of natural products have drawn considerable interest owing to their pharmacological properties [1–6]. Naturally-occurring chalcones and their synthetic analogs displayed significant cytotoxic activity against various cancer cells. One of the most widely proposed anticancer mechanisms of chalcones is its prevention of tubulin polymerization by binding to the colchicine-binding site [5–7]. The natural chalcone, licochalcone A (Fig. 1), isolated from Chinese licorice roots was revealed to exhibit potential antimalarial activity [8]. Numerous chalcones have been extensively studied for their antimalarial activity, and the results showed that the activity was exerted by plasmodial aspartate protease [9], cysteine protease [10–12] and cyclin-dependent protein kinase (CDK), Pfmrk [13] inhibitors. In addition, inhibition of new permeation pathways induced by malarial parasite in the erythrocyte membranes have been disclosed [14]. Structure–activity relationship (SAR) elucidation of antimalarial chalcones demonstrated that the presence of the α,β-unsaturated ketone linker [11] and *E* configuration [15] are critical for their activities in which the alkoxylated chalcones displayed superior antimalarial activity than those of the hydroxylated analogs [14,16].

Pharmacological applications of synthetic and natural coumarins (Fig. 1) have previously been reviewed [17–20]. For example, 7-hydroxycoumarin was shown to inhibit the release of cyclin D1, which is overexpressed in many types of cancers [19]. Daphnetin, the Chinese herbal product, exhibited potency against malarial parasite both *in vitro* and *in vivo* [21].

The design and development of new bioactive agents based on the molecular hybridization strategy, involving the integration of two or more pharmacophoric units having different mechanisms of action in the same molecule, is a rationally attractive approach [22,23]. These combined pharmacophores probably offer some advantages such as in overcoming drug resistance [24] as well as improving their biological potency [25]. Such hybrid approaches had previously reported the coupling of chalcones with various bioactive compounds including nucleosides [26], quinolines

* Corresponding author.
E-mail address: ratchanok@swu.ac.th (R. Pingaew).

http://dx.doi.org/10.1016/j.ejmech.2014.07.087
0223-5234/© 2014 Elsevier Masson SAS. All rights reserved.

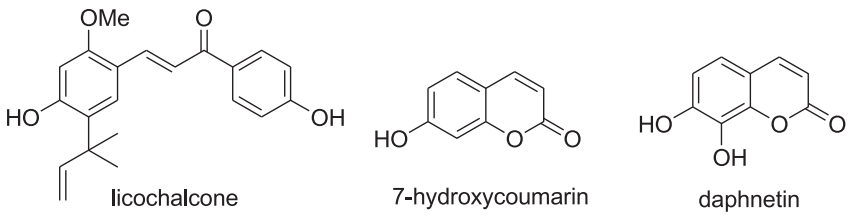

Fig. 1. Bioactive chalcone and coumarins.

[26–28], pyrrolobenzodiazepines [29], ciprofloxacin [30], β-lactam [31], nitric oxide donors [32,33], thiolactone [12] and isatin [12]. In addition, a number of new chalcone–coumarin hybrids affording anticancer, antimalarial, vasorelaxant, anti-inflammatory, antioxidant and trypanocidal activities have been documented [10,34–39]. For instance, hybrid (**1**) (Fig. 2) has been found to exert significant cytotoxic activity against the paclitaxel-resistant cancer cells [37]. Derivative (**2**) has shown cytotoxic activity against cervical carcinoma cells (IC_{50} = 3.59 μM) without affecting normal fibroblast NIH3T3 cells [38]. Additionally, conjugate (**3**) exhibited antimalarial activity against both chloroquine sensitive and chloroquine-resistant strains with IC_{50} values of 3.1 and 4 μg/mL, respectively [39]. Such chalcone analogs (**1**–**3**) constitute coumaryl group, but the different substituents are pyridyl and phenyl groups on the 2-propen-1-one core structure.

Triazole moiety is commonly found in diverse bioactive compounds. Its distinct property is its metabolically stable heterocyclic ring that is capable of forming hydrogen bonds. Furthermore, it can be used as linkers of various molecules as to give rise to new compounds and which might increase their bioavailability [40].

The reported cytotoxic and antimalarial activities of chalcone analogs led to our rational design and synthesis of new molecular hybrids of chalcone and coumarin tethered by the triazole ring. In this article, the synthetic approaches have been designed as follows (Fig. 3):

(i) use 1,3-diphenylpropenone (rings A and B) as the core structure
(ii) vary methoxy groups substituted on ring B (2,3-dimethoxy-, 3,4-dimethoxy-, 2,3,4-trimethoxy- or 3,4,5-trimethoxy substituents)
(iii) vary the position of 1,2,3-triazole ring on ring A (3- or 4-position)
(iv) vary coumaryl ring substituted on the triazole moiety (4-chromenone or 7-chromenone).

Herein, a variety of novel target chalcone–coumarin molecules containing triazole linker (**9**–**19**) were synthesized and evaluated for their cytotoxic and antimalarial activities. In addition, molecular docking studies of these compounds toward their target proteins, tubulin and falcipain-2, have been carried out to gain insight into the biological results.

2. Results and discussion

2.1. Chemistry

The novel target chalcone–coumarin hybrids (**9**–**19**) were synthesized in three steps (Scheme 1). Initially, chalcones **6** were synthesized using the base-catalyzed Claisen–Schmidt condensation of various aromatic aldehydes **4** with two aminoacetophenones **5** (3- or 4-NH_2). Subsequently, azotization reaction of the aminochalcones **6** using sodium nitrite and sodium azide in a mixture of glacial acetic acid and concentrated hydrochloric acid afforded the corresponding azidochalcones **7**. The azide/alkyne dipolar cycloaddition, represented as the Click-type reaction, is the key route to the synthesis of 1,2,3-triazole linkage. Finally, the azides **7** readily underwent cycloaddition with alkynes (**8**) to afford the novel desired hybrid molecules (**9**–**19**) in moderate to good yields (50–88%). The starting alkynes (**8**) were derived from the alkylation of either 4-hydroxycoumarin or 7-hydroxycoumarin with propargyl bromide.

Structures of the hybrids (**9**–**19**) were characterized by ^{1}H NMR spectra, which showed the existence of the singlet of methine proton at δ 8–10 ppm indicating that the triazole linkage was formed. In addition, triazole methylene ether linker displayed the singlet of methylene proton at δ 5–6 ppm. The chalcone part was shown to be in the *trans*-configuration of double bond as represented by the coupling constant (J) values of 15–16 Hz. Structures of all obtained compounds were further supported by ^{13}C NMR, IR and HRMS. Such spectral data using the chalcone–coumarin hybrid **9** as an example are provided below.

The hybrid **9** showed molecular ion $[M+Na]^+$ peak at 532.1464 corresponding to the molecular formula of $C_{29}H_{23}N_3NaO_6$. The IR spectra of the compound **9** exhibited absorption bands of C=O groups of coumarin and chalcone moieties at 1723 and 1660 cm^{-1}, respectively. In the ^{1}H NMR spectra, two singlets at δ 3.92 and 3.94 ppm were assigned to two methoxy protons on ring B of the chalcone part. The methylene protons connected to the triazole moiety appeared as a singlet at δ 5.35 ppm. Two protons of the

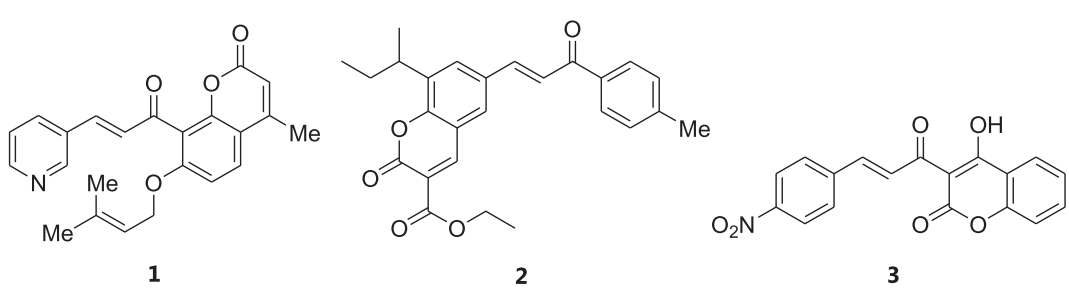

Fig. 2. Chalcone containing coumarin derivatives.

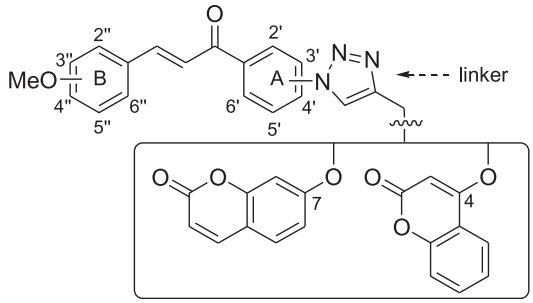

Fig. 3. Newly designed chalcone–coumarin hybrids linked by triazole.

propenone moiety were observed as two doublets at δ 7.38 and 7.82 ppm with J value of 15.6 Hz. Two doublets at δ 6.25 and 7.62 ppm with J value of 9.5 Hz were attributed to two protons of coumarin ring at positions 3 and 4. The rest of aromatic protons of this ring at C-6 and C-8 appeared as multiplet at δ 6.92–6.98 ppm, and a proton at position 5 was found to be displayed as a doublet at δ 7.39 ppm with J value of 8.9 Hz. The aromatic ring B protons of chalcone at position 5″, 2″ and 6″ were observed at δ 6.89 (d, $J = 8.3$ Hz), 7.16 (s) and 7.25 (d, $J = 8.3$ Hz) ppm, respectively. The aromatic protons at position 5′ and 2′ of chalcone (ring A) were visible as a triplet at δ 7.68 ppm with J value of 7.9 Hz and as a singlet at δ 8.32 ppm, respectively, whereas position 4′ and 6′ appeared as two doublets at δ 8.01 ($J = 8.0$ Hz) and 8.07 ($J = 7.7$ Hz) ppm. A singlet of a methine proton of the triazole ring appeared at δ 8.20 ppm. In the ^{13}C NMR spectra, two methoxy carbons (at C-3″ and C-4″) of chalcone part (ring B) were observed at δ 56.1 ppm whereas a methylene carbon adjacent to triazole ring was noted at 62.3 ppm. Two carbonyl groups of ketone and lactone were seen at 188.9 and 161.0 ppm, respectively. Nine quaternary aromatic carbons (ArC) were observed at chemical shift 113.2, 127.5, 137.3, 140.2, 144.1, 149.4, 151.9, 155.8 and 161.2 ppm. Eleven tertiary aromatic carbons (ArCH) and four olefinic carbons appeared at chemical shift 102.2, 110.3, 111.2, 112.7, 113.6, 119.0, 120.1, 121.3, 123.6, 124.3, 128.7, 129.0, 130.2, 143.2 and 146.5 ppm.

2.2. Biological activities

2.2.1. Cytotoxic activity

Cytotoxicity of the synthesized chalcone–coumarin hybrids (**9**–**19**) were assayed against human cancer cell lines; HuCCA-1 (cholangiocarcinoma), HepG2 (hepatocellular carcinoma), A549 (lung carcinoma) and MOLT-3 (lymphoblastic leukemia), as summarized in Table 1. These compounds were also evaluated for non-cancerous cell line (Vero) derived from African green monkey kidney.

Results showed that most of the tested hybrid molecules exerted significant cytotoxicity, especially against MOLT-3 cancer cell line, except for the hybrid **11**. Among these, triazole hybrid **16** was shown to be the most potent cytotoxic compound against MOLT-3 cells with an IC_{50} of 0.53 μM. Aside from MOLT-3 cells, compounds **9**–**11** and **15**–**17** also showed inhibitory effect against HuCCA-1 cells. However, tri-substituted methoxy hybrids **12**, **13**, **14** and **19** selectively inhibited MOLT-3 cells with IC_{50} in the range of 3.89–79.49 μM. Significant cytotoxic activity toward A549 cells was noted for 2,3-dimethoxy analogs **10**, **11** and **16**, in which **11** was the most potent compound ($IC_{50} = 7.95$ μM). The investigated chalcone–coumarin hybrids bear a variety of substituents on ring B (2,3-, 3,4-, 2,3,4- and 3,4,5-methoxys) and ring A (3- and 4-substituted triazoles) of the chalcone moiety while the coumarins linked to triazoles as a series of 7- (**9**–**14**) and 4- (**15**–**19**) substituted coumarins. SAR investigation of the compounds revealed that the most potent and promising cytotoxicity depended on the substitution pattern of substituents on rings A and B as well as coumaryl moieties. Apparently, compounds with 2,3-dimethoxy groups on ring B and 3-substituted ring A of 4-oxycoumaryl series exhibited higher inhibitory potency (HuCCA-1 cells) than the corresponding 3,4-dimethoxy (ring B) as observed for **16** ($IC_{50} = 2.36$ μM) and **15** ($IC_{50} = 38.57$ μM). Similar cytotoxic effect against HuCCA-1 was noted for 7-oxycoumaryl analogs **10** ($IC_{50} = 11.13$ μM) and **9** ($IC_{50} = 33.37$ μM). Obviously, 2,3-dimethoxy (ring B), 3-substituent (ring A) of 4-coumaryl analog **16** exerted higher cytotoxicity towards all of the tested cancer cells as compared to its 7-coumaryl analog (**10**). In addition, other 4-coumaryl derivatives exerted

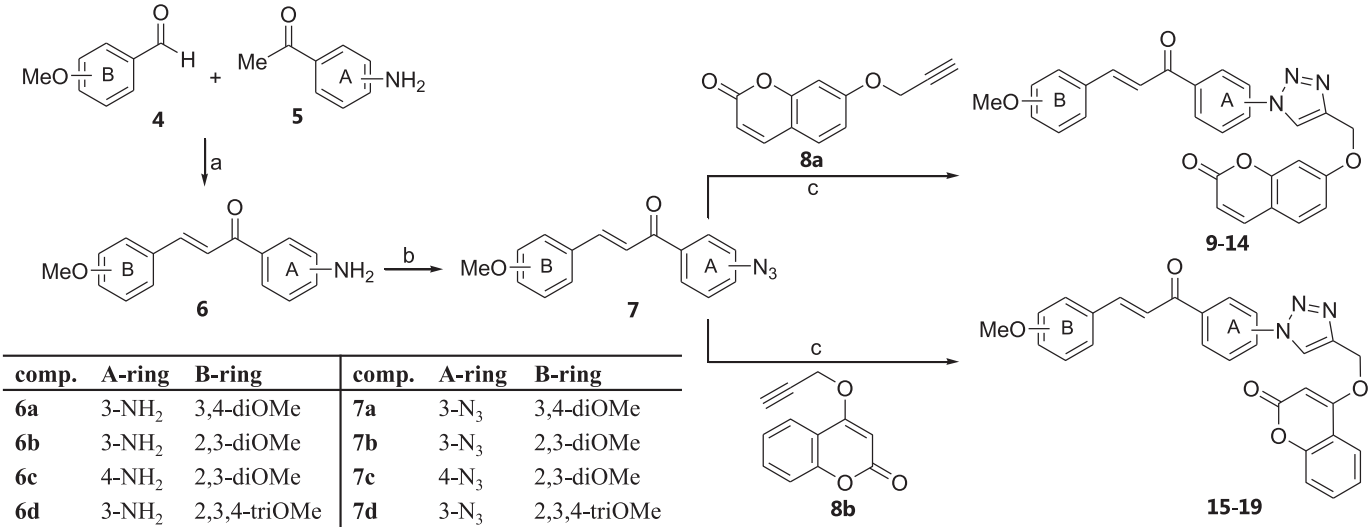

comp.	A-ring	B-ring	comp.	A-ring	B-ring
6a	3-NH_2	3,4-diOMe	**7a**	3-N_3	3,4-diOMe
6b	3-NH_2	2,3-diOMe	**7b**	3-N_3	2,3-diOMe
6c	4-NH_2	2,3-diOMe	**7c**	4-N_3	2,3-diOMe
6d	3-NH_2	2,3,4-triOMe	**7d**	3-N_3	2,3,4-triOMe
6e	4-NH_2	2,3,4-triOMe	**7e**	4-N_3	2,3,4-triOMe
6f	4-NH_2	3,4,5-triOMe	**7f**	4-N_3	3,4,5-triOMe

Reagents and conditions:
(a) 40% KOH, EtOH, rt
(b) $NaNO_2$, HCl/CH_3COOH, 0 °C, 15 min then NaN_3, rt, 30 min
(c) $CuSO_4 \cdot 5H_2O$, sodium ascorbate, t-BuOH/H_2O, rt

Scheme 1. Synthesis of chalcone–coumarin hybrids (**9**–**19**) through the Click reaction.

Table 1
Cytotoxic and antimalarial activities (IC_{50}, μM) of hybrid compounds (**9**–**19**).

Compound	A-ring	B-ring	Cancer cell lines[a]				Antimalarial[b]	Vero cell line
			HuCCA-1	HepG2	A549	MOLT-3		
9	3-Triazole	3,4-DiOMe	33.37 ± 0.84	Non-cytotoxic	Non-cytotoxic	3.12 ± 0.11	Inactive	Non-cytotoxic
10	3-Triazole	2,3-DiOMe	11.13 ± 0.40	15.70 ± 2.00	31.40 ± 1.00	5.16 ± 0.69	6.63	35.03
11	4-Triazole	2,3-DiOMe	4.81 ± 0.92	8.18 ± 0.76	7.95 ± 3.04	Non-cytotoxic	Inactive	Non-cytotoxic
12	3-Triazole	2,3,4-TriOMe	Non-cytotoxic	Non-cytotoxic	Non-cytotoxic	3.89 ± 0.28	13.03	Non-cytotoxic
13	4-Triazole	2,3,4-TriOMe	Non-cytotoxic	Non-cytotoxic	Non-cytotoxic	22.50 ± 3.63	Inactive	Non-cytotoxic
14	4-Triazole	3,4,5-TriOMe	Non-cytotoxic	Non-cytotoxic	Non-cytotoxic	79.49 ± 1.44	Inactive	Non-cytotoxic
15	3-Triazole	3,4-DiOMe	38.57 ± 1.48	Non-cytotoxic	Non-cytotoxic	3.91 ± 0.34	Inactive	Non-cytotoxic
16	3-Triazole	2,3-DiOMe	2.36 ± 0.14	4.26 ± 0.29	18.06 ± 1.07	0.53 ± 0.08	4.73	3.91
17	3-Triazole	2,3,4-TriOMe	6.13 ± 0.06	Non-cytotoxic	Non-cytotoxic	1.13 ± 0.18	7.47	Non-cytotoxic
18	4-Triazole	2,3,4-TriOMe	Non-cytotoxic	22.85 ± 0.51	Non-cytotoxic	12.33 ± 1.78	1.60	Non-cytotoxic
19	4-Triazole	3,4,5-TriOMe	Non-cytotoxic	Non-cytotoxic	Non-cytotoxic	6.58 ± 1.78	Inactive	Non-cytotoxic
Etoposide[c]			ND	30.16 ± 0.50	ND	0.051 ± 0.002	ND	ND
Doxorubicin[c]			0.83 ± 0.07	0.79 ± 0.08	0.44 ± 0.01	ND	ND	ND
Dihydroartemisinine[c]			ND	ND	ND	ND	0.0011	ND
Ellipticine[c]			ND	ND	ND	ND	ND	1.94

Non-cytotoxic = IC_{50} > 50 μg/mL.
Inactive = IC_{50} > 10 μg/mL.
Vero cell line = African green monkey kidney cell line.
ND, not determined.
[a] Cancer cell lines comprise the following: HuCCA-1 human cholangiocarcinoma cell line, HepG2 human hepatocellular carcinoma cell line, A549 human lung carcinoma cell line, MOLT-3 human lymphoblastic leukemia cell line.
[b] Antimalarial against *Plasmodium falciparum*.
[c] Etoposide, doxorubicin, ellipticine and dihydroartemisinine were used as reference drugs.

better cytotoxic activity than 7-coumaryls were shown to be in the following order **17** > **12**, **18** > **13** and **19** > **14**. Interestingly, HepG2 cells inhibitory action was observed for hybrids containing 2,3-dimethoxy (**10**, **11** and **16**) and 2,3,4-trimethoxy (**18**) on ring B. Such compounds (**10**, **11**, **16** and **18**) were shown to be more potent anticancer agents as compared to etoposide, the reference drug. Particularly, the most potent hybrid **16** (IC_{50} of 4.26 μM) displayed 7-fold stronger activity than the etoposide (IC_{50} = 30.16 μM). So far, the 2,3-dimethoxy derivatives **10** and **16** containing triazole ring at position 3 showed cytotoxicity against the Vero cell with IC_{50} of 35.03 and 3.91 μM, respectively. It should be noted that the hybrid **11** showed cytotoxicity in a broad spectrum of cancer cells (i.e., HuCCA-1, HepG2 and A549 cells) with IC_{50} values in the range of 4.81–8.18 μM without affecting normal cells. Molecular docking of the anticancer hybrids to their target proteins, tubulins have been described herein.

2.2.2. Antimalarial activity

Antimalarial activity of the hybrids (**9**–**19**) was examined against *Plasmodium falciparum* (K1, multidrug resistant strain) as shown in Table 1. The synthesized hybrids of 2,3-dimethoxy (**10** and **16**) and 2,3,4-trimethoxy (**12**, **17** and **18**) showed significant antimalarial activity with IC_{50} values in the range of 1.60–13.03 μM. At this point, it seemed reasonable that the presence of methoxy groups at *ortho*- and *para*-positions of chalcones (ring B) played crucial role for antimalarial activity. In addition, a series of 4-coumarinoxymethyl derivatives showed superior potency than the corresponding 7-coumarinoxymethyl analogs as seen for **16** > **10**, **17** > **12** and **18** > **13**. Notably, the 2,3,4-trimethoxy analog **18** was shown to be the most potent compound (IC_{50} = 1.60 μM) and was non-toxic to normal cells. Results from the molecular docking of antimalarial analogs are discussed hereafter.

2.3. Validation of docking protocol

Co-crystallized ligands, colchicine and *trans*-epoxysuccinyl-*L*-leucylamido-(4-guanidino)butane (E64), were re-docked to their target proteins, tubulin and falcipain-2, as to validate the docking protocol. Owing to limitations of the available docking software, covalent bonds between E64 and the falcipain-2 active site were disrupted and re-docked *via* non-covalent docking. Colchicine and E64 could be re-docked to their respective target proteins with a root mean squared deviation (RMSD) of 0.697 Å (Fig. 4A) and 1.157 Å (Fig. 4B), respectively.

2.3.1. Molecular docking of chalcone–triazole–coumarin derivatives to α- and β-tubulin complexes

As previously mentioned, the cytotoxic activity of chalcone is often associated with its ability to inhibit β-tubulin formation *via* binding of compounds to the colchicine binding site [5–7]. Molecular docking was performed to investigate the binding modalities of chalcone–triazole–coumarin derivatives against tubulin. Results suggested that all chalcone–triazole–coumarin analogs could snugly occupy the colchicine binding site of β-tubulin as shown in Fig. 4C. Binding energies for these compounds are in the range of −9.6 to −10.8 kcal/mol (Table 2). It was observed that all chalcone–triazole–coumarin derivatives afforded stronger binding energies than that of the colchicine found in the co-crystallized structure thereby suggesting promising inhibitory effect for this set of compounds. The observed tubulin binding energies for these compounds are in accordance with their cytotoxic activities, in which the more potent compounds as seen for the dimethoxy analogs (**9**–**11**, **15** and **16**) displayed lower binding energies (−10.5 to −10.8 kcal/mol) than the trimethoxy analogs (**12**–**14** and **17**–**19**) with the binding energies in the range of −9.6 to −10.3 kcal/mol. Particularly, the lowest cytotoxic activity of compound **14** showed the highest tubulin binding energy of −9.6 kcal/mol. Interestingly, docking poses of these compounds revealed that they could also occupy the GTP binding site of α-tubulin that is adjacent to the colchicine binding site of β-tubulin. These findings suggest that chalcone–triazole–coumarin derivatives could plausibly act as dual site inhibitors of α- and β-tubulin complexes. Molecular modeling analysis of the crystal structure revealed that the co-crystallized colchicine interacts with β-tubulin *via* the formation of hydrogen bonds involving a methoxy group to Cys241 and engaging in hydrophobic interactions with Leu255 and Ala316 (Fig. 4A). The GTP binds α-tubulin *via* the formation of hydrogen bonding network between the phosphate moiety to Ala12, Asp69,

Table 2
Binding energy of chalcone–triazole–coumarin derivatives (**9**–**19**).

Compounds	Binding energy (kcal/mol)[a]	
	Tubulin	Falcipain-2
9	−10.8	ND
10	−10.6	−8.6
11	−10.5	ND
12	−10.2	−8.9
13	−9.8	ND
14	−9.6	ND
15	−10.6	ND
16	−10.7	−8.3
17	−10.3	−8.1
18	−10.1	−8.4
19	−10.0	ND
Colchicine	−9.4	ND
E64[b]	ND	−7.3

[a] *ND*, not determined.
[b] E64 was covalently bound to falcipain-2. Binding energy was obtained from non-covalent docking.

Ser140, Thr145, Ser178 and Glu183 while the guanine ring forms hydrogen bonds with Asn206 and Asn288 as well as π–π stacking with Tyr224. Moreover, hydrophobic interaction between Ala12 and Tyr224 of α-tubulin with GTP were also observed. These aforementioned residues could be the essential site for ligand binding as to inhibit microtubule formation.

Compound **11**, which provided cytotoxicity against a broad spectrum of cancer cells (i.e., HuCCA-1, HepG2 and A549 cells) without affecting normal cells, could interact with both colchicine and GTP binding sites of β- and α-tubulins, respectively (Fig. 5A). The coumarin moiety of the compound could occupy the hydrophobic pocket as defined by Leu248, Ala316 and Ala354 residues of β-tubulin, which are located inside the colchicine binding site. In addition, ring B of chalcone moiety of the compound could form hydrophobic interaction with Ala12 and Tyr224 together with π–π interaction with Tyr224 of α-tubulin, which constitutes the GTP binding pocket. The less potency of trimethoxy analogs (**13**, **14**, **18** and **19**) compared to the 2,3-dimethoxy analog (**11**) may be due to the steric reason in this hydrophobic area. In addition, such interaction was strengthened by hydrogen bonding as afforded by the N atom at position 2 of triazole ring to Asn101 of α-tubulin and π–cation interaction of chalcone ring A to the positively-charged side chain of Lys254 from β-tubulin. These finding suggested that the cytotoxicity of chalcone–triazole–coumarin derivatives could be possibly due to their dual inhibition of α- and β-tubulins.

2.3.2. *Molecular docking of chalcone–coumarin derivatives to falcipain-2*

Many chalcone derivatives have been revealed to inhibit malarial cysteine protease [10–12], the enzyme plays an essential role in the degradation of host hemoglobin into small peptides as nutrients occurring within the acidic food vacuole of the parasite. Accordingly, molecular docking was performed against the cysteine protease-like falcipain-2 using selected compounds (i.e., **10**, **12**, **16**, **17** and **18**) that have been shown to exert antimalarial activity. The crystal structure of falcipain-2 was co-crystallized with inhibitor E64, which was covalently-bonded to the enzyme as to block substrates from reaching the catalytic triad as defined by Gln36, Cys42 and His174 residues [41]. Docking results suggested that all selected compounds could bind the active site of falcipain-2 (Fig. 4D) with binding energies in the range of −8.1 to −8.9 kcal/mol (Table 2). Unfortunately, due to the limitation of available docking software in performing covalent docking, therefore the

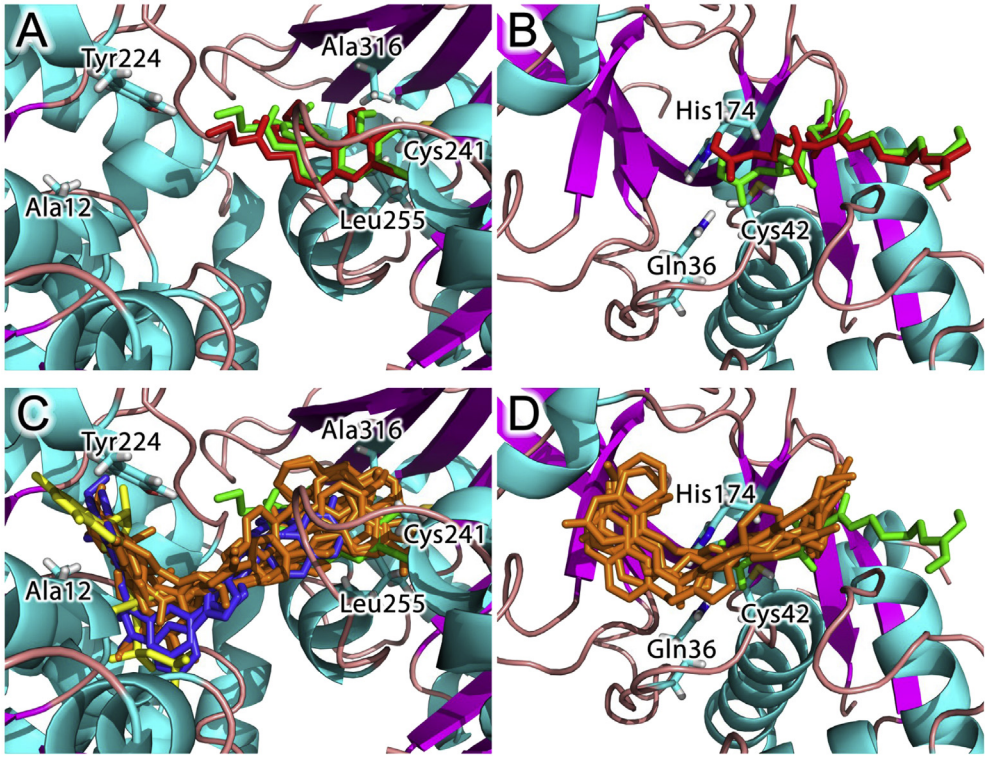

Fig. 4. Molecular docking of chalcone–triazole–coumarin ligands to tubulin. Re-docking poses of colchicine to tubulin (A) and E64 to falcipain-2 (B) are shown with original ligand structures colored in green while re-docking poses colored in red. Docking poses of chalcone–triazole–coumarin ligands to tubulin (C) are shown with colchicine colored in green, GTP colored in yellow, ligands colored in orange and blue. Docking poses of chalcone–triazole–coumarin ligands to falcipain-2 (D) are shown with E64 colored in green and ligands colored in orange. (For interpretation of the references to color in this figure legend, the reader is referred to the web version of this article.)

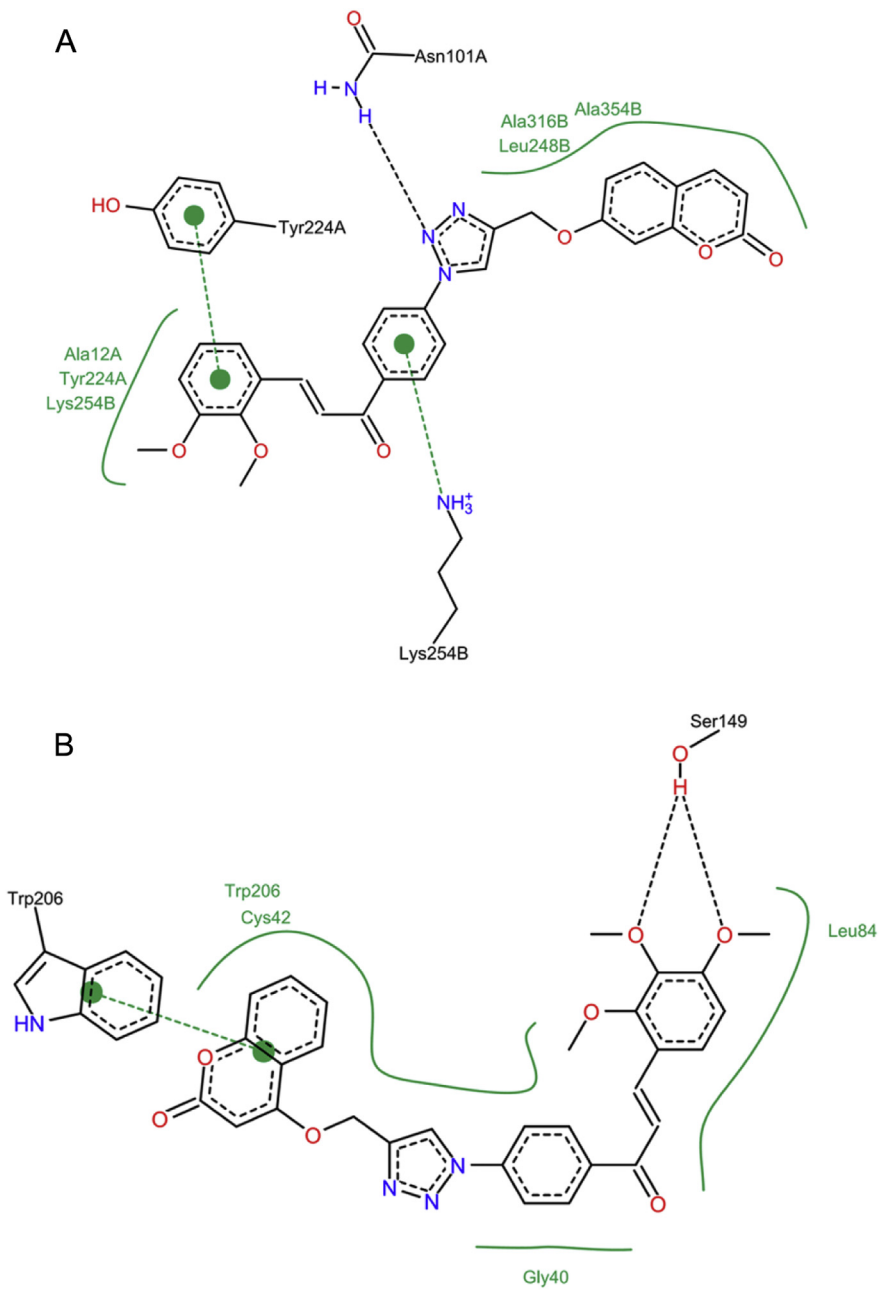

Fig. 5. Two-dimensional schematics of the protein-ligand interaction of compound **11** to tubulin (A) and compound **18** to falcipain-2 (B). The amino acid residues such as Ala12A, A is denoted as α-tubulin; and Ala316B, B is denoted as β-tubulin.

binding energy of E64 was obtained by disrupting the covalent bond and re-docked non-covalently. Owing to these inherent differences in the binding mechanism, thus it cannot be assumed that the chalcone–triazole–coumarins could possess higher potency than E64 by judging from their binding energies. Compound **18**, which had the highest antimalarial activity, could bind the active site of falcipain-2 *via* the interaction scheme shown in Fig. 5B. As such, the coumarin moiety of the compound could occupy the binding site of falcipain-2 *via* hydrophobic interaction with Cys42 and Trp206 residues together with the formation of π–π stacking with Trp206. Such interaction afforded strong stability because ring A and ring B of chalcone moiety formed hydrophobic interaction with Gly40 and Leu84, respectively. Moreover, 3,4-dimethoxy substituents of chalcone ring B provided hydrogen bonding with Ser149 thereby resulting in tight binding of compound **18** to the falcipain-2 active site. The docking results suggested that the antimalarial activity of the chalcone–triazole–coumarin derivatives might be due to their inhibitions of falcipain-2.

Furthermore, metabolic pathways in intracellular parasites (i.e., *P. falciparum*) and cancer cells are more sensitive to oxidative stress than normal cells [42]. It could be presumably explained that dimethoxychalcone moieties might be metabolized to catechols, then to phenoxy radicals and ultimately to superoxide anions, which are toxic to the cells [5].

3. Conclusions

Eleven conjugated molecules (**9**–**19**) derived from chalcones and coumarins linked by 1,2,3-triazole ring have been successfully synthesized *via* the Click reaction. Cytotoxic activity testing

revealed that most of the hybrids displayed cytotoxicity against MOLT-3 cell line. In particular, the chalcone–coumarin **16** was the most potent cytotoxic agent ($IC_{50} = 0.53$ μM). Compounds **10**, **11**, **16** and **18** displayed higher cytotoxic potency against HepG2 cells than the control drug, etoposide. The hybrid **16** was shown to be the most potent one ($IC_{50} = 4.26$ μM), but unfortunately it was toxic toward non-cancerous (Vero) cells. Significantly, the analog **11** displayed the second most potent activity (HepG2) with IC_{50} value of 8.18 μM and non-toxic to Vero cells. Importantly, antimalarial activity results concluded that the conjugate **18** exhibited the most potent activity ($IC_{50} = 1.60$ μM) without affecting non-cancerous cells. Docking results suggested that the cytotoxic and antimalarial activities of the hybrids might be due to their inhibition of tubulin and falcipain-2, respectively. This study provides novel chalcone–coumarin hybrids as potential lead molecules for further structural optimization as anticancer and antimalarial agents.

4. Experimental

4.1. Chemistry

Column chromatography was carried out using silica gel 60 (70–230 mesh ASTM). Analytical thin-layer chromatography (TLC) was performed on silica gel 60 F_{254} aluminum sheets. ^{1}H and ^{13}C NMR spectra were recorded on a Bruker AVANCE 300 NMR spectrometer (operating at 300 MHz for ^{1}H and 75 MHz for ^{13}C). FTIR spectra were obtained using a universal attenuated total reflectance attached on a Perkin–Elmer Spectrum One spectrometer. High resolution mass spectra (HRMS) were recorded on a Bruker Daltonics (microTOF). Melting points were determined using a Griffin melting point apparatus and were uncorrected.

4.2. General procedure for the synthesis of aminochalcones (**6**)

To a stirred solution of benzaldehyde **4** (5 mmol) and aminoacetophenone **5** (5 mmol) in ethanol (15 mL) at 5 °C, then 40% KOH (10 mL) was added dropwise, and stirred at room temperature overnight. The reaction mixture was neutralized with 2 M HCl, and then extracted with ethyl acetate (3 × 30 mL). The combined organic phases were washed with water (25 mL), dried over anhydrous sodium sulfate and evaporated to dryness. The crude product was purified using silica gel column chromatography and eluted with 12% acetone–hexane.

4.2.1. (E)-1-(3-aminophenyl)-3-(3,4-dimethoxyphenyl)prop-2-en-1-one (**6a**)

Yellow solid. 57%. mp 68–69 °C. IR (UATR) cm^{-1}: 3448, 3362, 3225, 1652, 1621, 1574, 1508. ^{1}H NMR (300 MHz, $CDCl_3$) δ 2.80 (br s, 2H, NH_2), 3.95, 3.96 (2s, 6H, 2 × OCH_3), 6.91 (d, $J = 8.3$ Hz, 1H, C5′-Ar*H*), 6.95 (d, $J = 7.7$ Hz, 1H, C4-Ar*H*), 7.16 (d, $J = 1.4$ Hz, 1H, C2′-Ar*H*), 7.23 (d, $J = 8.3$ Hz, 1H, C6′-Ar*H*), 7.30 (t, $J = 7.2$ Hz, 1H, C5-Ar*H*), 7.35 (d, $J = 15.4$ Hz, 1H, CH=C*H*CO), 7.38 (s, 1H, C2-Ar*H*), 7.42 (d, $J = 7.5$ Hz, 1H, C6-Ar*H*), 7.75 (d, $J = 15.6$ Hz, 1H, C*H*=CHCO). ^{13}C NMR (75 MHz, $CDCl_3$) δ 56.0, 110.1, 111.1, 114.8, 119.2, 119.6, 120.3, 123.1, 127.9, 129.4, 139.6, 144.8, 146.0, 149.2, 151.4, 190.8. HRMS-TOF: *m*/*z* $[M+Na]^+$ 306.1102 (Calcd for $C_{17}H_{17}NNaO_3$: 306.1101).

4.2.2. (E)-1-(3-aminophenyl)-3-(2,3-dimethoxyphenyl)prop-2-en-1-one (**6b**)

Yellow oil. 41%. IR (UATR) cm^{-1}: 3462, 3367, 3229, 1656, 1623, 1575, 1477. ^{1}H NMR (300 MHz, $CDCl_3$) δ 2.90 (br s, 2H, NH_2), 3.86, 3.87 (2s, 6H, 2 × OCH_3), 6.87 (d, $J = 7.9$ Hz, 1H, C4-Ar*H*), 6.94 (d, $J = 8.1$ Hz, 1H, C4′-Ar*H*), 7.07 (t, $J = 8.0$ Hz, 1H, C5′-Ar*H*), 7.21–7.28 (m, 2H, C5-Ar*H*, C6′-Ar*H*), 7.31 (s, 1H, C2-Ar*H*), 7.37 (d, $J = 7.6$ Hz, 1H, C6-Ar*H*), 7.53 (d, $J = 15.9$ Hz, 1H, CH=C*H*CO), 8.05 (d, $J = 15.9$ Hz, 1H, C*H*=CHCO). ^{13}C NMR (75 MHz, $CDCl_3$) δ 55.9, 61.3, 114.1, 114.6, 119.0, 119.4, 119.6, 123.9, 124.2, 129.2, 129.4, 139.3, 139.4, 146.7, 149.0, 153.2, 191.0. HRMS-TOF: *m*/*z* HRMS-TOF: *m*/*z* $[M+Na]^+$ 306.1113 (Calcd for $C_{17}H_{17}NNaO_3$: 306.1101).

4.2.3. (E)-1-(4-aminophenyl)-3-(2,3-dimethoxyphenyl)prop-2-en-1-one (**6c**)

Yellow solid. 65%. mp 133–134 °C (135.6–136.8 °C [43]). IR (UATR) cm^{-1}: 3453, 3351, 3228, 1623, 1602, 1579, 1478. ^{1}H NMR (300 MHz, $CDCl_3$) δ 3.90, 3.91 (2s, 6H, 2 × OCH_3), 4.17 (br s, 2H, NH_2), 6.72 (d, $J = 8.7$ Hz, 2H, C3-Ar*H*, C5-Ar*H*), 6.97 (d, $J = 8.0$ Hz, 1H, C-4′-Ar*H*), 7.10 (t, $J = 8.0$ Hz, 1H, C-5′-Ar*H*), 7.29 (d, $J = 8.0$ Hz, 1H, C-6′-Ar*H*), 7.62 (d, $J = 15.8$ Hz, 1H, CH=C*H*CO), 7.95 (d, $J = 8.6$ Hz, 2H, C2-Ar*H*, C6-Ar*H*), 8.07 (d, $J = 15.8$ Hz, 1H, C*H*=CHCO). ^{13}C NMR (75 MHz, $CDCl_3$) δ 55.9, 61.3, 113.8, 113.9, 119.6, 123.8, 124.1, 128.7, 129.6, 131.1, 138.0, 148.8, 151.0, 153.2, 188.5. HRMS-TOF: *m*/*z* $[M+H]^+$ 284.1285 (Calcd for $C_{17}H_{18}NO_3$: 284.1281).

4.2.4. (E)-1-(3-aminophenyl)-3-(2,3,4-trimethoxyphenyl)prop-2-en-1-one (**6d**)

Yellow solid. 62%. mp 94–95 °C. IR (UATR) cm^{-1}: 3458, 3364, 3233, 1653, 1627, 1577, 1494. ^{1}H NMR (300 MHz, $CDCl_3$) δ 3.85 (br s, 2H, NH_2), 3.91, 3.93, 3.96 (3s, 9H, 3 × OCH_3), 6.74 (d, $J = 8.8$ Hz, 1H, C5′-Ar*H*), 6.90 (dd, $J = 8.0$, 1.9 Hz, 1H, C4-Ar*H*), 7.29 (t, $J = 7.8$ Hz, 1H, C5-Ar*H*), 7.34 (t, $J = 1.9$ Hz, 1H, C2-Ar*H*), 7.40 (d, $J = 8.7$ Hz, 2H, C6-Ar*H*, C6′-Ar*H*), 7.53 (d, $J = 15.8$ Hz, 1H, CH=C*H*CO), 7.99 (d, $J = 15.8$ Hz, 1H, C*H*=CHCO). ^{13}C NMR (75 MHz, $CDCl_3$) δ 56.1, 60.9, 61.4, 107.6, 114.5, 118.8, 119.2, 121.7, 122.1, 123.8, 129.4, 139.7, 139.8, 142.5, 146.8, 153.8, 155.7, 191.1. HRMS-TOF: *m*/*z* $[M+H]^+$ 314.1390 (Calcd for $C_{18}H_{20}NO_4$: 314.1387).

4.2.5. (E)-1-(4-aminophenyl)-3-(2,3,4-trimethoxyphenyl)prop-2-en-1-one (**6e**)

Yellow solid. 80%. mp 125–126 °C. IR (UATR) cm^{-1}: 3458, 3343, 3234, 1633, 1595, 1580, 1494. ^{1}H NMR (300 MHz, $CDCl_3$) δ 3.87, 3.88, 3.91 (3s, 9H, 3 × OCH_3), 4.15 (br s, 2H, NH_2), 6.67 (d, $J = 8.7$ Hz, 2H, C3-Ar*H*, C5-Ar*H*), 6.69 (d, $J = 8.8$ Hz, 1H, C5′-Ar*H*), 7.35 (d, $J = 8.8$ Hz, 1H, C6′-Ar*H*), 7.55 (d, $J = 15.7$ Hz, 1H, CH=C*H*CO), 7.90 (d, $J = 8.7$ Hz, 2H, C2-Ar*H*, C6-Ar*H*), 7.93 (d, $J = 15.7$ Hz, 1H, C*H*=CHCO). ^{13}C NMR (75 MHz, $CDCl_3$) δ 56.1, 60.9, 61.4, 107.6, 113.9, 121.5, 122.5, 123.7, 128.9, 131.0, 138.4, 142.5, 150.9, 153.6, 155.4, 188.6. HRMS-TOF: *m*/*z* $[M+H]^+$ 314.1395 (Calcd for $C_{18}H_{20}NO_4$: 314.1387).

4.2.6. (E)-1-(4-aminophenyl)-3-(3,4,5-trimethoxyphenyl)prop-2-en-1-one (**6f**)

Yellow solid. 72%. mp 156–157 °C (160 °C [44]). IR (UATR) cm^{-1}: 3457, 3361, 3234, 1628, 1604, 1584, 1504. ^{1}H NMR (300 MHz, $CDCl_3$) δ 3.91, 3.94 (2s, 9H, 3 × OCH_3), 4.20 (br s, 2H, NH_2), 6.72 (d, $J = 8.5$ Hz, 2H, C3-Ar*H*, C5-Ar*H*), 6.87 (s, 2H, C2′-Ar*H*, C6′-Ar*H*), 7.43 (d, $J = 15.5$ Hz, 1H, CH=C*H*CO), 7.72 (d, $J = 15.5$ Hz, 1H, C*H*=CHCO),7.95 (d, $J = 8.5$ Hz, 2H, C2-Ar*H*, C6-Ar*H*). ^{13}C NMR (75 MHz, $CDCl_3$) δ 56.2, 61.0, 105.5, 113.9, 121.4, 128.6, 130.9, 131.1, 140.1, 143.3, 151.1, 153.5, 188.0. HRMS-TOF: *m*/*z* $[M+H]^+$ 314.1390 (Calcd for $C_{18}H_{20}NO_4$: 314.1387).

4.3. General procedure for the synthesis of azidochalcones (**7**)

To a cold solution of aminochalcone **6** (3 mmol) in HCl:CH_3COOH (3:3 mL) at 0 °C, a solution of sodium nitrite (9 mmol) in water (5 mL) was added. The stirred reaction mixture was maintained for 15 min and then added dropwise a solution of sodium azide (9 mmol) in water (5 mL). The reaction mixture was allowed to stir at room temperature for 0.5 h, then the precipitate was filtered, washed with cold water and recrystallized from methanol.

*4.3.1. (E)-1-(3-azidophenyl)-3-(3,4-dimethoxyphenyl)prop-2-en-1-one (**7a**)*

Yellow solid. 77%. mp 75–76 °C. IR (UATR) cm^{-1}: 2105, 1660, 1576, 1511. ^1H NMR (300 MHz, $CDCl_3$) δ 3.92, 3.94 (2s, 6H, 2 × OCH_3), 6.89 (d, J = 8.3 Hz, 1H, C5′-ArH), 7.13 (d, J = 1.9 Hz, 1H, C2′-ArH), 7.19–7.24 (m, 2H, C4-ArH, C6′-ArH), 7.31 (d, J = 15.6 Hz, 1H, CH=CHCO), 7.47 (t, J = 7.9 Hz, 1H, C5-ArH), 7.64 (d, J = 1.9 Hz, 1H, C2-ArH), 7.74 (d, J = 7.9 Hz, 1H, C6-ArH), 7.75 (d, J = 15.6 Hz, 1H, CH=CHCO). ^{13}C NMR (75 MHz, $CDCl_3$) δ 56.0, 110.1, 111.1, 118.8, 119.6, 122.9, 123.4, 124.8, 127.6, 130.0, 140.2, 140.9, 145.8, 149.3, 151.7, 189.6. HRMS-TOF: m/z $[M+H]^+$ 310.1200 (Calcd for $C_{17}H_{16}N_3O_3$: 310.1186).

*4.3.2. (E)-1-(3-azidophenyl)-3-(2,3-dimethoxyphenyl)prop-2-en-1-one (**7b**)*

Yellow solid. 78%. mp 73–74 °C. IR (UATR) cm^{-1}: 2109, 1663, 1577, 1479. ^1H NMR (300 MHz, $CDCl_3$) δ 3.87, 3.88 (2s, 6H, 2 × OCH_3), 6.97 (dd, J = 8.1, 1.3 Hz, 1H, C4′-ArH), 7.09 (t, J = 7.9 Hz, 1H, C5′-ArH), 7.18–7.28 (m, 2H, C4-ArH, C6′-ArH), 7.45 (t, J = 8.0 Hz, 1H, C5-ArH), 7.48 (d, J = 15.8 Hz, 1H, CH=CHCO), 7.65 (t, J = 1.8 Hz, 1H, C2-ArH), 7.75 (d, J = 7.7 Hz, 1H, C6-ArH), 8.09 (d, J = 15.8 Hz, 1H, CH=CHCO). ^{13}C NMR (75 MHz, $CDCl_3$) δ 55.9, 61.3, 114.5, 118.9, 119.7, 123.1, 123.2, 124.2, 125.0, 128.9, 130.0, 140.0, 140.5, 140.9, 153.3, 189.9. HRMS-TOF: m/z $[M+H]^+$ 310.1191 (Calcd for $C_{17}H_{16}N_3O_3$: 310.1186).

*4.3.3. (E)-1-(4-azidophenyl)-3-(2,3-dimethoxyphenyl)prop-2-en-1-one (**7c**)*

Orange-yellow solid. 69%. mp 82–83 °C. IR (UATR) cm^{-1}: 2122, 1660, 1601, 1577, 1479. ^1H NMR (300 MHz, $CDCl_3$) δ 3.91 (s, 6H, 2 × OCH_3), 7.00 (dd, J = 8.0, 1.3 Hz, 1H, C4′-ArH), 7.12 (t, J = 8.0 Hz, 1H, C5′-ArH), 7.15 (d, J = 8.7 Hz, 2H, C3-ArH, C5-ArH), 7.29 (d, J = 8.0 Hz, 1H, C6′-ArH), 7.59 (d, J = 15.9 Hz, 1H, CH=CHCO), 8.07 (d, J = 8.7 Hz, 2H, C2-ArH, C6-ArH), 8.12 (d, J = 15.9 Hz, 1H, CH=CHCO). ^{13}C NMR (75 MHz, $CDCl_3$) δ 55.9, 61.3, 114.3, 119.0, 119.7, 123.2, 124.2, 129.1, 130.5, 135.0, 139.8, 144.6, 149.0, 153.3, 189.1. HRMS-TOF: m/z $[M+H]^+$ 310.1195 (Calcd for $C_{17}H_{16}N_3O_3$: 310.1186).

*4.3.4. (E)-1-(3-azidophenyl)-3-(2,3,4-trimethoxyphenyl)prop-2-en-1-one (**7d**)*

Yellow solid. 93%. mp 65–66 °C. IR (UATR) cm^{-1}: 2107, 1660, 1576, 1495. ^1H NMR (300 MHz, $CDCl_3$) δ 3.91, 3.94, 3.98 (3s, 9H, 3 × OCH_3), 6.75 (d, J = 8.8 Hz, 1H, C5′-ArH), 7.23 (dd, J = 7.8, 1.8 Hz, 1H, C4-ArH), 7.41 (d, J = 8.8 Hz, 1H, C6′-ArH), 7.50 (t, J = 7.8 Hz, 1H, C5-ArH), 7.52 (d, J = 15.8 Hz, 1H, CH=CHCO), 7.68 (t, J = 1.8 Hz, 1H, C2-ArH), 7.78 (d, J = 7.8 Hz, 1H, C6-ArH), 8.03 (d, J = 15.8 Hz, 1H, CH=CHCO). ^{13}C NMR (75 MHz, $CDCl_3$) δ 56.1, 60.9, 61.4, 107.6, 118.8, 120.9, 121.8, 122.9, 124.1, 124.9, 129.9, 140.3, 140.8, 141.0, 142.5, 154.0, 156.0, 189.9. HRMS-TOF: m/z $[M+H]^+$ 340.1299 (Calcd for $C_{18}H_{18}N_3O_4$: 340.1292).

*4.3.5. (E)-1-(4-azidophenyl)-3-(2,3,4-trimethoxyphenyl)prop-2-en-1-one (**7e**)*

Yellow solid. 93%. mp 115–116 °C. IR (UATR) cm^{-1}: 2126, 1654, 1598, 1584, 1494. ^1H NMR (300 MHz, $CDCl_3$) δ 3.92, 3.94, 3.97 (3s, 6H, 3 × OCH_3), 6.75 (d, J = 8.8 Hz, 1H, C5′-ArH), 7.15 (d, J = 8.5 Hz, 2H, C3-ArH, C5-ArH), 7.41 (d, J = 8.8 Hz, 1H, C6′-ArH), 7.56 (d, J = 15.7 Hz, 1H, CH=CHCO), 8.02 (d, J = 15.7 Hz, 1H, CH=CHCO), 8.06 (d, J = 8.5 Hz, 2H, C2-ArH, C6-ArH). ^{13}C NMR (75 MHz, $CDCl_3$) δ 56.1, 60.9, 61.4, 107.6, 119.0, 120.9, 122.0, 124.0, 130.4, 135.3, 140.3, 142.6, 144.4, 153.9, 155.9, 189.1. HRMS-TOF: m/z HRMS-TOF: m/z $[M+H]^+$ 340.1283 (Calcd for $C_{18}H_{18}N_3O_4$: 340.1292).

*4.3.6. (E)-1-(4-azidophenyl)-3-(3,4,5-trimethoxyphenyl)prop-2-en-1-one (**7f**)*

Yellow solid. 90%. mp 70–71 °C. IR (UATR) cm^{-1}: 2122, 1658, 1599, 1579, 1502. ^1H NMR (300 MHz, $CDCl_3$) δ 3.92, 3.94 (2s, 6H, 3 × OCH_3), 6.88 (s, 2H, C2′-ArH, C6′-ArH), 7.15 (d, J = 8.1 Hz, 2H, C3-ArH, C5-ArH), 7.39 (d, J = 15.5 Hz, 1H, CH=CHCO), 7.75 (d, J = 15.5 Hz, 1H, CH=CHCO), 8.05 (d, J = 8.1 Hz, 2H, C2-ArH, C6-ArH). ^{13}C NMR (75 MHz, $CDCl_3$) δ 56.3, 61.0, 105.8, 119.1, 120.9, 130.3, 130.5, 134.9, 140.6, 144.7, 145.1, 153.5, 188.7. HRMS-TOF: m/z HRMS-TOF: m/z $[M+H]^+$ 340.1288 (Calcd for $C_{18}H_{18}N_3O_4$: 340.1292).

*4.4. General procedure for the synthesis of propynyloxy derivatives (**8a–b**)*

A propargyl bromide (2.4 mmol) was added to a suspension of an appropriate coumarin (2 mmol) and potassium carbonate (4 mmol) in acetone (15 mL). The suspension was heated under reflux for 2 h. The reaction was allowed to cool and then concentrated under reduced pressure. Water (30 mL) was added and extracted with EtOAc (3 × 30 mL). The organic extracts were combined and washed with water (20 mL) and brine (20 mL). The organic layer was dried over anhydrous sodium sulfate, filtered and concentrated *in vacuo*. The crude product was purified by column chromatography.

^1H NMR spectra of 7-(propynyloxy)-2*H*-chromen-2-one (**8a**) [45] and 4-(propynyloxy)-2*H*-chromen-2-one (**8b**) [46] were consistent with those reported in the literatures.

*4.5. General procedure for the synthesis of chalcone–coumarin hybrids (**9–19**)*

To a stirred solution of azidochalcone **7** (0.2 mmol) and alkyne **8** (0.22 mmol) in *t*-BuOH:H_2O (3:3 mL), $CuSO_4 \cdot 5H_2O$ (0.22 mmol) and sodium ascorbate (0.5 mmol) was added. The reaction mixture was stirred at room temperature for 2 h and then concentrated under reduced pressure. The residue was added water (10 mL) and extracted with dichloromethane (3 × 20 mL). The combined organic phases were washed with water (20 mL), dried over anhydrous sodium sulfate and evaporated to dryness. The crude product was purified using silica gel column chromatography and eluted with methanol:dichloromethane (1:50).

*4.5.1. (E)-7-((1-(3-(3-(3,4-dimethoxyphenyl)acryloyl)phenyl)-1H-1,2,3-triazol-4-yl)methoxy)-2H-chromen-2-one (**9**)*

Starting from azidochalcone **7a** and alkyne **8a**. Yellow solid. 65%. mp 132–133 °C. IR (UATR) cm^{-1}: 1723, 1660, 1611, 1576, 1509, 1464. ^1H NMR (300 MHz, $CDCl_3$) δ 3.92, 3.94 (2s, 6H, 2 × OCH_3), 5.35 (s, 2H, CH_2O), 6.25 (d, J = 9.5 Hz, 1H, C3), 6.89 (d, J = 8.3 Hz, 1H, C5″-ArH), 6.92–6.98 (m, 2H, C6 and C8), 7.16 (s, 1H, C2″-ArH), 7.25 (d, J = 8.3 Hz, 1H, C6″-ArH), 7.38 (d, J = 15.6 Hz, 1H, CH=CHCO), 7.39 (d, J = 8.9 Hz, 2H, C5), 7.62 (d, J = 9.5 Hz, 1H, C4), 7.68 (t, J = 7.9 Hz, 1H, C5′-ArH), 7.82 (d, J = 15.6 Hz, 1H, CH=CHCO), 8.01 (d, J = 8.0 Hz, 1H, C4′-ArH), 8.07 (d, J = 7.7 Hz, 1H, C6′-ArH), 8.20 (s, 1H, CHN), 8.32 (s, 1H, C2′-ArH). ^{13}C NMR (75 MHz, $CDCl_3$) δ 56.1, 62.3, 102.2, 110.3, 111.2, 112.7, 113.2, 113.6, 119.0, 120.1, 121.3, 123.6, 124.3, 127.5, 128.7, 129.0, 130.2, 137.3, 140.2, 143.2, 144.1, 146.5, 149.4, 151.9, 155.8, 161.0, 161.2, 188.9. HRMS-TOF: m/z $[M+Na]^+$ 532.1464 (Calcd for $C_{29}H_{23}N_3NaO_6$: 532.1479).

*4.5.2. (E)-7-((1-(3-(3-(2,3-dimethoxyphenyl)acryloyl)phenyl)-1H-1,2,3-triazol-4-yl)methoxy)-2H-chromen-2-one (**10**)*

Starting from azidochalcone **7b** and alkyne **8a**. Pale yellow solid. 61%. mp 131–132 °C. IR (UATR) cm^{-1}: 1726, 1663, 1610, 1587, 1576, 1506, 1478. ^1H NMR (300 MHz, $CDCl_3$) δ 3.88 (s, 6H, 2 × OCH_3), 5.35 (s, 2H, CH_2O), 6.26 (d, J = 9.5 Hz, 1H, C3), 6.93–7.00 (m, 2H, C6, C8

and C4″-Ar*H*), 7.10 (t, *J* = 7.9 Hz, 1H, C5″-Ar*H*), 7.28 (dd, *J* = 7.9, 1.2 Hz, 1H, C6″-Ar*H*), 7.39 (d, *J* = 9.3 Hz, 1H, C5), 7.55–7.71 (m, 3H, C4, C5′-Ar*H* and CH=C*H*CO), 8.05–8.14 (m, 2H, C4′-Ar*H* and C6′-Ar*H*), 8.18 (d, *J* = 15.9 Hz, 1H, C*H*=CHCO), 8.25 (s, 1H, C*H*N), 8.36 (t, *J* = 1.8 Hz, 1H, C2′-Ar*H*). ^{13}C NMR (75 MHz, $CDCl_3$) δ 56.0, 61.4, 62.3, 102.2, 112.7, 113.2, 113.6, 114.7, 119.7, 120.2, 121.2, 122.8, 124.3, 124.4, 128.7, 128.8, 129.0, 130.3, 137.3, 139.9, 141.2, 143.2, 144.1, 149.2, 153.3, 155.8, 161.0, 161.2, 189.3. HRMS-TOF: *m*/*z* [M+Na]$^+$ 532.1488 (Calcd for $C_{29}H_{23}N_3NaO_6$: 532.1479).

4.5.3. (E)-7-((1-(4-(3-(2,3-dimethoxyphenyl)acryloyl)phenyl)-1H-1,2,3-triazol-4-yl)methoxy)-2H-chromen-2-one (**11**)

Starting from azidochalcone **7c** and alkyne **8a**. White solid. 80%. mp 228–229 °C. IR (UATR) cm^{-1}: 1741, 1659, 1621, 1608, 1577, 1479. ^{1}H NMR (300 MHz, DMSO-d_6) δ 3.82, 3.85 (2s, 6H, 2 × OC*H*$_3$), 5.40 (s, 2H, C*H*$_2$O), 6.32 (d, *J* = 9.5 Hz, 1H, C3), 7.06 (dd, *J* = 8.6, 2.4 Hz, 1H, C6), 7.15–7.24 (m, 3H, C8 and C4″-Ar*H*, C5″-Ar*H*), 7.67 (d, *J* = 8.8 Hz, 2H, C5 and C6″-Ar*H*), 7.93–8.08 (m, 3H, C4 and C*H*=C*H*CO), 8.15 (d, *J* = 8.7 Hz, 2H, C3′-Ar*H* and C5′-Ar*H*), 8.37 (d, *J* = 8.7 Hz, 2H, C2′-Ar*H* and C6′-Ar*H*), 9.17 (s, 1H, C*H*N). ^{13}C NMR (75 MHz, DMSO-d_6) δ 56.3, 61.5, 62.1, 102.1, 113.2, 113.3, 113.4, 115.8, 119.7, 120.5, 123.1, 123.8, 124.8, 128.6, 130.1, 130.9, 137.8, 139.0, 139.9, 144.0, 144.7, 148.9, 153.3, 155.8, 160.7, 161.5, 188.6. HRMS-TOF: *m*/*z* [M+Na]$^+$ 532.1480 (Calcd for $C_{29}H_{23}N_3NaO_6$: 532.1479).

4.5.4. (E)-7-((1-(3-(3-(2,3,4-trimethoxyphenyl)acryloyl)phenyl)-1H-1,2,3-triazol-4-yl)methoxy)-2H-chromen-2-one (**12**)

Starting from azidochalcone **7d** and alkyne **8a**. Yellow solid. 74%. mp 120–121 °C. IR (UATR) cm^{-1}: 1725, 1657, 1611, 1578, 1494. ^{1}H NMR (300 MHz, $CDCl_3$) δ 3.92, 3.95, 3.99 (3s, 9H, 3 × OC*H*$_3$), 5.40 (s, 2H, C*H*$_2$O), 6.30 (d, *J* = 9.5 Hz, 1H, C3), 6.76 (d, *J* = 8.8 Hz, 1H, C5″-Ar*H*), 6.97–7.03 (m, 2H, C6 and C8), 7.41–7.47 (m, 2H, C5 and C6″-Ar*H*), 7.58 (d, *J* = 15.8 Hz, 1H, CH=C*H*CO), 7.67 (d, *J* = 9.3 Hz, 2H, C4), 7.71 (t, *J* = 7.9 Hz, 1H, C5′-Ar*H*), 8.02–8.10 (m, 2H, C4′-Ar*H* and C6′-Ar*H*), 8.09 (d, *J* = 15.8 Hz, 1H, C*H*=CHCO), 8.23 (s, 1H, C*H*N), 8.36 (t, *J* = 1.7 Hz, 1H, C2′-Ar*H*). ^{13}C NMR (75 MHz, $CDCl_3$) δ 56.1, 61.0, 61.5, 62.3, 102.2, 107.7, 112.7, 113.2, 113.6, 120.1, 120.4, 121.2, 121.6, 124.2, 128.7, 129.0, 130.2, 137.2, 140.3, 141.6, 142.5, 143.3, 144.1, 154.0, 155.8, 156.3, 161.0, 161.2, 189.3. HRMS-TOF: *m*/*z* [M+Na]$^+$ 562.1585 (Calcd for $C_{30}H_{25}N_3NaO_7$: 562.1585).

4.5.5. (E)-7-((1-(4-(3-(2,3,4-trimethoxyphenyl)acryloyl)phenyl)-1H-1,2,3-triazol-4-yl)methoxy)-2H-chromen-2-one (**13**)

Starting from azidochalcone **7e** and alkyne **8a**. Yellow solid. 50%. mp 221–222 °C. IR (UATR) cm^{-1}: 1737, 1658, 1623, 1605, 1499, 1464. ^{1}H NMR (300 MHz, $CDCl_3$) δ 3.92, 3.94, 3.98 (3s, 9H, 3 × OC*H*$_3$), 5.39 (s, 2H, C*H*$_2$O), 6.30 (d, *J* = 9.6 Hz, 1H, C3), 6.76 (d, *J* = 8.8 Hz, 1H, C5″-Ar*H*), 6.96–7.02 (m, 2H, C6 and C8), 7.40–7.47 (m, 2H, C5 and C6″-Ar*H*), 7.58 (d, *J* = 15.8 Hz, 1H, CH=C*H*CO), 7.67 (d, *J* = 9.5 Hz, 1H, C4), 7.93 (d, *J* = 8.8 Hz, 2H, C3′-Ar*H* and C5′-Ar*H*), 8.06 (d, *J* = 15.8 Hz, 1H, C*H*=CHCO), 8.20 (d, *J* = 8.8 Hz, 2H, C2′-Ar*H* and C6′-Ar*H*), 8.22 (s, 1H, C*H*N). ^{13}C NMR (75 MHz, $CDCl_3$) δ 56.1, 60.9, 61.4, 62.2, 102.2, 107.7, 112.7, 113.2, 113.7, 120.2, 120.6, 121.0, 121.7, 124.2, 129.0, 130.2, 130.6, 138.8, 139.4, 141.3, 142.5, 143.2, 144.2, 154.0, 155.8, 156.2, 161.0, 161.2, 189.3. HRMS-TOF: *m*/*z* [M+H]$^+$ 540.1767 (Calcd for $C_{30}H_{26}N_3O_7$: 540.1765).

4.5.6. (E)-7-((1-(4-(3-(3,4,5-trimethoxyphenyl)acryloyl)phenyl)-1H-1,2,3-triazol-4-yl)methoxy)-2H-chromen-2-one (**14**)

Starting from azidochalcone **7f** and alkyne **8a**. Yellow solid. 87%. mp 223–224 °C. IR (UATR) cm^{-1}: 1705, 1662, 1606, 1580, 1502. ^{1}H NMR (300 MHz, DMSO-d_6) δ 3.72, 3.87 (2s, 9H, 3 × OC*H*$_3$), 5.40 (s, 2H, C*H*$_2$O), 6.32 (d, *J* = 9.5 Hz, 1H, C3), 7.07 (d, *J* = 8.6 Hz, 1H, C6), 7.22 (s, 1H, C8), 7.26 (s, 2H, C2″-Ar*H* and C6″-Ar*H*), 7.67 (d, *J* = 8.6 Hz, 1H, C5), 7.75 (d, *J* = 15.5 Hz, 1H, CH=C*H*CO), 7.95 (d, *J* = 15.5 Hz, 1H, C*H*=CHCO), 7.99 (d, *J* = 9.6 Hz, 1H, C4), 8.14 (d, *J* = 8.4 Hz, 2H, C3′-Ar*H* and C5′-Ar*H*), 8.39 (d, *J* = 8.4 Hz, 2H, C2′-Ar*H* and C6′-Ar*H*), 9.16 (s, 1H, C*H*N). ^{13}C NMR (75 MHz, DMSO-d_6) δ 56.7, 60.6, 62.0, 102.1, 107.2, 113.2, 113.3, 113.4, 120.5, 121.5, 123.8, 126.9, 130.1, 130.6, 130.9, 137.9, 139.9, 140.4, 144.0, 144.7, 145.6, 153.6, 155.8, 160.7, 161.5, 188.5. HRMS-TOF: *m*/*z* [M+Na]$^+$ 562.1569 (Calcd for $C_{30}H_{25}N_3NaO_7$: 562.1585).

4.5.7. (E)-4-((1-(3-(3-(3,4-dimethoxyphenyl)acryloyl)phenyl)-1H-1,2,3-triazol-4-yl)methoxy)-2H-chromen-2-one (**15**)

Starting from azidochalcone **7a** and alkyne **8b**. Yellow solid. 62%. mp 201–202 °C. IR (UATR) cm^{-1}: 1713, 1660, 1622, 1609, 1568, 1510, 1454. ^{1}H NMR (300 MHz, $CDCl_3$) δ 3.96, 3.98 (2s, 6H, 2 × OC*H*$_3$), 5.47 (s, 2H, C*H*$_2$O), 5.94 (s, 1H, C3), 6.93 (d, *J* = 8.3 Hz, 1H, C5″-Ar*H*), 7.20 (s, 1H, C2″-Ar*H*), 7.24–7.37 (m, 3H, C6, C8 and C6″-Ar*H*), 7.44 (d, *J* = 15.6 Hz, 1H, CH=C*H*CO), 7.57 (t, *J* = 8.4 Hz, 1H, C7), 7.73 (t, *J* = 7.9 Hz, 1H, C5′-Ar*H*), 7.87 (d, *J* = 7.9 Hz, 1H, C5), 7.87 (d, *J* = 15.8 Hz, 1H, C*H*=CHCO), 8.03 (d, *J* = 8.0 Hz, 1H, C4′-Ar*H*), 8.13 (d, *J* = 7.7 Hz, 1H, C6′-Ar*H*), 8.33 (s, 1H, C*H*N), 8.39 (s, 1H, C2′-Ar*H*). ^{13}C NMR (75 MHz, $CDCl_3$) δ 56.1, 62.6, 91.3, 110.2, 111.2, 115.4, 116.8, 118.9, 120.1, 121.8, 123.1, 123.7, 124.0, 124.4, 127.4, 128.8, 130.3, 132.6, 137.2, 140.2, 142.6, 146.6, 149.4, 151.9, 153.4, 162.6, 164.9, 188.8. HRMS-TOF: *m*/*z* [M+Na]$^+$ 532.1458 (Calcd for $C_{29}H_{23}N_3NaO_6$: 532.1479).

4.5.8. (E)-4-((1-(3-(3-(2,3-dimethoxyphenyl)acryloyl)phenyl)-1H-1,2,3-triazol-4-yl)methoxy)-2H-chromen-2-one (**16**)

Starting from azidochalcone **7b** and alkyne **8b**. White solid. 88%. mp 137–138 °C. IR (UATR) cm^{-1}: 1713, 1663, 1622, 1608, 1587, 1575, 1478. ^{1}H NMR (300 MHz, $CDCl_3$) δ 3.92 (s, 6H, 2 × OC*H*$_3$), 5.47 (s, 2H, C*H*$_2$O), 5.94 (s, 1H, C3), 7.02 (dd, *J* = 8.1, 1.2 Hz, 1H, C4″-Ar*H*), 7.14 (t, *J* = 8.0 Hz, 1H, C5″-Ar*H*), 7.25–7.37 (m, 3H, C6, C8 and C6″-Ar*H*), 7.57 (dt, *J* = 7.9, 1.5 Hz, 1H, C7), 7.63 (d, *J* = 15.6 Hz, 1H, CH=C*H*CO), 7.74 (t, *J* = 7.9 Hz, 1H, C5′-Ar*H*), 7.85 (dd, *J* = 7.9, 1.4 Hz, 1H, C5), 8.08–8.17 (m, 2H, C4′-Ar*H* and C6′-Ar*H*), 8.19 (d, *J* = 15.9 Hz, 1H, C*H*=CHCO), 8.32 (t, *J* = 1.7 Hz, 1H, C*H*N), 8.38 (s, 1H, C2′-Ar*H*). ^{13}C NMR (75 MHz, $CDCl_3$) δ 55.9, 61.4, 62.6, 91.3, 114.7, 115.4, 116.8, 119.7, 120.2, 121.7, 122.7, 123.2, 124.0, 124.3, 124.5, 128.7, 128.9, 130.3, 132.6, 137.2, 140.0, 141.2, 149.2, 153.3, 153.4, 162.6, 164.9, 189.3. HRMS-TOF: *m*/*z* [M+Na]$^+$ 532.1476 (Calcd for $C_{29}H_{23}N_3NaO_6$: 532.1479).

4.5.9. (E)-4-((1-(3-(3-(2,3,4-trimethoxyphenyl)acryloyl)phenyl)-1H-1,2,3-triazol-4-yl)methoxy)-2H-chromen-2-one (**17**)

Starting from azidochalcone **7d** and alkyne **8b**. Yellow solid. 79%. mp 198–199 °C. IR (UATR) cm^{-1}: 1713, 1660, 1622, 1609, 1579, 1565, 1494, 1464. ^{1}H NMR (300 MHz, $CDCl_3$) δ 3.93, 3.95, 3.97 (3s, 9H, 3 × OC*H*$_3$), 5.47 (s, 2H, C*H*$_2$O), 5.94 (s, 1H, C3), 6.76 (d, *J* = 8.8 Hz, 1H, C5″-Ar*H*), 7.28 (dt, *J* = 7.6, 1.0 Hz, 1H, C6), 7.35 (d, *J* = 8.4 Hz, 1H, C8), 7.44 (d, *J* = 8.8 Hz, 1H, C6″-Ar*H*), 7.58 (dt, *J* = 7.8, 1.6 Hz, 1H, C7), 7.59 (d, *J* = 15.8 Hz, 1H, CH=C*H*CO), 7.73 (t, *J* = 7.9 Hz, 1H, C5′-Ar*H*), 7.85 (dd, *J* = 7.9, 1.5 Hz, 1H, C5), 8.09 (d, *J* = 15.8 Hz, 1H, C*H*=CHCO), 8.08–8.16 (m, 2H, C4′-Ar*H* and C6′-Ar*H*), 8.32 (s, 1H, C*H*N), 8.38 (t, *J* = 1.7 Hz, 1H, C2′-Ar*H*). ^{13}C NMR (75 MHz, $CDCl_3$) δ 56.1, 61.0, 61.5, 62.6, 91.3, 107.7, 115.4, 116.8, 120.2, 120.3, 121.6, 121.7, 123.2, 124.0, 124.2, 124.3, 128.9, 130.3, 132.6, 137.1, 140.3, 141.7, 142.5, 153.4, 154.0, 156.3, 162.6, 165.0, 189.3. HRMS-TOF: *m*/*z* [M+Na]$^+$ 562.1591 (Calcd for $C_{30}H_{25}N_3NaO_7$: 562.1585).

4.5.10. (E)-4-((1-(4-(3-(2,3,4-trimethoxyphenyl)acryloyl)phenyl)-1H-1,2,3-triazol-4-yl)methoxy)-2H-chromen-2-one (**18**)

Starting from azidochalcone **7e** and alkyne **8b**. Yellow solid. 70%. mp 151–152 °C. IR (UATR) cm^{-1}: 1717, 1660, 1621, 1606, 1563, 1494, 1464. ^{1}H NMR (300 MHz, $CDCl_3$) δ 3.88, 3.91, 3.95 (3s, 9H, 3 × OC*H*$_3$), 5.43 (s, 2H, C*H*$_2$O), 5.90 (s, 1H, C3), 6.73 (d, *J* = 8.8 Hz, 1H, C5″-Ar*H*),

7.25 (t, J = 7.2 Hz, 1H, C6), 7.31 (d, J = 8.3 Hz, 2H, C8), 7.40 (d, J = 8.8 Hz, 1H, C6″-Ar*H*), 7.54 (t, J = 7.3 Hz, 1H, C7), 7.55 (d, J = 15.8 Hz, 1H, CH=C*H*CO), 7.80 (d, J = 7.8 Hz, 1H, C5), 7.92 (d, J = 8.6 Hz, 2H, C3′-Ar*H* and C5′-Ar*H*), 8.03 (d, J = 15.8 Hz, 1H, C*H*=CHCO), 8.18 (d, J = 8.6 Hz, 2H, C2′-Ar*H* and C6′-Ar*H*), 8.29 (s, 1H, C*H*N). ^{13}C NMR (75 MHz, $CDCl_3$) δ 56.1, 61.0, 61.5, 62.5, 91.4, 107.7, 115.4, 116.8, 120.3, 120.6, 121.7, 123.1, 124.0, 124.2, 130.3, 132.7, 139.0, 139.3, 141.4, 153.4, 154.0, 156.2, 162.5, 164.9, 189.3. HRMS-TOF: m/z $[M+H]^+$ 540.1776 (Calcd for $C_{30}H_{26}N_3O_7$: 540.1765).

4.5.11. (E)-4-((1-(4-(3-(3,4,5-trimethoxyphenyl)acryloyl)phenyl)-1H-1,2,3-triazol-4-yl)methoxy)-2H-chromen-2-one (**19**)

Starting from azidochalcone **7f** and alkyne **8b**. Yellow solid. 86%. mp 229–230 °C. IR (UATR) cm^{-1}: 1712, 1687, 1659, 1623, 1606, 1583, 1505, 1455. ^{1}H NMR (300 MHz, DMSO-d_6) δ 3.72, 3.88 (2s, 9H, 3 × OC*H*$_3$), 5.56 (s, 2H, C*H*$_2$O), 6.22 (s, 1H, C3), 7.27 (s, 2H, C2″-Ar*H* and C6″-Ar*H*), 7.36 (t, J = 7.7 Hz, 1H, C6), 7.42 (d, J = 8.3 Hz, 1H, C8), 7.67 (dt, J = 8.3, 1.4 Hz, 1H, C7), 7.76 (d, J = 15.5 Hz, 1H, CH=C*H*CO), 7.85 (dd, J = 7.8, 1.2 Hz, 1H, C5), 7.96 (d, J = 15.6 Hz, 1H, C*H*=CHCO), 8.18 (d, J = 8.6 Hz, 2H, C3′-Ar*H* and C5′-Ar*H*), 8.40 (d, J = 8.7 Hz, 2H, C2′-Ar*H* and C6′-Ar*H*), 9.25 (s, 1H, C*H*N). ^{13}C NMR (75 MHz, DMSO-d_6) δ 56.7, 60.6, 63.2, 92.0, 107.2, 115.5, 116.9, 120.6, 121.5, 123.5, 124.1, 124.7, 130.6, 130.9, 133.4, 138.0, 139.9, 143.1, 145.6, 153.3, 153.6, 162.0, 164.8, 188.5. HRMS-TOF: m/z $[M+Na]^+$ 562.1581 (Calcd for $C_{30}H_{25}N_3NaO_7$: 562.1585).

4.6. Cytotoxic assay: cancer cell lines

The cells suspended in the corresponding culture medium were inoculated in 96-well microtiter plates (Corning Inc., NY, USA) at a density of 10,000–20,000 cells per well, and incubated for 24 h at 37 °C in a humidified atmosphere with 95% air and 5% CO_2. An equal volume of additional medium containing either the serial dilutions of the test compounds, positive control (etoposide and/or doxorubicin), or negative control (DMSO) was added to the desired final concentrations, and the microtiter plates were further incubated for an additional 48 h. The number of surviving cells in each well was determined using MTT assay [47,48] (for adherent cells: HuCCA-1, HepG2, and A549 cells) and XTT assay [49] (for suspended cells: MOLT-3 cells). The IC_{50} value is defined as the drug (or compound) concentration that inhibits cell growth by 50% (relative to negative control).

4.7. Antimalarial assay: radioisotope techniques

P. falciparum (K1, multidrug resistant strain) was cultivated *in vitro* conditions, according to Trager & Jensen (1976) [50], in RPMI 1640 medium containing 20 mM HEPES (*N*-2-hydroxyethylpiperazine-*N*′-2-ethanesulfonic acid), 32 mM $NaHCO_3$ and 10% heat activated human serum with 3% erythrocytes, in humidified 37 °C incubator with 3% CO_2. The culture was passaged with fresh mixture of erythrocytes and medium for every day to maintain cell growth. Quantitative assessment of antimalarial activity *in vitro* was determined by microculture radioisotope techniques based upon the methods described by Desjardins et al. (1979) [51]. Briefly, a mixture of 200 μL of 1.5% erythrocytes with 1% parasitemia at the early ring stage was pre-exposed to 25 μL of the medium containing a test sample dissolved in 1% DMSO (0.1% final concentration) for 24 h. Subsequently, 25 μL of [3H] hypoxanthine (Amersham, USA) in culture medium (0.5 μCi) was added to each well and the plates were incubated for an additional 24 h. Levels of incorporated radioactive labeled hypoxanthine, indicating parasite growth, were determined using the Top Count microplate scintillation counter (Packard, USA). The percentage of parasite growth was calculated using the signal count per minute of treated (CPMT) and untreated conditions (CPMU) as shown by the following equation;

$$\%\ \text{parasite growth} = \text{CPMT}/\text{CPMU} \times 100$$

4.8. Cytotoxicity assay: primate cell line (Vero)

The cytotoxicity assay was performed using the Green Fluorescent Protein (GFP) detection method [52]. The GFP-expressing Vero cell line was generated in-house by stably transfecting the African green monkey kidney cell line (Vero, ATCC CCL-81), with pEGFP-N1 plasmid (Clontech). The cell line was maintained in a minimal essential medium supplemented with 10% heat-inactivated fetal bovine serum, 2 mM L-glutamine, 1 mM sodium pyruvate, 1.5 g/L sodium bicarbonate and 0.8 mg/mL geneticin, at 37 °C in a humidified incubator with 5% CO_2. The assay was carried out by adding 45 μL of cell suspension at 3.3×10^4 cells/mL to each well of 384-well plates containing 5 μL of test compounds previously diluted in 0.5% DMSO, and then incubating for 4 days at 37 °C incubator with 5% CO_2. Fluorescence signals were measured by using SpectraMax M5 microplate reader (Molecular Devices, USA) in the bottom reading mode with excitation and emission wavelengths of 485 and 535 nm, respectively. Fluorescence signal at day 4 was subtracted with background fluorescence at day 0. IC_{50} values were derived from dose–response curves, using 6 concentrations of 3-fold serially diluted samples, by the SOFTMax Pro software (Molecular device). Ellipticine and 0.5% DMSO were used as a positive and a negative control, respectively.

4.9. Molecular docking

Molecular docking was performed to investigate the binding modalities of ligands toward possible targets comprising of falcipain-2 (PDB id 3BPF), a cysteine protease from *P. falciparum*, as well as α- and β-tubulin complexes (PDB id 1SA0) from Bos taurus. Protein structures were prepared for docking by adding essential hydrogen atoms and modeling missing side chains using the WHAT IF web server version 10.1a [53]. Furthermore, non-polar hydrogen atoms were merged, Gasteiger atomic charges were assigned, and atom type of receptors were specified using AutoDock Tools version 1.5.6. [54,55]. Chalcone–triazole–coumarin ligands were constructed using Marvin Sketch version 6.1.4 [56] and geometrically optimized with Gaussian 09 [57] at the B3LYP/6-31G(d) level of theory. Ligand structures were prepared for docking by merging non-polar hydrogen atoms and defining rotatable bonds using AutoDock Tools version 1.5.6. Partial atomic charges calculated by Gaussian 09 were assigned to ligands for further use in the docking process. A grid box size of 25.0, 25.0, 25.0 Å was generated and allocated at the center of the receptor binding site using x, y and z coordinates of −91.5906, 5.0925 and −21.4080 for falcipain-2 and 118.4155, 89.6890 and 6.2141 for α- and β-tubulin complexes. Molecular docking simulations were performed using AutoDock Vina as part of the PyRx 0.8 software [58]. Co-crystallized ligands were re-docked as validation of the docking protocol. Docked structures were visualized using PyMOL [59]. Two-dimensional schematic representation of protein-ligand interaction was generated using PoseViewWeb version 1.97.0 [60].

Acknowledgments

This project is supported by the research grants from Srinakharinwirot University under the Government Budget (B.E. 2559). We would like to thank the Thailand Research Fund, the office of the Higher Education Commission, and Srinakharinwirot University

(Grant No. MRG5680001) for financial support. Great supports from the office of the Higher Education Commission and Mahidol University under the National Research Universities Initiative are appreciated. We are also indebted to Chulabhorn Research Institute for recording mass spectra and bioactivity testing.

Appendix A. Supplementary data

Supplementary data related to this article can be found at http://dx.doi.org/10.1016/j.ejmech.2014.07.087.

References

[1] N.K. Sahu, S.S. Balbhadra, J. Choudhary, D.V. Kohli, Exploring pharmacological significance of chalcone scaffold: a review, Curr. Med. Chem. 19 (2012) 209–225.
[2] L. Ni, C.Q. Meng, J.A. Sikorski, Recent advances in therapeutic chalcones, Expert Opin. Ther. Pat. 14 (2004) 1669–1691.
[3] D.I. Batovska, I.T. Todorova, Trends in utilization of the pharmacological potential of chalcones, Curr. Clin. Pharmacol. 5 (2010) 1–29.
[4] J.R. Dimmock, D.W. Elias, M.A. Beazely, N.M. Kandepu, Bioactivities of chalcones, Curr. Med. Chem. 6 (1999) 1125–1149.
[5] M.L. Go, X. Wu, X.L. Liu, Chalcones: an update on cytotoxic and chemoprotective properties, Curr. Med. Chem. 12 (2005) 483–499.
[6] S. Ducki, Antimitotic chalcones and related compounds as inhibitors of tubulin assembly, Anticancer Agents Med. Chem. 9 (2009) 336–347.
[7] C. Dyrager, M. Wickström, M. Fridén-Saxin, A. Friberg, K. Dahlén, E.A.A. Wallén, J. Gullbo, M. Grøtli, K. Luthman, Inhibitors and promoters of tubulin polymerization: synthesis and biological evaluation of chalcones and related dienones as potential anticancer agents, Bioorg. Med. Chem. 19 (2011) 2659–2665.
[8] M. Chen, T.G. Theander, S.B. Christensen, L. Hviid, L. Zhai, A. Kharazmi, Licochalcone A, a new antimalarial agent, inhibits *in vitro* growth of the human malaria parasite *Plasmodium falciparum* and protects mice from *P. yoelii* infection, Antimicrob. Agents Chemother. 38 (1994) 1470–1475.
[9] N. Sriwilaijaroen, M. Liu, M.-L. Go, P. Wilairat, Plasmepsin II inhibitory activity of alkoxylated and hydroxylated chalcones, Southeast Asian J. Trop. Med. Public Health 37 (2006) 607–612.
[10] G. Wanare, R. Aher, N. Kawathekar, R. Ranjan, N.K. Kaushik, D. Sahal, Synthesis of novel alpha-pyranochalcones and pyrazoline derivatives as *Plasmodium falciparum* growth inhibitors, Bioorg. Med. Chem. Lett. 420 (2010) 4675–4678.
[11] R. Li, G.L. Kenyon, F.E. Cohen, X. Chen, B. Gong, J.N. Dominguez, E. Davidson, G. Kurzban, R.E. Miller, E.O. Nuzum, P.J. Rosenthal, J.H. McKerrow, *In vitro* antimalarial activity of chalcones and their derivatives, J. Med. Chem. 38 (1995) 5031–5037.
[12] R.H. Hans, J. Gut, P.J. Rosenthal, K. Chibale, Comparison of the antiplasmodial and falcipain-2 inhibitory activity of β-amino alcohol thiolactone-chalcone and isatin-chalcone hybrids, Bioorg. Med. Chem. Lett. 20 (2010) 2234–2237.
[13] J.A. Geyer, S.M. Keenan, C.L. Woodard, P.A. Thompson, L. Gerena, D.A. Nichols, C.E. Gutteridge, N.C. Waters, Selective inhibition of Pfmrk, a *Plasmodium falciparum* CDK, by antimalarial 1,3-diaryl-2-propenones, Bioorg. Med. Chem. Lett. 19 (2009) 1982–1985.
[14] M.-L. Go, M. Liu, P. Wilairat, P.J. Rosenthal, K.J. Saliba, K. Kirk, Antiplasmodial chalcones inhibit sorbitol-induced hemolysis of *Plasmodium falciparum*-infected erythrocytes, Antimicrob. Agents Chemother. 48 (2004) 3241–3245.
[15] M. Larsen, H. Kromann, A. Kharazmi, S.F. Nielsen, Conformationally restricted anti-plasmodial chalcones, Bioorg. Med. Chem. Lett. 15 (2005) 4858–4861.
[16] M. Liu, P. Wilairat, M.-L. Go, Antimalarial alkoxylated and hydroxylated chalcones: structure-activity relationship analysis, J. Med. Chem. 44 (2001) 4443–4452.
[17] F. Borges, F. Roleira, N. Milhazes, L. Santana, E. Uriarte, Simple coumarins and analogues in medicinal chemistry: occurrence, synthesis and biological activity, Curr. Med. Chem. 12 (2005) 887–916.
[18] I. Kostova, Synthetic and natural coumarins as cytotoxic agents, Curr. Med. Chem. Anticancer Agents 5 (2005) 29–46.
[19] A. Lacy, R. O'Kennedy, Studies on coumarins and coumarin-related compounds to determine their therapeutic role in the treatment of cancer, Curr. Pharm. Des. 10 (2004) 3797–3811.
[20] Coumarins. Biology, Applications and Mode of Action, Wiley, New York, 1997.
[21] Y.-Z. Yang, A. Ranz, H.-Z. Pan, Z.-N. Zhang, X.-B. Lin, S.R. Meshnick, Daphnetin: a novel antimalarial agent with *in vitro* and *in vivo* activity, Am. J. Trop. Med. Hyg. 46 (1992) 15–20.
[22] K. Nepali, S. Sharma, M. Sharma, P.M.S. Bedi, K.L. Dhar, Rational approaches, design strategies, structure activity relationship and mechanistic insights for anticancer hybrids, Eur. J. Med. Chem. 77 (2014) 422–487.
[23] F.W. Muregi, A. Ishih, Next-generation antimalarial drugs: hybrid molecules as a new strategy in drug design, Drug Dev. Res. 71 (2010) 20–32.
[24] C. Hubschwerlen, J.L. Specklin, C. Sigwalt, S. Schroeder, H.H. Locher, Design, synthesis and biological evaluation of oxazolidinone-quinolone hybrids, Bioorg. Med. Chem. 11 (2003) 2313–2319.
[25] R. Pingaew, S. Prachayasittikul, S. Ruchirawat, V. Prachayasittikul, Synthesis and cytotoxicity of novel 4-(4-(substituted)-1*H*-1,2,3-triazol-1-yl)-*N*-phenethylbenzenesulfonamides, Med. Chem. Res. 23 (2014) 1768–1780.
[26] E.M. Guantai, K. Ncokazi, T.J. Egan, J. Gut, P.J. Rosenthal, P.J. Smith, K. Chibale, Design, synthesis and *in vitro* antimalarial evaluation of triazole-linked chalcone and dienone hybrid compounds, Bioorg. Med. Chem. 18 (2010) 8243–8256.
[27] K.V. Sashidhara, S.R. Avula, G.R. Palnati, S.V. Singh, K. Srivastava, S.K. Puri, J.K. Saxena, Synthesis and *in vitro* evaluation of new chloroquine-chalcone hybrids against chloroquine-resistant strain of *Plasmodium falciparum*, Bioorg. Med. Chem. Lett. 22 (2012) 5455–5459.
[28] K.V. Sashidhara, M. Kumar, R.K. Modukuri, R.K. Srivastava, A. Soni, K. Srivastava, S.V. Singh, J.K. Saxena, H.M. Gauniyal, S.K. Puri, Antiplasmodial activity of novel keto-enamine chalcone-chloroquine based hybrid pharmacophores, Bioorg. Med. Chem. 20 (2012) 2971–2981.
[29] A. Kamal, S. Prabhakar, M.J. Ramaiah, P.V. Reddy, Ch.R. Reddy, A. Mallareddy, N. Shankaraiah, T.L.N. Reddy, S.N.C.V.L. Pushpavalli, M. Pal-Bhadra, Synthesis and anticancer activity of chalcone-pyrrolobenzodiazepine conjugates linked *via* 1,2,3-triazole ring side-armed with alkane spacers, Eur. J. Med. Chem. 46 (2011) 3820–3831.
[30] M. Abdel-Aziz, S.-E. Park, G.E.-D.A.A. Abuo-Rahma, M.A. Sayed, Y. Kwon, Novel *N*-4-piperazinyl-ciprofloxacin-chalcone hybrids: synthesis, physicochemical properties, anticancer and topoisomerase I and II inhibitory activity, Eur. J. Med. Chem. 69 (2013) 427–438.
[31] P. Singh, R. Raj, V. Kumar, M.P. Mahajan, P.M.S. Bedi, T. Kaur, A.K. Saxena, 1,2,3-Triazole tethered β-lactam-chalcone bifunctional hybrids: synthesis and anticancer evaluation, Eur. J. Med. Chem. 47 (2012) 594–600.
[32] M.A.E. Mourad, M. Abdel-Aziz, G.E.-D.A.A. Abuo-Rahma, H.H. Farag, Design, synthesis and anticancer activity of nitric oxide donating/chalcone hybrids, Eur. J. Med. Chem. 54 (2012) 907–913.
[33] X. Dong, L. Du, Z. Pan, T. Liu, B. Yang, Y. Hu, Synthesis and biological evaluation of novel hybrid chalcone derivatives as vasorelaxant agents, Eur. J. Med. Chem. 45 (2010) 3986–3992.
[34] F. Pérez-Cruz, S. Vazquez-Rodriguez, M.J. Matos, A. Herrera-Morales, F.A. Villamena, A. Das, B. Gopalakrishnan, C. Olea-Azar, L. Santana, E. Uriarte, Synthesis and electrochemical and biological studies of novel coumarin-chalcone hybrid compounds, J. Med. Chem. 56 (2013) 6136–6145.
[35] S. Vazquez-Rodriguez, R. Figueroa-Guíñez, M.J. Matos, L. Santana, E. Uriarte, M. Lapier, J.D. Maya, C. Olea-Azar, Synthesis of coumarin-chalcone hybrids and evaluation of their antioxidant and trypanocidal properties, MedChemComm 4 (2013) 993–1000.
[36] K.V. Sashidhara, M. Kumar, R.K. Modukuri, R. Sonkar, G. Bhatia, A.K. Khanna, S. Rai, R. Shukla, Synthesis and anti-inflammatory activity of novel biscoumarin–chalcone hybrids, Bioorg. Med. Chem. Lett. 21 (2011) 4480–4484.
[37] E. Bombardelli, P. Valenti, Preparation of 8-(Arylpropenoyl)coumarins as Antiproliferative Agents. PCT Int. Pub. No. WO 01/17984 A1, 2001.
[38] K.V. Sashidhara, A. Kumar, M. Kumar, J. Sarkar, S. Sinha, Synthesis and *in vitro* evaluation of novel coumarin-chalcone hybrids as potential anticancer agents, Bioorg. Med. Chem. Lett. 20 (2010) 7205–7211.
[39] K. Patel, C. Karthikeyan, N.S. Hari Narayana Moorthy, G.S. Deora, V.R. Solomon, H. Lee, P. Trivedi, Design, synthesis and biological evaluation of some novel 3-cinnamoyl-4-hydroxy-2*H*-chromen-2-ones as antimalarial agents, Med. Chem. Res. 21 (2012) 1780–1784.
[40] S.G. Agalave, S.R. Maujan, V.S. Pore, Click chemistry: 1,2,3-triazoles as pharmacophores, Chem. Asian J. 6 (2011) 2696–2718.
[41] I.D. Kerr, J.H. Lee, K.C. Pandey, A. Harrison, M. Sajid, P.J. Rosenthal, L.S. Brinen, Structures of falcipain-2 and falcipain-3 bound to small molecule inhibitors: implications for substrate specificity, J. Med. Chem. 52 (2009) 852–857.
[42] V. Prachayasittikul, S. Prachayasittikul, S. Ruchirawat, V. Prachayasittikul, 8-Hydroxyquinolines: a review of their metal chelating properties and medicinal applications, Drug Des. Dev. Ther. 7 (2013) 1157–1178.
[43] J. Wu, J. Li, Y. Cai, Y. Pan, F. Ye, Y. Zhang, Y. Zhao, S. Yang, X. Li, G. Liang, Evaluation and discovery of novel synthetic chalcone derivatives as anti-inflammatory agents, J. Med. Chem. 54 (2011) 8110–8123.
[44] Y.R. Prasad, A.S. Rao, R. Rambabu, Synthesis of some 4′-amino chalcones and their antiinflammatory and antimicrobial activity, Asian J. Chem. 21 (2009) 907–914.
[45] I. Kosiova, S. Kovackova, P. Kois, Synthesis of coumarin–nucleoside conjugates *via* Huisgen 1,3-dipolar cycloaddition, Tetrahedron 63 (2007) 312–320.
[46] C.P. Rao, G. Srimannarayana, Claisen rearrangement of 4-propargloxycoumarins: formation of 2*H*,5*H*-Pyrano[3,2-*c*][1]benzopyran-5-ones, Syn. Comm. 20 (1990) 535–540.
[47] J. Carmichael, W.G. DeGraff, A.F. Gazdar, J.D. Minna, J.B. Mitchell, Evaluation of a tetrazolium-based semiautomated colorimetric assay: assessment of radiosensitivity, Cancer Res. 47 (1987) 943–946.
[48] T. Mosmann, Rapid colorimetric assay for cellular growth and survival: application to proliferation and cytotoxicity assays, J. Immunol. Methods 65 (1983) 55–63.
[49] A. Doyle, J.B. Griffiths, Mammalian Cell Culture: Essential Techniques, John Wiley & Sons, Chichester, UK, 1997.
[50] W. Trager, J.B. Jensen, Human malaria parasites in continuous culture, Science 193 (1976) 673–675.
[51] R.E. Desjardins, C.J. Canfield, J.D. Haynes, J.D. Chulay, Quantitative assessment of antimalarial activity *in vitro* by a semiautomated microdilution technique, Antimicrob. Agents Chemother. 16 (1979) 710–718.

[52] L. Hunt, M. Jordan, M. De Jesus, F.M. Wurm, GFP-expressing mammalian cells for fast, sensitive, noninvasive cell growth assessment in a kinetic mode, Biotechnol. Bioeng. 65 (1999) 201–205.
[53] R. Rodriguez, G. Chinea, N. Lopez, T. Pons, G. Vriend, Homology modeling, model and software evaluation: three related resources, Bioinformatics 14 (1998) 523–528.
[54] M.F. Sanner, Python: a programming language for software integration and development, J. Mol. Graph. Mod. 17 (1999) 57–61.
[55] G.M. Morris, R. Huey, W. Lindstrom, M.F. Sanner, R.K. Belew, D.S. Goodsell, A.J. Olson, Autodock4 and AutoDockTools4: automated docking with selective receptor flexibility, J. Comput. Chem. 16 (2009) 2785–2791.
[56] ChemAxon Marvin Sketch Version 6.0, 2013 (Budapest, Hungary).
[57] M.J. Frisch, G.W. Trucks, H.B. Schlegel, G.E. Scuseria, M.A. Robb, J.R. Cheeseman, G. Scalmani, V. Barone, B. Mennucci, G.A. Petersson, H. Nakatsuji, M. Caricato, X. Li, H.P. Hratchian, A.F. Izmaylov, J. Bloino, G. Zheng, J.L. Sonnenberg, M. Hada, M. Ehara, K. Toyota, R. Fukuda, J. Hasegawa, M. Ishida, T. Nakajima, Y. Honda, O. Kitao, H. Nakai, T. Vreven, J.A. Montgomery, J.E. Peralta, F. Ogliaro, M. Bearpark, J.J. Heyd, E. Brothers, K.N. Kudin, V.N. Staroverov, R. Kobayashi, J. Normand, K. Raghavachari, A. Rendell, J.C. Burant, S.S. Iyengar, J. Tomasi, M. Cossi, N. Rega, J.M. Millam, M. Klene, J.E. Knox, J.B. Cross, V. Bakken, C. Adamo, J. Jaramillo, R. Gomperts, R.E. Stratmann, O. Yazyev, A.J. Austin, R. Cammi, C. Pomelli, J.W. Ochterski, R.L. Martin, K. Morokuma, V.G. Zakrzewski, G.A. Voth, P. Salvador, J.J. Dannenberg, S. Dapprich, A.D. Daniels, Farkas, J.B. Foresman, J.V. Ortiz, J. Cioslowski, D.J. Fox, Gaussian 09, 2009 (Wallingford, Connecticut).
[58] S. Dallakyan, PyRx Version 0.8, 2013. http://pyrx.scripps.edu.
[59] W. Delano, PyMOL Release 0.99, DeLano Scientific LLC, Palo Alto, CA, 2002.
[60] K. Stierand, M. Rarey, Drawing the PDB: protein-ligand complexes in two dimensions, ACS Med. Chem. Lett. 1 (2010) 540–545.

European Journal of Medicinal Chemistry 81 (2014) 192–203

Contents lists available at ScienceDirect

European Journal of Medicinal Chemistry

journal homepage: http://www.elsevier.com/locate/ejmech

Original article

Design, synthesis and molecular docking studies of novel *N*-benzenesulfonyl-1,2,3,4-tetrahydroisoquinoline-based triazoles with potential anticancer activity

Ratchanok Pingaew [a,*], Prasit Mandi [b,c], Chanin Nantasenamat [b,c], Supaluk Prachayasittikul [b], Somsak Ruchirawat [d,e,f], Virapong Prachayasittikul [c]

[a] Department of Chemistry, Faculty of Science, Srinakharinwirot University, Bangkok 10110, Thailand
[b] Center of Data Mining and Biomedical Informatics, Faculty of Medical Technology, Mahidol University, Bangkok 10700, Thailand
[c] Department of Clinical Microbiology and Applied Technology, Faculty of Medical Technology, Mahidol University, Bangkok 10700, Thailand
[d] Laboratory of Medicinal Chemistry, Chulabhorn Research Institute, Bangkok 10210, Thailand
[e] Program in Chemical Biology, Chulabhorn Graduate Institute, Bangkok 10210, Thailand
[f] Center of Excellence on Environmental Health and Toxicology, Commission on Higher, Education (CHE), Ministry of Education, Thailand

ARTICLE INFO

Article history:
Received 23 December 2013
Received in revised form
1 May 2014
Accepted 4 May 2014
Available online 6 May 2014

Keywords:
Isoquinoline
Triazole
Pictet–Spengler reaction
Antiproliferative activity
Molecular docking
AKR1C3

ABSTRACT

A novel series of *N*-benzenesulfonyl-1,2,3,4-tetrahydroisoquinolines (**14**–**33**) containing triazole moiety were designed and synthesized through rational cycloadditions using the modified Pictet–Spengler reaction and the Click chemistry. Antiproliferative activity against four cancer cell lines (e.g., HuCCA-1, HepG2, A549 and MOLT-3) revealed that many substituted triazole analogs of benzoates (**20**, **29**) and benzaldehydes (**30**, **32**) exhibited anticancer activity against all of the tested cancer cell lines in which the ester analog **20** was shown to be the most potent compound against HuCCA-1 ($IC_{50} = 0.63$ μM) and A549 ($IC_{50} = 0.57$ μM) cell lines. Triazoles bearing phenyl (**15**, **24**), tolyl (**26**, **27**), acetophenone (**19**), benzoate (**20**, **29**), benzaldehyde (**21**, **30**) and naphthalenyl (**25**) substituents showed stronger anticancer activity against HepG2 cells than that of the etoposide. Interestingly, the *p*-tolyl analog (**27**) displayed the most potent inhibitory activity ($IC_{50} = 0.56$ μM) against HepG2 cells without affecting normal cells. Of the investigated tetrahydroisoquinoline-triazoles, the promising compounds **20** and **27** were selected for molecular docking against AKR1C3, which was identified to be a plausible target site.

© 2014 Elsevier Masson SAS. All rights reserved.

1. Introduction

Isoquinoline alkaloid is a class of natural products that possess a broad spectrum of pharmacological actions, particularly, anticancer activity [1–3]. A variety of bioactive 1,2,3,4-tetrahydroisoquinolines (THIQs) have been reported. Generally, THIQs are synthesized by the Pictet–Spengler reaction involving the cyclization of iminium ions derived from the condensation of β-arylethylamines with aldehydes [4,5]. The modified Pictet–Spengler protocol was accomplished by increasing the electrophilicity of the iminium intermediates using *N*-sulfonylphenethylamines as starting materials to yield *N*-sulfonyl-1,2,3,4-tetrahydroisoquinoline products. Such *N*-sulfonyl-THIQs have been proven to be interesting scaffolds for medical applications [6,7]. 1,2,3,4-Tetrahydro-6,7-dimethoxy-2-[(4-methylphenyl)sulfonyl]-1-(2-hydroxyphenylisoquinoline) (**1**) and 1-acetyl-6,7-dimethoxy-*N*-4-methoxybenzenesulfonyl-1,2,3,4-tetrahydroisoquinoline thiosemicarbazone (**2**) exhibited cytotoxic activity reported by our group as shown in Fig. 1 [6,7]. Furthermore, *N*-sulfonyl-THIQ (**3**) and *N*-sulfonyl-THIQs with hydroxamate (**4**) and carboxylate (**5**) have been revealed to act as carbonic anhydrase and matrix-matalloproteinase inhibitors, respectively (Fig. 1) [8–10]. Additionally, 3-(3,4-dihydroisoquinolin-2(1*H*)-ylsulfonyl)benzoic acid (**6**) was shown to be selective and potent inhibitor of an aldo-keto reductase 1C3 (AKR1C3) [11]. Replacement of the carboxyl group with pyrrolidin-2-one core as compound **7** retained the activity, but with 3-fold less potent than the parent compound **6**. The structure–activity relationship (SAR) results of THIQs **6** and **7** showed that the sulfonamide moiety was critical for AKR1C3 inhibitory activity [12].

AKR1C3, a member of the aldo-keto reductase superfamily of enzymes, plays an important role in stereospecific reduction of carbonyl groups on both steroid and prostaglandin substrates using

* Corresponding author.
E-mail address: ratchanok@swu.ac.th (R. Pingaew).

http://dx.doi.org/10.1016/j.ejmech.2014.05.019
0223-5234/© 2014 Elsevier Masson SAS. All rights reserved.

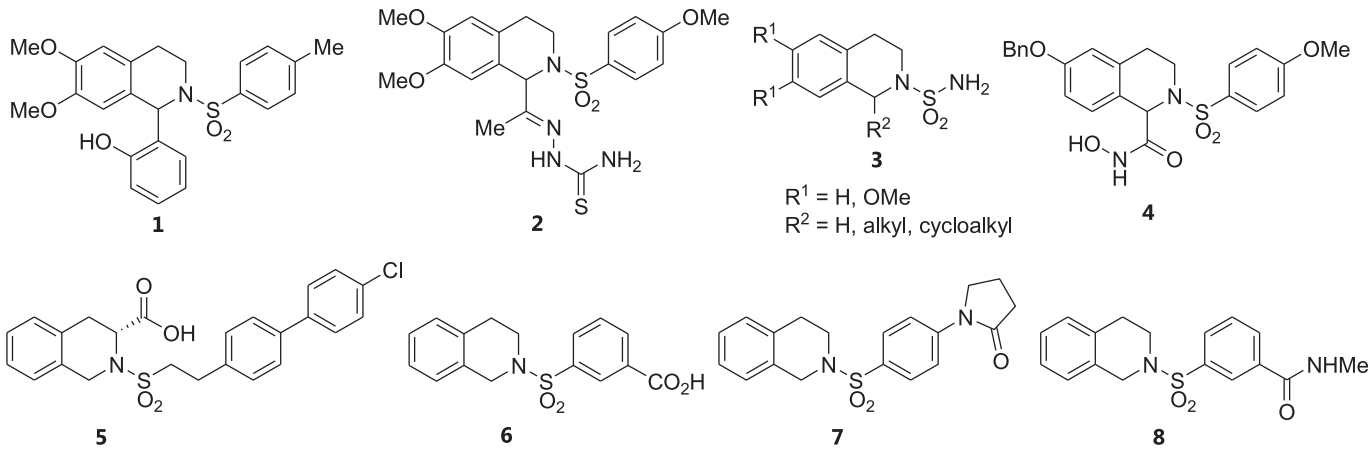

Fig. 1. Representative structures of bioactive *N*-sulfonyl-1,2,3,4-tetrahydroisoquinolines **1**–**8**.

NADPH as a cofactor [13–16]. The reduction products of AKR1C3-promoted reaction such as testosterone, 17β-estradiol, 20α-hydroxy progesterone and $PGF_{2\alpha}$ can stimulate tumor growth, therefore AKR1C3 expression levels are correlated with both hormone-dependent and hormone-independent cancers [15]. AKR1C3 is over-expressed in a number of cancers, particularly, in the prostate and mammary gland where it is responsible for the production of a series of growth-stimulatory steroid hormones. Consequently, inhibition of the catalytic activity renders AKR1C3 as an attractive therapeutic target for treating various types of cancer and for the development of novel anticancer drugs.

Triazole moiety is a common pharmacophore found in a diverse range of biologically active molecules [17,18]. Potential structural features of bioactive triazole include capability of hydrogen bonding, stable to metabolic degradation, high selectivity and less unfavorable reactions. Molecules linking with triazole scaffold are considered to improve their pharmacological activities [19,20]. Importantly, substituted triazole analogs **9**–**12** (Fig. 2) have been used in clinical trials for cancer therapy [17,18]. Recently, our group reported that an open chain analog of *N*-sulfonyl-THIQ bearing triazole, methyl 2-((1-(4-(*N*-phenethylsulfamoyl)phenyl)-1*H*-1,2,3-triazol-4-yl)methoxy)benzoate (**13**), displayed antiproliferative activity against cancer cell lines (e.g., HepG2 and MOLT-3) [20].

The reported bioactive pharmacophores lead to the rational design of new THIQ rigid analogs based on the triazole moiety. As part of our ongoing research, a new series of hybrid molecules containing both THIQ and triazole were designed and synthesized. Thus, target molecules **14**–**33** (Fig. 3) were obtained by the replacement of a phenethylamine moiety of compound **13** with a restricted THIQ ring and by the replacement of a carboxyl group of compound **6** with a triazole ring. A variety of expected novel hybrids were then evaluated for their *in vitro* antiproliferative activity against cancer cell lines and normal cells. Molecular docking of these compounds against AKR1C3 has been carried out.

2. Results and discussion

2.1. Chemistry

Several new *N*-benzenesulfonyl-1,2,3,4-tetrahydroisoquinolines (**14**–**33**) were synthesized using the modified Pictet–Spengler reaction and the Click chemistry approaches as key steps shown in Scheme 1. Initially, treatments of nitrobenzenesulfonamides **34** [7] with paraformaldehyde in refluxing formic acid were smoothly cyclized *via* the modified Pictet–Spengler reaction [6] to furnish 1,2,3,4-tetrahydroisoquinolines **35** [21,22] in good yields. Reduction of the nitro derivatives **35** was performed using stannous chloride in refluxing ethanol to give aminobenzenesulfonamides **36**. Conversion of the amino compounds **36** to the corresponding azidobenzensulfonamides **37** was readily achieved through diazotization

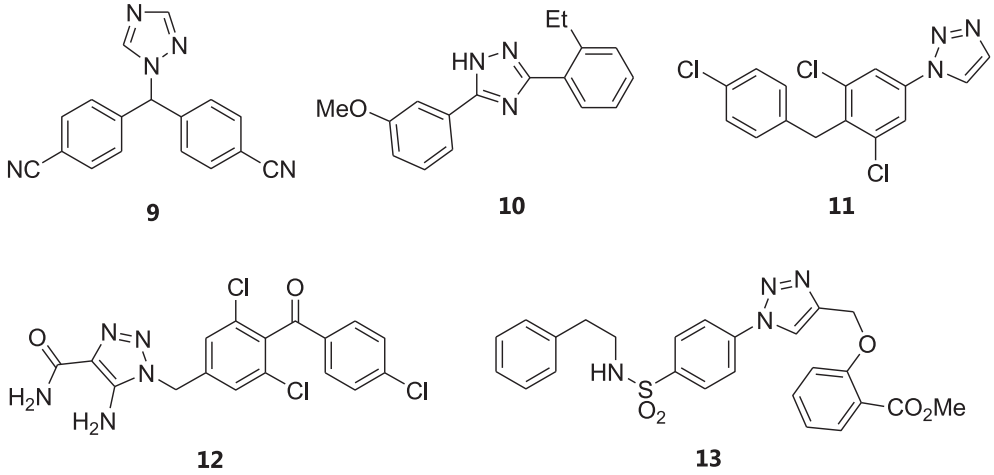

Fig. 2. Representative structures of bioactive triazoles **9**–**13**.

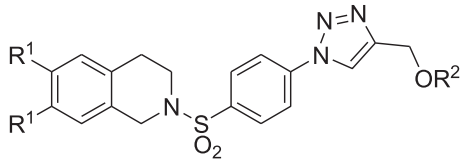

14-33

R^1 = H, OMe
R^2 = H, phenyl, naphthalenyl, coumaryl

Fig. 3. Synthetic *N*-benzenesulfonyl-1,2,3,4-tetrahydroisoquinoline based triazoles **14–33**.

reaction using sodium nitrite in a mixture of glacial acetic acid and concentrated hydrochloric acid in the presence of sodium azide. Finally, cycloaddition reaction (the Click chemistry) of the azides **37** with various alkynes **38** obtaining from alkylation of the appropriate phenol derivatives with propargyl bromide afforded a variety of the desired triazoles **14–33** (Scheme 1) in moderate to good yields (45–94%).

Structures of the desired 1,2,3-triazoles **14–33** were identified based on their HRMS, IR and NMR spectra. For example, the HRMS-TOF of hydroxymethyltriazole **23** showed its molecular ion $[M+H]^+$ peak at 431.1389 corresponding to the molecular formula of $C_{20}H_{23}N_4O_5S$. The IR spectra of the compound **23** exhibited absorption bands of O–H group at 3280 cm^{-1} and of C=C moiety at 1599 cm^{-1}. The ^1H NMR spectra revealed two triplets at δ 2.78 and 3.33 ppm which were assigned to the methylene protons of C4- and C3-THIQ, respectively. The methylene protons at C1-THIQ ring appeared as a singlet at δ 4.16 ppm whereas two methoxy protons at C6- and C7-positions of the THIQ part appeared as two singlets at δ 3.67 and 3.68 ppm. In addition, the methylene protons of $-CH_2OH$ group were found to be displayed as a doublet at δ 4.62 ppm, and the hydroxyl proton was observed as a triplet at δ 5.41 ppm. Aromatic protons of THIQ ring (H-5 and H-8) displayed as two singlets at δ 6.67 ppm and 6.76 ppm. Two doublets at δ 7.99 and 8.19 ppm with *J* value of 8.8 Hz were attributed to four aromatic protons of benzenesulfonyl moiety at position 2′(6′) and 3′(5′). A singlet of a methine proton of the triazole ring appeared down field chemical shift at δ 8.83 ppm. In the ^{13}C NMR spectra, three methylene carbons (C-1, C-3 and C-4) of THIQ ring were visible at δ 28.0, 44.1 and 47.4 ppm whereas a methylene carbon of $-CH_2OH$ group was observed at δ 55.4 ppm. Two methoxy carbons (at C-6 and C-7) of THIQ ring were noted at 55.9 and 56.0 ppm. Seven quaternary aromatic carbons (ArC) were observed at chemical shift 123.6, 125.2, 136.0, 140.2, 147.8, 148.1 and 150.1 ppm, and seven tertiary aromatic carbons (ArCH) appeared at chemical shift 110.3, 112.3, 120.8 (2ArCH), 121.7 and 129.8 (2ArCH) ppm.

2.2. Biological activity

A series of *N*-benzenesulfonyl-1,2,3,4-tetrahydroisoquinolines (**14–33**) (i.e., with or without 6,7-dimethoxy substituents) were preliminarily evaluated *in vitro* as antiproliferative agents against four human cancer cell lines including HuCCA-1 (cholangiocarcinoma), HepG2 (hepatocellular carcinoma), A549 (lung carcinoma) and MOLT-3 (lymphoblastic leukemia) cell lines as summarized in Table 1. These compounds were also tested against the noncancerous (Vero) cell line derived from African green monkey kidney (Table 1). Results showed that substituents (R^1) on the isoquinoline ring and substituents (R^2) on the triazole core play important roles in governing their cytotoxicities. SAR studies of the tested compounds are discussed hereafter.

It was observed that in a series of 1,2,3,4-tetrahydroisoquinoline (**14–22**) without 6,7-dimethoxy substituents (R^1 = H), the triazole (**14**) bearing hydroxymethyl substituent (R^2 = H) showed selective inhibition against HuCCA-1 cells. The cytotoxic activity of compound **14** in HuCCA-1 cells was lost when the H atom (R^2) of the OH group was replaced with a phenyl group as seen for compound **15**. On the other hand, the cytotoxic activity of compound **15** showed

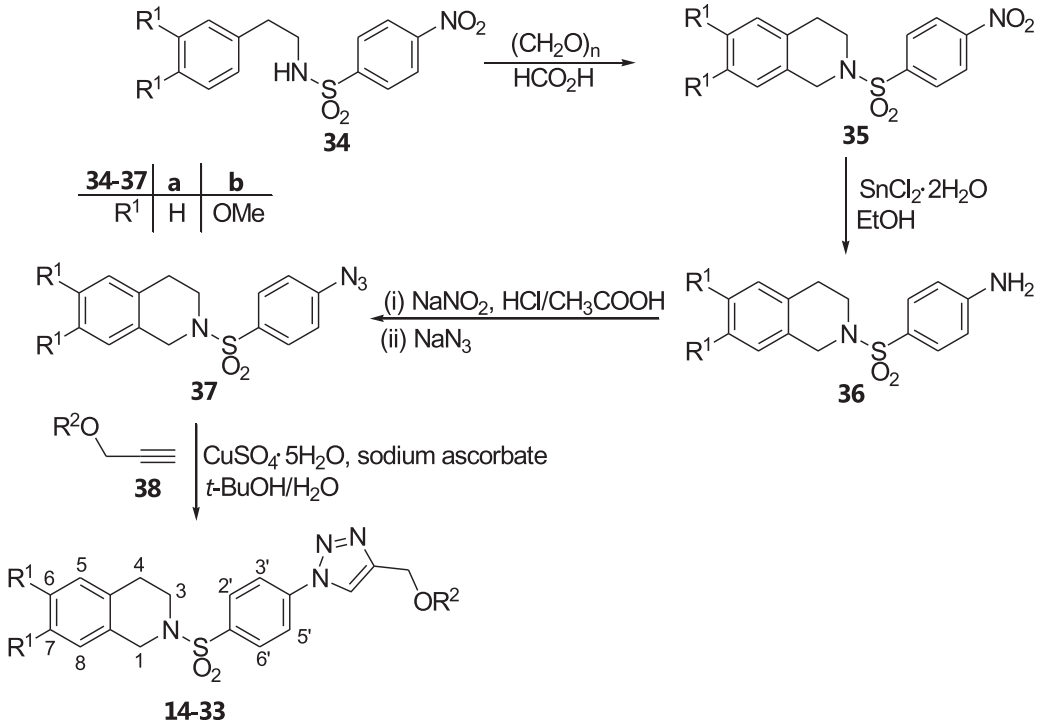

Scheme 1. Synthesis of *N*-benzenesulfonyl-1,2,3,4-tetrahydroisoquinoline based triazoles **14–33** through the Pictet–Spengler reaction and the Click reaction.

Table 1
Cytotoxic activity (IC_{50}, μM) of compounds (**14**–**33**) against four cancer cell lines and Vero cell line.

Compound	R^1	R^2	Cancer cell lines[a]				Vero cell line
			HuCCA-1	HepG2	A549	MOLT-3	
14	H	H	51.35 ± 5.66	Non-cytotoxic	Non-cytotoxic	Non-cytotoxic	Non-cytotoxic
15	H		Non-cytotoxic	6.50 ± 0.14	Non-cytotoxic	Non-cytotoxic	Non-cytotoxic
16	H	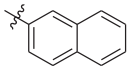	Non-cytotoxic	60.48 ± 14.14	Non-cytotoxic	Non-cytotoxic	Non-cytotoxic
17	H	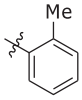	Non-cytotoxic	Non-cytotoxic	66.30 ± 0.70	Non-cytotoxic	Non-cytotoxic
18	H	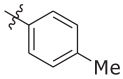	Non-cytotoxic	Non-cytotoxic	Non-cytotoxic	Non-cytotoxic	Non-cytotoxic
19	H	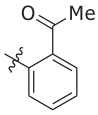	30.16 ± 4.07	19.12 ± 3.06	14.90 ± 1.02	21.86 ± 3.67	Non-cytotoxic
20	H	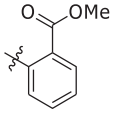	0.63 ± 0.04	12.36 ± 1.97	0.57 ± 0.02	18.63 ± 1.62	4.98
21	H	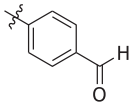	Non-cytotoxic	5.27 ± 0.71	59.07 ± 11.31	Non-cytotoxic	Non-cytotoxic
22	H	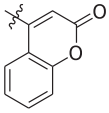	24.80 ± 2.19	Non-cytotoxic	25.29 ± 10.78	80.78 ± 10.23	28.58
23	OMe	H	72.0 ± 10.54	31.79 ± 2.89	41.04 ± 9.40	Non-cytotoxic	Non-cytotoxic
24	OMe		Non-cytotoxic	2.57 ± 0.99	Non-cytotoxic	Non-cytotoxic	Non-cytotoxic
25	OMe	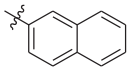	Non-cytotoxic	1.26 ± 0.42	Non-cytotoxic	36.35 ± 1.36	Non-cytotoxic
26	OMe	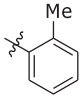	39.71 ± 1.48	1.48 ± 0.61	27.21 ± 1.77	Non-cytotoxic	Non-cytotoxic
27	OMe	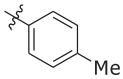	Non-cytotoxic	0.56 ± 0.01	Non-cytotoxic	Non-cytotoxic	Non-cytotoxic
28	OMe	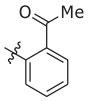	Non-cytotoxic	Non-cytotoxic	Non-cytotoxic	Non-cytotoxic	37.23
29	OMe	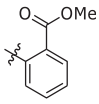	4.79 ± 0.28	3.37 ± 0.96	8.43 ± 2.79	11.74 ± 4.97	2.82
30	OMe	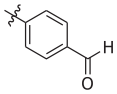	31.09 ± 8.91	12.49 ± 2.47	31.84 ± 8.13	34.12 ± 0.97	Non-cytotoxic

(*continued on next page*)

Table 1 (*continued*)

Compound	R^1	R^2	Cancer cell lines[a]				Vero cell line
			HuCCA-1	HepG2	A549	MOLT-3	
31	OMe	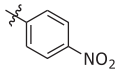	Non-cytotoxic	Non-cytotoxic	Non-cytotoxic	Non-cytotoxic	Non-cytotoxic
32	OMe	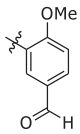	76.15 ± 1.77	41.36 ± 2.89	31.91 ± 9.76	5.82 ± 0.85	Non-cytotoxic
33	OMe	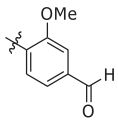	39.98 ± 4.03	Non-cytotoxic	Non-cytotoxic	5.50 ± 0.61	Non-cytotoxic
Etoposide[b]			ND	30.16 ± 0.50	ND	0.051 ± 0.002	ND
Doxorubicin[b]			0.83 ± 0.07	0.79 ± 0.08	0.44 ± 0.01	ND	ND
Ellipticine[b]			ND	ND	ND	ND	1.94

Non-cytotoxic = IC_{50} > 50 μg/mL.
Vero cell line = African green monkey kidney cell line.
ND not determined.
[a] Cancer cell lines comprise the following: HuCCA-1 human cholangiocarcinoma cell line, HepG2 human hepatocellular carcinoma cell line, A549 human lung carcinoma cell line, MOLT-3 human lymphoblastic leukemia cell line.
[b] Etoposide, doxorubicin and ellipticine were used as reference drugs.

remarkably enhanced effect (IC_{50} = 6.50 μM) in HepG2 cells. Replacement of the phenyl ring (R^2) with the naphthalenyl ring as observed in compound **16** afforded a decrease in the cytotoxic potency against HepG2. *o*-Tolyloxymethyl analog (**17**) was shown to be a selective cytotoxic compound against A549 cells. However, isomeric effect of tolyl group on the cytotoxic activity was seen in triazole **18** bearing *p*-tolyl group (R^2) in which its activity was totally lost. Significantly, phenyl groups (R^2) possessing *ortho*-substituents on the phenyl ring such as COMe (**19**) and CO_2Me (**20**) displayed cytotoxic activities toward all tested cancer cell lines in which methylbenzoate (**20**) was shown to be the most potent compound having comparable IC_{50} value (0.57 μM) with that of the control drug, doxorubicin (IC_{50} = 0.44 μM), in A549 cells. It was also found that the ester analog **20** was the most active compound (IC_{50} = 0.63 μM) against HuCCA-1 cells and exerted higher activity than that of the doxorubicin. Enhancement in anticancer activity of the phenoxytriazole compound **15** ($R^2 = C_6H_5$) against HepG2 and A549 cells was observed when a formyl group was introduced at the *para* position of the phenyl moiety as noted for compound **21**. Apparently, the phenoxy compound (**15**) and its derivatives bearing ketone (**19**), ester (**20**) and aldehyde (**21**) groups displayed high cytotoxic activity against HepG2 cells as compared to the reference drug, etoposide. When the phenyl group of compound **15** was replaced with a coumaryl ring as found in compound **22**, the enhanced cytotoxic potency was observed against HuCCA-1, A549 and MOLT-3 cell lines whereas the activity was lost in HepG2 cells.

In a 6,7-dimethoxy-1,2,3,4-tetrahydroisoquinoline series (**23**–**33**, R^1 = OMe), the hydroxymethyltriazole (**23**) (R^2 = H) was shown to be active against HuCCA-1, HepG2 and A549 cell lines. Such cytotoxic activity in HuCCA-1 and A549 cells of compound **23** was lost when the H atom was replaced with a phenyl group as seen for compound **24**. Cytotoxic activity against HepG2 cells was distinctively enhanced when the H atom of **23** was substituted with phenyl (**24**), naphthalenyl (**25**) and tolyl (**26**, **27**) groups. Significant results showed that *p*-tolyloxy compound (**27**) displayed selective inhibition and exerted the highest cytotoxic activity against HepG2 cells with IC_{50} of 0.56 μM (i.e., 53.9-fold and 1.4-fold stronger activity than etoposide and doxorubicin, respectively). Obviously, it was found that triazoles bearing the phenoxymethyl (**24**) moiety and phenoxymethyl (**26**, **27**, **29**, **30**) with substituents (CH_3, CO_2Me, CHO) on the phenyl ring as well as naphthalenoxymethyl (**25**) exhibited superior inhibitory potency toward HepG2 cells than that of the etoposide. The order of decreasing cytotoxic potency of these cytotoxic triazoles was shown by the following trend: **27** > **25** > **26** > **29** > **30**. Inhibition effect in HepG2 cells of *p*-tolyloxymethyltriazole (**27**) was found to decrease when methyl group on the phenyl ring was replaced with polar substituents (i.e., COMe, CO_2Me, CHO and NO_2). At this point, it was suggested that lipophilic groups, thus seems to be important sites responsible for strong cytotoxic activity as observed in HepG2 cells. Phenoxymethyl compounds constituting methyl ester (**29**) and formyl (**30**) groups on the phenyl ring were found to be active towards all of the tested cancer cell lines whereas compounds with acetylphenyl (**28**) and nitrophenyl (**31**) moieties displayed no cytotoxic activity toward all of the tested cells. Furthermore, additional introduction of methoxyl to the phenyl moiety containing *m*- and *p*-formyl groups as indicated by compounds **32** and **33** led to enhanced cytotoxic activity against MOLT-3 cell line.

Interestingly, most triazole compounds were shown to be non-cytotoxic toward normal cells except for triazole derivatives having methyl esters (**20**, **29**), coumaryl (**22**) and acetyl (**28**) substituents.

SAR analysis revealed that substituents (R^1 and R^2) on the target triazoles play a crucial role in governing their anticancer activity. The strongest activities against HuCCA-1 and A549 cells were noted for compounds bearing polar substituents (R^2) such as triazole ester **20** (R^1 = H, $R^2 = C_6H_4$–CO_2Me-*o*). Promisingly, compounds having high lipophilic substituents (R^1 and R^2), particularly *p*-tolyl triazole **27** (R^1 = OMe, $R^2 = C_6H_4$–Me-*p*) provided the most potent anticancer activity against HepG2 cells without affecting the normal cell line. It was conceivable that such difference in potency and selectivity of compounds in exerting anticancer activity was dependent upon the functionality of their R^1 and R^2 substituents. The strongest activity (HuCCA-1 and A549 cells) may require the compound (**20**) to have polar (CO) electrophilic center for

interacting with cellular nucleophiles. For higher potency in HepG2 cells, higher hydrophobic effect such as those afforded by the tolyl group (**27**) may be involved in binding with the hydrophobic area of the target site.

2.3. Molecular docking

A search for the putative target of 1,2,3,4-tetrahydroisoquinoline-triazoles investigated herein was carried out using the promising triazole analogs **20** and **27** as the query molecules in PubChem. It was revealed that 4-phenylpyrrolidine-2-one analog of 1,2,3,4-tetrahydroisoquinoline (**7**) provided nanomolar potency against AKR1C3 with IC_{50} values of 42 and 52 nM as elucidated by two separate bioactivity experiments [11,12]. Molecular docking was performed as to evaluate the binding modalities of the 1,2,3,4-tetrahydroisoquinoline-triazoles against AKR1C3. The results suggested that all 1,2,3,4-tetrahydroisoquinoline-triazole analogs (**14**–**33**) could snugly occupy the active site of AKR1C3 (Fig. 4) with binding energies in the range of −9.5 to −14.5 kcal/mol (Table 2). It was observed that many of the 1,2,3,4-tetrahydroisoquinoline-triazole analogs afforded binding energy lower than the co-complexed ligand found in the crystal structure, 3-(3,4-dihydroisoquinolin-2(1*H*)-ylsulfonyl)-*N*-methylbenzamide **8**, which provided binding energy of −11.0 kcal/mol indicating possibly higher potency for AKR1C3 inhibition.

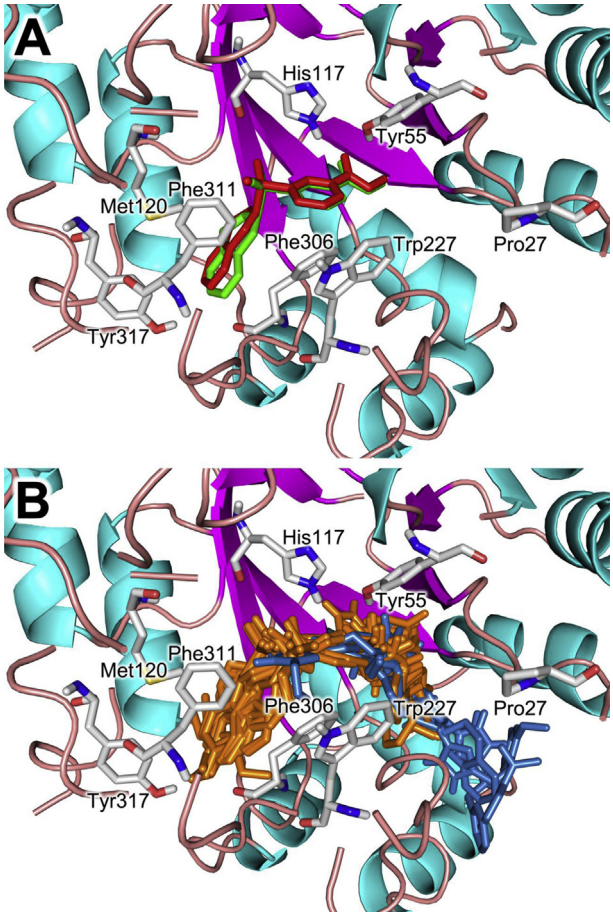

Fig. 4. Molecular docking of tetrahydroisoquinoline-triazole derivatives to AKR1C3. Re-docking of the co-crystallized ligand 3-(3,4-dihydroisoquinolin-2(1*H*)-ylsulfonyl)-*N*-methylbenzamide **8** yielded RMSD of 0.692 Å (A). Poses of docked tetrahydroisoquinoline-triazole derivatives are shown inside the binding cavity (B).

Table 2
Binding energy of 1,2,3,4-tetrahydroisoquinoline-triazole derivatives (**14**–**33**).

Compound	Binding energy (Kcal/mol)	Compound	Binding energy (kcal/mol)
14	−11.1	**24**	−10.1
15	−12.8	**25**	−12.7
16	−14.5	**26**	−11.7
17	−13.2	**27**	−11.5
18	−10.8	**28**	−10.0
19	−13.2	**29**	−11.2
20	−13.1	**30**	−11.3
21	−12.9	**31**	−11.7
22	−14.5	**32**	−11.5
23	−9.5	**33**	−11.1
8[a]	−11.0		

[a] 3-(3,4-Dihydroisoquinolin-2(1*H*)-ylsulfonyl)-*N*-methylbenzamide (**8**) is the co-crystallized ligand found in the crystal structure of AKR1C3.

Molecular modeling analysis of the crystal structure revealed that the co-complexed inhibitor **8**, binds the active site of AKR1C3 *via* hydrogen bonding of amide oxygen to Tyr55 and His117 while the phenyl group engages in hydrophobic interaction with Leu54 and forms π-π stacking with Trp227. The 1,2,3,4-tetrahydroisoquinoline moiety of **8** occupies the hydrophobic pocket inside the active site bounded by Met120, Phe306, Phe311 and Tyr317 residues (Fig. 5A). The triazole **20** could plausibly bind the active site of AKR1C3 with a similar modality as deduced from its docked conformer, particularly the 1,2,3,4-tetrahydroisoquinoline moiety of compound **20** sits inside the hydrophobic pocket formed by Met120, Phe311 and Phe306 residues whereas the phenyl ring (next to the sulfonyl group) is located in a pocket defined by Phe306 and Tyr216 residues. It was observed that the methoxy group of ester (R^2) at the other end of the compound is responsible for hydrogen bond formation with Tyr55. Moreover, compound **20** was found to also engage in hydrogen bonding with Gln222 (using phenoxy O-atom), π-stacking with Tyr24 (using the triazole ring) and hydrophobic interaction with Leu268 and Lys270 (using phenyl ring of R^2 substituent) as shown in Fig. 5B. Interestingly, compound **27**, which exerts specific activity towards the HepG2 cell line, was shown to interact with AKR1C3 through a different mechanism (Fig. 5C). Particularly, the methoxy substituent at the R^1 position sterically hinders the 1,2,3,4-tetrahydroisoquinoline moiety in occupying the hydrophobic pocket as defined by Met120, Phe306 and Phe311. However, the *p*-tolyl substituent at the R^2 position counters the previously mentioned moiety by allowing the ligand to occupy the aforementioned pocket. This instance enabled the triazole ring and the adjacent phenyl ring of sulfonamide **27** to form π-π stacking with Phe306 and Tyr216. Such interaction was strengthen by a hydrogen bonding network formed between the sulfonyl oxygen and Tyr55 as well as the between the oxygen atom of two methoxy substituents at R^1 positions to Lys270 and Ser221.

Taken together, the docking results support the viewpoint that AKR1C3 is a plausible target of 1,2,3,4-tetrahydroisoquinoline-triazoles for which it was shown to interact strongly. It is notable that substituents (R^1 and R^2) on the triazoles (**14**–**33**) are crucial for binding the active site of AKR1C3. Most THIQs without 6,7-dimethoxy substituents (R^1 = H) had lower binding energy than the corresponding compounds with 6,7-dimethoxy substituents (R^1 = OMe). However, the lowest binding energy (−14.5 kcal/mol) was observed for compounds having more bulky planar lipophilic groups (R^2) such as those found in naphthalenyl (**16**) and coumaryl (**22**). Such results could be reasonably explained that the chemical properties of R^1 and R^2 governed the compounds in interacting or fitting inside the hydrophobic pocket areas of AKR1C3.

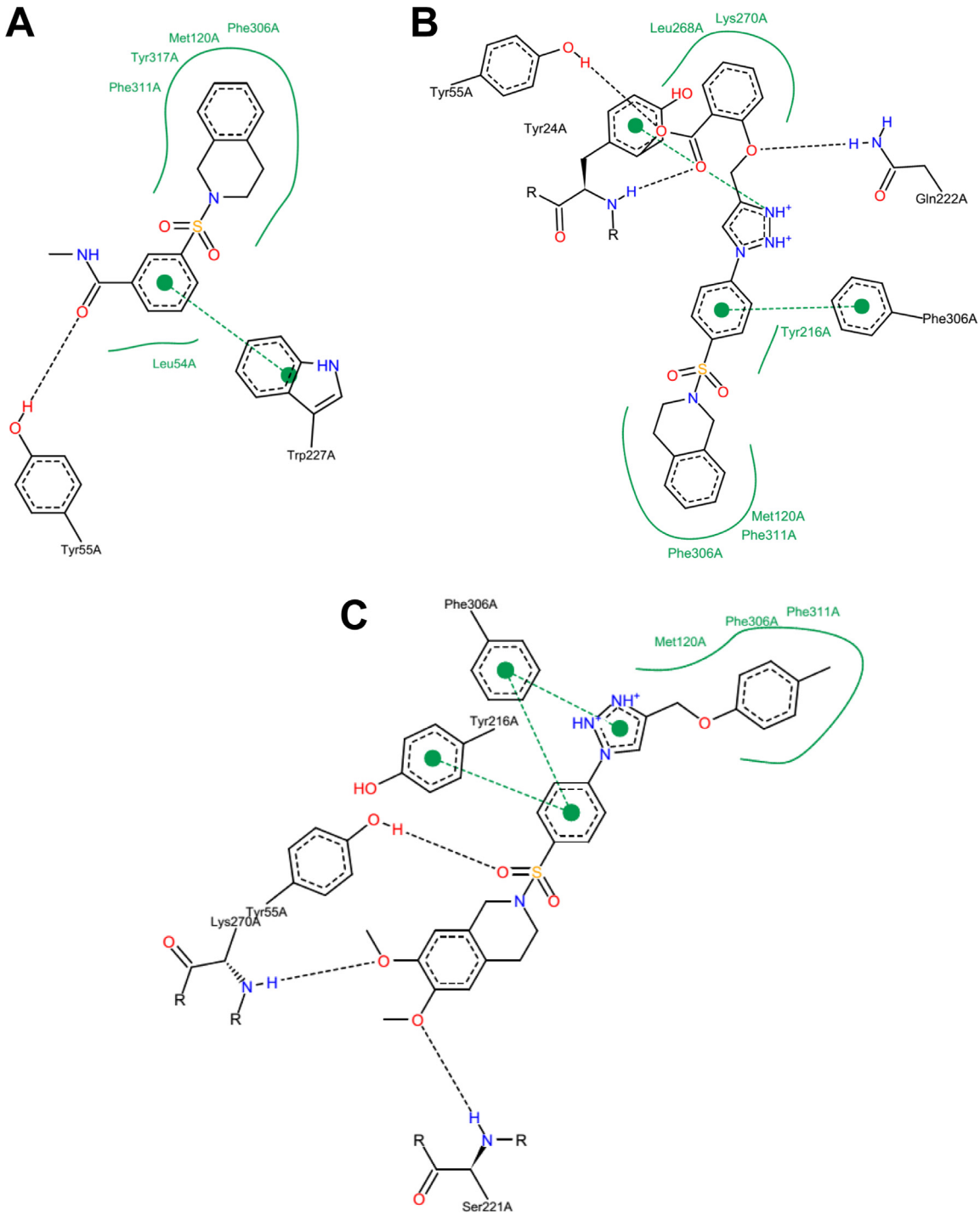

Fig. 5. 2D ligand–protein interaction schemes of the co-crystallized ligand 3-(3,4-dihydroisoquinolin-2(1*H*)-ylsulfonyl)-*N*-methylbenzamide **8** (A), the docked pose of compound **20** (B) and the docked pose of compound **27** (C).

3. Conclusions

A novel series of tetrahydroisoquinoline-triazole hybrids (**14**–**33**) have been synthesized *via* two key steps using the modified Pictet–Spengler reaction and the click reaction. Their antiproliferative activity against four cancer (HuCCA-1, HepG2, A549 and MOLT-3) cell lines and molecular docking with AKR1C3 were studied. It was observed that triazole esters (**20** and **29**) with R^2 = methylbenzoate were active toward all of the tested cell lines in which the ester analog **20** was shown to be the most potent compound against HuCCA-1 (IC_{50} = 0.63 μM) and A549 (IC_{50} = 0.57 μM) cell lines. The triazole **27** containing 6,7-dimethoxy substituent (R^1) on the isoquinoline core and *p*-tolyl group (R^2) on the triazole part was a promising compound showing the strongest and selective cytotoxicity in HepG2 cells (IC_{50} 0.56 μM) without affecting the normal cell line. The potent and selective action of compounds may be a direct function of their substituents at R^1 and R^2 positions. Activities against HuCCA-1 and A549 cells may require the compound (**20**) to have polar electrophilic center in interacting with cellular nucleophiles. The potent

activity against HepG2 cells may be rationalized to be due to the hydrophobic group (**27**) in which it binds the hydrophobic region of the target site of action. Furthermore, molecular docking study indicated that all of the investigated triazoles could snugly occupy the active site of AKR1C3, which had been identified to be a plausible target site of such compounds.

4. Experimental section

4.1. Chemistry

Column chromatography was carried out using silica gel 60 (70–230 mesh ASTM). Analytical thin-layer chromatography (TLC) was performed with silica gel 60 F254 aluminum sheets. ^{1}H- and ^{13}C-NMR spectra were recorded on a Bruker AVANCE 300 NMR spectrometer (operating at 300 MHz for 1H and 75 MHz for ^{13}C). The following standard abbreviations were used for signal multiplicities: singlet (s), doublet (d), triplet (t), quartet (q), multiplet (m), and broad (br). FTIR spectra were obtained using a universal attenuated total reflectance attached on a Perkin–Elmer Spectrum One spectrometer. Mass spectra were recorded on a Bruker Daltonics (microTOF). Melting points were determined using a Griffin melting point apparatus and were uncorrected.

4.2. General procedure for the synthesis of 1,2,3,4-tetrahydroisoquinolines (*35*)

A mixture of sulfonamide **34** (0.67 mmol) and paraformaldehyde (0.72 mmol) in formic acid (15 mL) was refluxed for 2 h, and then allowed to cool to room temperature. The reaction mixture was added to 30 mL of water, and the product was extracted with CH_2Cl_2 (2 × 30 mL). Combined extracts were washed with saturated aqueous $NaHCO_3$, dried (anh. Na_2SO_4) and evaporated to dryness under reduced pressure. The crude product was recrystallized from methanol.

^{1}H NMR of 2-((4-nitrophenyl)sulfonyl)-1,2,3,4-tetrahydroisoquinoline (**35a**) and 6,7-dimethoxy-2-((4-nitrophenyl)sulfonyl)-1,2,3,4-tetrahydroisoquinoline (**35b**) were consistent with those reported in the literatures [21,22].

4.3. General procedure for the synthesis of 1,2,3,4-tetrahydroisoquinolines (*36*)

A mixture of nitroisoquinoline **35** (4 mmol) and $SnCl_2 \cdot 2H_2O$ (20 mmol) in absolute ethanol (20 mL) was stirred under reflux for 4 h then concentrated under reduced pressure. Water (20 mL) was added and extracted with EtOAc (3 × 20 mL). The organic extracts were combined and washed with water (20 mL) and brine (20 mL). The organic layer was dried over anhydrous sodium sulfate, filtered and concentrated. The crude product was purified using silica gel column chromatography and eluted with acetone:hexane (3:7).

4.3.1. 2-((4-Aminophenyl)sulfonyl)-1,2,3,4-tetrahydroisoquinoline (*36a*)

Pale yellow solid. 82%. mp 175–176 °C (175.0–175.5 °C [23]). IR (UATR) cm^{-1}: 3454, 3362, 1591, 1503, 1324, 1155. ^{1}H NMR (300 MHz, DMSO-d$_6$) δ 2.84 (t, J = 5.8 Hz, 2H, C4–*H*), 3.16 (t, J = 5.8 Hz, 2H, C3–*H*), 4.06 (s, 2H, C1–*H*), 6.08 (s, 2H, N*H*$_2$), 6.64 (d, J = 8.7 Hz, 2H, Ar*H*), 7.05–7.18 (m, 4H, Ar*H*), 7.44 (d, J = 8.7 Hz, 2H, Ar*H*). ^{13}C NMR (75 MHz, DMSO-d$_6$) δ 28.1, 43.6, 47.4, 112.7, 120.0, 126.0, 126.4, 126.5, 128.6, 129.5, 131.9, 133.1, 153.2. HRMS-TOF: *m*/*z* [M+Na]$^+$ 311.0829 (Calcd for $C_{15}H_{16}N_2NaO_2S$: 311.0825).

4.3.2. 2-((4-Aminophenyl)sulfonyl)-6,7-dimethoxy-1,2,3,4-tetrahydroisoquinoline (*36b*)

Pale yellow solid. 80%. mp 185–186 °C. IR (UATR) cm^{-1}: 3468, 3372, 1596, 1518, 1316, 1153. ^{1}H NMR (300 MHz, DMSO-d$_6$) δ 2.75 (t, J = 5.9 Hz, 2H, C4–*H*), 3.12 (t, J = 5.9 Hz, 2H, C3–*H*), 3.68 (s, 6H, 2 × OC*H*$_3$), 3.92 (s, 2H, C1–*H*), 6.65 (d, J = 8.4 Hz, 2H, Ar*H*), 6.66 (s, 1H, Ar*H*), 6.73 (s, 1H, Ar*H*), 7.42 (d, J = 8.4 Hz, 2H, Ar*H*). ^{13}C NMR (75 MHz, DMSO-d$_6$) δ 28.2, 44.2, 47.6, 55.9, 110.3, 112.1, 113.2, 120.4, 123.9, 125.2, 130.0, 147.7, 147.9, 153.6. HRMS-TOF: *m*/*z* [M+Na]$^+$ 371.1035 (Calcd for $C_{17}H_{20}N_2NaO_4S$: 371.1036).

4.4. General procedure for the synthesis of 2-((4-azidophenyl)sulfonyl)-1,2,3,4-tetrahydroisoquinolines (*37*)

To a cold solution of amine **36** (3 mmol) in HCl:CH_3COOH (3:3 mL) at 0 °C, a solution of sodium nitrite (9 mmol) in water (5 mL) was added. The stirred reaction mixture was maintained for 15 min and then added dropwise a solution of sodium azide (9 mmol) in water (5 mL). The reaction mixture was allowed to stir at room temperature for 0.5 h, then the precipitate was filtered and washed with cold water. The crude product was purified using silica gel column chromatography and eluted with acetone:hexane (2:8).

4.4.1. 2-((4-Azidophenyl)sulfonyl)-1,2,3,4-tetrahydroisoquinoline (*37a*)

Pale yellow solid. 94%. mp 126–127 °C. IR (UATR) cm^{-1}: 2129, 2099, 1589, 1489, 1337, 1287, 1163. ^{1}H NMR (300 MHz, $CDCl_3$) δ 2.90 (t, J = 6.0 Hz, 2H, C4–*H*), 3.36 (t, J = 6.0 Hz, 2H, C3–*H*), 4.25 (s, 2H, C1–*H*), 6.96–7.18 (m, 6H, Ar*H*), 7.80 (d, J = 8.7 Hz, 2H, Ar*H*). ^{13}C NMR (75 MHz, $CDCl_3$) δ 28.8, 43.7, 47.5, 119.4, 126.3, 126.4, 126.9, 128.8, 129.6, 131.4, 132.9, 133.0, 144.9. HRMS-TOF: *m*/*z* [M+Na]$^+$ 337.0726 (Calcd for $C_{15}H_{14}N_4NaO_2S$: 337.0730).

4.4.2. 2-((4-Azidophenyl)sulfonyl)-6,7-dimethoxy-1,2,3,4-tetrahydroisoquinoline (*37b*)

Pale yellow solid. 85%. mp 145–146 °C. IR (UATR) cm^{-1}: 2126, 2100, 1588, 1519, 1345, 1284, 1163. ^{1}H NMR (300 MHz, $CDCl_3$) δ 2.81 (t, J = 5.9 Hz, 2H, C4–*H*), 3.33 (t, J = 5.9 Hz, 2H, C3–*H*), 3.80 (s, 6H, 2 × OC*H*$_3$), 4.17 (s, 2H, C1–*H*), 6.48 (s, 1H, Ar*H*), 6.53 (s, 1H, Ar*H*), 7.12 (d, J = 8.7 Hz, 2H, Ar*H*), 7.79 (d, J = 8.7 Hz, 2H, Ar*H*). ^{13}C NMR (75 MHz, $CDCl_3$) δ 28.3, 43.7, 47.2, 55.9, 56.0, 108.9, 111.4, 119.4, 123.2, 124.9, 129.5, 132.8, 144.9, 147.8, 148.0. HRMS-TOF: *m*/*z* [M+Na]$^+$ 397.0946 (Calcd for $C_{17}H_{18}N_4NaO_4S$: 397.0941).

4.5. General procedure for the synthesis of propynyloxy derivatives (*38*)

A propargyl bromide (2.4 mmol) was added to a suspension of an appropriate phenol (2 mmol) and potassium carbonate (4 mmol) in acetone (15 mL). The suspension was heated to reflux for 2–6 h (monitored by TLC). The reaction was allowed to cool and then concentrated under reduced pressure. Water (30 mL) was added and extracted with CH_2Cl_2 (3 × 30 mL). The organic extracts were combined and washed with water (20 mL) and brine (20 mL). The organic layer was dried over anhydrous sodium sulfate, filtered and concentrated. The crude product was purified by column chromatography.

^{1}H NMR spectra of propynyloxy derivatives (**38**) including (2-propynyloxy)benzene [24], 2-(2-propynyloxy)naphthalene [25], 1-methyl-2-(2-propynyloxy)benzene [26], 1-methyl-4-(2-propynyloxy)benzene [27], 1-(2-(prop-2-ynyloxy)phenyl)ethanone [28], methyl 2-(2-propynyloxy)benzoate [29], 4-(2-propynyloxy) benzaldehyde [28], 4-(propynyloxy)-2*H*-chromen-2-one [30], 1-nitro-4-(2-propynyloxy)benzene [25], 4-methoxy-3-(2-

propynyloxy)benzaldehyde [31] and 3-methoxy-4-(2-propynyloxy) [31] were consistent with those reported in the literatures.

4.6. General procedure for the synthesis of 4-(4-(substituted)-1H-1,2,3-triazol-1-yl)-N-phenethylbenzenesulfonamides (**14**–**33**)

To a stirred solution of azido **37** (0.2 mmol) and alkyne **38** (0.2 mmol) in *t*-BuOH:H_2O (3:3 mL), $CuSO_4 \cdot 5H_2O$ (0.2 mmol) and ascorbic acid (0.5 mmol) were added. The reaction mixture was stirred at room temperature for 2–12 h (monitored by TLC), then concentrated under reduced pressure. The residue was added water (10 mL) and extracted with dichloromethane (3 × 20 mL). The combined organic phases were washed with water (20 mL), dried over anhydrous sodium sulfate and evaporated to dryness. The crude product was purified using silica gel column chromatography and eluted with methanol:dichloromethane (1:50).

4.6.1. (1-(4-((3,4-Dihydroisoquinolin-2(1H)-yl)sulfonyl)phenyl)-1H-1,2,3-triazol-4-yl)methanol (**14**)

White solid. 45%. mp 111–112 °C. IR (UATR) cm^{-1}: 3280, 1597, 1503, 1336, 1243, 1161. ^1H NMR (300 MHz, DMSO-d_6) δ 2.87 (br t, 2H, C4–*H*), 3.35 (br t, 2H, C3–*H*), 4.27 (s, 2H, C1–*H*), 4.62 (d, $J = 5.4$ Hz, 2H, CH_2OH), 5.41 (t, $J = 5.4$ Hz, 1H, CH_2OH), 7.05–7.20 (m, 4H, Ar*H*), 8.03 (d, $J = 8.7$ Hz, 2H, Ar*H*), 7.97 (d, $J = 8.6$ Hz, 2H, Ar*H*), 8.85 (s, 1H, C*H*N). ^{13}C NMR (75 MHz, DMSO-d_6) δ 28.4, 44.0, 47.7, 55.4, 120.8, 121.7, 126.6, 126.9, 127.2, 129.1, 129.8, 132.0, 133.4, 136.0, 140.2, 150.1. HRMS-TOF: *m*/*z* $[M+Na]^+$ 393.0988 (Calcd for $C_{18}H_{18}N_4NaO_3S$: 393.0992).

4.6.2. 2-((4-(4-(Phenoxymethyl)-1H-1,2,3-triazol-1-yl)phenyl)sulfonyl)-1,2,3,4-tetrahydroisoquinoline (**15**)

White solid. 84%. mp 186–187 °C. IR (UATR) cm^{-1}: 1598, 1497, 1337, 1243, 1162. ^1H NMR (300 MHz, $CDCl_3$) δ 2.92 (t, $J = 6.0$ Hz, 2H, C4–*H*), 3.43 (t, $J = 6.0$ Hz, 2H, C3–*H*), 4.32 (s, 2H, C1–*H*), 5.29 (s, 2H, CH_2O), 6.94–7.33 (m, 9H, Ar*H*), 7.91 (d, $J = 8.8$ Hz, 2H, Ar*H*), 7.98 (d, $J = 8.8$ Hz, 2H, Ar*H*), 8.10 (s, 1H, C*H*N). ^{13}C NMR (75 MHz, $CDCl_3$) δ 28.7, 43.7, 47.5, 61.9, 114.7, 120.6, 121.5, 126.3, 126.5, 127.0, 128.9, 129.4, 129.7, 131.2, 132.9, 137.1, 139.9, 145.9, 158.0. HRMS-TOF: *m*/*z* $[M+Na]^+$ 469.1292 (Calcd for $C_{24}H_{22}N_4NaO_3S$: 469.1305).

4.6.3. 2-((4-(4-((Naphthalen-2-yloxy)methyl)-1H-1,2,3-triazol-1-yl)phenyl)sulfonyl)-1,2,3,4-tetrahydroisoquinoline (**16**)

White solid. 52%. mp 241–242 °C. IR (UATR) cm^{-1}: 1597, 1508, 1337, 1243, 1161. ^1H NMR (300 MHz, $CDCl_3$) δ 2.91 (t, $J = 5.6$ Hz, 2H, C4–*H*), 3.43 (t, $J = 5.8$ Hz, 2H, C3–*H*), 4.32 (s, 2H, C1–*H*), 5.26 (s, 2H, CH_2O), 6.85–7.18 (m, 11H, Ar*H*), 7.91 (d, $J = 8.6$ Hz, 2H, Ar*H*), 7.98 (d, $J = 8.6$ Hz, 2H, Ar*H*), 8.09 (s, 1H, C*H*N). ^{13}C NMR (75 MHz, $CDCl_3$) δ 28.7, 43.7, 47.5, 62.1, 114.6, 120.6, 126.3, 126.5, 127.0, 128.9, 129.4, 130.1, 130.9, 131.2, 132.9, 137.2, 139.9, 146.1, 156.0. HRMS-TOF: *m*/*z* $[M+H]^+$ 497.1647 (Calcd for $C_{28}H_{25}N_4O_3S$: 497.1653).

4.6.4. 2-((4-(4-((o-Tolyloxy)methyl)-1H-1,2,3-triazol-1-yl)phenyl)sulfonyl)-1,2,3,4-tetrahydroisoquinoline (**17**)

White solid. 77%. mp 168–169 °C. IR (UATR) cm^{-1}: 1596, 1495, 1339, 1240, 1164. ^1H NMR (300 MHz, $CDCl_3$) δ 2.28 (s, 3H, CH_3), 2.96 (t, $J = 5.9$ Hz, 2H, C4–*H*), 3.47 (t, $J = 5.9$ Hz, 2H, C3–*H*), 4.36 (s, 2H, C1–*H*), 5.34 (s, 2H, CH_2O), 6.90–7.24 (m, 8H, Ar*H*), 7.95 (d, $J = 8.9$ Hz, 2H, Ar*H*), 8.03 (d, $J = 8.8$ Hz, 2H, Ar*H*), 8.11 (s, 1H, C*H*N). ^{13}C NMR (75 MHz, $CDCl_3$) δ 16.3, 28.7, 43.7, 47.5, 62.2, 111.5, 120.4, 120.6, 121.3, 126.3, 126.5, 127.0, 128.9, 129.4, 131.0, 131.2, 132.9, 139.9, 146.3, 156.2. HRMS-TOF: *m*/*z* $[M+H]^+$ 461.1637 (Calcd for $C_{25}H_{25}N_4O_3S$: 461.1653).

4.6.5. 2-((4-(4-((p-Tolyloxy)methyl)-1H-1,2,3-triazol-1-yl)phenyl)sulfonyl)-1,2,3,4-tetrahydroisoquinoline (**18**)

White solid. 88%. mp 196–197 °C. IR (UATR) cm^{-1}: 1598, 1512, 1338, 1244, 1162. ^1H NMR (300 MHz, $CDCl_3$) δ 2.27 (s, 3H, CH_3), 2.92 (t, $J = 6.0$ Hz, 2H, C4–*H*), 3.43 (t, $J = 6.0$ Hz, 2H, C3–*H*), 4.32 (s, 2H, C1–*H*), 5.26 (s, 2H, CH_2O), 6.89 (d, $J = 8.5$ Hz, 2H, Ar*H*), 7.00–7.16 (m, 6H, Ar*H*), 7.90 (d, $J = 8.8$ Hz, 2H, Ar*H*), 7.98 (d, $J = 8.8$ Hz, 2H, Ar*H*), 8.09 (s, 1H, C*H*N). ^{13}C NMR (75 MHz, $CDCl_3$) δ 20.5, 28.7, 43.7, 47.5, 62.1, 114.6, 120.5, 126.3, 126.5, 126.6, 128.9, 129.4, 130.1, 130.9, 131.2, 132.9, 137.1, 139.9, 146.1, 155.9. HRMS-TOF: *m*/*z* $[M+H]^+$ 461.1646 (Calcd for $C_{25}H_{25}N_4O_3S$: 461.1653).

4.6.6. 1-(2-((1-(4-((3,4-Dihydroisoquinolin-2(1H)-yl)sulfonyl)phenyl)-1H-1,2,3-triazol-4-yl)methoxy)phenyl)ethanone (**19**)

White solid. 78%. mp 185–186 °C. IR (UATR) cm^{-1}: 1655, 1595, 1450, 1358, 1161. ^1H NMR (300 MHz, $CDCl_3$) δ 2.58 (s, 3H, $COCH_3$), 2.91 (t, $J = 6.0$ Hz, 2H, C4–*H*), 3.42 (t, $J = 6.0$ Hz, 2H, C3–*H*), 4.31 (s, 2H, C1–*H*), 5.38 (s, 2H, CH_2O), 6.99–7.15 (m, 6H, Ar*H*), 7.46 (dt, $J = 7.7$, 1.7 Hz, 1H, Ar*H*), 7.69 (dd, $J = 7.7$, 1.7 Hz, 1H, Ar*H*), 7.92 (d, $J = 8.8$ Hz, 2H, Ar*H*), 7.99 (d, $J = 8.8$ Hz, 2H, Ar*H*), 8.15 (s, 1H, C*H*N). ^{13}C NMR (75 MHz, $CDCl_3$) δ 28.7, 31.7, 43.7, 47.5, 62.4, 113.1, 120.7, 120.8, 121.5, 126.3, 126.5, 127.0, 128.9, 129.0, 129.5, 130.5, 131.2, 132.9, 133.6, 137.2, 139.7, 145.1, 157.0, 199.7. HRMS-TOF: *m*/*z* $[M+Na]^+$ 511.1391 (Calcd for $C_{26}H_{24}N_4NaO_4S$: 511.1410).

4.6.7. Methyl 2-((1-(4-((3,4-dihydroisoquinolin-2(1H)-yl)sulfonyl)phenyl)-1H-1,2,3-triazol-4-yl)methoxy)benzoate (**20**)

White solid. 91%. mp 162–163 °C. IR (UATR) cm^{-1}: 1696, 1599, 1453, 1306, 1254, 1160. ^1H NMR (300 MHz, $CDCl_3$) δ 2.92 (t, $J = 6.0$ Hz, 2H, C4–*H*), 3.43 (t, $J = 6.0$ Hz, 2H, C3–*H*), 3.88 (s, 3H, CO_2CH_3), 4.32 (s, 2H, C1–*H*), 5.39 (s, 2H, CH_2O), 7.00–7.18 (m, 6H, Ar*H*), 7.48 (dt, $J = 7.8$, 1.7 Hz, 1H, Ar*H*), 7.82 (dd, $J = 7.8$, 1.7 Hz, 1H, Ar*H*), 7.93 (d, $J = 8.9$ Hz, 2H, Ar*H*), 7.99 (d, $J = 8.9$ Hz, 2H, Ar*H*), 8.31 (s, 1H, C*H*N). ^{13}C NMR (75 MHz, $CDCl_3$) δ 28.7, 43.7, 47.5, 52.0, 63.4, 114.1, 120.6, 121.0, 121.3, 126.3, 126.5, 127.0, 128.9, 129.4, 131.2, 131.8, 132.9, 133.8, 137.0, 139.9, 146.0, 157.8, 166.1. HRMS-TOF: *m*/*z* $[M+Na]^+$ 527.1365 (Calcd for $C_{26}H_{24}N_4NaO_5S$: 527.1360).

4.6.8. 4-((1-(4-((3,4-dihydroisoquinolin-2(1H)-yl)sulfonyl)phenyl)-1H-1,2,3-triazol-4-yl)methoxy)benzaldehyde (**21**)

White solid. 81%. mp 189–190 °C. IR (UATR) cm^{-1}: 1686, 1605, 1578, 1500, 1357, 1243, 1160. ^1H NMR (300 MHz, $CDCl_3$) δ 2.92 (t, $J = 5.9$ Hz, 2H, C4–*H*), 3.43 (t, $J = 5.9$ Hz, 2H, C3–*H*), 4.32 (s, 2H, C1–*H*), 5.37 (s, 2H, CH_2O), 7.00–7.18 (m, 6H, Ar*H*), 7.84 (d, $J = 8.8$ Hz, 2H, Ar*H*), 7.92 (d, $J = 8.8$ Hz, 2H, Ar*H*), 7.99 (d, $J = 8.8$ Hz, 2H, Ar*H*), 8.14 (s, 1H, C*H*N), 9.88 (s, 3H, C*H*O). ^{13}C NMR (75 MHz, $CDCl_3$) δ 28.7, 43.7, 47.5, 62.0, 115.1, 120.7, 120.9, 126.3, 126.5, 127.0, 128.9, 129.5, 130.6, 131.2, 132.2, 132.8, 137.4, 139.7, 144.8, 162.9, 190.7. HRMS-TOF: *m*/*z* $[M+H]^+$ 475.1450 (Calcd for $C_{25}H_{23}N_4O_4S$: 475.1446).

4.6.9. 4-((1-(4-((3,4-Dihydroisoquinolin-2(1H)-yl)sulfonyl)phenyl)-1H-1,2,3-triazol-4-yl)methoxy)-2H-chromen-2-one (**22**)

White solid. 94%. mp 150–151 °C. IR (UATR) cm^{-1}: 1687, 1618, 1456, 1354, 1248, 1161. ^1H NMR (300 MHz, $CDCl_3$) δ 2.96 (t, $J = 5.9$ Hz, 2H, C4–*H*), 3.47 (t, $J = 5.9$ Hz, 2H, C3–*H*), 4.36 (s, 2H, C1–*H*), 5.46 (s, 2H, CH_2O), 5.92 (s, 1H, C*H*CO), 7.04–7.36 (m, 6H, Ar*H*), 7.57 (dt, $J = 7.7$, 1.4 Hz, 1H, Ar*H*), 7.82 (dd, $J = 7.9$, 1.4 Hz, 1H, Ar*H*), 7.99 (d, $J = 8.7$ Hz, 2H, Ar*H*), 8.05 (d, $J = 8.7$ Hz, 2H, Ar*H*), 8.27 (s, 1H, C*H*N). ^{13}C NMR (75 MHz, $CDCl_3$) δ 28.7, 43.7, 47.5, 62.4, 91.4, 115.4, 116.8, 120.8, 121.5, 123.1, 124.0, 126.3, 126.6, 127.0, 128.9, 129.5, 131.2, 132.7, 132.8, 139.6, 142.9, 153.4, 162.4, 164.8. HRMS-TOF: *m*/*z* $[M+H]^+$ 515.1384 (Calcd for $C_{27}H_{23}N_4O_5S$: 515.1384).

*4.6.10. (1-(4-((6,7-Dimethoxy-3,4-dihydroisoquinolin-2(1H)-yl) sulfonyl)phenyl)-1H-1,2,3-triazol-4-yl)methanol (**23**)*

Pale yellow solid. 58%. mp 159–160 °C. IR (UATR) cm^{-1}: 3280, 1599, 1523, 1342, 1226, 1158. ^1H NMR (300 MHz, DMSO-d_6) δ 2.78 (t, J = 5.5 Hz, 2H, C4–*H*), 3.33 (t, J = 5.8 Hz, 2H, C3–*H*), 3.67, 3.68 (2s, 6H, 2 × OC*H*$_3$), 4.16 (s, 2H, C1–*H*), 4.62 (d, J = 5.5 Hz, 2H, C*H*$_2$OH), 5.41 (t, J = 5.4 Hz, 1H, CH$_2$O*H*), 6.67 (s, 1H, Ar*H*), 6.76 (s, 1H, Ar*H*), 7.99 (d, J = 8.8 Hz, 2H, Ar*H*), 8.19 (d, J = 8.8 Hz, 2H, Ar*H*), 8.83 (s, 1H, C*H*N). ^{13}C NMR (75 MHz, DMSO-d_6) δ 28.0, 44.1, 47.4, 55.4, 55.9, 56.0, 110.3, 112.3, 120.8, 121.7, 123.6, 125.2, 129.8, 136.0, 140.2, 147.8, 148.1, 150.1. HRMS-TOF: m/z $[M+H]^+$ 431.1389 (Calcd for $C_{20}H_{23}N_4O_5S$: 431.1384).

*4.6.11. 6,7-Dimethoxy-2-((4-(4-(phenoxymethyl)-1H-1,2,3-triazol-1-yl)phenyl)sulfonyl)-1,2,3,4-tetrahydroisoquinoline (**24**)*

White solid. 91%. mp 158–159 °C. IR (UATR) cm^{-1}: 1597, 1519, 1348, 1227, 1163. ^1H NMR (300 MHz, $CDCl_3$) δ 2.82 (t, J = 6.0 Hz, 2H, C4–*H*), 3.40 (t, J = 6.0 Hz, 2H, C3–*H*), 3.80 (s, 6H, 2 × OC*H*$_3$), 4.24 (s, 2H, C1–*H*), 5.29 (s, 2H, C*H*$_2$O), 6.49 (s, 1H, Ar*H*), 6.53 (s, 1H, Ar*H*), 6.94–7.02 (m, 3H, Ar*H*), 7.24–7.34 (m, 2H, Ar*H*), 7.91 (d, J = 8.8 Hz, 2H, Ar*H*), 7.98 (d, J = 8.8 Hz, 2H, Ar*H*), 8.10 (s, 1H, C*H*N). ^{13}C NMR (75 MHz, $CDCl_3$) δ 28.2, 43.8, 47.2, 55.9, 56.0, 61.9, 109.0, 111.4, 114.7, 120.6, 121.6, 123.0, 124.8, 129.4, 129.7, 137.2, 139.8, 145.9, 147.9, 148.1, 158.0. HRMS-TOF: m/z $[M+H]^+$ 507.1706 (Calcd for $C_{26}H_{27}N_4O_5S$: 507.1697).

*4.6.12. 6,7-Dimethoxy-2-((4-(4-((naphthalen-2-yloxy)methyl)-1H-1,2,3-triazol-1-yl)phenyl)sulfonyl)-1,2,3,4-tetrahydroisoquinoline (**25**)*

Pale yellow solid. 83%. mp 210–211 °C. IR (UATR) cm^{-1}: 1598, 1519, 1463, 1347, 1257, 1163. ^1H NMR (300 MHz, $CDCl_3$) δ 2.86 (t, J = 5.7 Hz, 2H, C4–*H*), 3.43 (t, J = 5.7 Hz, 2H, C3–*H*), 3.83, 3.84 (2s, 6H, 2 × OC*H*$_3$), 4.27 (s, 2H, C1–*H*), 5.45 (s, 2H, C*H*$_2$O), 6.53 (s, 1H, Ar*H*), 6.56 (s, 1H, Ar*H*), 7.22 (dd, J = 8.9, 2.5 Hz, 1H, Ar*H*), 7.31 (d, J = 2.4 Hz, 1H, Ar*H*), 7.38 (t, J = 8.1 Hz, 1H, Ar*H*), 7.47 (t, J = 8.1 Hz, 1H, Ar*H*), 7.75–7.82 (m, 3H, Ar*H*), 7.95 (d, J = 8.9 Hz, 2H, Ar*H*), 8.01 (d, J = 8.9 Hz, 2H, Ar*H*), 8.17 (s, 1H, C*H*N). ^{13}C NMR (75 MHz, $CDCl_3$) δ 28.2, 43.8, 47.2, 55.9, 56.0, 61.9, 107.3, 108.9, 111.4, 118.6, 120.6, 120.7, 123.0, 124.1, 124.8, 126.6, 126.9, 127.7, 129.3, 129.4, 129.7, 134.4, 137.2, 139.8, 145.8, 147.9, 148.1, 155.9. HRMS-TOF: m/z $[M+H]^+$ 557.1843 (Calcd for $C_{30}H_{29}N_4O_5S$: 557.1853).

*4.6.13. 6,7-Dimethoxy-2-((4-(4-((o-tolyloxy)methyl)-1H-1,2,3-triazol-1-yl)phenyl)sulfonyl)-1,2,3,4-tetrahydroisoquinoline (**26**)*

White solid. 87%. mp 138–139 °C. IR (UATR) cm^{-1}: 1596, 1519, 1463, 1346, 1237, 1160. ^1H NMR (300 MHz, $CDCl_3$) δ 2.28 (s, 3H, C*H*$_3$), 2.86 (t, J = 5.9 Hz, 2H, C4–*H*), 3.44 (t, J = 5.9 Hz, 2H, C3–*H*), 3.84 (s, 6H, 2 × OC*H*$_3$), 4.28 (s, 2H, C1–*H*), 5.34 (s, 2H, C*H*$_2$O), 6.53 (s, 1H, Ar*H*), 6.57 (s, 1H, Ar*H*), 6.90–7.02 (m, 2H, Ar*H*), 7.16–7.23 (m, 2H, Ar*H*), 7.96 (d, J = 8.9 Hz, 2H, Ar*H*), 8.02 (d, J = 8.9 Hz, 2H, Ar*H*), 8.11 (s, 1H, C*H*N). ^{13}C NMR (75 MHz, $CDCl_3$) δ 16.3, 28.2, 43.8, 47.2, 55.9, 56.0, 62.1, 109.0, 111.5, 120.6, 121.3, 123.0, 124.2, 124.8, 127.0, 129.4, 129.5, 131.0, 137.2, 139.9, 146.3, 147.9, 148.1, 156.2. HRMS-TOF: m/z $[M+H]^+$ 521.1859 (Calcd for $C_{27}H_{29}N_4O_5S$: 521.1853).

*4.6.14. 6,7-Dimethoxy-2-((4-(4-((p-tolyloxy)methyl)-1H-1,2,3-triazol-1-yl)phenyl)sulfonyl)-1,2,3,4-tetrahydroisoquinoline (**27**)*

White solid. 92%. mp 168–169 °C. IR (UATR) cm^{-1}: 1596, 1509, 1464, 1346, 1225, 1162. ^1H NMR (300 MHz, $CDCl_3$) δ 2.31 (s, 3H, C*H*$_3$), 2.86 (t, J = 5.7 Hz, 2H, C4–*H*), 3.44 (t, J = 5.7 Hz, 2H, C3–*H*), 3.84 (s, 6H, 2 × OC*H*$_3$), 4.28 (s, 2H, C1–*H*), 5.30 (s, 2H, C*H*$_2$O), 6.53 (s, 1H, Ar*H*), 6.56 (s, 1H, Ar*H*), 6.92 (d, J = 8.5 Hz, 2H, Ar*H*), 7.12 (d, J = 8.5 Hz, 2H, Ar*H*), 7.94 (d, J = 8.7 Hz, 2H, Ar*H*), 8.01 (d, J = 8.7 Hz, 2H, Ar*H*), 8.13 (s, 1H, C*H*N). ^{13}C NMR (75 MHz, $CDCl_3$) δ 20.5, 28.2, 43.8, 47.2, 55.9, 56.0, 62.0, 109.0, 111.4, 114.6, 120.6, 123.0, 129.4, 130.1, 130.9, 137.2, 139.9, 146.1, 147.9, 148.1, 155.9. HRMS-TOF: m/z $[M+H]^+$ 521.1842 (Calcd for $C_{27}H_{29}N_4O_5S$: 521.1853).

*4.6.15. 1-(2-((1-(4-((6,7-Dimethoxy-3,4-dihydroisoquinolin-2(1H)-yl)sulfonyl)phenyl)-1H-1,2,3-triazol-4-yl)methoxy)phenyl)ethanone (**28**)*

White solid. 70%. mp 171–172 °C. IR (UATR) cm^{-1}: 1670, 1596, 1519, 1450, 1347, 1226, 1161. ^1H NMR (300 MHz, $CDCl_3$) δ 2.58 (s, 3H, COC*H*$_3$), 2.81 (t, J = 5.7 Hz, 2H, C4–*H*), 3.39 (t, J = 5.7 Hz, 2H, C3–*H*), 3.79, 3.80 (2s, 6H, 2 × OC*H*$_3$), 4.23 (s, 2H, C1–*H*), 5.38 (s, 2H, C*H*$_2$O), 6.49 (s, 1H, Ar*H*), 6.52 (s, 1H, Ar*H*), 7.03 (t, J = 8.0 Hz, 1H, Ar*H*), 7.12 (d, J = 8.2 Hz, 1H, Ar*H*), 7.46 (dt, J = 8.2, 1.8 Hz, 1H, Ar*H*), 7.69 (dd, J = 7.7, 1.8 Hz, 1H, Ar*H*), 7.91 (d, J = 8.9 Hz, 2H, Ar*H*), 7.98 (d, J = 8.9 Hz, 2H, Ar*H*), 8.15 (s, 1H, C*H*N). ^{13}C NMR (75 MHz, $CDCl_3$) δ 28.3, 31.7, 43.8, 47.2, 55.9, 56.0, 62.4, 108.9, 111.4, 113.1, 120.7, 120.8, 121.5, 122.9, 124.8, 129.0, 129.5, 130.5, 133.6, 137.3, 139.7, 145.1, 147.9, 148.1, 157.0, 199.7. HRMS-TOF: m/z $[M+Na]^+$ 571.1608 (Calcd for $C_{28}H_{28}N_4NaO_6S$: 571.1622).

*4.6.16. Methyl 2-((1-(4-((6,7-dimethoxy-3,4-dihydroisoquinolin-2(1H)-yl)sulfonyl)phenyl)-1H-1,2,3-triazol-4-yl)methoxy)benzoate (**29**)*

White solid. 94%. mp 142–143 °C. IR (UATR) cm^{-1}: 1723, 1598, 1519, 1451, 1347, 1258, 1162. ^1H NMR (300 MHz, $CDCl_3$) δ 2.83 (t, J = 5.8 Hz, 2H, C4–*H*), 3.40 (t, J = 5.8 Hz, 2H, C3–*H*), 3.80 (s, 6H, 2 × OC*H*$_3$), 3.87 (s, 3H, CO$_2$C*H*$_3$), 4.24 (s, 2H, C1–*H*), 5.38 (s, 2H, C*H*$_2$O), 6.50 (s, 1H, Ar*H*), 6.53 (s, 1H, Ar*H*), 7.02 (t, J = 8.2 Hz, 1H, Ar*H*), 7.12 (d, J = 8.3 Hz, 1H, Ar*H*), 7.48 (dt, J = 8.2, 1.8 Hz, 1H, Ar*H*), 7.82 (dd, J = 7.8, 1.7 Hz, 1H, Ar*H*), 7.94 (d, J = 8.9 Hz, 2H, Ar*H*), 7.99 (d, J = 8.9 Hz, 2H, Ar*H*), 8.31 (s, 1H, C*H*N). ^{13}C NMR (75 MHz, $CDCl_3$) δ 28.3, 43.8, 47.2, 52.0, 55.9, 56.0, 63.4, 108.9, 111.4, 114.0, 120.5, 120.6, 121.0, 121.3, 123.0, 124.8, 129.4, 131.9, 133.8, 137.0, 139.9, 146.0, 147.8, 148.0, 157.8, 166.1. HRMS-TOF: m/z $[M+H]^+$ 565.1737 (Calcd for $C_{28}H_{29}N_4O_7S$: 565.1752).

*4.6.17. 4-((1-(4-((6,7-Dimethoxy-3,4-dihydroisoquinolin-2(1H)-yl) sulfonyl)phenyl)-1H-1,2,3-triazol-4-yl)methoxy)benzaldehyde (**30**)*

White solid. 80%. mp 186–187 °C. IR (UATR) cm^{-1}: 1692, 1604, 1519, 1348, 1231, 1162. ^1H NMR (300 MHz, $CDCl_3$) δ 2.86 (t, J = 5.8 Hz, 2H, C4–*H*), 3.45 (t, J = 5.8 Hz, 2H, C3–*H*), 3.84 (s, 6H, 2 × OC*H*$_3$), 4.29 (s, 2H, C1–*H*), 5.42 (s, 2H, C*H*$_2$O), 6.53 (s, 1H, Ar*H*), 6.56 (s, 1H, Ar*H*), 7.15 (d, J = 8.7 Hz, 2H, Ar*H*), 7.88 (d, J = 8.7 Hz, 2H, Ar*H*), 7.95 (d, J = 8.8 Hz, 2H, Ar*H*), 8.04 (d, J = 8.8 Hz, 2H, Ar*H*), 8.17 (s, 1H, C*H*N), 9.92 (s, 1H, C*H*O). ^{13}C NMR (75 MHz, $CDCl_3$) δ 28.2, 43.8, 47.2, 55.9, 56.0, 62.0, 109.0, 111.5, 115.1, 120.6, 120.9, 123.0, 124.8, 129.5, 130.6, 132.1, 137.5, 139.7, 144.8, 147.9, 148.1, 162.9, 190.6. HRMS-TOF: m/z $[M+H]^+$ 535.1645 (Calcd for $C_{27}H_{27}N_4O_6S$: 535.1646).

*4.6.18. 6,7-Dimethoxy-2-((4-(4-((4-nitrophenoxy)methyl)-1H-1,2,3-triazol-1-yl)phenyl)sulfonyl)-1,2,3,4-tetrahydroisoquinoline (**31**)*

White solid. 77%. mp 173–174 °C. IR (UATR) cm^{-1}: 1592, 1518, 1464, 1341, 1257, 1162. ^1H NMR (300 MHz, $CDCl_3$) δ 2.86 (t, J = 5.9 Hz, 2H, C4–*H*), 3.45 (t, J = 5.9 Hz, 2H, C3–*H*), 3.84 (s, 6H, 2 × OC*H*$_3$), 4.29 (s, 2H, C1–*H*), 5.42 (s, 2H, C*H*$_2$O), 6.53 (s, 1H, Ar*H*), 6.56 (s, 1H, Ar*H*), 7.12 (d, J = 7.3 Hz, 2H, Ar*H*), 7.96 (d, J = 8.8 Hz, 2H, Ar*H*), 8.03 (d, J = 8.8 Hz, 2H, Ar*H*), 8.19 (s, 1H, C*H*N), 8.25 (d, J = 7.3 Hz, 2H, Ar*H*). ^{13}C NMR (75 MHz, $CDCl_3$) δ 28.2, 43.8, 47.2, 55.9, 56.0, 62.3, 108.9, 111.4, 114.8, 120.7, 121.0, 122.9, 124.8, 126.0, 129.5, 137.5, 139.5, 142.1, 144.3, 148.1, 162.8. HRMS-TOF: m/z $[M+H]^+$ 552.1539 (Calcd for $C_{26}H_{26}N_5O_7S$: 552.1548).

4.6.19. 3-((1-(4-((6,7-dimethoxy-3,4-dihydroisoquinolin-2(1H)-yl) sulfonyl)phenyl)-1H-1,2,3-triazol-4-yl)methoxy)-4-methoxybenzaldehyde (**32**)

Pale yellow solid. 76%. mp 141–142 °C. IR (UATR) cm^{-1}: 1682, 1587, 1519, 1464, 1346, 1260, 1161. ^1H NMR (300 MHz, $CDCl_3$) δ 2.86 (t, J = 5.8 Hz, 2H, C4–*H*), 3.44 (t, J = 5.8 Hz, 2H, C3–*H*), 3.83, 3.84, 3.95 (3s, 9H, 3 × OC*H*$_3$), 4.27 (s, 2H, C1–*H*), 5.48 (s, 2H, C*H*$_2$O), 6.53 (s, 1H, Ar*H*), 6.56 (s, 1H, Ar*H*), 7.24 (d, J = 7.9 Hz, 1H, Ar*H*), 7.46 (s, 1H, Ar*H*), 7.47 (d, J = 8.0 Hz, 1H, Ar*H*), 7.94 (d, J = 8.8 Hz, 2H, Ar*H*), 8.01 (d, J = 8.8 Hz, 2H, Ar*H*), 8.21 (s, 1H, C*H*N), 9.88 (s, 1H, C*H*O). ^{13}C NMR (75 MHz, $CDCl_3$) δ 28.2, 43.8, 47.2, 55.9, 56.0, 62.7, 109.0, 109.5, 111.5, 112.6, 120.6, 121.2, 123.0, 124.8, 126.6, 129.4, 130.9, 137.4, 139.7, 144.8, 147.9, 148.1, 150.0, 152.8, 190.8. HRMS-TOF: m/z $[M+H]^+$ 565.1759 (Calcd for $C_{28}H_{29}N_4O_7S$: 565.1752).

4.6.20. 4-((1-(4-((6,7-Dimethoxy-3,4-dihydroisoquinolin-2(1H)-yl) sulfonyl)phenyl)-1H-1,2,3-triazol-4-yl)methoxy)-3-methoxybenzaldehyde (**33**)

Pale yellow solid. 77%. mp 116–117 °C. IR (UATR) cm^{-1}: 1683, 1596, 1518, 1437, 1346, 1264, 1162. ^1H NMR (300 MHz, $CDCl_3$) δ 2.87 (t, J = 5.7 Hz, 2H, C4–*H*), 3.46 (t, J = 5.9 Hz, 2H, C3–*H*), 3.84, 3.99 (2s, 9H, 3 × OC*H*$_3$), 4.28 (s, 2H, C1–*H*), 5.44 (s, 2H, C*H*$_2$O), 6.54 (s, 1H, Ar*H*), 6.57 (s, 1H, Ar*H*), 7.04 (d, J = 8.3 Hz, 1H, Ar*H*), 7.55 (dd, J = 8.2, 1.8 Hz, 1H, Ar*H*), 7.61 (d, J = 1.8 Hz, 1H, Ar*H*), 7.95 (d, J = 8.8 Hz, 2H, Ar*H*), 8.02 (d, J = 8.8 Hz, 2H, Ar*H*), 8.20 (s, 1H, C*H*N), 9.88 (s, 1H, C*H*O). ^{13}C NMR (75 MHz, $CDCl_3$) δ 28.2, 43.8, 47.2, 56.0, 56.2, 62.8, 108.9, 111.1, 111.4, 112.0, 120.7, 121.0, 123.0, 124.8, 127.2, 129.4, 130.1, 137.3, 139.8, 144.9, 148.1, 155.0, 190.6. HRMS-TOF: m/z $[M+H]^+$ 565.1753 (Calcd for $C_{28}H_{29}N_4O_7S$: 565.1752).

4.7. Cytotoxic assay: cancer cell lines

Cell lines suspended in the corresponding culture medium were inoculated in 96-well microtiter plates (Corning Inc., NY, USA) at a density of 10,000–20,000 cells per well and incubated at 37 °C in a humidified atmosphere with 95% air and 5% CO_2. After 24 h, an equal volume of additional medium containing either the serial dilutions of the test compounds, positive control (etoposide and/or doxorubicin) or negative control (DMSO) was added to the desired final concentrations, and the microtiter plates were further incubated for an additional 48 h. The number of surviving cells in each well was determined using either MTT assay [32,33] (for adherent cells: HuCCA-1, HepG2, and A549 cells) or XTT assay [34] (for suspended cells: MOLT-3 cells) in order to determine the IC_{50}, which is defined as the concentration that inhibits cell growth by 50% (relative to negative control) after 48 h of continuous exposure to each test compound.

4.8. Cytotoxicity assay: primate cell line (Vero)

The cytotoxicity was performed by using the Green Fluorescent Protein (GFP) detection method [35]. The GFP-expressing Vero cell line was generated in-house by stably transfecting the African green monkey kidney cell line (Vero, ATCC CCL-81), with pEGFP-N1 plasmid (Clontech). The cell line was maintained in a minimal essential medium supplemented with 10% heat-inactivated fetal bovine serum, 2 mM L-glutamine, 1 mM sodium pyruvate, 1.5 g/L sodium bicarbonate and 0.8 mg/mL geneticin, at 37 °C in a humidified incubator with 5% CO_2. The assay was carried out by adding 45 μL of cell suspension at 3.3×10^4 cells/mL to each well of 384-well plates containing 5 μL of test compounds previously diluted in 0.5% DMSO, and then incubating for 4 days in 37 °C incubator with 5% CO_2. Fluorescence signals were measured by using SpectraMax M5 microplate reader (Molecular Devices, USA) in the bottom reading mode with excitation and emission wavelengths of 485 and 535 nm. Fluorescence signal at day 4 was subtracted with background fluorescence at day 0. IC_{50} values were derived from dose–response curves, using 6 concentrations of 3-fold serially diluted samples, by the SOFTMax Pro software (Molecular device). Ellipticine and 0.5% DMSO were used as a positive and a negative control, respectively.

4.9. Identification of putative targets of 1,2,3,4-tetrahydroisoquinolines

A structure similarity search was performed in PubChem using compounds **20** and **27** as the query molecules, which identified 1-[4-(3,4-dihydro-1*H*-isoquinolin-2-ylsulfonyl)phenyl]pyrrolidin-2-one **7** (CID 18096680) as homologous structure. Analysis on the previously tested bioactivity of this compound revealed 17β-hydroxysteroid dehydrogenase type 5, belonging to the aldo-keto reductase family 1 member C3 (AKR1C3), as a putative target affording potent nanomolar inhibitory activity with IC_{50} values of 42 and 52 nM as verified by two separate bioactivity experiments [11,12]. In addition, the X-ray crystallographic structure of AKR1C3 as obtained from the Protein Data Bank (PDB id 4FAL) was co-complexed with 3-(3,4-dihydroisoquinolin-2(1*H*)-ylsulfonyl)-*N*-methylbenzamide (**8**), which displayed 2-(benzenesulfonyl)-1,2,3,4-tetrahydroisoquinoline as a similar moiety to compounds investigated herein.

4.10. Molecular docking

Molecular docking was performed as to shed light on the binding modalities of investigated ligands toward its putative target AKR1C3 using a similar protocol as previously described [36]. Preparation of the AKR1C3 protein structure prior to docking was performed by adding essential hydrogen atoms using Kollman united atom charges and solvation parameters as provided by AutoDock Tools in PyRx 0.6 [37]. 1,2,3,4-Tetrahydroisoquinoline-triazole structures were constructed using Marvin Sketch Version 6.0 [38] and geometrically optimized with Gaussian 09 [39] using the B3LYP/6-31G(d) method. Ligand structures were prepared for docking by merging non-polar hydrogen atoms, adding Gasteiger partial charges and defining rotatable bonds. A maximum grid box size of 47.27 × 49.52 × 59.94 Å was generated to cover the entire AKR1C3 protein using Auto Grid. The grid box was allocated at the center of the protein using *x,y,z* coordinates of 7.1616, 5.6316, 11.0790, respectively. Molecular docking simulations were performed using AutoDock Vina as part of the PyRx 0.6 software. The co-crystallized ligand was re-docked as validation of the docking protocol. Docked structures were visualized using PyMOL [40]. A 2-dimensional schematic representation of protein-ligand interaction was generated using PoseViewWeb version 1.97.0 [41].

Acknowledgments

This project was financially supported from Srinakharinwirot University under the Government Budget (B.E. 2558) and the Thailand Research Fund under the Young Scholars Research Fellowship (MRG5680001 to R.P.). Great supports from the Office of Higher Education Commission and Mahidol University under the National Research Universities Initiative are appreciated. We are also indebted to Chulabhorn Research Institute for recording mass spectra and bioactivity testing.

Appendix A. Supplementary data

Supplementary data related to this article can be found at http://dx.doi.org/10.1016/j.ejmech.2014.05.019.

References

[1] K.W. Bentley, in: The Isoquinoline Alkaloids, Harwood Academic Publishers, Amsterdam, 1998.
[2] J.D. Scott, R.M. Williams, Chemistry and biology of the tetrahydroisoquinoline antitumor antibiotics, Chem. Rev. 102 (2002) 1669–1730.
[3] P. Siengalewicz, U. Rinner, J. Mulzer, Recent progress in the total synthesis of naphthyridnomycin and lemonomycin tetrahydroisoquinoline antibiotics (TAAs), Chem. Soc. Rev. 37 (2008) 2676–2690.
[4] E.D. Cox, J.M. Cook, The Pictet-Spengler condensation: a new direction for an old reaction, Chem. Rev. 95 (1995) 1797–1842.
[5] E.L. Larghi, M. Amongero, A.B.J. Bracca, T.S. Kaufman, The intermolecular Pictet-Spengler condensation with chiral carbonyl derivatives in the stereoselective syntheses of optically active isoquinoline and indole alkaloids, ARKIVOC 12 (2005) 98–153.
[6] R. Pingaew, A. Worachartcheewan, C. Nantasenamat, S. Prachayasittikul, S. Ruchirawat, V. Prachayasittikul, Synthesis, cytotoxicity and QSAR study of *N*-tosyl-1,2,3,4-tetrahydroisoquinoline derivatives, Arch. Pharm. Res. 36 (2013) 1066–1077.
[7] R. Pingaew, S. Prachayasittikul, S. Ruchirawat, V. Prachayasittikul, Synthesis and cytotoxicity of novel *N*-sulfonyl-1,2,3,4-tetrahydroisoquinoline thiosemicarbazone derivatives, Med. Chem. Res. 22 (2013) 267–277.
[8] R. Gitto, S. Agnello, S. Ferro, L. De Luca, D. Vullo, J. Brynda, P. Mader, C.T. Supuran, A. Chimirri, Identification of 3,4-dihydroisoquinoline-2(1*H*)-sulfonamide as potent carbonic anhydrase inhibitors: synthesis, biological evaluation, and enzyme–ligand X-ray studies, J. Med. Chem. 53 (2010) 2401–2408.
[9] D. Ma, W. Wu, G. Yang, J. Li, J. Li, Q. Ye, Tetrahydroisoquinoline based sulfonamide hydroxamates as potent matrix metalloproteinase inhibitors, Bioorg. Med. Chem. Lett. 14 (2004) 47–50.
[10] H. Matter, M. Schudok, W. Schwab, W. Thorwart, D. Barbier, G. Billen, B. Haase, B. Neises, K. Weithmann, T. Wollmann, Tetrahydroisoquinoline-3-carboxylate based matrix-metalloproteinase inhibitors: design, synthesis and structure–activity relationship, Bioorg. Med. Chem. 10 (2002) 3529–3544.
[11] S.M.F. Jamieson, D.G. Brooke, D. Heinrich, G.J. Atwell, S. Silva, E.J. Hamilton, A.P. Turnbull, L.J.M. Rigoreau, E. Trivier, C. Soudy, S.S. Samlal, P.J. Owen, E. Schroeder, T. Raynham, J.U. Flanagan, W.A.J. Denny, 3-(3,4-Dihydroisoquinolin-2(1*H*)-ylsulfonyl)benzoic Acids: highly potent and selective inhibitors of the type 5 17-β-hydroxysteroid dehydrogenase AKR1C3, J. Med. Chem. 55 (2012) 7746–7758.
[12] D.M. Heinrich, J.U. Flanagan, S.M.F. Jamieson, S. Silva, L.J.M. Rigoreau, E. Trivier, T. Raynham, A.P. Turnbull, W.A. Denny, Synthesis and structure-activity relationships for 1-(4-(piperidin-1-ylsulfonyl)phenyl)pyrrolidin-2-ones as novel non-carboxylate inhibitors of the aldo-keto reductase enzyme AKR1C3, Eur. J. Med. Chem. 62 (2013) 738–744.
[13] O.A. Barski, S.M. Tipparaju, A. Bhatnagar, The aldo-keto reductase superfamily and its role in drug metabolism and detoxification, Drug Metab. Rev. 40 (2008) 553–624.
[14] T.M. Penning, M.E. Burczynski, J.M. Jez, C.F. Hung, H.K. Lin, H. Ma, M. Moore, N. Palackal, K. Ratnam, Human 3α-hydroxysteroid dehydrogenase isoforms (AKR1C1-AKR1C4) of the aldo-keto reductase superfamily: functional plasticity and tissue distribution reveals roles in the inactivation and formation of male and female sex hormones, Biochem. J. 351 (2000) 67–77.
[15] M.C. Byrns, Y. Jin, T.M. Penning, Inhibitors of type 5 17β-hydroxysteroid dehydrogenase (AKR1C3): overview and structural insights, J. Steroid Biochem. Mol. Biol. 125 (2011) 95–104.
[16] J.U. Flanagan, Y. Yosaatmadja, R.M. Teague, M.Z.L. Chai, A.P. Turnbull, C.J. Squire, Crystal structures of three classes of non-steroidal anti-inflammatory drugs in complex with aldo-keto reductase 1C3, PLoS One 7 (2012) e43965.
[17] S.G. Agalave, S.R. Maujan, V.S. Pore, Click chemistry: 1,2,3-triazoles as pharmacophores, Chem. Asian J. 6 (2011) 2696–2718.
[18] X. Li, Y. Lin, Y. Yuan, K. Liu, X. Qian, Novel efficient anticancer agents and DNA-intercalators of 1,2,3-triazol-1,8-naphthalimides: design, synthesis, and biological activity, Tetrahedron 67 (2011) 2299–2304.
[19] X.L. Wang, K. Wan, C.H. Zhou, Synthesis of novel sulfanilamide-derived 1,2,3-triazoles and their evaluation for antibacterial and antifungal activities, Eur. J. Med. Chem. 45 (2010) 4631–4639.
[20] R. Pingaew, S. Prachayasittikul, S. Ruchirawat, V. Prachayasittikul, Synthesis and cytotoxicity of novel 4-(4-(substituted)-1*H*-1,2,3-triazol-1-yl)-*N*-phenethylbenzenesulfonamides, Med. Chem. Res. 23 (2014) 1768–1780.
[21] S.P. Miller, Y.L. Zhong, Z. Liu, M. Simeone, N. Yasuda, J. Limanto, Z. Chen, J. Lynch, V. Capodanno, Practical and cost-effective manufacturing route for the synthesis of a β-lactamase inhibitor, Org. Lett. 16 (2014) 174–177.
[22] R. Pingaew, S. Prachayasittikul, S. Ruchirawat, V. Prachayasittikul, Tungstophosphoric acid catalyzed synthesis of *N*-sulfonyl-1,2,3,4-tetrahydroisoquinoline analogs, Chin. Chem. Lett. 24 (2013) 941–944.
[23] R.J. Pagliero, R. Mercado, V. McCracken, M.R. Mazzieri, M.J. Nieto, Rapid and facile synthesis of *N*-benzenesulfonyl derivatives of heterocycles and their antimicrobial properties, Lett. Drug Des. Discov. 8 (2011) 778–791.
[24] E.M. Guantai, K. Ncokazi, T.J. Egan, J. Gut, P.J. Rosenthal, P.J. Smith, K. Chibale, Design, synthesis and in vitro antimalarial evaluation of triazole-linked chalcone and dienone hybrid compounds, Bioorg. Med. Chem. 18 (2010) 8243–8256.
[25] Y. Tsuzuki, T.K.N. Nguyen, D.R. Garud, B. Kuberan, M. Koketsu, 4-Deoxy-4-fluoro-xyloside derivatives as inhibitors of glycosaminoglycan biosynthesis, Bioorg. Med. Chem. Lett. 20 (2010) 7269–7273.
[26] T. Achard, A. Lepronier, Y. Gimbert, H. Clavier, L. Giordano, A. Tenaglia, G. Buono, A regio- and diastereoselective platinum-catalyzed tandem [2+1]/[3+2] cycloaddition sequence, Angew. Chem. Int. Ed. 50 (2011) 3552–3556.
[27] C. Efe, I.N. Lykakis, M. Stratakis, Gold nanoparticles supported on TiO_2 catalyse the cycloisomerisation/oxidative dimerisation of aryl propargyl ethers, Chem. Commun. 47 (2011) 803–805.
[28] R.H. Hans, E.M. Guantai, C. Lategan, P.J. Smith, B. Wan, S.G. Franzblau, J. Gut, P.J. Rosenthal, K. Chibale, Synthesis, antimalarial and antitubercular activity of acetylenic chalcones, Bioorg. Med. Chem. Lett. 20 (2010) 942–944.
[29] I.N. Lykakis, C. Efe, C. Gryparis, M. Stratakis, $Ph_3PAuNTf_2$ as a superior catalyst for the selective synthesis of 2*H*-chromenes: application to the concise synthesis of benzopyran natural products, Eur. J. Org. Chem. (2011) 2334–2338.
[30] C.P. Rao, G. Srimannarayana, Claisen rearrangement of 4-propargloxycoumarins: formation of 2*H*,5*H*-Pyrano[3,2-*c*][1]benzopyran-5-ones, Syn. Commun. 20 (1990) 535–540.
[31] S.C. Zammit, A.J. Cox, R.M. Gow, Y. Zhang, D.J. Kelly, S.J. Williamsa, Evaluation and optimization of antifibrotic activity of cinnamoyl anthranilates, Bioorg. Med. Chem. Lett. 19 (2009) 7003–7006.
[32] J. Carmichael, W.G. DeGraff, A.F. Gazdar, J.D. Minna, J.B. Mitchell, Evaluation of a tetrazolium-based semiautomated colorimetrie assay: assessment of radiosensitivity, Cancer Res. 47 (1987) 943–946.
[33] T. Mosmann, Rapid colorimetric assay for cellular growth and survival: application to proliferation and cytotoxicity assays, J. Immunol. Methods 65 (1983) 55–63.
[34] A. Doyle, J.B. Griffiths, Mammalian Cell Culture: Essential Techniques, John Wiley & Sons, Chichester, UK, 1997.
[35] L. Hunt, M. Jordan, M. De Jesus, F.M. Wurm, GFP-expressing mammalian cells for fast, sensitive, noninvasive cell growth assessment in a kinetic mode, Biotechnol. Bioeng. 65 (1999) 201–205.
[36] N. Suvannang, C. Nantasenamat, C. Isarankura-Na-Ayudhya, V. Prachayasittikul, Molecular docking of aromatase inhibitors, Molecules 16 (2011) 3597–3617.
[37] S. Dallakyan, PyRx Version 0.6, 2013. http://pyrx.scripps.edu.
[38] ChemAxon, Marvin Sketch Version 6.0, 2013. Budapest, Hungary.
[39] M.J. Frisch, G.W. Trucks, H.B. Schlegel, G.E. Scuseria, M.A. Robb, J.R. Cheeseman, G. Scalmani, V. Barone, B. Mennucci, G.A. Petersson, H. Nakatsuji, M. Caricato, X. Li, H.P. Hratchian, A.F. Izmaylov, J. Bloino, G. Zheng, J.L. Sonnenberg, M. Hada, M. Ehara, K. Toyota, R. Fukuda, J. Hasegawa, M. Ishida, T. Nakajima, Y. Honda, O. Kitao, H. Nakai, T. Vreven, J.A. Montgomery, J.E. Peralta, F. Ogliaro, M. Bearpark, J.J. Heyd, E. Brothers, K.N. Kudin, V.N. Staroverov, R. Kobayashi, J. Normand, K. Raghavachari, A. Rendell, J.C. Burant, S.S. Iyengar, J. Tomasi, M. Cossi, N. Rega, J.M. Millam, M. Klene, J.E. Knox, J.B. Cross, V. Bakken, C. Adamo, J. Jaramillo, R. Gomperts, R.E. Stratmann, O. Yazyev, A.J. Austin, R. Cammi, C. Pomelli, J.W. Ochterski, R.L. Martin, K. Morokuma, V.G. Zakrzewski, G.A. Voth, P. Salvador, J.J. Dannenberg, S. Dapprich, A.D. Daniels, Farkas, J.B. Foresman, J.V. Ortiz, J. Cioslowski, D.J. Fox, Gaussian 09, 2009. Wallingford, Connecticut.
[40] W. Delano, PyMOL Release 0.99, DeLano Scientific LLC, Palo Alto, CA, 2002.
[41] K. Stierand, M. Rarey, Drawing the PDB: protein-ligand complexes in two dimensions, ACS Med. Chem. Lett. 1 (2010) 540–545.

Med Chem Res (2014) 23:1768–1780
DOI 10.1007/s00044-013-0777-z

MEDICINAL CHEMISTRY RESEARCH

ORIGINAL RESEARCH

Synthesis and cytotoxicity of novel 4-(4-(substituted)-1*H*-1,2,3-triazol-1-yl)-*N*-phenethylbenzenesulfonamides

Ratchanok Pingaew · Supaluk Prachayasittikul · Somsak Ruchirawat · Virapong Prachayasittikul

Received: 22 May 2013 / Accepted: 29 August 2013 / Published online: 13 September 2013
© Springer Science+Business Media New York 2013

Abstract A new series of 4-(4-(substituted)-1*H*-1,2,3-triazol-1-yl)-*N*-phenethylbenzenesulfonamide derivatives **5** were synthesized through the Click approach and evaluated for their cytotoxic activity against four cancer cell lines (HuCCA-1, HepG2, A549, and MOLT-3). Most of the synthesized triazoles **5** displayed cytotoxicity against MOLT-3 cell line, except for analogs **5a–c** and **5e**. Significantly, 4-phenyltriazoles (**5a** and **5n**), 4-(naphthalen-2-yloxy) methyltriazole **5d**, as well as 4-((2-oxo-2*H*-chromen-7-yl)oxy)methyltriazole **5l** showed higher cytotoxic activity against HepG2 cells than the reference drug, etoposide. Interestingly, the 4-phenyltriazole **5a** was the most potent and promising compound with IC_{50} value of 9.07 μM against HepG2 cell line. The analog **5a** also exerted the highest cytotoxic activity against HuCCA-1 cells. This finding provides the novel lead molecules for further development.

Keywords Sulfonamide · Triazole · Click reaction · Cytotoxicity

R. Pingaew (✉)
Department of Chemistry, Faculty of Science, Srinakharinwirot University, Bangkok 10110, Thailand
e-mail: ratchanok@swu.ac.th

S. Prachayasittikul
Center of Data Mining and Biomedical Informatics, Faculty of Medical Technology, Mahidol University, Bangkok 10700, Thailand

S. Ruchirawat
Laboratory of Medicinal Chemistry, Chulabhorn Research Institute, Bangkok 10210, Thailand

S. Ruchirawat
Program in Chemical Biology, Chulabhorn Graduate Institute, Bangkok 10210, Thailand

S. Ruchirawat
Center of Excellence on Environmental Health and Toxicology, Commission on Higher Education (CHE), Ministry of Education, Bangkok, Thailand

V. Prachayasittikul
Department of Clinical Microbiology and Applied Technology, Faculty of Medical Technology, Mahidol University, Bangkok 10700, Thailand

Introduction

Nitrogen heterocycles display a vast arrays of bioactivities, in particular, triazoles have been attracted considerable interest due to their wide use as antitubercular, antibacterial, antifungal, antiviral, anti-HIV, antiinflammatory, and cytotoxic agents (Agalave *et al.*, 2011). Triazoles showed various promising structural features, such as stable to metabolic degradation, capable of hydrogen bonding, high selectivity, and less adverse effects. Furthermore, the triazole scaffold can be used for the linkage of biomolecules (e.g., polyamines, amino acids, and carbohydrates), drugs, and other functional molecules with the point of improving their pharmacological activities (Agalave *et al.*, 2011).

The azide/alkyne dipolar cycloaddition, represented as the Click-type reaction, is a significant route to the synthesis of 1,2,3-triazoles. The approach has endowed with high thermodynamic driving force (i.e., usually greater than 20 kcal mol^{-1}) (Kolb *et al.*, 2001), therefore leading to a powerful reaction of high yield, short reaction time, and high selectivity.

Sulfonamide-containing molecules also possess a broad spectrum of pharmacological actions including antitumor, antibacterial, antimalarial, and antioxidative activities (Hu *et al.*, 2008; Scozzafava *et al.*, 2003; Supuran *et al.*, 2004; Winum *et al.*, 2008). A large number of novel sulfonamide

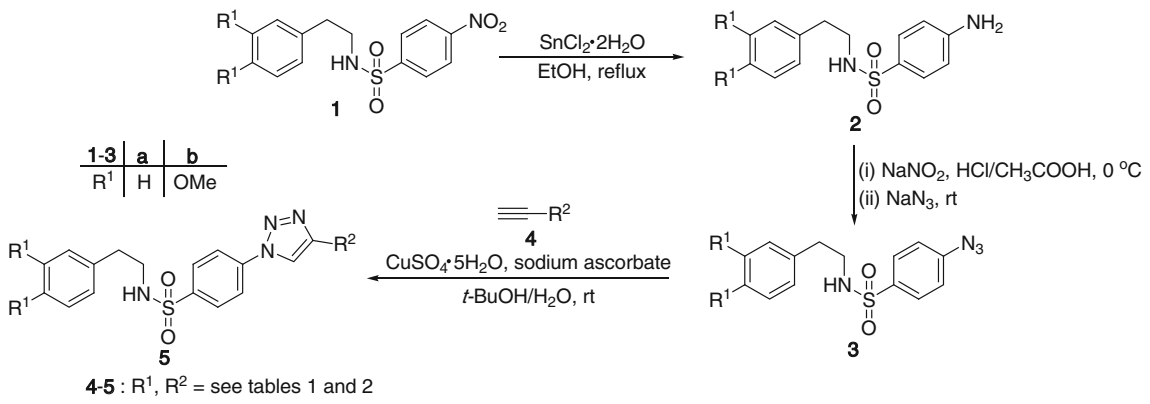

Scheme 1 Synthesis of 4-(4-(substituted)-1*H*-1,2,3-triazol-1-yl)-*N*-phenethylbenzenesulfonamides **5** through the Click reaction

derivatives as cytotoxic agent revealed several advantages including simplicity of the synthesis and effectiveness against multidrug resistant cell lines (MDR). Moreover, some compounds have better pharmacological profiles such as oral absorption with low side effects.

Furthermore, triazoles bearing sulfonamide moiety have been reported to exert antimicrobial (Ezabadi *et al*., 2008; Faidallah *et al*., 2011; Thomas *et al*., 2011; Wang *et al*., 2010; Wilkinson *et al*., 2007), antimalarial (Boechat *et al*., 2011), and antitumor (Ou *et al*., 2011) activities.

In the design of new bioactive agents, the development of hybrid structures using a combination of two or more pharmacophores that have different mechanisms of action in the same molecule is the method of choice. These merged pharmacophores offer the possibility to overcome the current drug resistance and to reduce the appearance of new resistant strains. In addition, the strategy can also reduce unwanted side effects and may enhance biological potency (Bektas *et al*., 2012; Hubschwerlen *et al*., 2003; Kaplancikli *et al*., 2008; Solomon *et al*., 2010).

In this article, a novel series of target molecules that contain both biologically active sulfonamide and triazole entities have been designed and synthesized. A variety of expected novel sulfonamide-triazole hybrids were evaluated for their in vitro cytotoxic activity against HuCCA-1, HepG2, A549, and MOLT-3 cell lines.

Results and discussion

Chemistry

A series of novel 4-substituted triazole sulfonamide analogs **5** as target molecules were synthesized via azidobenzenesulfonamides **3** as shown in Scheme 1. Nitrobenzenesulfonamides **1** were prepared by treatment of 2-phenylethylamines with 4-nitrobenzenesulfonyl chloride in the presence of sodium carbonate (Pingaew *et al*., 2013). Reduction of the nitro derivatives **1** with stannous chloride in refluxing ethanol provided the corresponding aminobenzenesulfonamides **2** which were converted to the azidobenzensulfonamides **3** using sodium nitrite and sodium azide in a mixture of glacial acetic acid and concentrated hydrochloric acid. Cycloaddition reaction of the azides **3** with various alkynes **4** readily afforded the triazoles **5** in good yields (70–98 %) (Scheme 1; Table 1).

Structures of the desired triazoles **5** were characterized by ^{1}H NMR spectra which showed the existing of the singlet of methine proton of triazole ring at δ 8–10 ppm indicating that the cycloadducts **5** were formed. The ^{1}H NMR spectra displayed two methylene groups (ArCH_2CH_2NH–) as triplet and as quartet at δ in the range of 2–4 ppm. The N*H* proton showed as triplet at δ 4–5 ppm (in $CDCl_3$) or at δ 7–8 ppm (in DMSO-d_6). In the latter case, the deshielded proton was observed due to the formation of H-bonding with the solvent. In addition, the ether derivatives (**5b**–**5m** and **5o**–**5p**) showed the singlet of ether methylene proton at δ 5–6 ppm. The structures of all obtained compounds were further supported by 2D NMR, IR, and HRMS.

Cytotoxic activity

Cytotoxicity of the synthesized triazoles (**5**) as well as amines (**2**) and azides (**3**) was assayed against HuCCA-1, HepG2, A549, and MOLT-3 human cancer cell lines as summarized in Table 2. Obviously, most of the triazoles (**5**) displayed higher cytotoxicity than the amino (**2**) and azido (**3**) derivatives, whereas the azido analogs (**3**) showed twofold stronger activity than the amino compounds (**2**) in MOLT-3 cells.

Substituents on the target 4-substituted triazoles **5** include phenyl, phenoxymethyl, naphthalenoxymethyl, and coumarinoxymethyl groups. Significant results showed that triazoles of various 4-substituents such as phenyl (**5a** and **5n**), phenoxymethyl (**5b**, **5e**–**5f**, and **5h**–**5k**), naphthalenoxymethyl

Table 1 Chemical yield of the 4-(4-(substituted)-1*H*-1,2,3-triazol-1-yl)-*N*-phenethylbenzenesulfonamides **5**

Azide **3**	Alkyne **4**	Triazole **5**	Yield (%)
3a	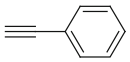 **4a**	**5a**	94
3a	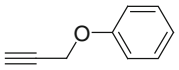 **4b**	**5b**	98
3a	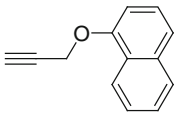 **4c**	**5c**	76
3a	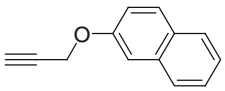 **4d**	**5d**	70
3a	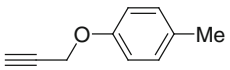 **4e**	**5e**	75
3a	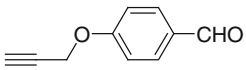 **4f**	**5f**	79
3a	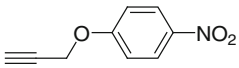 **4g**	**5g**	93
3a	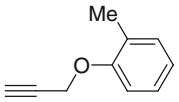 **4h**	**5h**	91
3a	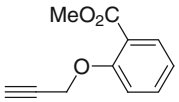 **4i**	**5i**	88
3a	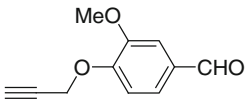 **4j**	**5j**	76
3a	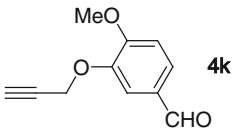 **4k**	**5k**	71
3a	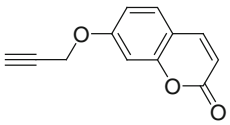 **4l**	**5l**	77

Table 1 continued

Azide **3**	Alkyne **4**	Triazole **5**	Yield (%)
3a	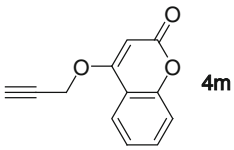 **4m**	**5m**	77
3b	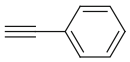 **4a**	**5n**	94
3b	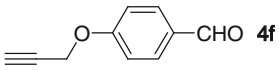 **4f**	**5o**	90
3b	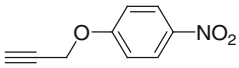 **4g**	**5p**	95

(**5d**), and coumarinoxymethyl (**5l**) displayed cytotoxicity against HepG2 cell line. Among these cytotoxic compounds, 4-phenyltriazole (**5a**) exerted the highest cytotoxic activity ($IC_{50} = 9.07$ μM) and higher than that of the reference drug, etoposide ($IC_{50} = 30.16$ μM). The analog **5a** also displayed the highest cytotoxicity against HuCCA-1 cell line with IC_{50} of 8.65 μM. Cytotoxic activity of triazole **5a** decreased when dimethoxy groups were introduced to 3,4-positions on phenethyl moiety as observed for triazole **5n** ($IC_{50} = 23.89$ μM). Similarly, when 4-phenyl group of compound **5a** was replaced by 4-phenoxymethyl group (**5b**), cytotoxic activity was remarkably decreased. In addition, 2-naphthalenoxymethyl (**5d**, $IC_{50} = 28.21$ μM) and 7-coumarinoxymethyl (**5l**, $IC_{50} = 12.44$ μM) displayed cytotoxic activity, but weaker than the phenyltriazole **5a**. It should be noted that positions of naphthalenyl and coumaryl groups linked to oxymethyl affect cytotoxic activity of the compounds. Apparently, 1-naphthalenyloxymethyl moiety afforded the triazole **5c** with total loss of the cytotoxic activity toward all the tested cells. It was also found that 4-coumaryloxymethyl triazole (**5m**) showed no inhibition effect against the tested cells, except for MOLT-3 cells. Interestingly, many 4-substituted triazoles **5** exerted promisingly high cytotoxic activity against HepG2 cells as compared to the etoposide. The order of decreasing cytotoxic potency of these triazoles against HepG2 cells was **5a** > **5l** > **5n** > **5d**. It was observed that 4-phenoxymethyltriazole (**5b**) and its derivatives having substituents (CH_3, OCH_3, CHO, CO_2CH_3, and NO_2) on phenoxy moiety exhibited cytotoxicity against different cell lines with different potencies. In HepG2 cell line, inhibition effect of phenoxymethyltriazole (**5b**) decreased when CH_3 CHO and NO_2 substituents were placed on *para*-position of phenoxymethyl group as seen for triazole analogs (**5e**, **5f**, and **5g**). The inhibition effect distinctively enhanced in MOLT-3 cells, when the triazole **5b** contained CH_3, CO_2CH_3, and OCH_3 groups on *ortho*-position of 4-phenoxytriazole as noted for compounds **5h**, **5i**, **5j**, and **5k**. The ester derivative of triazole (**5i**) was shown to be the most active compound (MOLT-3 cells) with IC_{50} of 8.81 μM. The triazoles that showed selective inhibition against MOLT-3 cells were *p*-NO_2 phenoxy (**5g** and **5p**) and 4-coumaryloxy (**5m**) derivatives. However, most of the investigated compounds exerted cytotoxicity against MOLT-3 cell line, except for triazoles **5a**–**5c** and **5e**. In HuCCA-1 cell line, 3,4-dimethoxy groups on phenethyl moiety of the triazole (**5n**) resulted in significant loss of cytotoxicity as compared to phenethyltriazole (**5a**). The results demonstrated that the insertion of 4-oxymethyl group between triazole and phenyl (or naphthalenyl or coumarinyl) moieties makes most target compounds lose their cytotoxic activity. From cytotoxicity results of 4-substituted triazoles (**5**), obviously, 4-phenyltriazole (**5a**) was shown to be the most potent compound against HepG2 cells. It is reasonable to assume that 4-phenyl ring is an appropriate hydrophobic group for potent cytotoxicity. Other 4-aryl- and heteroaryloxymethyltriazoles exhibited lower cytotoxicity, particularly, toward HepG2 cells. This could be possibly due to the steric effect of 4-aryloxymethyl group that hindered the molecule in interacting with the target site of action. It could be postulated that cytotoxic activity of 4-substituted triazole (**5**) against HepG2 cells requires the planarity of 1-benzenesulfonamide and 4-phenyl moieties on the triazole ring together with unsubstituted phenethyl group. Therefore, both ends of the target

Table 2 Cytotoxic activity of compounds (**2**–**3** and **5**) against four cancer cell lines

Compound	Cytotoxic activity (IC_{50}, μM)[a]			
	HuCCA-1	HepG2	A549	MOLT-3
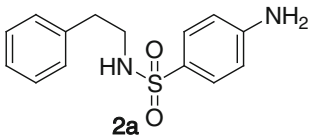 **2a**	Inactive	Inactive	Inactive	166.60 ± 1.96
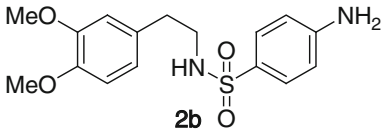 **2b**	Inactive	Inactive	Inactive	104.49 ± 2.93
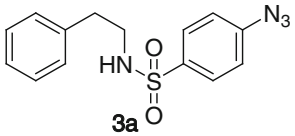 **3a**	Inactive	92.61 ± 3.00	138.91 ± 9.90	60.10 ± 1.13
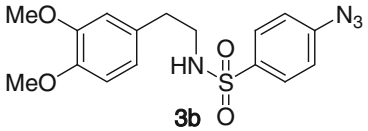 **3b**	Inactive	122.32 ± 5.51	Inactive	48.51 ± 0.81
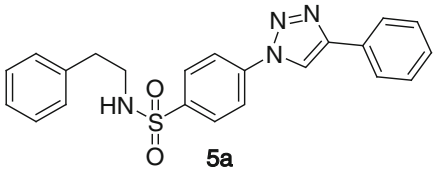 **5a**	8.65 ± 1.70	9.07 ± 1.15	34.54 ± 0.89	Inactive
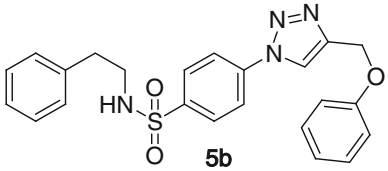 **5b**	Inactive	57.54 ± 8.66	Inactive	Inactive
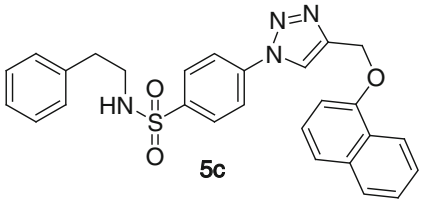 **5c**	Inactive	Inactive	Inactive	Inactive
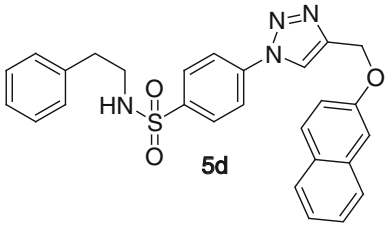 **5d**	Inactive	28.21 ± 2.89	Inactive	74.23 ± 5.08

Table 2 continued

Compound	Cytotoxic activity (IC_{50}, μM)[a]			
	HuCCA-1	HepG2	A549	MOLT-3
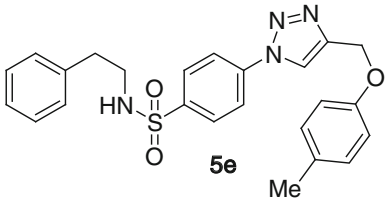 5e	Inactive	81.75 ± 2.89	Inactive	Inactive
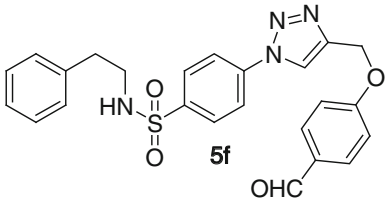 5f	87.89 ± 0.92	100.54 ± 2.12	Inactive	32.02 ± 0.76
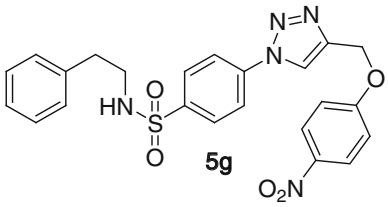 5g	Inactive	Inactive	Inactive	61.42 ± 1.01
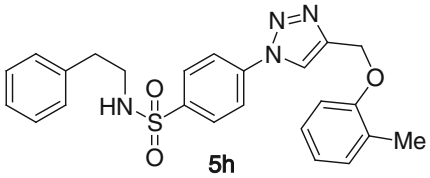 5h	Inactive	41.62 ± 1.15	Inactive	34.24 ± 3.11
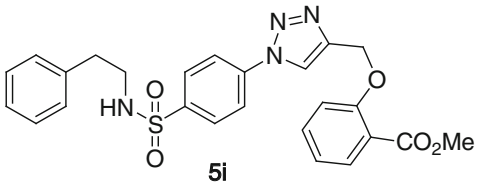 5i	Inactive	49.40 ± 4.04	Inactive	8.81 ± 0.42
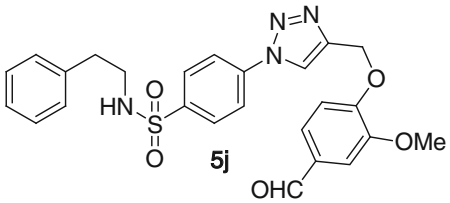 5j	Inactive	57.52 ± 6.51	79.18 ± 14.15	9.22 ± 0.48
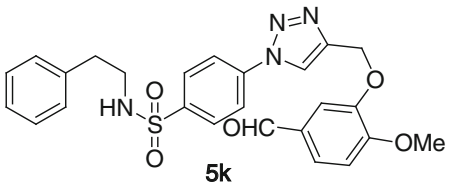 5k	Inactive	34.51 ± 4.36	39.04 ± 0.37	10.33 ± 0.08

Table 2 continued

Compound	Cytotoxic activity (IC_{50}, μM)[a]			
	HuCCA-1	HepG2	A549	MOLT-3
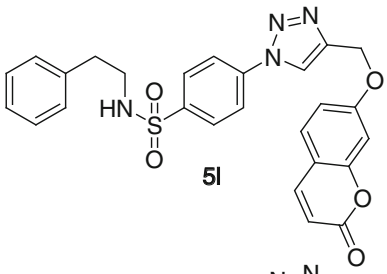 5l	16.12 ± 0.71	12.44 ± 1.71	19.60 ± 2.33	88.97 ± 3.42
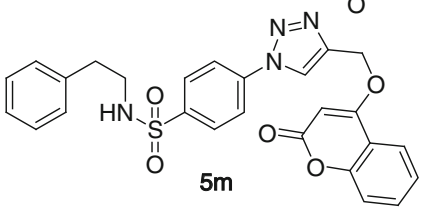 5m	Inactive	Inactive	Inactive	10.65 ± 0.48
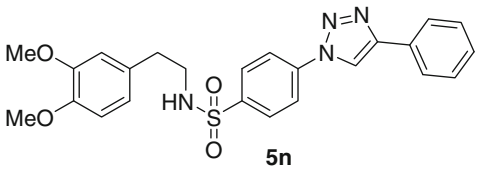 5n	Inactive	23.89 ± 3.00	18.19 ± 0.35	60.99 ± 6.66
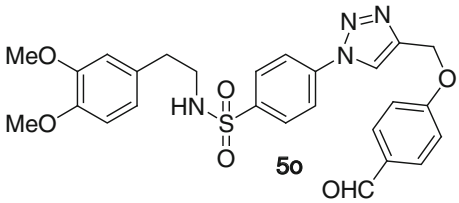 5o	Inactive	Inactive	28.03 ± 1.63	17.43 ± 0.41
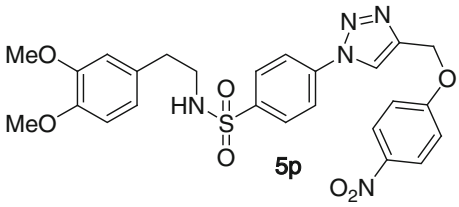 5p	Inactive	Inactive	Inactive	10.10 ± 0.27
Etoposide[b]	ND	30.16 ± 0.50	ND	0.051 ± 0.002
Doxorubicin[c]	0.83 ± 0.07	0.79 ± 0.08	0.44 ± 0.01	ND

Inactive = IC_{50} > 50 μg/mL. Cancer cell lines comprise the following: HuCCA-1 human cholangiocarcinoma cell line, HepG2 human hepatocellular carcinoma cell line, A549 human lung carcinoma cell line, MOLT-3 human lymphoblastic leukemia cell line

ND not determined

[a] The assays were performed in triplicate

[b,c] Etoposide and doxorubicin were used as reference drugs

triazole require hydrophobic phenyl groups to bind lipophilic sites of action. However, the effect of triazole core structure on the target site of action and its mode of action remain to be elucidated.

Conclusion

A series of triazoles-based sulfonamide (**5**) have been accomplished via the Click reaction. Cytotoxic activity

testing revealed that most of the triazole analogs displayed cytotoxicity against MOLT-3 cell line. It was observed that the 4-phenoxymethyl-triazole scaffolds, especially methylbenzoate analog **5i**, seem to be the most important core structure responsible for strong cytotoxic activity (MOLT-3 cells). Significantly, triazoles (**5a**, **5d**, **5l**, and **5n**) showed higher cytotoxic activity against HepG2 cells than the control drug, etoposide. In particular, the 4-phenyl-triazole **5a** was the most potent and promising cytotoxic agent (IC_{50} = 9.07 μM). The analog **5a** also displayed the highest inhibition potency against HuCCA-1 cell line (IC_{50} = 8.65 μM). The synthesis of the novel triazole analogs of phenethylbenzenesulfonamides **5** provides potential lead molecules for further drug discovery and development.

Experimental

Chemistry

Column chromatography was carried out using silica gel 60 (70–230 mesh ASTM). Analytical thin-layer chromatography (TLC) was performed with silica gel 60 F_{254} aluminum sheets. ^{1}H- and ^{13}C-NMR spectra were recorded on a Bruker AVANCE 300 NMR spectrometer (operating at 300 MHz for ^{1}H and 75 MHz for ^{13}C). FTIR spectra were obtained using a universal attenuated total reflectance attached on a Perkin-Elmer Spectrum One spectrometer. High-resolution mass spectra (HRMS) were recorded on a Bruker Daltonics (microTOF). Melting points were determined using a Griffin melting point apparatus and were uncorrected.

Propynyoxy derivatives (**4b–m**) were prepared according to the literature procedures (Banday *et al.*, 2010) and confirmed by ^{1}H-NMR spectra.

General procedure for the synthesis of 4-amino-*N*-phenethylbenzenesulfonamides (**2**)

A mixture of nitrosulfonamide **1** (4 mmol) and $SnCl_2 \cdot 2H_2O$ (20 mmol) in absolute ethanol (20 mL) was stirred under reflux for 4 h then concentrated under reduced pressure. Water (20 mL) was added and extracted with EtOAc (3 × 20 mL). The organic extracts were combined and washed with water (20 mL) and brine (20 mL). The organic layer was dried over anhydrous sodium sulfate, filtered, and concentrated. The crude product was recrystallized from methanol.

*4-Amino-N-phenethylbenzenesulfonamide (**2a**)*

Light brown solid. 82 %. mp 147–148 °C. IR (UATR) cm^{-1}: 3460 (NH), 3366 (NH), 3273 (NH), 1597 (ar C=C), 1497 (ar C=C), 1312 (S=O), 1153 (S=O). ^{1}H NMR (300 MHz, DMSO-d_6) δ 2.63 (t, J = 8.0 Hz, 2H, ArCH_2), 2.82 (br q, 2H, CH_2NH), 5.92 (s, 2H, NH_2), 6.59 (d, J = 8.6 Hz, 2H, C3′-Ar*H* and C5′-Ar*H*), 7.10–7.29 (m, 6H, Ar*H* and N*H*SO_2), 7.40 (d, J = 8.7 Hz, 2H, C2′-Ar*H* and C6′-Ar*H*). ^{13}C NMR (75 MHz, DMSO-d_6) δ 35.2 (CH_2), 44.1 (CH_2), 112.7 (CH), 126.1 (C), 128.3 (CH), 128.4 (CH), 128.6 (CH), 138.9 (C), 152.4 (C). HRMS–TOF: *m*/*z* [M+Na]$^+$ 299.0814 (Calcd for $C_{14}H_{16}N_2NaO_2S$: 299.0825).

*4-Amino-N-(3,4-dimethoxyphenethyl)benzenesulfonamide (**2b**)*

Light brown solid. 94 %. mp 144–145 °C. IR (UATR) cm^{-1}: 3467 (NH), 3371 (NH), 3256 (NH), 1596 (ar C=C), 1515 (ar C=C), 1309 (S=O), 1145 (S=O). ^{1}H NMR (300 MHz, $CDCl_3$) δ 2.68 (t, J = 6.6 Hz, 2H, ArCH_2), 3.12 (q, J = 6.6 Hz, 2H, CH_2NH), 3.79, 3.83 (2s, 6H, 2 × OCH_3), 4.12 (s, 2H, NH_2), 4.30 (br q, 1H, N*H*SO_2), 6.55 (d, J = 1.8 Hz, 1H, C2-Ar*H*), 6.58–6.65 (m, 3H, C6-Ar*H*, C3′-Ar*H* and C5′-Ar*H*), 6.74 (d, J = 8.1 Hz, 1H, C5-Ar*H*), 7.52 (d, J = 8.7 Hz, 2H, C2′-Ar*H* and C6′-Ar*H*). ^{13}C NMR (75 MHz, $CDCl_3$) δ 35.2 (CH_2), 44.2 (CH_2), 55.8 (OCH_3), 55.9 (OCH_3), 111.4 (CH), 111.7 (CH), 114.0 (CH), 120.8 (CH), 127.8 (C), 129.2 (CH), 130.3 (C), 147.8 (C), 149.1 (C), 150.5 (C). HRMS–TOF: *m*/*z* [M+H]$^+$ 337.1224 (Calcd for $C_{16}H_{21}N_2O_4S$: 337.1216).

General procedure for the synthesis of 4-azido-*N*-phenethylbenzenesulfonamides (**3**)

To a cool solution of amine **2** (3 mmol) in HCl:CH_3COOH (3:3 mL) at 0 °C, a solution of sodium nitrite (9 mmol) in water (5 mL) was added. The stirred reaction mixture was maintained for 15 min and then added dropwise a solution of sodium azide (9 mmol) in water (5 mL). The reaction mixture was allowed to stir at room temperature for 0.5 h, then the precipitate was filtered, washed with cool water, and recrystallized from methanol.

*4-Azido-N-phenethylbenzenesulfonamide (**3a**)*

Light brown solid. 95 %. mp 72–73 °C. IR (UATR) cm^{-1}: 3279 (NH), 2120 (N=N$^+$=N$^-$), 2097 (N=N$^+$=N$^-$), 1588 (ar C=C), 1490 (ar C=C), 1324 (S=O), 1155 (S=O). ^{1}H NMR (300 MHz, $CDCl_3$) δ 2.79 (t, J = 6.8 Hz, 2H, ArCH_2), 3.26 (q, J = 6.8 Hz, 2H, CH_2NH), 4.42 (br s, 1H, N*H*SO_2), 7.08–7.33 (m, 7H, Ar*H*), 7.79 (d, J = 8.5 Hz, 2H, C2′-Ar*H* and C6′-Ar*H*). ^{13}C NMR (75 MHz, $CDCl_3$) δ 35.8 (CH_2), 44.2 (CH_2), 119.4 (CH), 126.9 (CH), 128.7 (CH), 128.8 (CH), 129.0 (CH), 137.5 (C), 144.6 (C). HRMS–TOF: *m*/*z* [M+Na]$^+$ 325.0733 (Calcd for $C_{14}H_{14}N_4NaO_2S$: 325.0741).

*4-Azido-N-(3,4-dimethoxyphenethyl)benzenesulfonamide (**3b**)*

Light brown solid. 84 %. mp 76–77 °C. IR (UATR) cm^{-1}: 3276 (NH), 2130 ($N=N^{+}=N^{-}$), 2101 ($N=N^{+}=N^{-}$), 1589 (ar C=C), 1517 (ar C=C), 1329 (S=O), 1160 (S=O). ^{1}H NMR (300 MHz, $CDCl_3$) δ 2.69 (t, $J = 6.6$ Hz, 2H, ArCH_2), 3.17 (q, $J = 6.6$ Hz, 2H, CH_2NH), 3.80, 3.83 (2 s, 6H, 2 × OCH_3), 4.44 (t, $J = 6.3$ Hz, 1H, N$H$$SO_2$), 6.55 (d, $J = 1.9$ Hz, 1H, C2-ArH), 6.59 (dd, $J = 8.0$, 1.9 Hz, 1H, C6-ArH), 6.74 (d, $J = 8.0$ Hz, 1H, C5-ArH), 7.06 (d, $J = 8.8$ Hz, 2H, C3′-ArH and C5′-ArH), 7.73 (d, $J = 8.8$ Hz, 2H, C2′-ArH and C6′-ArH). ^{13}C NMR (75 MHz, $CDCl_3$) δ 35.3 (CH_2), 44.3 (CH_2), 55.8 (OCH_3), 55.9 (OCH_3), 111.4 (CH), 111.8 (CH), 119.4 (CH), 120.7 (CH), 129.0 (CH), 129.9 (C), 136.0 (C), 144.7 (C), 148.0 (C), 149.2 (C). HRMS–TOF: *m/z* $[M+H]^{+}$ 363.1119 (Calcd for $C_{16}H_{19}N_4O_4S$: 363.1122).

General procedure for the synthesis of 4-(4-(substituted)-1*H*-1,2,3-triazol-1-yl)-*N*-phenethylbenzenesulfonamides (**5**)

To a stirred solution of azido **3** (0.2 mmol) and alkyne **4** (0.2 mmol) in *t*-BuOH:H_2O (3:3 mL), $CuSO_4 \cdot 5H_2O$ (0.2 mmol) and ascorbic acid (0.5 mmol) were added. The reaction mixture was stirred at room temperature for 2 h, then concentrated under reduced pressure. The residue was added water (10 mL) and extracted with dichloromethane (3 × 20 mL). The combined organic phases were washed with water (20 mL), dried over anhydrous sodium sulfate, and evaporated to dryness. The crude product was purified using silica gel column chromatography and eluted with methanol:dichloromethane (1:50).

*N-Phenethyl-4-(4-phenyl-1H-1,2,3-triazol-1-yl)benzenesulfonamide (**5a**)*

White solid. 94 %. mp 219–220 °C. IR (UATR) cm^{-1}: 3315 (NH), 1597 (ar C=C), 1504 (ar C=C), 1328 (S=O), 1153 (S=O). ^{1}H NMR (300 MHz, DMSO-d_6) δ 2.71 (t, $J = 7.5$ Hz, 2H, ArCH_2), 3.04 (q, $J = 6.9$ Hz, 2H, CH_2NH), 7.13–7.30 (m, 5H, ArH), 7.41 (t, $J = 7.5$ Hz, 1H, ArH), 7.52 (t, $J = 7.2$ Hz, 2H, ArH), 7.87–8.05 (m, 5H, ArH and N$H$$SO_2$), 8.17 (d, $J = 8.7$ Hz, 2H, ArH), 9.42 (s, 1H, CHN). ^{13}C NMR (75 MHz, DMSO-d_6) δ 35.7 (CH_2), 44.5 (CH_2), 120.3 (CH), 120.9 (CH), 125.9 (CH), 126.7 (CH), 128.8 (CH), 128.9 (CH), 129.1 (CH), 129.5 (CH), 130.4 (C), 139.1 (C), 139.5 (C), 140.6 (C), 148.1 (C). HRMS–TOF: *m/z* $[M+H]^{+}$ 405.1371 (Calcd for $C_{22}H_{21}N_4O_2S$: 405.1380).

*N-Phenethyl-4-(4-(phenoxymethyl)-1H-1,2,3-triazol-1-yl)benzenesulfonamide (**5b**)*

White solid. 98 %. mp 149–150 °C. IR (UATR) cm^{-1}: 3278 (NH), 1597 (ar C=C), 1496 (ar C=C), 1331 (S=O), 1159 (S=O). ^{1}H NMR (300 MHz, $CDCl_3$) δ 2.83 (t, $J = 6.8$ Hz, 2H, ArCH_2), 3.31 (q, $J = 6.8$ Hz, 2H, CH_2NH), 4.56 (t, $J = 6.1$ Hz, 1H, N$H$$SO_2$), 5.34 (s, 2H, CH_2O), 7.00–7.38 (m, 10H, ArH), 7.90 (d, $J = 8.9$ Hz, 2H, ArH), 7.97 (d, $J = 8.9$ Hz, 2H, ArH), 8.15 (s, 1H, CHN). ^{13}C NMR (75 MHz, $CDCl_3$) δ 35.8 (CH_2), 44.3 (CH_2), 61.9 (OCH_2), 114.8 (CH), 120.6 (CH), 121.6 (CH), 127.0 (CH), 128.7 (CH), 128.9 (CH), 129.7 (CH), 137.3 (C), 139.7 (C), 140.2 (C), 145.9 (C), 158.0 (C). HRMS–TOF: *m/z* $[M+H]^{+}$ 435.1473 (Calcd for $C_{23}H_{23}N_4O_3S$: 435.1496).

*4-(4-((Naphthalen-1-yloxy)methyl)-1H-1,2,3-triazol-1-yl)-N-phenethylbenzenesulfonamide (**5c**)*

White solid. 76 %. mp 166–167 °C. IR (UATR) cm^{-1}: 3250 (NH), 1596 (ar C=C), 1507 (ar C=C), 1331 (S=O), 1154 (S=O). ^{1}H NMR (300 MHz, $CDCl_3$) δ 2.78 (t, $J = 6.8$ Hz, 2H, ArCH_2), 3.26 (q, $J = 6.7$ Hz, 2H, CH_2NH), 4.51 (t, $J = 6.1$ Hz, 1H, N$H$$SO_2$), 5.50 (s, 2H, CH_2O), 6.95 (d, $J = 7.5$ Hz, 1H, ArH), 7.11 (dd, $J = 7.9$, 1.6 Hz, 2H, ArH), 7.17–7.29 (m, 3H, ArH), 7.38 (t, $J = 7.6$ Hz, 1H, ArH), 7.42–7.52 (m, 3H, ArH), 7.77–7.96 (m, 5H, ArH), 8.20 (s, 1H, CHN), 8.23–8.28 (m, 1H, ArH). ^{13}C NMR (75 MHz, $CDCl_3$) δ 35.8 (CH_2), 44.3 (CH_2), 62.3 (OCH_2), 105.4 (CH), 120.6 (CH), 120.7 (CH), 121.2 (CH), 121.8 (CH), 125.4 (CH), 125.8 (CH), 126.6 (CH), 127.0 (CH), 127.6 (CH), 128.7 (CH), 128.9 (CH), 134.6 (C), 137.3 (C), 139.7 (C), 140.2 (C), 145.9 (C), 153.7 (C). HRMS–TOF: *m/z* $[M+H]^{+}$ 485.1652 (Calcd for $C_{27}H_{25}N_4O_3S$: 485.1642).

*4-(4-((Naphthalen-2-yloxy)methyl)-1H-1,2,3-triazol-1-yl)-N-phenethylbenzenesulfonamide (**5d**)*

White solid. 70 %. mp 179–180 °C. IR (UATR) cm^{-1}: 3247 (NH), 1598 (ar C=C), 1505 (ar C=C), 1312 (S=O), 1154 (S=O). ^{1}H NMR (300 MHz, DMSO-d_6) δ 2.70 (t, $J = 7.6$ Hz, 2H, ArCH_2), 3.03 (q, $J = 7.0$ Hz, 2H, CH_2NH), 5.39 (s, 2H, CH_2O), 7.12–7.29 (m, 6H, ArH), 7.37 (t, $J = 8.1$ Hz, 1H, ArH), 7.49 (t, $J = 7.9$ Hz, 1H, ArH), 7.56 (d, $J = 2.2$ Hz, 1H, ArH), 7.81–7.95 (m, 4H, ArH and N$H$$SO_2$), 7.98 (d, $J = 8.6$ Hz, 2H, ArH), 8.16 (d, $J = 8.7$ Hz, 2H, ArH), 9.14 (s, 1H, CHN). ^{13}C NMR (75 MHz, DMSO-d_6) δ 35.7 (CH_2), 44.5 (CH_2), 61.5 (OCH_2), 107.8 (CH), 119.1 (CH), 121.1 (CH), 123.7 (CH), 124.3 (CH), 126.7 (CH), 127.0 (CH), 127.3 (CH), 128.0 (CH), 128.8 (CH), 128.9 (CH), 129.1 (CH), 129.9 (CH), 134.6 (C), 139.1 (C), 139.4 (C), 140.7 (C), 144.7 (C), 156.3

(C). HRMS–TOF: *m/z* $[M+H]^+$ 485.1635 (Calcd for $C_{27}H_{25}N_4O_3S$: 485.1642).

*N-Phenethyl-4-(4-((p-tolyloxy)methyl)-1H-1,2,3-triazol-1-yl)benzenesulfonamide (**5e**)*

White solid. 75 %. mp 150–151 °C. IR (UATR) cm^{-1}: 3273 (NH), 1597 (ar C=C), 1508 (ar C=C), 1331 (S=O), 1159 (S=O). ^1H NMR (300 MHz, $CDCl_3$) δ 2.32 (s, 3H, ArCH_3), 2.82 (t, $J = 6.8$ Hz, 2H, ArCH_2), 3.30 (q, $J = 6.4$ Hz, 2H, CH_2NH), 4.55 (br s, 1H, N*H*SO_2), 5.31 (s, 2H, CH_2O), 6.94 (d, $J = 8.6$ Hz, 2H, Ar*H*), 7.08–7.17 (m, 4H, Ar*H*), 7.22–7.33 (m, 3H, Ar*H*), 7.90 (d, $J = 8.8$ Hz, 2H, Ar*H*), 7.97 (d, $J = 8.8$ Hz, 2H, Ar*H*), 8.14 (s, 1H, C*H*N). ^{13}C NMR (75 MHz, $CDCl_3$) δ 20.5 (CH_3), 35.8 (CH_2), 44.3 (CH_2), 62.0 (OCH_2), 114.6 (CH), 120.6 (CH), 127.0 (CH), 128.7 (CH), 128.9 (CH), 130.1 (CH), 130.9 (C), 137.3 (C), 139.7 (C), 140.2 (C), 146.0 (C), 155.9 (C). HRMS–TOF: *m/z* $[M+H]^+$ 449.1641 (Calcd for $C_{24}H_{25}N_4O_3S$: 449.1642).

*4-(4-((4-Formylphenoxy)methyl)-1H-1,2,3-triazol-1-yl)-N-phenethylbenzenesulfonamide (**5f**)*

White solid. 79 %. mp 141–142 °C. IR (UATR) cm^{-1}: 3267 (NH), 1687 (C=O), 1597 (ar C=C), 1507 (ar C=C), 1330 (S=O), 1158 (S=O). ^1H NMR (300 MHz, $CDCl_3$) δ 2.83 (t, $J = 6.8$ Hz, 2H, ArCH_2), 3.31 (q, $J = 6.8$ Hz, 2H, CH_2NH), 4.62 (t, $J = 6.1$ Hz, 1H, N*H*SO_2), 5.42 (s, 2H, CH_2O), 7.08–7.34 (m, 7H, Ar*H*), 7.85–8.01 (m, 6H, Ar*H*), 8.19 (s, 1H, C*H*N), 9.92 (s, 1H, C*H*O). ^{13}C NMR (75 MHz, $CDCl_3$) δ 35.8 (CH_2), 44.3 (CH_2), 62.0 (OCH_2), 115.1 (CH), 120.7 (CH), 120.9 (CH), 127.0 (CH), 128.7 (CH), 128.9 (CH), 129.0 (CH), 130.6 (C), 132.1 (CH), 137.3 (C), 139.5 (C), 140.5 (C), 144.8 (C), 162.9 (C), 190.7 (C=O). HRMS–TOF: *m/z* $[M+H]^+$ 463.1428 (Calcd for $C_{24}H_{23}N_4O_4S$: 463.1434).

*4-(4-((4-Nitrophenoxy)methyl)-1H-1,2,3-triazol-1-yl)-N-phenethylbenzenesulfonamide (**5g**)*

White solid. 93 %. mp 192–193 °C. IR (UATR) cm^{-1}: 3280 (NH), 1590 (ar C=C), 1506 (ar C=C), 1338 (S=O), 1158 (S=O). ^1H NMR (300 MHz, DMSO-d_6) δ 2.70 (t, $J = 7.6$ Hz, 2H, ArCH_2), 3.03 (q, $J = 6.9$ Hz, 2H, CH_2NH), 5.45 (s, 2H, CH_2O), 7.13–7.35 (m, 7H, Ar*H*), 7.91 (t, $J = 5.7$ Hz, 1H, N*H*SO_2), 7.98 (d, $J = 8.7$ Hz, 2H, Ar*H*), 8.14 (d, $J = 8.7$ Hz, 2H, Ar*H*), 8.25 (d, $J = 9.0$ Hz, 2H, Ar*H*), 9.11 (s, 1H, C*H*N). ^{13}C NMR (75 MHz, DMSO-d_6) δ 35.7 (CH_2), 44.5 (CH_2), 62.2 (OCH_2), 115.9 (CH), 121.2 (CH), 124.0 (CH), 126.4 (CH), 126.7 (CH), 128.8 (CH), 128.9 (CH), 129.1 (CH), 139.0 (C), 139.3 (C), 140.8 (C), 141.7 (C), 143.8 (C), 163.6 (C). HRMS–TOF: *m/z* $[M+H]^+$ 480.1337 (Calcd for $C_{23}H_{22}N_5O_5S$: 480.1336).

*N-Phenethyl-4-(4-((o-tolyloxy)methyl)-1H-1,2,3-triazol-1-yl)benzenesulfonamide (**5h**)*

White solid. 91 %. mp 172–173 °C. IR (UATR) cm^{-1}: 3187 (NH), 1594 (ar C=C), 1496 (ar C=C), 1333 (S=O), 1161 (S=O). ^1H NMR (300 MHz, DMSO-d_6) δ 2.16 (s, 3H, ArCH_3), 2.70 (t, $J = 7.6$ Hz, 2H, ArCH_2), 3.02 (q, $J = 7.1$ Hz, 2H, CH_2NH), 5.26 (s, 2H, CH_2O), 6.83–6.90 (m, 1H, Ar*H*), 7.12–7.29 (m, 8H, Ar*H*), 7.91 (t, $J = 5.7$ Hz, 1H, N*H*SO_2), 7.98 (d, $J = 8.8$ Hz, 2H, Ar*H*), 8.15 (d, $J = 8.8$ Hz, 2H, Ar*H*), 9.06 (s, 1H, C*H*N). ^{13}C NMR (75 MHz, DMSO-d_6) δ 16.5 (CH_3), 35.7 (CH_2), 44.5 (CH_2), 61.7 (OCH_2), 112.4 (CH), 121.1 (CH), 121.2 (CH), 123.3 (CH), 126.5 (C), 126.7 (CH), 127.4 (CH), 128.8 (CH), 129.1 (CH), 131.0 (CH), 139.0 (C), 139.4 (C), 140.7 (C), 145.2 (C), 156.5 (C). HRMS–TOF: *m/z* $[M+H]^+$ 449.1629 (Calcd for $C_{24}H_{25}N_4O_3S$: 449.1642).

*Methyl 2-((1-(4-(N-phenethylsulfamoyl)phenyl)-1H-1,2,3-triazol-4-yl)methoxy)benzoate (**5i**)*

White solid. 88 %. mp 135–136 °C. IR (UATR) cm^{-1}: 3275 (NH), 1717 (C=O), 1599 (ar C=C), 1490 (ar C=C), 1307 (S=O), 1159 (S=O). ^1H NMR (300 MHz, $CDCl_3$) δ 2.82 (t, $J = 6.8$ Hz, 2H, ArCH_2), 3.31 (br t, 2H, CH_2NH), 3.92 (s, 3H, CO_2CH_3), 4.62 (br s, 1H, N*H*SO_2), 5.44 (s, 2H, CH_2O), 7.04–7.33 (m, 7H, Ar*H*), 7.49–7.57 (m, 1H, Ar*H*), 7.85–8.00 (m, 5H, Ar*H*), 8.36 (s, 1H, C*H*N). ^{13}C NMR (75 MHz, $CDCl_3$) δ 35.8 (CH_2), 44.3 (CH_2), 52.0 (OCH_3), 63.4 (OCH_2), 114.1 (CH), 120.6 (CH), 121.1 (C), 121.3 (CH), 127.0 (CH), 128.7 (CH), 128.9 (CH), 131.8 (CH), 133.8 (C), 137.4 (C), 139.7 (C), 140.1 (C), 157.8 (C), 166.2 (C=O). HRMS–TOF: *m/z* $[M+Na]^+$ 515.1359 (Calcd for $C_{25}H_{24}N_4NaO_5S$: 515.1371).

*4-(4-((4-Formyl-2-methoxyphenoxy)methyl)-1H-1,2,3-triazol-1-yl)-N-phenethylbenzenesulfonamide (**5j**)*

Pale yellow solid. 76 %. mp 100–101 °C. IR (UATR) cm^{-1}: 3300 (NH), 1677 (C=O), 1586 (ar C=C), 1504 (ar C=C), 1334 (S=O), 1156 (S=O). ^1H NMR (300 MHz, $CDCl_3$) δ 2.78 (t, $J = 6.8$ Hz, 2H, ArCH_2), 3.26 (q, $J = 6.7$ Hz, 2H, CH_2NH), 3.92 (s, 3H, OCH_3), 4.67 (t, $J = 6.1$ Hz, 1H, N*H*SO_2), 5.44 (s, 2H, CH_2O), 7.06 (dd, $J = 7.9$, 1.7 Hz, 2H, Ar*H*), 7.18–7.28 (m, 4H, Ar*H*), 7.40–7.47 (m, 2H, Ar*H*), 7.85 (d, $J = 8.8$ Hz, 2H, Ar*H*), 7.92 (d, $J = 8.7$ Hz, 2H, Ar*H*), 8.18 (s, 1H, C*H*N), 9.84 (s, 1H, C*H*O). ^{13}C NMR (75 MHz, $CDCl_3$) δ 35.8 (CH_2), 44.3 (CH_2), 56.1 (OCH_3), 62.7 (OCH_2), 109.5 (CH), 112.6 (CH), 120.7 (CH), 121.2 (C), 126.6 (CH), 127.0 (CH),

128.7 (CH), 128.9 (CH), 130.9 (C), 137.4 (C), 139.5 (C), 140.4 (C), 150.0 (C), 152.8 (C), 190.9 (C=O). HRMS–TOF: *m/z* $[M+H]^+$ 493.1545 (Calcd for $C_{25}H_{25}N_4O_5S$: 493.1540).

*4-(4-((5-Formyl-2-methoxyphenoxy)methyl)-1H-1,2,3-triazol-1-yl)-N-phenethylbenzenesulfonamide (**5k**)*

Light brown solid. 71 %. mp 204–205 °C. IR (UATR) cm^{-1}: 3304 (NH), 1686 (C=O), 1583 (ar C=C), 1514 (ar C=C), 1335 (S=O), 1162 (S=O). ^1H NMR (300 MHz, DMSO-d_6) δ 2.70 (t, $J = 6.8$ Hz, 2H, ArCH_2), 3.02 (q, $J = 6.8$ Hz, 2H, CH_2NH), 3.87 (s, 3H, OCH_3), 5.33 (s, 2H, CH_2O), 7.13–7.30 (m, 6H, Ar*H*), 7.62 (dd, $J = 8.2$, 1.7 Hz, 1H, Ar*H*), 7.66 (d, $J = 1.7$ Hz, 1H, Ar*H*), 7.90 (t, $J = 5.7$ Hz, 1H, N*H*SO_2), 7.98 (d, $J = 8.7$ Hz, 2H, Ar*H*), 8.15 (d, $J = 8.7$ Hz, 2H, Ar*H*), 9.07 (s, 1H, C*H*N), 9.86 (s, 1H, C*H*O). ^{13}C NMR (75 MHz, DMSO-d_6) δ 35.7 (CH_2), 44.5 (CH_2), 56.4 (OCH_3), 62.1 (OCH_2), 112.2 (CH), 112.3 (CH), 121.1 (CH), 123.9 (CH), 126.7 (CH), 126.9 (CH), 128.8 (CH), 129.1 (CH), 130.1 (C), 139.1 (C), 139.4 (C), 140.8 (C), 144.3 (C), 148.2 (C), 155.0 (C), 191.8 (C=O). HRMS–TOF: *m/z* $[M+H]^+$ 493.1536 (Calcd for $C_{25}H_{25}N_4O_5S$: 493.1540).

*4-(4-(((2-Oxo-2H-chromen-7-yl)oxy)methyl)-1H-1,2,3-triazol-1-yl)-N-phenethylbenzenesulfonamide (**5l**)*

White solid. 77 %. mp 130–131 °C. IR (UATR) cm^{-1}: 3246 (NH), 1718 (C=O), 1618 (C=C), 1595 (ar C=C), 1505 (ar C=C), 1277 (S=O), 1153 (S=O). ^1H NMR (300 MHz, $CDCl_3$) δ 2.79 (t, $J = 6.8$ Hz, 2H, ArCH_2), 3.27 (q, $J = 6.6$ Hz, 2H, CH_2NH), 4.60 (t, $J = 5.8$ Hz, 1H, N*H*SO_2), 5.35 (s, 2H, CH_2O), 6.26 (d, $J = 9.5$, 1H, COC*H*=CH), 6.91–6.98 (m, 2H, Ar*H*), 7.07 (d, $J = 6.6$ Hz, 2H, Ar*H*), 7.17–7.29 (m, 3H, Ar*H*), 7.40 (d, $J = 9.2$ Hz, 1H, Ar*H*), 7.63 (d, $J = 9.5$ Hz, 1H, COCH=C*H*), 7.87 (d, $J = 8.7$ Hz, 2H, Ar*H*), 7.93 (d, $J = 8.7$ Hz, 2H, Ar*H*), 8.50 (s, 1H, C*H*N). ^{13}C NMR (75 MHz, $CDCl_3$) δ 35.8 (CH_2), 44.3 (CH_2), 62.2 (OCH_2), 102.2 (CH), 112.7 (CH), 113.2 (CH), 113.7 (CH), 120.7 (CH), 121.0 (C), 127.0 (CH), 128.7 (CH), 128.9 (CH), 129.0 (CH), 137.4 (C), 139.5 (C), 140.4 (C), 143.2 (C), 155.8 (C), 161.0 (C), 161.1 (C). HRMS–TOF: *m/z* $[M+H]^+$ 503.1392 (Calcd for $C_{26}H_{23}N_4O_5S$: 503.1384).

*4-(4-(((2-Oxo-2H-chromen-4-yl)oxy)methyl)-1H-1,2,3-triazol-1-yl)-N-phenethylbenzenesulfonamide (**5m**)*

White solid. 77 %. mp 181–182 °C. IR (UATR) cm^{-1}: 3147 (NH), 1719 (C=O), 1624 (C=C), 1328 (S=O), 1157 (S=O). ^1H NMR (300 MHz, DMSO-d_6) δ 2.70 (t, $J = 6.8$ Hz, 2H, ArCH_2), 3.02 (q, $J = 6.8$ Hz, 2H, CH_2NH), 5.56 (s, 2H, CH_2O), 6.22 (s, 1H, COC*H*), 7.13–7.46 (m, 5H, Ar*H*), 7.36 (t, $J = 8.0$, 1H, Ar*H*), 7.43 (d, $J = 7.8$ Hz, 1H, Ar*H*), 7.66 (dt, $J = 8.0$, 1.4 Hz, 1H, Ar*H*), 7.85 (dd, $J = 7.9$, 1.4 Hz, 1H, Ar*H*), 7.92 (t, $J = 5.7$ Hz, 1H, N*H*SO_2), 7.99 (d, $J = 8.8$ Hz, 2H, Ar*H*), 8.18 (d, $J = 8.8$ Hz, 2H, Ar*H*), 9.21 (s, 1H, C*H*N). ^{13}C NMR (75 MHz, DMSO-d_6) δ 35.7 (CH_2), 44.5 (CH_2), 63.2 (OCH_2), 92.0 (CH), 115.5 (CH), 116.9 (CH), 121.2 (CH), 123.5 (CH), 124.1 (CH), 124.7 (CH), 126.7 (CH), 128.8 (CH), 128.9 (CH), 133.3 (C), 139.0 (C), 139.3 (C), 140.9 (C), 143.1 (C), 153.3 (C), 162.0 (C), 164.8. HRMS–TOF: *m/z* $[M+H]^+$ 503.1383 (Calcd for $C_{26}H_{23}N_4O_5S$: 503.1384).

*N-(3,4-Dimethoxyphenethyl)-4-(4-phenyl-1H-1,2,3-triazol-1-yl)benzenesulfonamide (**5n**)*

Pale yellow solid. 94 %. mp 147–148 °C. IR (UATR) cm^{-1}: 3271 (NH), 1596 (ar C=C), 1516 (ar C=C), 1330 (S=O), 1157 (S=O). ^1H NMR (300 MHz, $CDCl_3$) δ 2.74 (t, $J = 6.8$ Hz, 2H, ArCH_2), 3.26 (q, $J = 6.8$ Hz, 2H, CH_2NH), 3.78, 3.81 (2s, 6H, 2 × OCH_3), 4.59 (t, $J = 6.2$ Hz, 1H, N*H*SO_2), 6.56 (d, $J = 1.7$ Hz, 1H, C2-Ar*H*), 6.61 (dd, $J = 8.1$,1.7 Hz, 1H, C6-Ar*H*), 6.74 (d, $J = 8.1$ Hz, 1H, C5-Ar*H*), 7.35–7.50 (m, 3H, Ar*H*), 7.87–7.98 (m, 6H, Ar*H*), 8.27 (s, 1H, C*H*N). ^{13}C NMR (75 MHz, $CDCl_3$) δ 35.4 (CH_2), 44.4 (CH_2), 55.9 (OCH_3), 56.0 (OCH_3), 111.6 (CH), 111.9 (CH), 117.3 (CH), 120.5 (CH), 120.8 (CH), 126.0 (CH), 128.8 (CH), 128.9 (CH), 129.7 (C), 129.9 (C), 139.7 (C), 140.0 (C), 148.1 (C), 149.0 (C), 149.2 (C). HRMS–TOF: *m/z* $[M+H]^+$ 465.1590 (Calcd for $C_{24}H_{25}N_4O_4S$: 465.1591).

*N-(3,4-Dimethoxyphenethyl)-4-(4-((4-formylphenoxy)methyl)-1H-1,2,3-triazol-1-yl)benzenesulfonamide (**5o**)*

Light brown solid. 90 %. mp 143–144 °C. IR (UATR) cm^{-1}: 3262 (NH), 1688 (C=O), 1597 (ar C=C), 1508 (ar C=C), 1330 (S=O), 1159 (S=O). ^1H NMR (300 MHz, $CDCl_3$) δ 2.73 (t, $J = 6.5$ Hz, 2H, ArCH_2), 3.24 (q, $J = 6.2$ Hz, 2H, CH_2NH), 3.76, 3.80 (2s, 6H, 2 × OCH_3), 4.58 (t, $J = 6.0$ Hz, 1H, N*H*SO_2), 5.38 (s, 2H, CH_2O), 6.55 (br d, 1H, C2-Ar*H*), 6.60 (d, $J = 7.8$ Hz, 1H, C6-Ar*H*), 6.73 (d, $J = 8.1$ Hz, 1H, C5-Ar*H*), 7.81–7.96 (m, 6H, Ar*H*), 7.12 (d, $J = 8.6$ Hz, 2H, Ar*H*), 8.17 (s, 1H, C*H*N), 9.88 (s, 1H, C*H*O). ^{13}C NMR (75 MHz, $CDCl_3$) δ 35.4 (CH_2), 44.4 (CH_2), 55.8 (OCH_3), 55.9 (OCH_3), 62.0 (OCH_2), 111.5 (CH), 111.8 (CH), 115.1 (CH), 120.6 (CH), 120.7 (CH), 120.8 (C), 121.0 (C), 128.9 (C), 129.8 (C), 130.6 (C), 132.0 (CH), 139.5 (C), 140.4 (C), 144.7 (C), 148.1 (C), 149.2 (C), 162.9 (C), 190.7 (C=O). HRMS–

TOF: *m/z* $[M+H]^+$ 523.1650 (Calcd for $C_{26}H_{27}N_4O_6S$: 523.1646).

*N-(3,4-Dimethoxyphenethyl)-4-(4-((4-nitrophenoxy)methyl)-1H-1,2,3-triazol-1-yl)benzenesulfonamide (**5p**)*

Light brown solid. 95 %. mp 183–184 °C. IR (UATR) cm^{-1}: 3257 (NH), 1593 (ar C=C), 1519 (ar C=C), 1343 (S=O), 1160 (S=O). ^1H NMR (300 MHz, DMSO-d_6) δ 2.62 (t, $J = 7.4$ Hz, 2H, ArCH_2), 3.03 (q, $J = 7.0$ Hz, 2H, CH_2NH), 3.65, 3.68 (2s, 6H, 2 × OCH_3), 5.45 (s, 2H, CH_2O), 6.64 (dd, $J = 8.1$, 1.8 Hz, 1H, C6-Ar*H*), 6.72 (d, $J = 1.7$ Hz, 1H, C2-Ar*H*), 6.78 (d, $J = 8.2$ Hz, 1H, C5-Ar*H*), 7.32 (d, $J = 9.3$ Hz, 2H, C2″-Ar*H* and C6″-Ar*H*), 7.85 (t, $J = 5.6$ Hz, 1H, N*H*SO_2), 7.94 (d, $J = 8.7$ Hz, 2H, C3′-Ar*H* and C5′-Ar*H*), 8.11 (d, $J = 8.7$ Hz, 2H, C2′-Ar*H* and C6′-Ar*H*), 8.25 (d, $J = 9.2$ Hz, 2H, C3″-Ar*H* and C5″-Ar*H*), 9.09 (s, 1H, C*H*N). ^{13}C NMR (75 MHz, DMSO-d_6) δ 35.3 (CH_2), 44.7 (CH_2), 55.8 (OCH_3), 55.9 (OCH_3), 62.2 (OCH_2), 112.2 (CH), 113.0 (CH), 115.9 (CH), 121.0 (CH), 123.9 (CH), 126.4 (CH), 128.8 (CH), 131.4 (C), 139.2 (C), 140.9 (C), 141.7 (C), 143.8 (C), 147.8 (C), 149.0 (C), 163.6 (C). HRMS–TOF: *m/z* $[M+H]^+$ 540.1563 (Calcd for $C_{25}H_{26}N_5O_7S$: 540.1548).

Cytotoxic assay

The cells suspended in the corresponding culture medium were inoculated in 96-well microtiter plates (Corning Inc., NY, USA) at a density of 10,000–20,000 cells per well, and incubated for 24 h at 37 °C in a humidified atmosphere with 95 % air and 5 % CO_2. An equal volume of additional medium containing either the serial dilutions of the test compounds, positive control (etoposide and/or doxorubicin) or negative control (DMSO) was added to the desired final concentrations, and the microtiter plates were further incubated for an additional 48 h. The number of surviving cells in each well was determined using MTT assay (Carmichael *et al*., 1987; Mosmann, 1983) (for adherent cells: HuCCA-1, HepG2, and A549 cells) and XTT assay (Doyle and Griffiths, 1997) (for suspended cells: MOLT-3 cells). The IC_{50} value is defined as the drug (or compound) concentration that inhibits cell growth by 50 % (relative to negative control).

Acknowledgments We gratefully acknowledge the research grants from Srinakharinwirot University under the Government Budget (B.E. 2557) and the Thailand Research Fund under the Young Scholars Research Fellowship (MRG5680001 to R.P.). This project is supported by the office of the Higher Education Commission and Mahidol University under the National Research Universities Initiative. We are also indebted to the Chulabhorn Research Institute for recording mass spectra and bioactivity testing.

References

Agalave SG, Maujan SR, Pore VS (2011) Click chemistry: 1,2,3-triazoles as pharmacophores. Chem Asian J 6:2696–2718

Banday AH, Shameem SA, Gupta BD, Sampath Kumar HM (2010) D-ring substituted 1,2,3-triazolyl 20-keto pregnenanes as potential anticancer agents: synthesis and biological evaluation. Steroids 75:801–804

Bektas H, Demirbas A, Demirbas N, Karaoglu SA (2012) Synthesis and biological activity studies of new hybrid molecules containing tryptamine moiety. Med Chem Res 21:212–223

Boechat N, Pinheiro LCS, Santos-Filho OA, Silva IC (2011) Design and synthesis of new *N*-(5-trifluoromethyl)-1*H*-1,2,4-triazol-3-yl benzenesulfonamides as possible antimalarial prototypes. Molecules 16:8083–8097

Carmichael J, DeGraff WG, Gazdar AF, Minna JD, Mitchell JB (1987) Evaluation of a tetrazolium-based semiautomated colorimetrie assay: assessment of radiosensitivity. Cancer Res 47: 943–946

Doyle A, Griffiths JB (1997) Mammalian cell culture: essential techniques. Wiley, Chichester

Ezabadi IR, Camoutsis C, Zoumpoulakis P, Geronikaki A, Soković M, Glamočlija J, Cirić A (2008) Sulfonamide-1,2,4-triazole derivatives as antifungal and antibacterial agents: synthesis, biological evaluation, lipophilicity, and conformational studies. Bioorg Med Chem 16:1150–1161

Faidallah HM, Khan KA, Asiri AM (2011) Synthesis and biological evaluation of new 3,5-di(trifluoromethyl)-1,2,4-triazolesulfonylurea and thiourea derivatives as antidiabetic and antimicrobial agents. J Fluorine Chem 132:870–877

Hu L, Li ZR, Jiang JD, Boykin DW (2008) Novel diaryl or heterocyclic sulfonamides as antimitotic agents. Anti Cancer Agents Med Chem 8:739–745

Hubschwerlen C, Specklin JL, Sigwalt C, Schroeder S, Locher HH (2003) Design, synthesis and biological evaluation of oxazolidinone–quinolone hybrids. Bioorg Med Chem 11:2313–2319

Kaplancikli ZA, Turan-Zitouni G, Ozdemir AA, Revial G (2008) New triazole and triazolothiadiazine derivatives as possible antimicrobial agents. Eur J Med Chem 43:155–159

Kolb HC, Finn MG, Sharpless KB (2001) Click chemistry: diverse chemical function from a few good reactions. Angew Chem Int Ed 40:2004–2021

Mosmann T (1983) Rapid colorimetric assay for cellular growth and survival: application to proliferation and cytotoxicity assays. J Immunol Methods 65:55–63

Ou L, Han S, Ding W, Jia P, Yang B, Medina-Franco JL, Giulianotti MA, Chen JZ, Yu Y (2011) Parallel synthesis of novel antitumor agents: 1,2,3-triazoles bearing biologically active sulfonamide moiety and their 3D-QSAR. Mol Divers 15:927–946

Pingaew R, Prachayasittikul S, Ruchirawat S, Prachayasittikul V (2013) Synthesis and cytotoxicity of novel *N*-sulfonyl-1,2,3,4-tetrahydroisoquinoline thiosemicarbazone derivatives. Med Chem Res 22:267–277

Scozzafava A, Owa T, Mastrolorenzo A, Supuran CT (2003) Cytotoxic and antiviral sulfonamides. Curr Med Chem 10: 925–953

Solomon VR, Hua C, Lee H (2010) Design and synthesis of anti-breast cancer agents from 4-piperazinylquinoline: a hybrid pharmacophore approach. Bioorg Med Chem 18:1563–1572

Supuran CT, Casini A, Mastrolorenzo A, Scozzafava A (2004) COX-2 selective inhibitors, carbonic anhydrase inhibition and cytotoxic properties of sulfonamides belonging to this class of pharmacological agents. Mini Rev Med Chem 4:625–632

Thomas KD, Adhikari AV, Chowdhury IH, Sumesh E, Pal NK (2011) New quinolin-4-yl-1,2,3-triazoles carrying amides and

amidopiperazines as potential antitubercular agents. Eur J Med Chem 46:2503–2512

Wang XL, Wan K, Zhou CH (2010) Synthesis of novel sulfanilamide-derived 1,2,3-triazoles and their evaluation for antibacterial and antifungal activities. Eur J Med Chem 45:4631–4639

Wilkinson BL, Bornaghi LF, Wright AD, Houston TA, Poulsen SA (2007) Anti-mycobacterial activity of a bis-sulfonamide. Bioorg Med Chem Lett 17:1355–1357

Winum JY, Rami M, Scozzafava A, Montero JL, Supuran C (2008) Carbonic anhydrase IX: a new druggable target for the design of antitumor agents. Med Res Rev 28:445–463

Synthesis and structure–activity relationship of mono-indole-, bis-indole-, and tris-indole-based sulfonamides as potential anticancer agents

Ratchanok Pingaew, Supaluk Prachayasittikul, Somsak Ruchirawat & Virapong Prachayasittikul

Molecular Diversity

ISSN 1381-1991
Volume 17
Number 3

Mol Divers (2013) 17:595-604
DOI 10.1007/s11030-013-9457-7

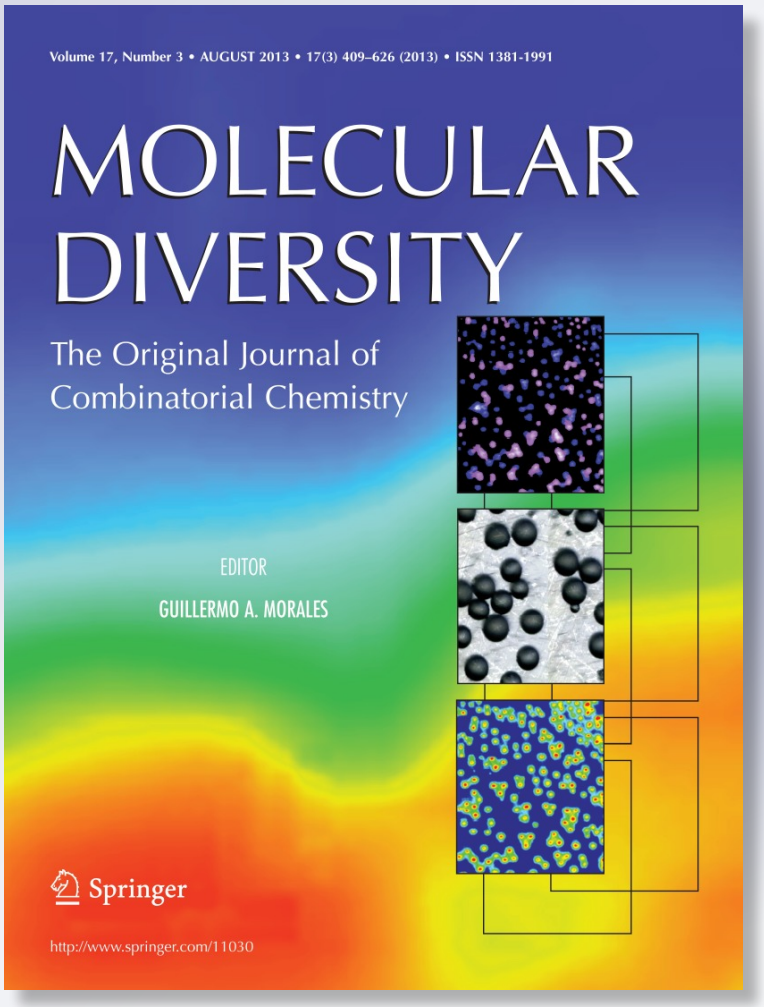

Springer

Your article is protected by copyright and all rights are held exclusively by Springer Science +Business Media Dordrecht. This e-offprint is for personal use only and shall not be self-archived in electronic repositories. If you wish to self-archive your article, please use the accepted manuscript version for posting on your own website. You may further deposit the accepted manuscript version in any repository, provided it is only made publicly available 12 months after official publication or later and provided acknowledgement is given to the original source of publication and a link is inserted to the published article on Springer's website. The link must be accompanied by the following text: "The final publication is available at link.springer.com”.

Springer

Author's personal copy

Mol Divers (2013) 17:595–604
DOI 10.1007/s11030-013-9457-7

FULL-LENGTH PAPER

Synthesis and structure–activity relationship of mono-indole-, bis-indole-, and tris-indole-based sulfonamides as potential anticancer agents

Ratchanok Pingaew · Supaluk Prachayasittikul · Somsak Ruchirawat · Virapong Prachayasittikul

Received: 25 February 2013 / Accepted: 8 June 2013 / Published online: 28 June 2013
© Springer Science+Business Media Dordrecht 2013

Abstract A series of arylsulfonyl mono-indoles (**10**–**15**), bis-indoles (**16**–**27**), and tris-indoles (**28**–**32**) have been synthesized and evaluated for their cytotoxicity toward four human cancer cell lines including HuCCA-1 (cholangiocarcinoma), HepG2 (hepatocellular carcinoma), A-549 (lung carcinoma), and MOLT-3 (lymphoblastic leukemia). Most of the synthesized indoles displayed cytotoxicity against the MOLT-3 cell line except for analogs **16**, **17**, and **32**. Significantly, the *N*-sulfonylphenolic bis-indole series (**18**–**27**) and the *N*-chlorobenzenesulfonyl tris-indole (**30**) showed higher antiproliferative activity against HepG2 cell than the reference drug, etoposide. Promisingly, the *N*-chlorobenzenesulfonyl bis-indole (**20**) and tris-indole (**30**) provided 3-fold and 2-fold stronger activity, respectively, against HepG2 cell than etoposide. Moreover, the phenolic bis-indole (**20**) was also shown to be the most potent cytotoxic agent against HuCCA-1 and A-549 cell lines with IC_{50} values of 7.75 and 8.74 μM, respectively. The tris-indole analogs **28**, **29**, and **31** also exhibited selectivity against MOLT-3 cell. The findings disclosed that *N*-arylsulfonyl bis-indoles-bearing phenolic groups are potentially interesting lead pharmacophores of anticancer agents that should be further investigated in more detail.

Keywords Indole · Sulfonamide · Heteropoly acid · Antiproliferative activity · Structure–activity relationship

Electronic supplementary material The online version of this article (doi:10.1007/s11030-013-9457-7) contains supplementary material, which is available to authorized users.

R. Pingaew (✉)
Department of Chemistry, Faculty of Science,
Srinakharinwirot University, Bangkok 10110, Thailand
e-mail: ratchanok@swu.ac.th

S. Prachayasittikul
Center of Data Mining and Biomedical Informatics,
Faculty of Medical Technology, Mahidol University,
Bangkok 10700, Thailand

S. Ruchirawat
Chulabhorn Research Institute and Chulabhorn Graduate Institute,
Bangkok 10210, Thailand

V. Prachayasittikul
Department of Clinical Microbiology and Applied Technology,
Faculty of Medical Technology, Mahidol University,
Bangkok 10700, Thailand

Introduction

Several natural products containing the indole ring system have received much interest due to their potent biological activities especially anticancer properties [1–4]. For instance, convolutamydine A (**1**), an indolin-2-one isolated from the Floridian bryozoans *Amathia convoluta*, was found to exhibit potent activity in the differentiation of HL-60 human promyelocytic leukemic cells [5]. Furthermore, 3,3-di(indol-3-yl)-indolin-2-one (**2**) isolated from the expression of *Rhodococcus*-derived oxygenase gene in *Escherichia coli* has been shown to exert cytotoxic effects toward both parental (MES-SA and HCT15) and multidrug-resistant (MDR; MES-SA/DX5 and HCT15/CL02) cell lines. It was found to be more effective in killing MDR cancer cells when compared with the control drug, etoposide [6].

Recently, a series of synthetic di(indolyl)indolin-2-ones (**3**) have been reported to display anticancer potencies without affecting normal cell lines [7]. Bis-indolylmethane (BIM) is recognized as one of the scaffolds that are found in many natural products isolated from both terrestrial and marine natural sources [8]. BIMs also exhibit a broad range of bioactivities including anticancer activ-

Author's personal copy

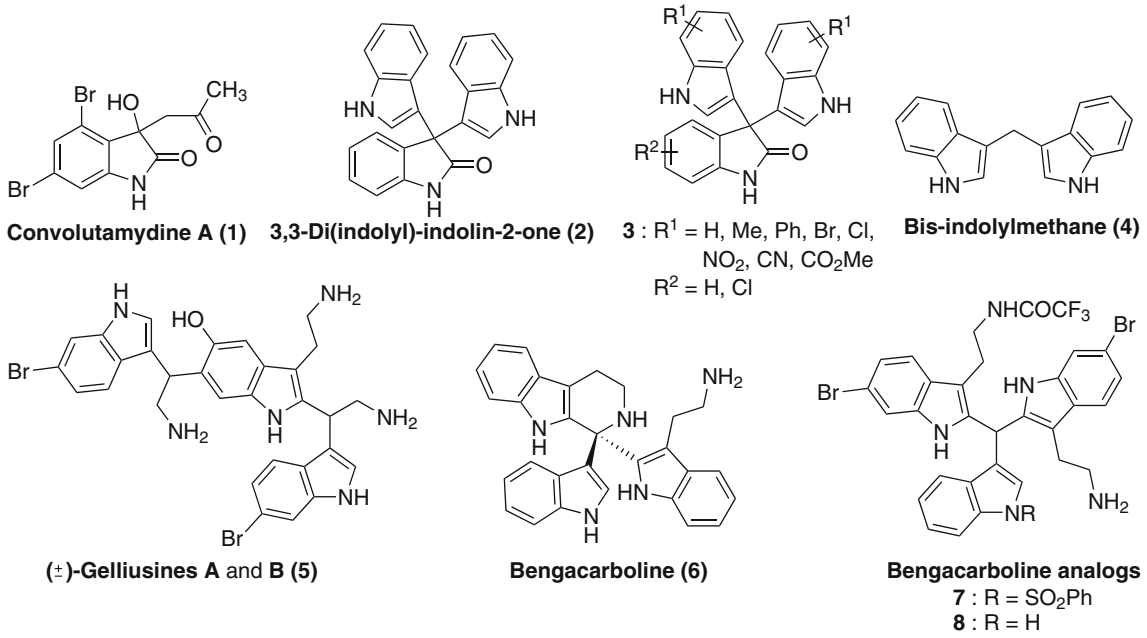

Fig. 1 Representative bioactive indole alkaloids (**1**–**8**)

ity against several common cancer cell lines [9]. Among the family of BIM, 3,3′-bis-indolylmethane (**4**) is a major metabolite of the anticancer agent belonging to indole-3-carbinol, which is found in vegetables of the *Brassica* genus. It has been shown to inhibit the proliferation of both estrogen-dependent and -independent breast cancer cell lines [10,11]. (±)-Gelliusines A and B (**5**), brominated tris-indole alkaloids isolated from the deep water New Caledonian sponge *Gellius* or *Orina* sp., could inhibit cancer cell lines (e.g., KB, P-388, P-388/dox, HT-29, and NSCLCN-6) with IC_{50} values in the range of 10–20 μg/mL [12]. In addition, bengacarboline (**6**) as cyclic tris-indolylmethane, isolated from the Fijian ascidian *Didemnum* sp., displayed *in vitro* cytotoxicity on a wide range of tumor cell lines with a mean IC_{50} value of 0.9 μg/mL. It acted as an inhibitor of topoisomerase II at 32 μM [13]. The synthetic tris-indolylmethane analogs **7** and **8** of bengacarboline were shown to be more potent cytotoxic agents than the parent compound (**6**). Analogs **7** and **8** exhibited anticancer activity as well as the ability to induce the accumulation of cells in the S phase of DNA synthesis [14] (Fig. 1).

Recently, our group had reported the synthesis and cytotoxic activity of *N*,*N*′-(2,2′-(2,2′-(aryl-methylene)bis(1*H*-indole-3,2-diyl)bis(ethane-2,1-diyl)bis(4-nitrobenzenesulfonamide) derivatives **9** (Fig. 2) [15]. The study revealed that the phenolic hydroxyl group plays an important role in cytotoxicity. Particularly, the *ortho*- and *para*-hydroxy phenyl (R = OH) BIM analogs (**9b** and **9c**) displayed cytotoxic potency toward HepG2 and MOLT-3 cancer cell lines,

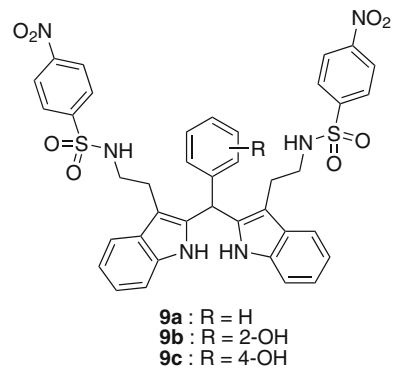

Fig. 2 Cytotoxic *N*-4-nitrobenzenesulfonyl-bis-indole derivatives (**9**)

whereas the unsubstituted phenyl (R = H) BIM compound **9a** was shown to be inactive.

Considering the reported cytotoxic property of indoles in the mono-, bis-, and tris-form, their indole rings were substituted at various positions, particularly at C-2, C-3, C-2,3, or C-2,3,3. It was noted that the indole moiety of the compounds was mostly substituted at the C-3 position. Taken together, we designed and synthesized indole analogs having sulfonamides at the C-3 position as a continuation of our ongoing efforts in the design of indole scaffolds that afford potential chemotherapeutic activities. The strategic design of the target indole analogs (**10**–**32**) was based on the reported literature and turned out as follows (Fig. 3):

(i) use the mono-indole (type I), bis-indole (type II–IV), and tris-indole (typeV) as core structures having 3-benzenesulfonamide moieties;

Author's personal copy

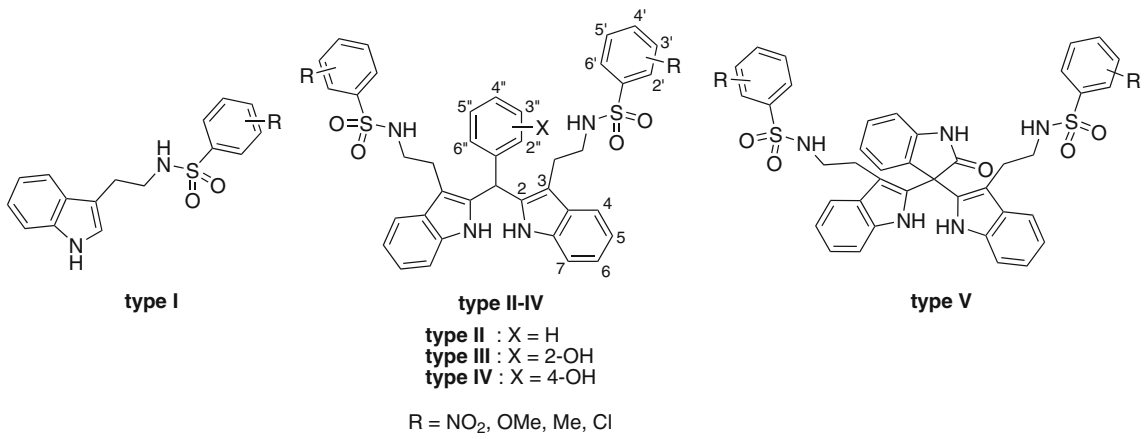

Fig. 3 Molecular structures of indole analogs

(ii) use different electron-donating or -withdrawing groups substituted on aryl rings of the benzenesulfonamide moiety (R = NO_2, OMe, Me, Cl); and
(iii) vary the substitution on the phenyl ring of the bis-indole portion (X = H, OH).

In this study, we employed the Friedel–Crafts reaction for the synthesis of BIM and tris-indole core structures as potential anticancer agents that are catalyzed by tungstosilicic acid hydrate ($H_4O_{40}SiW_{12} \cdot aq$). Thus far, the catalyst has received considerable attention owing to its environmental-friendly property, high catalytic activities, commercial availability, high stability toward humidity and air, as well as ease of handing [15–18]. Herein, the antiproliferative activity of the synthesized indole analogs on cancer cell lines, as well as their structure–activity relationship (SAR), is reported.

Results and discussion

Chemistry

Five series of *N*-arylsulfonylindole derivatives mono-indoles (type I), bis-indoles (type II–IV), and tris-indoles (type V) were synthesized. Various mono-indoles **10–15** were readily prepared by the condensation of tryptamine with corresponding arylsulfonyl chlorides in the presence of sodium carbonate in good yields (85–95 %) as shown in Scheme 1 [15]. Subsequently, alkylations of *N*-sulfonyltryptamines **11–15** with benzaldehyde (**a**), *o*-hydroxybenzaldehyde (**b**), or *p*-hydroxybenzaldehyde (**c**) catalyzed by 20 mol % $H_4O_{40}SiW_{12} \cdot aq$ in acetonitrile were investigated. The reactions readily furnished three series of BIMs (type II–IV) in moderate to good yields (38–75 %) (Scheme 2).

Structures of the desired bis-indoles (**16–27**) were characterized by ^{1}H NMR spectra, which showed the existence of a singlet of methine proton at δ in the range of 5–7 ppm indicating that the alkylation products (**16–27**) were formed. In addition, the spectra displayed a typical symmetrical signal of two *N*-arylsulfonyl tryptamine parts.

Analogously, treatment of the *N*-sulfonyltryptamines **11–15** with isatin (**d**) under similar conditions gave the desired tris-indoles (**28–32**) (Scheme 2). To the best of our knowledge, these are the first few reports using the application of this catalyst for the synthesis of tris-indoles (**28–32**). ^{1}H NMR spectra of tris-indoles displayed the presence of a symmetrical signal of two *N*-sulfonyltryptamine moieties, while the indolinone scaffold showed the NH amide singlet proton at δ in the range of 10–11 ppm. ^{13}C NMR signal showed the rest of the amide carbonyls in the δ range of 170–180 ppm. These observations confirmed that the alkylation took place at a ketone group. The structures of all obtained compounds were further supported by 2D NMR, IR, and HRMS.

A plausible mechanism for the formation of BIMs and TIMs may be rationalized by the nucleophilic addition of indole to the carbonyl component, the formation of a vinylogous iminium ion by losing a water molecule, followed by re-addition of another molecule of indole [15].

Anticancer activity

The cytotoxicity [19] of the synthesized mono-indole (**10–15**), bis-indole (**16–27**), and tris-indole (**28–32**) analogs was evaluated against HuCCA-1, HepG2, A549, and MOLT-3 human cancer cell lines as summarized in Table 1.

Most compounds of the mono-indole series (**10–15**) showed poor cytotoxicity against all of the tested cell lines, whereas *p*-chloro (**13**) and *m*-nitro (**14**) derivatives were inactive toward HuCCA-1 cells. The *o*-nitro compound (**15**) was shown to be selectively active against MOLT-3 cells. Significant cytotoxicities were noted for phenolic bis-indoles (**18–27**) and tris-indoles (**28–32**) against the tested cell lines.

Author's personal copy

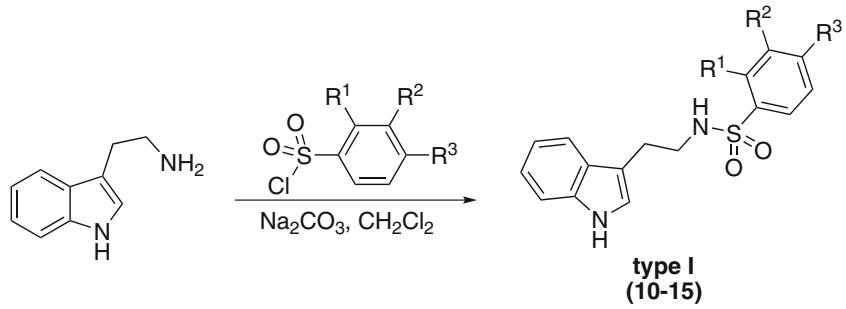

Scheme 1 Synthesis of *N*-(2-(1*H*-indol-3-yl)ethyl)-benzenesulfonamides (**10**–**15**)

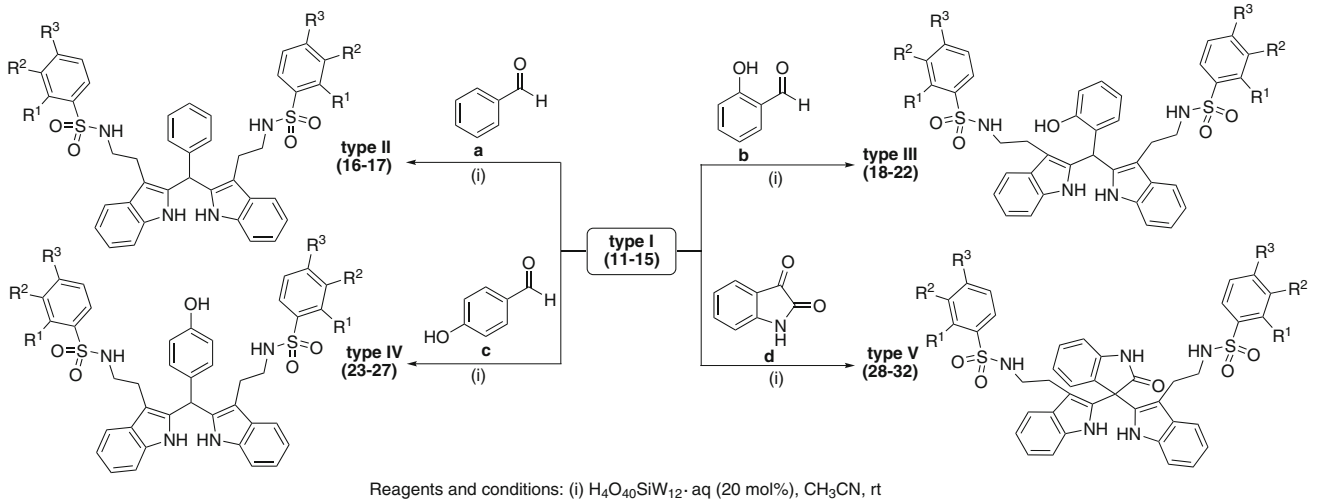

Scheme 2 Synthesis of bis-indole and tris-indole derivatives (**16**–**32**)

Structure–activity relationship (SAR)

As noted, the phenolic bis-indole and tris-indole core structures bear diverse substituents (R^1–R^3) on the aryl ring of the benzenesulfonamide moiety. Thus, SAR information of the compounds is discussed as follows.

Cytotoxic potencies were totally lost when mono-indoles (**10**, **11**, and **12**) were alkylated with benzaldehyde to form bis-indoles (**9a**, **16**, and **17**) incorporating the phenyl ring. The results indicated that the bis-indoles required a phenolic moiety for their cytotoxicities. Notably, this was seen for bis-indole analogs (**18**–**27**) bearing *o*- and *p*-hydroxyl groups (phenolics) that exhibited greater activity than their phenyl counterparts (**16** and **17**). The results were in accordance with the previous observation for bis-indoles (**9b** and **9c** vs. **9a**) [15]. It was suggested that compounds **9b** and **9c** required H-bonding from the phenolic moiety for their cytotoxic activities. *Para*-substitution (R^3 = Me, OMe, Cl) on the benzenesulfonamide group of bis-indoles (**18**–**20**, **23**–**25**) displayed superior inhibitory potency than analogs containing *o*-, *m*-, and *p*-nitro groups (**9b**, **9c**, **21**–**22**, **26**–**27**) against HuCCA-1, HepG2, and A549 cells. Apparently, the cytotoxic potency decreased in the following series: Cl > Me > OMe > NO_2. In the case of nitro group substitutions on the benzenesulfonyl moiety, they were shown to afford different cytotoxicity. Particularly, the results showed that the nitro group at the *ortho* site was preferred over the *para* and *meta* positions as observed for compounds **22** vs. **9b** and **21**, as well as **27** vs. **9c** and **26** against HuCCA-1 cell. It should be noted that all bis-indoles (**9b**, **9c**, **18**–**27**) containing phenolic groups displayed antiproliferative activity against HepG2 and MOLT-3 cell lines. Significantly, they were shown to exhibit higher activity against the HepG2 cell than the control drug etoposide, in which the chloro derivative **20** had the lowest IC_{50} value of 8.62 μM (i.e., 3-fold stronger activity than etoposide). This may be attributed to the hydrophobic effect of the Cl group, which enhanced the absorption of the compound into the cells. Moreover, analog **20** also showed the highest potency toward HuCCA-1 and A549 cells. Cytotoxicity tests in MOLT-3 cell line of bis-indoles bearing the phenol ring reported IC_{50} in the range of 2.04 − 9.95 μM, whereas the bis-indole **9c** was shown to be the most potent compound. At this point, it was observed that substituents (R^3) on the benzene sulfonamide moiety and the phenolic group of bis-indoles played important roles in cytotoxicity. The most remarkable activity against HepG2 was seen for compound **20** (R^3 = Cl) possessing the *o*-phenolic group. On the other hand, the *p*-nitro bis-indole (**9c**, R^3 = NO_2) showed the most potent cytotoxicity against the MOLT-3 cell line.

Author's personal copy

Table 1 Cytotoxic activity of compounds (**10–32**) against four cancer cell lines

Compounds	R^1	R^2	R^3	Cytotoxic activity (IC_{50}, μM)[a]			
				HuCCA-1	HepG2	A549	MOLT-3
10	H	H	NO_2	136.09 ± 1.14	95.55 ± 2.82	124.50 ± 1.41	68.91 ± 2.63
11	H	H	Me	128.18 ± 1.53	83.75 ± 4.73	132.00 ± 2.12	50.41 ± 1.69
12	H	H	OMe	134.69 ± 6.36	86.77 ± 2.08	119.55 ± 0.71	50.15 ± 1.41
13	H	H	Cl	Inactive	69.68 ± 2.89	71.68 ± 0.64	46.23 ± 1.65
14	H	NO_2	H	Inactive	99.40 ± 4.04	128.85 ± 4.95	54.38 ± 2.34
15	NO_2	H	H	Inactive	Inactive	Inactive	59.21 ± 3.13
9a[b]	H	H	NO_2	Inactive	Inactive	Inactive	Inactive
16	H	H	Me	Inactive	Inactive	Inactive	Inactive
17	H	H	OMe	Inactive	Inactive	Inactive	Inactive
9b[b]	H	H	NO_2	Inactive	22.23 ± 2.08	Inactive	4.97 ± 0.13
18	H	H	Me	15.69 ± 0.71	11.15 ± 1.44	64.13 ± 1.41	6.94 ± 0.90
19	H	H	OMe	30.72 ± 0.71	18.73 ± 2.08	47.06 ± 2.83	7.35 ± 0.54
20	H	H	Cl	7.75 ± 0.37	8.62 ± 1.04	8.74 ± 0.79	6.06 ± 0.81
21	H	NO_2	H	Inactive	26.00 ± 4.04	Inactive	5.47 ± 0.68
22	NO_2	H	H	61.65 ± 1.41	22.02 ± 3.79	Inactive	9.95 ± 0.82
9c[b]	H	H	NO_2	Inactive	22.02 ± 2.08	Inactive	2.04 ± 0.10
23	H	H	Me	14.33 ± 2.12	9.55 ± 1.73	15.69 ± 0.71	6.30 ± 0.91
24	H	H	OMe	33.99 ± 1.41	13.30 ± 1.44	Inactive	7.22 ± 1.21
25	H	H	Cl	9.69 ± 0.16	9.91 ± 1.04	12.39 ± 0.58	7.13 ± 0.34
26	H	NO_2	H	Inactive	26.00 ± 1.15	Inactive	8.49 ± 1.19
27	NO_2	H	H	20.93 ± 3.76	9.94 ± 1.93	Inactive	5.06 ± 0.56
28	H	H	Me	Inactive	Inactive	Inactive	5.49 ± 0.58
29	H	H	OMe	Inactive	Inactive	Inactive	53.84 ± 8.25
30	H	H	Cl	15.95 ± 0.37	12.52 ± 0.58	Inactive	6.25 ± 0.35
31	H	NO_2	H	Inactive	Inactive	Inactive	31.57 ± 4.71
32	NO_2	H	H	Inactive	Inactive	Inactive	Inactive
Etoposide[c]				ND	30.92 ± 5.35	ND	0.032 ± 0.001
Doxorubicin[d]				0.79 ± 0.06	1.01 ± 0.13	0.70 ± 0.11	ND

Inactive = IC_{50} > 50 μg/mL
Cancer cell lines comprise the following: *HuCCA-1* human cholangiocarcinoma cancer cell, *HepG2* human hepatocellular carcinoma cell line, *A549* human lung carcinoma cell line, *MOLT-3* human lymphoblastic leukemia cell line
[a] The assays were performed in triplicate
[b] Data from reference number 15
[c,d] Etoposide and doxorubicin were used as reference drugs
ND not determined

All of the tris-indoles (**28–32**) displayed cytotoxic activities against MOLT-3 cells except for *o*-nitro analog **32**. In addition, analog **32** also exhibited no cytotoxicity against the other tested cell lines. However, all tris-indoles were shown to be inactive against the A549 cell line. Significant cytotoxicity of *p*-chloro tris-indole **30** (R^3 = Cl) was observed against HepG2 cell that provided 2-fold stronger activity (IC_{50} 12.52 μM) than etoposide (IC_{50} 30.92 μM).

Conclusion

A variety of mono-, bis-, and tris-indole sulfonamide derivatives have been synthesized and evaluated for their cytotoxic activity. Most of the indole analogs (**10–15**, **18–31**) with various substituents (R^1–R^3) on the benzene ring of the sulfonamide moiety displayed cytotoxicity against MOLT-3 cell lines. Significantly, bis-indoles containing phenolic groups and chloro tris-indole showed higher anticancer activity against HepG2 cell than the control drug, etoposide. The phenolic bis-indoles seem to be the most important core structures responsible for the strong antiproliferative activity observed in all of the tested cancer cell lines. Promisingly, the chloro bis-indole (**20**) and tris-indole (**30**) provided 3-fold and 2-fold stronger activity, respectively, against HepG2 cell than etoposide. Moreover, chloro bis-indole (**20**) was the most potent compound against HuCCA-1 and A549 cell lines affording IC_{50} of 7.75 and 8.74 μM, respectively. The *p*-nitro phenolic bis-indole analog **9c** was shown to be the most potent compound against MOLT-3 cells providing IC_{50} of 2.04 μM. In summary, cytotoxic bis- and tris-indole analogs have been successfully synthesized using environmental-friendly

Author's personal copy

tungstosilicic acid. Significant antiproliferative activity was observed for bis- and tris-indole core structures endowed with a phenolic group or with a functional group that can form H-bonding together with the highly hydrophobic *p*-substituent on the benzenesulfonamide moiety.

Experimental

Chemistry

Column chromatography was carried out using silica gel 60 (70–230 mesh ASTM). Analytical thin-layer chromatography (TLC) was performed with silica gel 60 F_{254} aluminium sheets. ^{1}H- and ^{13}C- NMR spectra were recorded on a Bruker AVANCE 300 NMR spectrometer (operating at 300 MHz for ^{1}H and 75 MHz for ^{13}C). Residual solvent shifts of the deuterated solvents were used as internal standards for calibration of spectra. The following standard abbreviations were used for signal multiplicities: singlet (s), doublet (d), triplet (t), quartet (q), multiplet (m), and broad (br). FTIR spectra were obtained using a universal attenuated total reflectance attached on a Perkin–Elmer Spectrum One spectrometer. Mass spectra were recorded on a Bruker Daltonics (microTOF). Melting points were determined using a Griffin melting point apparatus and were uncorrected.

General procedure for the synthesis of *N*-(2-(1*H*-indol-3-yl)ethyl)-benzenesulfonamides (**10**–**15**)

A solution of tryptamine (10 mmol) in dichloromethane (50 mL) was added in a dropwise manner to a stirred mixture of appropriate benzenesulfonyl chloride (10 mmol) and sodium carbonate (14 mmol) in dichloromethane (20 mL). The reaction mixture was stirred at room temperature overnight, and distilled water (20 mL) was added. The organic phase was separated and the aqueous phase was extracted with dichloromethane (2 × 30 mL). The organic extracts were combined and washed with water (30 mL). The organic layer was dried over anhydrous sodium sulfate, filtered, and evaporated to dryness under reduced pressure. The crude product was further purified by column chromatography on silica gel to obtain the pure product.

^{1}H NMR spectra of 4-nitro-*N*-(2-(1*H*-indol-3-yl)ethyl)-benzenesulfonamide (**10**) [15], 4-methyl-*N*-(2-(1*H*-indol-3-yl)ethyl)-benzenesulfonamide (**11**) [20] and 2-nitro-*N*-(2-(1*H*-indol-3-yl)ethyl)-benzenesulfonamide (**15**) [21] were consistent with those reported in the literature.

*4-Methoxy-N-(2-(1H-indol-3-yl)ethyl)-benzenesulfonamide (**12**)*

White solid. 85 % Yield; mp 100–101 °C; IR (UATR) cm^{-1}: 3406, 3298, 1596, 1498, 1321, 1260, 1151. ^{1}H NMR (300 MHz, DMSO-d$_6$) δ 2.77 (t, J = 7.1 Hz, 2H, ArCH_2), 2.96 (q, J = 6.8 Hz, 2H, CH_2NH), 3.82 (s, 3H, OCH_3), 6.95 (t, J = 7.6 Hz, 1H, C5-Ar*H*), 7.00–7.14 (m, 4H, C2-Ar*H*, C6-Ar*H*, C3′-Ar*H* and C5′-Ar*H*), 7.31 (d, J = 8.0 Hz, 1H, C7-Ar*H*), 7.37 (d, J = 7.8 Hz, 1H, C4-Ar*H*), 7.59 (t, J = 5.6 Hz, 1H, N*H*SO$_2$), 7.72 (d, J = 8.8 Hz, 2H, C2′-Ar*H* and C6′-Ar*H*), 10.82 (s, 1H, N*H*). ^{13}C NMR (75 MHz, DMSO-d$_6$) δ 25.8, 43.9, 56.1, 111.4, 111.9, 114.7, 118.4, 118.7, 121.4, 123.4, 127.4, 129.1, 132.7, 136.6, 162.5. TOF-MS m/z: 331.1116 (Calcd. for $C_{17}H_{19}N_2O_3S$: 331.1111).

*4-Chloro-N-(2-(1H-indol-3-yl)ethyl)-benzenesulfonamide (**13**)*

White solid. 90 % Yield; mp 126–127 °C; IR (UATR) cm^{-1}: 3400, 3260, 1587, 1315, 1156. ^{1}H NMR (300 MHz, DMSO-d$_6$) δ 2.78 (t, J = 7.2 Hz, 2H, ArCH_2), 3.01 (t, J = 7.2 Hz, 2H, CH_2NH), 6.94 (t, J = 7.7 Hz, 1H, C5-Ar*H*), 7.05 (t, J = 7.7 Hz, 1H, C6-Ar*H*), 7.10 (d, J = 1.7 Hz, 1H, C2-Ar*H*), 7.31 (d, J = 8.0 Hz, 1H, C7-Ar*H*), 7.36 (d, J = 7.8 Hz, 1H, C4-Ar*H*), 7.61 (d, J = 8.5 Hz, 2H, C3′-Ar*H* and *C*5′-Ar*H*), 7.76 (d, J = 8.6 Hz, 2H, C2′-Ar*H* and C6′-Ar*H*), 7.87 (s, 1H, N*H*SO$_2$), 10.81 (s, 1H, N*H*). ^{13}C NMR (75 MHz, DMSO-d$_6$) δ 25.8, 43.9, 111.3, 111.9, 118.4, 118.8, 121.4, 123.4, 127.4, 128.8, 129.7, 136.6, 137.6, 139.9. TOF-MS m/z: 335.0610 (Calcd. for $C_{16}H_{16}ClN_2O_2S$: 335.0616).

*3-Nitro-N-(2-(1H-indol-3-yl)ethyl)-benzenesulfonamide (**14**)*

Yellow solid. 95 % Yield; mp 108–109 °C; IR (UATR) cm^{-1}: 3412, 3309, 1607, 1529, 1350, 1162. ^{1}H NMR (300 MHz, DMSO-d$_6$) δ 2.79 (t, J = 7.3 Hz, 2H, ArCH_2), 3.10 (q, J = 7.3 Hz, 2H, CH_2NH), 6.91 (t, J = 7.8 Hz, 1H, C5-Ar*H*), 7.02 (t, J = 7.8 Hz, 1H, C6-Ar*H*), 7.09 (d, J = 2.2 Hz, 1H, C2-Ar*H*), 7.26 (d, J = 7.8 Hz, 1H, C7-Ar*H*), 7.36 (d, J = 8.0 Hz, 1H, C4-Ar*H*), 7.77 (t, J = 8.0 Hz, 1H, C5′-Ar*H*), 8.07–8.16 (m, 2H, C4′-Ar*H* and C6′-Ar*H*), 8.34–8.45 (m, 2H, N*H*SO$_2$, C2′-Ar*H*), 10.78 (s, 1H, N*H*). ^{13}C NMR (75 MHz, DMSO-d$_6$) δ 25.8, 43.8, 111.1, 111.8, 118.4, 118.7, 121.4, 121.5, 123.6, 127.2, 131.4, 132.7, 136.5, 142.6, 148.1. TOF-MS m/z: 368.0665 (Calcd. for $C_{16}H_{15}N_3NaO_4S$: 368.0676).

Author's personal copy

General procedure for the synthesis of bis- and tris-indoles (**16–32**)

A mixture of *N*-sulfonyltryptamine (**11–15**) (0.5 mmol), benzaldehyde (**a**), 2-hydroxybenzaldehyde (**b**), 4-hydroxybenzaldehyde (**c**) or isatin (**d**) (0.3 mmol), and $H_4O_{40}SiW_{12} \cdot aq$ (20 mol %) in acetonitrile (5 mL) was stirred at room temperature for 2–6 h. After complete conversion, as indicated by TLC, the reaction mixture was concentrated in a vacuum and purified by silica gel column chromatography to obtain the corresponding bis- or tris-indole pure products.

*N,N′-((2,2′-(Phenylmethylene)bis(1H-indole-3,2-diyl))bis(ethane-2,1-diyl))bis(4-methylbenzenesulfonamide) (**16**)*

Light brown solid. 52 % Yield; mp 166–167 °C; IR (UATR) cm^{-1}: 3378, 1598, 1458, 1320, 1155. ^1H NMR (300 MHz, acetone-d_6) δ 2.36 (s, 6H, 2 × CH_3), 2.80–3.00 (m, 8H, 4 × CH_2), 6.16 (s, 1H, C*H*), 6.39 (br t, 2H, 2 × N*H*SO_2), 6.97–7.08 (m, 4H, Ar*H*), 7.14–7.30 (m, 11H, Ar*H*), 7.45 (d, J = 7.1 Hz, 2H, Ar*H*), 7.58 (d, J = 8.2 Hz, 4H, 2C2′-Ar*H*, 2C6′-Ar*H*), 9.66 (s, 2H, 2 × N*H*). ^{13}C NMR (75 MHz, acetone-d_6) δ 20.5, 25.0, 40.5, 43.6, 108.8, 111.3, 118.1, 119.0, 121.1, 126.8, 128.4, 128.5, 128.6, 129.5, 135.2, 136.1, 138.0, 141.2, 142.7. TOF-MS m/z: 717.2568 (Calcd. for $C_{41}H_{41}N_4O_4S_2$: 717.2564).

*N,N′-((2,2′-(Phenylmethylene)bis(1H-indole-3,2-diyl))bis(ethane-2,1-diyl))bis(4-methoxybenzenesulfonamide) (**17**)*

Light brown solid. 60 % Yield; mp 119–120 °C; IR (UATR) cm^{-1}: 3292, 1596, 1497, 1321, 1259, 1149. ^1H NMR (300 MHz, acetone-d_6) δ 2.80–3.00 (m, 8H, 4 × CH_2), 3.80 (s, 6H, 2 × OCH_3), 6.14 (s, 1H, C*H*), 6.34 (br t, 2H, 2 × N*H*SO_2), 6.89 (d, J = 8.8 Hz, 4H, 2C3′-Ar*H* and 2C5′-Ar*H*), 6.99 (2t, J = 7.1 Hz, 4H, 2C5-Ar*H* and 2C6-Ar*H*), 7.10–7.30 (m, 7H, 2C7-ArH, C2″-Ar*H*, C3″-Ar*H*, C4″-Ar*H*, C5″-Ar*H* and C6″-Ar*H*), 7.42 (d, J = 7.2 Hz, 2H, 2C4-Ar*H*), 7.58 (d, J = 8.8 Hz, 4H, 2C2′-Ar*H* and 2C6′-Ar*H*), 9.66 (s, 1H, N*H*). ^{13}C NMR (75 MHz, acetone-d_6) δ 25.0, 40.4, 43.6, 55.2, 108.9, 111.3, 114.0, 118.1, 119.0, 121.1, 126.9, 128.4, 128.6, 128.9, 132.5, 135.2, 136.1, 141.2, 162.6. TOF-MS m/z: 749.2431 (Calcd. for $C_{41}H_{41}N_4O_6S_2$: 749.2462).

*N,N′-((2,2′-((2-Hydroxyphenyl)methylene)bis(1H-indole-3,2-diyl))bis(ethane-2,1-diyl))bis(4-methylbenzenesulfonamide) (**18**)*

Yellow solid. 63 % Yield; mp 149–150 °C; IR (UATR) cm^{-1}: 3384, 1597, 1456, 1318, 1153. ^1H NMR (300 MHz, dmso-d_6) δ 2.32 (s, 6H, 2 × CH_3), 2.50–2.70 (m, 8H, 4 × CH_2), 6.06 (s, 1H, C*H*), 6.67 (t, J = 7.3 Hz, 1H, C5″-Ar*H*), 6.79 (d, J = 8.1 Hz, 1H, C3″-Ar*H*), 6.85 (d, J = 6.8 Hz, 1H, C6″-Ar*H*), 6.90–7.10 (m, 5H, 2 × C5-Ar*H*, 2 × C6-Ar*H*, C4″-Ar*H*), 7.20–7.31 (m, 8H, 2 × C4-Ar*H*, 2 × C7-Ar*H*, 2 × C3′-Ar*H*, 2 × C5′-Ar*H*), 7.45 (br t, 2H, 2 × N*H*SO_2), 7.52 (d, J = 8.1 Hz, 4H, 2 × C2′-Ar*H*, 2 × C6′-Ar*H*, 9.56 (s, 1H, O*H*), 10.21 (s, 2H, 2 × N*H*). ^{13}C NMR (75 MHz, dmso-d_6) δ 21.4, 25.2, 34.9, 43.5, 108.0, 111.8, 115.5, 117.9, 118.8, 119.4, 120.9, 126.4, 126.9, 127.8, 128.3, 128.5, 129.6, 129.9, 135.6, 135.9, 138.0, 142.8, 154.9. TOF-MS m/z: 755.2317 (Calcd. for $C_{41}H_{40}N_4NaO_5S_2$: 755.2332).

*N,N′-((2,2′-((2-Hydroxyphenyl)methylene)bis(1H-indole-3,2-diyl))bis(ethane-2,1-diyl))bis(4-methoxybenzenesulfonamide) (**19**)*

Yellow solid. 75 % Yield; mp 157–158 °C; IR (UATR) cm^{-1}: 3383, 1596, 1498, 1456, 1259, 1147. ^1H NMR (300 MHz, dmso-d_6) δ 2.50–2.74 (m, 8H, 4 × CH_2), 3.78 (s, 6H, 2 × OCH_3), 6.09 (s, 1H, C*H*), 6.67 (t, J = 7.6 Hz, 1H, C5″-Ar*H*), 6.80 (d, J = 8.0 Hz, 1H, C3″-Ar*H*), 6.86 (d, J = 7.7 Hz, 1H, C6″-Ar*H*), 6.90–7.09 (m, 9H, 2 × C5-Ar*H*, 2 × C6-Ar*H*, 2 × C3′-Ar*H*, 2 × C5′-Ar*H*, C4″-Ar*H*), 7.26 (d, J = 7.7 Hz, 2H, 2 × C7-Ar*H*), 7.29 (d, J = 7.6 Hz, 2H, 2 × C4-Ar*H*), 7.38 (br t, 2H, 2 × N*H*SO_2), 7.55 (d, J = 8.1 Hz, 4H, 2 × C2′-Ar*H*, 2 × C6′-Ar*H*), 9.57 (s, 1H, O*H*), 10.23 (s, 2H, 2 × N*H*). ^{13}C NMR (75 MHz, dmso-d_6) δ 25.2, 34.9, 43.5, 56.0, 108.0, 111.9, 114.6, 115.5, 117.9, 118.9, 119.5, 120.9, 127.8, 128.3, 128.5, 129.0, 129.6, 132.6, 135.7, 135.9, 154.9, 162.4. TOF-MS m/z: 787.2231 (Calcd. for $C_{41}H_{40}N_4NaO_7S_2$: 787.2231).

*N,N′-((2,2′-((2-Hydroxyphenyl)methylene)bis(1H-indole-3,2-diyl))bis(ethane-2,1-diyl))bis(4-chlorobenzenesulfonamide) (**20**)*

Light brown solid. 38 % Yield; mp 134–135 °C; IR (UATR) cm^{-1}: 3385, 3306, 1587, 1456, 1320, 1156. ^1H NMR (300 MHz, dmso-d_6) δ 2.55–2.70 (m, 8H, 4 × CH_2), 6.08 (s, 1H, C*H*), 6.66 (t, J = 7.1 Hz, 1H, C5″-Ar*H*), 6.79 (d, J = 8.0 Hz, 1H, C3″-Ar*H*), 6.85 (d, J = 7.1 Hz, 1H, C6″-Ar*H*), 6.91–7.09 (m, 5H, 2 × C5-Ar*H*, 2 × C6-Ar*H*, C4″-Ar*H*), 7.23-7.31 (m, 4H, 2 × C4-Ar*H*, 2 × C7-Ar*H*), 7.46 (d, J = 8.6 Hz, 4H, 2 × C3′-Ar*H*, 2 × C5′-Ar*H*), 7.58 (d, J = 8.6 Hz, 4H, 2 × C2′-Ar*H*, 2 × C6′-Ar*H*), 7.68 (br t, 2H, 2 × N*H*SO_2), 9.58 (s, 1H, O*H*), 10.24 (s, 2H, 2 × N*H*). ^{13}C NMR (75 MHz, dmso-d_6) δ 25.2, 34.9, 43.4, 107.8, 111.9, 115.4, 117.9, 118.9, 119.5, 120.9, 127.7, 128.3, 128.5, 128.7, 129.6, 135.7, 135.9, 137.5, 139.7, 154.8. TOF-MS m/z: 790.1677 (Calcd. for $C_{39}H_{38}Cl_2N_5O_5S_2$: 790.1686).

Author's personal copy

*N,N′-((2,2′-((2-Hydroxyphenyl)methylene)bis(1H-indole-3,2-diyl))bis(ethane-2,1-diyl))bis(3-nitrobenzenesulfonamide) (**21**)*

Yellow solid. 57 % Yield; mp 141–142 °C; IR (UATR) cm^{-1}: 3404, 3314, 1606, 1530, 1456, 1351, 1267, 1162. ^{1}H NMR (300 MHz, dmso-d_6) δ 2.60–2.80 (m, 8H, 4 × CH_2), 6.07 (s, 1H, C*H*), 6.64 (t, J = 7.6 Hz, 1H, C5″-Ar*H*), 6.76 (d, J = 7.9 Hz, 1H, *C*3″-Ar*H*), 6.85–7.05 (m, 6H, 2 × C5-Ar*H*, 2 × C6-Ar*H*, C4″-Ar*H*, C6″-Ar*H*), 7.23 (d, J = 7.8 Hz, 2H, 2 × C7-Ar*H*), 7.27 (d, J = 7.5 Hz, 2H, 2 × C4-Ar*H*), 7.68 (t, J = 8.1 Hz, 2H, C5′-Ar*H*), 7.92 (d, J = 7.7 Hz, 4H, 2 × C6′-Ar*H*, 2 × C4′-Ar*H*), 8.38 (s, 2H, 2 × C2′-Ar*H*), 8.34 (br t, 2H, 2 × N*H*SO_2), 9.60 (s, 1H, O*H*), 10.22 (s, 2H, 2 × N*H*). ^{13}C NMR (75 MHz, dmso-d_6) δ 25.1, 34.8, 43.5, 107.8, 111.8, 115.5, 117.9, 118.9, 119.4, 120.9, 121.5, 127.3, 127.6, 128.3, 128.4, 129.7, 131.4, 132.7, 135.7, 135.8, 142.5, 148.1, 154.8. TOF-MS m/z: 817.1706 (Calcd. for $C_{39}H_{34}N_6NaO_9S_2$: 817.1721).

*N,N′-((2,2′-((2-Hydroxyphenyl)methylene)bis(1H-indole-3,2-diyl))bis(ethane-2,1-diyl))bis(2-nitrobenzenesulfonamide) (**22**)*

Light brown solid. 43 % Yield; mp 156–157 °C; IR (UATR) cm^{-1}: 3398, 1594, 1538, 1457, 1338, 1163. ^{1}H NMR (300 MHz, dmso-d_6) δ 2.65–2.85 (m, 8H, 4 × CH_2), 6.12 (s, 1H, C*H*), 6.65 (t, J = 7.6 Hz, 1H, C5″-Ar*H*), 6.79 (d, J = 7.6 Hz, 1H, C3″-Ar*H*), 6.85–7.08 (m, 6H, 2 × C5-Ar*H*, 2 × C6-Ar*H*, C4″-Ar*H*, C6″-Ar*H*), 7.28 (d, J = 7.8 Hz, 2H, 2 × C7-Ar*H*), 7.35 (d, J = 7.5 Hz, 2H, 2 × C4-Ar*H*), 7.60-7.81 (m, 6H, 2 × C4′-Ar*H*, 2 × C5′-Ar*H*, 2 × C6′-Ar*H*), 7.90 (d, J = 7.9 Hz, 2H, 2 × C3′-Ar*H*), 7.97 (br t, 2H, 2 × N*H*SO_2), 9.62 (s, 1H, O*H*), 10.26 (s, 2H, 2 × N*H*). ^{13}C NMR (75 MHz, dmso-d_6) δ 25.4, 35.0, 43.6, 107.7, 111.9, 115.5, 118.0, 118.9, 120.9, 124.9, 127.7, 128.5, 129.6, 129.7, 132.9, 133.2, 134.3, 135.8, 135.9, 148.0, 154.9. TOF-MS m/z: 817.1686 (Calcd. for $C_{39}H_{34}N_6NaO_9S_2$: 817.1721).

*N,N′-((2,2′-((4-Hydroxyphenyl)methylene)bis(1H-indole-3,2-diyl))bis(ethane-2,1-diyl))bis(4-methylbenzenesulfonamide) (**23**)*

Red-brown solid. 54 % Yield; mp 150–151 °C; IR (UATR) cm^{-1}: 3382, 1598, 1512, 1458, 1319, 1155. ^{1}H NMR (300 MHz, dmso-d_6) δ 2.33 (s, 6H, 2 × CH_3), 2.60–2.85 (m, 8H, 4 × CH_2), 5.73 (s, 1H, C*H*), 6.65 (d, J = 8.4 Hz, 2H, C3″-Ar*H*, C5″-Ar*H*), 6.79 (d, J = 8.4 Hz, 2H, C2″-Ar*H*, C6″-Ar*H*), 6.95 (t, J = 7.2 Hz, 2H, 2 × C5-Ar*H*), 7.02 (t, J = 7.2 Hz, 2H, 2 × C6-Ar*H*), 7.22-7.35 (m, 8H, 2 × C4-Ar*H*, 2 × C7-Ar*H*, 2 × C3′-Ar*H*, 2 × C5′-Ar*H*), 7.55 (d, J = 8.0 Hz, 6H, 2 × C2′-Ar*H*, 2 × C6′-Ar*H*, 2 × N*H*SO_2), 9.36 (s, 1H, O*H*), 10.38 (s, 2H, 2 × N*H*). ^{13}C NMR (75 MHz, dmso-d_6) δ 21.4, 25.0, 39.7 (superimposed with dmso-d_6 peaks), 44.0, 108.7, 111.7, 115.6, 118.2, 119.0, 121.2, 127.0, 128.1, 129.4, 130.0, 131.6, 135.9, 136.1, 137.9, 142.9, 156.6. TOF-MS m/z: 755.2346 (Calcd. for $C_{41}H_{40}N_4NaO_5S_2$: 755.2332).

*N,N′-((2,2′-((4-Hydroxyphenyl)methylene)bis(1H-indole-3,2-diyl))bis(ethane-2,1-diyl))bis(4-methoxybenzenesulfonamide) (**24**)*

Red-brown solid. 61 % Yield; mp 166–167 °C; IR (UATR) cm^{-1}: 3376, 1596, 1459, 1150. ^{1}H NMR (300 MHz, dmso-d_6) δ 2.60–2.85 (m, 8H, 4 × CH_2), 3.79 (s, 6H, 2 × OCH_3), 5.77 (s, 1H, C*H*), 6.67 (d, J = 8.4 Hz, 2H, C3″-Ar*H*, C5″-Ar*H*), 6.81 (d, J = 8.4 Hz, 2H, C2″-Ar*H*, C6″-Ar*H*), 6.91–7.06 (m, 8H, 2 × C5-Ar*H*, 2 × C6-Ar*H*, 2 × C3′-Ar*H*, 2 × C5′-Ar*H*), 7.28 (d, J = 7.9 Hz, 2H, 2 × C7-Ar*H*), 7.32 (d, J = 7.6 Hz, 2H, 2 × C4-Ar*H*), 7.47 (br t, 2H, 2 × N*H*SO_2), 7.58 (d, J = 8.7 Hz, 4H, 2 × C2′-Ar*H*, 2 × C6′-Ar*H*), 9.37 (s, 1H, O*H*), 10.37 (s, 2H, 2 × N*H*). ^{13}C NMR (75 MHz, dmso-d_6) δ 25.0, 39.7 (superimposed with dmso-d_6 peaks), 44.0, 56.0, 108.7, 111.7, 114.6, 115.6, 118.2, 119.0, 121.2, 128.1, 129.1, 129.5, 131.7, 132.4, 135.9, 136.1, 156.5, 162.4. TOF-MS m/z: 787.2230 (Calcd. for $C_{41}H_{40}N_4NaO_7S_2$: 787.2231).

*N,N′-((2,2′-((4-Hydroxyphenyl)methylene)bis(1H-indole-3,2-diyl))bis(ethane-2,1-diyl))bis(4-chlorobenzenesulfonamide) (**25**)*

Red-brown solid. 44 % Yield; mp 157–158 °C; IR (UATR) cm^{-1}: 3291, 1641, 1528, 1319, 1158. ^{1}H NMR (300 MHz, dmso-d_6) δ 2.65–2.85 (m, 8H, 4 × CH_2), 5.78 (s, 1H, C*H*), 6.68 (d, J = 8.6 Hz, 2H, C3″-Ar*H*, C5″-Ar*H*), 6.82 (d, J = 8.5 Hz, 2H, C2″-Ar*H*, C6″-Ar*H*), 6.96 (t, J = 7.3 Hz, 2H, 2 × C5-Ar*H*), 7.03 (t, J = 6.9 Hz, 2H, 2 × C6-Ar*H*), 7.28 (d, J = 7.7 Hz, 2H, 2 × C7-Ar*H*), 7.33 (d, J = 7.7 Hz, 2H, 2 × C4-Ar*H*), 7.50 (d, J = 8.6 Hz, 4H, 2 × C3′-Ar*H*, 2 × C5′-Ar*H*), 7.62 (d, J = 8.6 Hz, 4H, 2 × C2′-Ar*H*, 2 × C6′-Ar*H*), 7.76 (br t, 2H, 2 × N*H*SO_2), 9.37 (s, 1H, O*H*), 10.37 (s, 2H, 2 × N*H*). ^{13}C NMR (75 MHz, dmso-d_6) δ 25.1, 39.7 (superimposed with dmso-d_6 peaks), 43.9, 108.5, 111.7, 115.7, 118.2, 119.0, 121.2, 128.1, 128.8, 129.5, 129.6, 131.6, 135.9, 136.1, 137.6, 139.7, 156.6. TOF-MS m/z: 790.1688 (Calcd. for $C_{39}H_{38}Cl_2N_5O_5S_2$: 790.1686).

Author's personal copy

*N,N′-((2,2′-((4-Hydroxyphenyl)methylene)bis(1H-indole-3,2-diyl))bis(ethane-2,1-diyl))bis(3-nitrobenzenesulfonamide) (**26**)*

Red-brown solid. 58 % Yield; mp 119–120 °C; IR (UATR) cm^{-1}: 3411, 3318, 1608, 1530, 1457, 1351, 1162. ^1H NMR (300 MHz, dmso-d_6) δ 2.70-2.90 (m, 8H, 4 × CH_2), 5.80 (s, 1H, C*H*), 6.64 (d, J = 8.5 Hz, 2H, C3″-Ar*H*, C5″-Ar*H*), 6.82–7.01 (m, 6H, 2 × C5-Ar*H*, 2 × C6-Ar*H*, C2″-Ar*H*, C6″-Ar*H*), 7.24 (d, J = 7.8 Hz, 2H, 2 × C7-Ar*H*), 7.33 (d, J = 7.6 Hz, 2H, 2 × C4-Ar*H*), 7.70 (t, J = 8.1 Hz, 2H, 2 × C5′-Ar*H*), 7.94 (d, J = 7.9 Hz, 2H, 2 × C6′-Ar*H*), 8.37 (d, J = 8.1 Hz, 2H, 2 × C4′-Ar*H*), 8.41 (s, 2H, 2 × C2′-Ar*H*), 8.01 (br t, 2H, 2 × N*H*SO_2), 9.33 (s, 1H, O*H*), 10.34 (s, 2H, 2 × N*H*). ^{13}C NMR (75 MHz, dmso-d_6) δ 25.0, 39.7 (superimposed with dmso-d_6 peaks), 43.9, 108.5, 111.7, 115.6, 118.1, 119.0, 121.2, 121.5, 127.3, 128.1, 129.5, 131.4, 131.5, 132.7, 136.0, 142.4, 148.2, 156.6. TOF-MS m/z: 817.1734 (Calcd. for $C_{39}H_{34}N_6NaO_9S_2$: 817.1721).

*N,N′-((2,2′-((4-Hydroxyphenyl)methylene)bis(1H-indole-3,2-diyl))bis(ethane-2,1-diyl))bis(2-nitrobenzenesulfonamide) (**27**)*

Red-brown solid. 52 % Yield; mp 129–130 °C; IR (UATR) cm^{-1}: 3393, 1614, 1594, 1538, 1338, 1163. ^1H NMR (300 MHz, dmso-d_6) δ 2.75-3.00 (m, 8H, 4 × CH_2), 5.84 (s, 1H, C*H*), 6.67 (d, J = 8.5 Hz, 2H, C3″-Ar*H*, C5″-Ar*H*), 6.87 (d, J = 8.5 Hz, 2H, C2″-Ar*H*, C6″-Ar*H*), 6.95 (t, J = 7.0 Hz, 2H, 2 × C5-Ar*H*), 7.02 (t, J = 7.3 Hz, 2H, 2 × C6-Ar*H*), 7.28 (d, J = 7.9 Hz, 2H, 2 × C7-Ar*H*), 7.39 (d, J = 7.6 Hz, 2H, 2 × C4-Ar*H*), 7.63–7.82 (m, 6H, 2 × C4′-Ar*H*, 2 × C5′-Ar*H*, 2 × C6′-Ar*H*), 7.90 (d, J = 7.9 Hz, 2H, 2 × C3′-Ar*H*), 8.03 (br t, 2H, 2 × N*H*SO_2), 9.36 (s, 1H, O*H*), 10.38 (s, 2H, 2 × N*H*). ^{13}C NMR (75 MHz, dmso-d_6) δ 25.3, 39.7 (superimposed with dmso-d_6 peaks), 44.0, 108.4, 111.7, 115.7, 118.2, 119.0, 121.2, 124.9, 128.2, 129.5, 129.7, 131.6, 132.9, 133.1, 134.3, 136.0, 136.1, 148.1, 156.6. TOF-MS m/z: 817.1696 (Calcd. for $C_{39}H_{34}N_6NaO_9S_2$: 817.1721).

*N,N′-((2′-Oxo-1′,2′-dihydro-1H,1″H-[2,3′:3′,2″-terindole]-3,3″-diyl)bis(ethane-2,1-diyl))bis(4-methylbenzenesulfonamide) (**28**)*

Yellow solid. 46 % Yield; mp 161–162 °C; IR (UATR) cm^{-1}: 3329, 1710, 1617, 1599, 1320, 1153. ^1H NMR (300 MHz, dmso-d_6) δ 2.35 (s, 6H, 2 × CH_3), 2.35–2.80 (m, 8H, 4 × CH_2), 6.88–7.05 (m, 6H, Ar*H*), 7.18–7.35 (m, 10H, Ar*H*), 7.50 (br t, 2H, 2 × N*H*SO_2), 7.59 (d, J = 7.8 Hz, 4H, 2 × C2′-Ar*H*, 2 × C6′-Ar*H*), 10.44 (s, 2H, 2 × N*H*), 10.85 (s, 1H, N*H*CO). ^{13}C NMR (75 MHz, dmso-d_6) δ 21.4, 25.4, 43.2, 55.0, 109.3, 110.8, 112.1, 118.3, 119.0, 121.6, 122.9, 125.7, 127.0, 128.7, 129.4, 129.9, 131.8, 132.2, 135.9, 138.1, 141.4, 142.8, 176.4. TOF-MS m/z: 780.2294 (Calcd. for $C_{42}H_{39}N_5NaO_5S_2$: 780.2285).

*N,N′-((2′-Oxo-1′,2′-dihydro-1H,1″H-[2,3′:3′,2″-terindole]-3,3″-diyl)bis(ethane-2,1-diyl))bis(4-methoxybenzenesulfonamide) (**29**)*

Light brown solid. 57 % Yield; mp 166–167 °C; IR (UATR) cm^{-1}: 3336, 1709, 1617, 1597, 1259, 1147. ^1H NMR (300 MHz, dmso-d_6) δ 2.35–2.74 (m, 8H, 4 × CH_2), 3.81 (s, 6H, 2 × OCH_3), 6.88–7.07 (m, 10H, Ar*H*), 7.20–7.30 (m, 6H, Ar*H*), 7.42 (br t, 2H, 2 × N*H*SO_2), 7.64 (d, J = 8.8 Hz, 4H, 2 × C2′-Ar*H*, 2 × C6′-Ar*H*), 10.45 (s, 2H, 2 × N*H*), 10.86 (s, 1H, N*H*CO). ^{13}C NMR (75 MHz, dmso-d_6) δ 25.4, 43.2, 55.0, 56.0, 110.84, 112.06, 114.64, 118.35, 119.0, 121.7, 122.9, 125.7, 128.7, 129.1, 129.4, 131.8, 132.2, 132.6, 135.9, 141.4, 162.4, 176.4. TOF-MS m/z: 812.2181 (Calcd. for $C_{42}H_{39}N_5NaO_7S_2$: 812.2183).

*N,N′-((2′-Oxo-1′,2′-dihydro-1H,1″H-[2,3′:3′,2″-terindole]-3,3″-diyl)bis(ethane-2,1-diyl))bis(4-chlorobenzenesulfonamide) (**30**)*

Light brown solid. 34 % Yield; mp 221–222 °C; IR (UATR) cm^{-1}: 3339, 1708, 1617, 1587, 1321, 1156. ^1H NMR (300 MHz, dmso-d_6) δ 2.35–2.80 (m, 8H, 4 × CH_2), 6.90–7.07 (m, 6H, Ar*H*), 7.20–7.30 (m, 6H, Ar*H*), 7.57 (d, J = 8.6 Hz, 4H, 2 × C3′-Ar*H*, 2 × C5′-Ar*H*), 7.68 (d, J = 8.7 Hz, 4H, 2 × C2′-Ar*H*, 2 × C6′-Ar*H*), 7.72 (br t, 2H, 2 × N*H*SO_2), 10.45 (s, 2H, 2 × N*H*), 10.86 (s, 1H, N*H*CO). ^{13}C NMR (75 MHz, dmso-d_6) δ 25.4, 43.2, 55.0, 112.1, 118.3, 119.0, 121.7, 123.0, 125.7, 128.7, 128.8, 129.6, 131.8, 132.2, 135.8, 137.5, 139.9, 141.4, 176.4. TOF-MS m/z: 820.1206 (Calcd. for $C_{40}H_{33}Cl_2N_5NaO_5S_2$: 820.1192).

*N,N′-((2′-Oxo-1′,2′-dihydro-1H,1″H-[2,3′:3′,2″-terindole]-3,3″-diyl)bis(ethane-2,1-diyl))bis(3-nitrobenzenesulfonamide) (**31**)*

Yellow solid. 50 % Yield; mp 163–164 °C; IR (UATR) cm^{-1}: 3367, 1706, 1617, 1529, 1350, 1163. ^1H NMR (300 MHz, dmso-d_6) δ 2.30–2.83 (m, 8H, 4 × CH_2), 6.84–7.02 (m, 6H, Ar*H*), 7.15–7.28 (m, 6H, Ar*H*), 7.74 (t, J = 7.9 Hz, 2H, 2 × N*H*SO_2), 7.93–8.05 (m, 4H, Ar*H*), 8.31–8.40 (m, 4H, Ar*H*), 10.41 (s, 2H, 2 × N*H*), 10.94 (s, 1H, N*H*CO). ^{13}C NMR (75 MHz, dmso-d_6) δ 25.3, 43.2, 55.0, 109.1, 110.9, 112.1, 118.2, 119.1, 121.5, 121.7, 123.0, 125.8, 127.3, 128.6, 129.4, 131.5, 131.7, 132.2, 132.7, 135.7, 141.4, 142.5, 148.1, 176.6. TOF-MS m/z: 842.1678 (Calcd. for $C_{40}H_{33}N_7NaO_9S_2$: 842.1673).

Author's personal copy

N,N′-((2′-Oxo-1′,2′-dihydro-1H,1″H-[2,3′:3′,2″-terindole]-3,3″-diyl)bis(ethane-2,1-diyl))bis(2-nitrobenzenesulfonamide) (**32**)

Yellow solid. 55 % Yield; mp 157–158 °C; IR (UATR) cm^{-1}: 3354, 1710, 1617, 1595, 1537, 1335, 1162. ^{1}H NMR (300 MHz, dmso-d_6) δ 2.45–3.00 (m, 8H, 4 × CH_2), 6.89–7.07 (m, 6H, Ar*H*), 7.20–7.39 (m, 6H, Ar*H*), 7.67–7.83 (m, 6H, Ar*H*), 7.90 (d, $J = 7.8$ Hz, 2H, 2 × C3′-Ar*H*), 8.05 (br t, 2H, 2 × N*H*SO_2), 10.48 (s, 2H, 2 × N*H*), 10.87 (s, 1H, N*H*CO). ^{13}C NMR (75 MHz, dmso-d_6) δ 25.6, 43.4, 55.0, 109.1, 110.9, 112.1, 118.5, 119.1, 121.7, 123.0, 124.8, 125.7, 128.7, 129.4, 129.7, 131.7, 132.3, 132.9, 133.2, 134.2, 135.9, 141.5, 148.2, 176.4. TOF-MS m/z: 842.1671 (Calcd. for $C_{40}H_{33}N_7NaO_9S_2$: 842.1673).

Cytotoxic assay

The cytotoxic assay was performed as previously described by Tengchaisri et al. [19]. Briefly, cell lines suspended in RPMI 1640 containing 10 % FBS were seeded at 1×10^4 cells (100 μL) per well in a 96-well plate and incubated in humidified atmosphere, 95 % air, 5 % CO_2 at 37 °C. After 24 h, additional medium (100 μL) containing the test compound and vehicle was added to a final concentration of 50 μg/mL, 0.2 % DMSO, and further incubated for 3 days. After that, the cells were fixed with EtOH–H_2O (95:5, v/v), stained with crystal violet solution, and lysed with a solution of 0.1 N HCl in MeOH. The absorbance was measured at 550 nm. The number of surviving cells was determined from the absorbance. Etoposide and/or doxorubicin were used as reference drugs.

Acknowledgments This project was financially supported by the Young Scholars Research Fellowship from the Thailand Research Fund to R.P. (MRG5680001). Great supports from the Office of Higher Education Commission and Mahidol University under the National Research Universities Initiative were appreciated. We are also indebted to Chulabhorn Research Institute for mass spectra and bioactivity tests and to Asst. Prof. Dr. Chanin Nantasenamat for the proofreading of this manuscript.

References

1. Gribble GW (2000) Recent developments in indole ring synthesis-methodology and applications. J Chem Soc Perkin Trans 1: 1045–1075. doi:10.1039/a909834h
2. Gul W, Hamann MT (2005) Indole alkaloid marine natural products: an established source of cancer drug leads with considerable promise for the control of parasitic, neurological and other diseases. Life Sci 78:442–453. doi:10.1016/j.lfs.2005.09.007
3. Ishikura M, Yamada K, Abe T (2010) Simple indole alkaloids and those with a nonrearranged monoterpenoid unit. Nat Prod Rep 27:1630–1680. doi:10.1039/c005345g
4. Kochanowska-Karamyan AJ, Hamann MT (2010) Marine indole alkaloids: potential new drug leads for the control of depression and anxiety. Chem Rev 110:4489–4497. doi:10.1021/cr900211p
5. Kamano Y, Zhang H-P, Ichihara Y, Kizu H, Komiyama K, Pettit GR (1995) Convolutamydine A, a novel bioactive hydroxyoxindole alkaloid from marine bryozoan *Amathia convoluta*. Tetrahedron Lett 36:2783–2784
6. Yoo M, Choi S-U, Choi KY, Yon GH, Chae J-C, Kim D, Zylstra G, Kim E (2008) Trisindoline synthesis and anticancer activity. Biochem Biophys Res Commun 376:96–99. doi:10.1016/j.bbrc.2008.08.092
7. Reddy BVS, Rajeswari N, Sarangapani M, Prashanthi Y, Ganji RJ, Addlagatta A (2012) Iodine-catalyzed condensation of isatin with indoles: a facile synthesis of di(indolyl)indolin-2-ones and evaluation of their cytotoxicity. Bioorg Med Chem Lett 22: 2460–2463. doi:10.1016/j.bmcl.2012.02.011
8. Shiri M, Zolfigol MA, Kruger HG, Tanbakouchian Z (2010) Bis- and trisindolylmethanes (BIMs and TIMs). Chem Rev 110: 2250–2293. doi:10.1021/cr900195a
9. Safe S, Papineni S, Chintharlapalli S (2008) Cancer chemotherapy with indole-3-carbinol, bis(3′-indolyl)methane and synthetic analogs. Cancer Lett 269:326–338. doi:10.1016/j.canlet.2008.04.021
10. Rahman KW, Li Y, Wang Z, Sarkar SH, Sarkar FH (2006) Gene expression profiling revealed survivin as a target of 3,3′-diindolylmethane-induced cell growth inhibition and apoptosis in breast cancer cells. Cancer Res 66:4952–4960. doi:10.1158/0008-5472.CAN-05-3918
11. Hong C, Firestone GL, Bjeldanes LF (2002) Bcl-2 family-mediated apoptotic effects of 3,3′-diindolylmethane (DIM) in human breast cancer cells. Biochem Pharmacol 63:1085–1097. doi:10.1016/S0006-2952(02)00856-0
12. Bifulco G, Bruno I, Minale L, Riccio R (1994) Gelliusines A and B, two diastereomeric brominated tris-indole alkaloids from a deep water new caledonian marine sponge (*Gellius* or *Orina* sp.). J Nat Prod 57:1294–1299
13. Foderato TA, Barrows LR, Lassota P, Ireland CM (1997) Bengacarboline, a new β-carboline from a marine ascidian *Didemnum* sp. J Org Chem 62:6064–6065. doi:10.1021/jo962422q
14. Pouilhès A, Kouklovsky C, Langlois Y, Baltaze J-P, Vispé S, Annereau J-P, Barret J-M, Kruczynskic A, Bailly C (2008) Synthesis and biological evaluation of bengacarboline derivatives. Bioorg Med Chem Lett 18:1212–1216. doi:10.1016/j.bmcl.2007.11.113
15. Pingaew R, Prachayasittikul S, Ruchirawat S, Prachayasittikul V (2012) Synthesis and cytotoxicity of novel 2,2′-bis- and 2,2′,2″-tris-indolylmethanes-based bengacarboline analogs. Arch Pharm Res 35:949–954. doi:10.1007/s12272-012-0601-1
16. Kozhevnikov IV (1995) Heteropoly acids and related compounds as catalysts for fine chemical synthesis. Catal Rev Sci Eng 37: 311–352. doi:10.1080/01614949508007097
17. Ueda T, Kotsuki H (2008) Heteropoly acids: green chemical catalysts in organic synthesis. Heterocycles 76:73–97
18. Romanelli GP, Autino JC (2009) Recent applications of heteropolyacids and related compounds in heterocycles synthesis. Mini-Rev Org Chem 6:359–366
19. Tengchaisri T, Chawengkirttikul R, Rachaphaew N, Reutrakul V, Sangsuwan R, Sirisinha S (1998) Antitumor activity of triptolide against cholangiocarcinoma growth in vitro and in hamsters. Cancer Lett 133:169–175. doi:10.1016/S0304-3835(98)00222-5
20. Priebbenow DL, Henderson LC, Pfeffer FM, Stewart S (2010) Domino Heck-Aza-Michael reaction: efficient access to 1-substituted tetrahydro-β-carbolines. J Org Chem 75:1787–1790. doi:10.1021/jo902652h
21. Matsuda Y, Kitajima M, Takayama H (2008) First total synthesis of trimericindole alkaloid, psychotrimine. Org Lett 10:125–128. doi:10.1021/ol702637r

NPCEOCA

UNIVERSITY OF MALAYA

The Leader in Research & Innovation

Asian Core Program Lectureship Award

Ratchanok Pingaew

(Srinakharinwirot University)

PB22

Design, synthesis and molecular docking of novel tetrahydroisoquinoline- triazole hybrids as potential anti-cancer agents

This is to certify that you have been selected by the coordinator of China on 4th December, 2014 to receive a Lectureship Award under the New Phase Asian Core Programme On Cutting-Edge Organic Chemistry in Asia. You will be invited to deliver a series of lectures during the one-week visit to China in the next fiscal year.

.....

Coordinator of China